

PNEUMATIC HYDROPOWER SYSTEMS

by

IAN CHRISTOPHER PARMEE, B.Sc.

**A dissertation submitted in partial fulfilment
of the requirements for the degree of
Doctor of Philosophy to
The Council for National Academic Awards**

June 1990

Collaborating Establishment:

**Energy Technology Support Unit (ETSU),
Harwell**

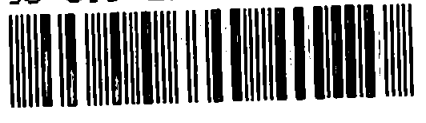
Sponsoring Establishment:

**Department of Civil and Structural Engineering,
Faculty of Technology,
Polytechnic South West**

REFERENCE ONLY

90 013 2714 8

TELEPEN



UNIVERSITY OF PLYMOUTH LIBRARY SERVICES	
Item No.	900 132714-8
Class No.	T-621.312134
Contl No.	X 702619212

PAR

PREFACE

As a result of changes within Higher Education, the author commenced this thesis under the auspices of Plymouth Polytechnic and completed it under the auspices of Polytechnic South West.

Polytechnic South West came into existence on 1st April, 1989 and embraces the formerly independent institutions of Plymouth Polytechnic, Exeter College of Art and Design, Rolle College at Exmouth and Seale-Hayne College at Newton Abbot.

PNEUMATIC HYDROPOWER SYSTEMS

by

IAN CHRISTOPHER PARMEE, B.Sc.

ABSTRACT

The following thesis investigates the performance and economics of a Pneumatic Water Engine capable of extracting energy from differential heads of water in the two to three metre range. Initial concepts are discussed and a system configuration is physically modelled at a laboratory scale. Outline designs using a variety of materials are developed and these provide a basis for the estimation of a probable capital cost using standard Civil Engineering methods.

The proposed system is mathematically modelled using a lumped-mass approach to the complex hydrodynamics. The resultant differential equations are solved by means of a variable Runge-Kutta numerical analysis. The model includes the thermodynamic aspects of the system's compressible airflow. A computer program has been developed from the mathematical model and is utilized in a series of parametric studies.

An economic assessment based upon both the average power output achieved during the parametric studies and the probable capital cost of the system is presented, together with an estimate of the cost per kilowatt-hour of the electricity produced. This assessment takes into account maintenance costs, expected value of the energy produced and the possible effects of both Water Abstraction Charges and Local Authority Rating.

In addition to the parametric studies a final, more rigorous optimization of the system involving a number of the many interacting variables has been undertaken. This optimization is achieved via Cumulative Evolutionary Design techniques involving the use of Genetic Algorithms. An optimal design of the chamber shape is achieved in the same manner.

ACKNOWLEDGEMENTS

The author wishes to thank Dr. G. N. Bullock for his supervision during the period of this research. He also wishes to thank AUR Hydropower Ltd for the use of some of their test data and Dr. T. Whittaker for information concerning the Wells Turbine. Thanks are also due to the many individuals and organizations that have provided information useful to the research project.

To Bev and Josie

CONTENTS

	Page
PREFACE	I
ABSTRACT	II
ACKNOWLEDGEMENTS	III
CONTENTS	v
1.0 INTRODUCTION	1
1.1 Overview	1
1.2 History and Background	3
1.2.1 Recent Developments	3
1.3 The Present Study	6
2.0 THE DESIGN OF A PWE SYSTEM	13
2.1 Design Criteria	13
2.2 Gate Design	13
2.3 Gate Size	15
2.4 Hydraulic Efficiency of Gate and Chamber Configuration	15
2.5 Gate Drive and Gate Access	16
2.6 Multi Chamber Arrangements	17
2.7 Conclusions	18
2.7.1 The Horizontal-Axis Radial Gate	18
2.7.2 The Vertical-Axis Radial Gate	18
2.7.3 The Vertical-Axis Butterfly Gate	19
3.0 HYDRAULIC MODEL TESTS	28
3.1 Introduction	28
3.2 Preliminary Tests (Series 1)	28
3.3 Main Series of Tests	29
3.3.1 Test Series 2	29
3.3.2 Test Series 3	29
3.3.3 Details of Test Series 3	31
3.3.4 Flow Within the Chamber	34
3.3.5 Gate Tuning and Latching	34
3.3.6 Linked Chambers	35
3.3.7 Further Refinements	35
3.4 Non-Circular Chambers	35
3.5 Calibration Data	36
3.5.1 Discharge Estimates	36
3.5.2 Gate Velocity	38
3.5.3 Classification of Vortices	39
3.6 Introduction of the "Stepped Gate"	40

CONTENTS (continued)

	Page
4.0 MATHEMATICAL MODEL	61
4.1 Introduction	61
4.2 Initial Approach	61
4.2.1 The Open Chamber Model	61
4.2.2 Calibration of the Initial Model	62
4.3 Further Development	63
4.4 Model Flexibility	64
4.5 Governing Equations	65
4.5.1 Continuity	65
4.5.2 Flow Through an Upstream Gate	66
4.5.3 Flow Through the Downstream Gate	66
4.5.4 Flow of Water Within a Chamber	67
4.6 The Air Turbine	68
4.7 Thermodynamics of the Airflow	69
4.7.1 Convective Entropy Transfer	69
4.7.2 Entropy Transfer With Heat	69
4.8 The Calibration of PWETWO	70
4.9 The Computer Program	71
4.9.1 PWEONE and PWETWO	72
4.9.2 EDIT and TEDIT	72
4.9.3 GATE and TGATE	72
4.9.4 RKF2 and TRKF2	72
4.9.5 AIR and TAIR	72
4.9.6 WATER and TWATER	73
4.9.7 CHECK and TCHECK	73
4.9.8 GAMCAL and TGAMCAL	73
5.0 THE WELLS TURBINE	82
5.1 Introduction	82
5.2 The Scale Factor	82
5.3 The Design Pressure Differential	84
5.3.1 The Optimization of the Turbine Output Via the Design Pressure Differential	86
5.4 The Off-line Turbine Model	87
5.4.1 Generation of Force Coefficients	89
5.5 Summary	91

CONTENTS (continued)

	Page
6.0 PARAMETRIC TESTING	101
6.1 Introduction	101
6.2 Energy Test 1	101
6.2.1 Parameter Selection	101
6.2.2 System Configuration	103
6.2.3 Test Format	103
6.2.4 Test Series 1: Results and Discussion	104
6.3 Test Series 9-12	106
6.3.1 System Configuration	106
6.3.2 Parameter Selection	106
6.3.3 Results and Discussion	107
6.4 Final Developments	108
6.4.1 Introduction	108
6.4.2 Test Series 22	109
6.5 Primary Optimization for Costing and Economic Assessment	110
6.6 Twin Rectangular Chamber PWE With Horizontal-Axis Radial Gate	111
7.0 OUTLINE DESIGN AND COSTING	129
7.1 Initial Concepts	129
7.2 Position	129
7.3 The Structure	131
7.4 Steel Sheetpile Construction	132
7.4.1 Introduction	132
7.4.2 Design Considerations	133
7.4.3 Chamber Design	133
7.4.4 Ground Conditions	133
7.4.5 Sliding	134
7.4.6 Overturning	136
7.4.7 Interlock Tension	137
7.4.8 Side Walls	138
7.4.9 Intermediate Wall	140
7.4.10 Temporary Cofferdams	140
7.4.11 Turbine Frame	140
7.4.12 Gate Section	142
7.4.13 Wallings	142
7.4.14 Sluices	143
7.4.15 Rock Foundation	143
7.4.16 Summary	143

CONTENTS (continued)

	Page
Section 7 (continued)	
7.5 Construction Sequence for Sheetpiled Chambers	144
7.5.1 Introduction	144
7.5.2 Programme of Works	144
7.6 Precast Concrete Construction	145
7.7 In-Situ Concrete Construction	148
7.8 Steel Chamber Construction	147
7.9 Plastic and Glass-Reinforced Construction	148
7.10 Components Common to all Systems	148
7.10.1 Site Investigation	149
7.10.2 Bank Protection and Bed Preparation	149
7.10.3 Site Set-Up and Temporary Works	149
7.10.4 Additional Plant Costs	149
7.10.6 Trashrack	150
7.10.7 Turbine, Generator and Ducting	150
7.10.8 Grid Connection	150
7.10.9 Professional Fees, etc.	151
7.11 Alternative System Configuration	151
7.12 Summary of Costs	153
8.0 ECONOMIC ASSESSMENT	178
8.1 Introduction	178
8.2 Annual Charges	178
8.2.1 Downtime	178
8.2.2 Water Abstraction Charges	179
8.2.3 Local Authority Rating	180
8.3 Economic Assessment	182
8.3.1 Methodology	182
8.3.2 Case 1, Circular Chamber, Butterfly-Gated System	183
8.3.3 Case 2, Rectangular Chamber, Horizontal-Axis Radial Gated System	184
8.4 Sensitivity Analysis	185
8.5 Cost Projections	186
8.5.1 Introduction	186
8.5.2 Possible Scenarios	186
8.5.3 Summary of Scenarios One to Five	188

CONTENTS (continued)

	Page
9.0 SYSTEM OPTIMIZATION VIA GENETIC ALGORITHM	195
9.1 Introduction	195
9.1.1 ZHCG, PADIFD and ST	195
9.1.2 Chamber Shape	195
9.2 The Search Space	196
9.2.1 Parameter Combination	196
9.2.2 The Variation of Chamber Shape	197
9.2.3 Negotiating the Search Space	197
9.3 History and Background of the Genetic Algorithm	198
9.4 Overall Methodology	200
9.4.1 The Natural System	200
9.4.2 Artificial Systems	201
9.4.3 The Fitness Proportionate Reproduction Operator	202
9.4.4 The Crossover Operator	205
9.4.5 The Random Mutation Operator	208
9.4.6 Schemata	208
10.0 CONCLUSIONS	230
10.1 Introduction	230
10.2 Initial Concepts	230
10.3 The Mathematical Model and Parametric Testing	231
10.4 Outline Design and Costing	233
10.5 Economic Assessment	234
10.6 System Optimization	236
10.6.1 The Evolutionary Technique	236
10.6.2 The Application of the Technique	236
10.6.3 Further Work	237
10.7 Further development of the Pneumatic Water Engine	238
10.7.1 PWE or Conventional Water Turbine	238
10.7.2 The 1989 Electricity Act	240
10.7.3 The PWE in the Developing World	241
10.7.4 The Operation of the PWE in a Tidal Situation	241
REFERENCES	248

CONTENTS (continued)

		Page
APPENDICES		
I	Physical Model Results	A1.1
II	Notation	A2.1
III	Parametric Test Results	A3.1
IV	Costing Sheets and Final Bills of Quantities	A4.1
FIGURES		
Fig. No.		
1.1	Representation of a PWE Barrage	9
1.2	Typical Mode of Operation	10
1.3	Perspective View of STO	11
1.4	The AUR Water Engine	11
1.5	The Pneumatic Bag Device	12
2.1	Horizontal-Axis Radial Gate	20
2.2	Vertical-Axis Radial Gate	21
2.3	Twin Chamber PWE Incorporating a Butterfly Gate	22
2.4	Double Vertical-Axis Radial Gate, Twin Chamber	24
2.5	Vertical-Axis Radial Gate, Single Chamber	25
2.6	Barrage With Horizontal-Axis Radial Gates	26
2.7	Vertical-Axis Radial Gate - Continuous Alignment	27
3.1	Model No. 1: Symmetric Gate, 65° Arc	47
3.2	Model No. 1: Non-Symmetric Gate, 65° Arc	48
3.3	Model No. 3.3: Definition Drawing	49
3.4	General Arrangement: Aerofoll and Fins	50
3.5	Final Configuration for Models 3.1, 3.2 and 3.3	51
3.6	Adjustable Pivot Gates for 45° Model	52
3.7	Streamlines as Gate Commences to Open	53
3.8	Introduction of Conventional Fin	54
3.9	Introduction of T-Shaped Flange	55
3.10	Introduction of Shaped Downstream Edges	56
3.11	Model 3.4: Non-Circular Chambers	57
3.13	Surface Profile of Vortices	59
3.14	Stepped Gate Designs	60

CONTENTS (continued)

Page

FIGURES (continued)

4.1	PWEONE/AUR Rise Times (Slow Gate)	74
4.2	PWEONE/AUR Rise Times (Fast Gate)	75
4.3	PWEONE/AUR Fall Times	76
4.4	Basic Notation	77
4.5	Twin Chamber PWE - Thermodynamic Aspects	78
4.6	Flow Diagram for PWETWO	79-81
5.1	The Wells Turbine	93
5.2	Turbine Efficiency	94
5.3	Off-Design Ratio	95
5.4	Optimization of the Design Pressure	96
5.5	Ideallised Drag Data	97
5.6	Ideallised Lift Data	98
5.7	Power Outputs From CEGB Test, PWETWO and Turb4	99
5.8	Efficiency Curve Generated by Turb4	100
6.1	Diagrammatic Representation of Relationship Between Turbine Scale and Leakage Through the System	112
6.2	Energy Tests S1.0 - S1.7, Variable Gate	113
6.3	Power Output and Efficiencies	114
6.4	Power Output and Cycle Time	115
6.5	Energy Test S1.4, ST = 2.5	116
6.6	Energy Test T1.4, ST = 1.5	117
6.7	Energy Tests T1.0-T1.7, Varying Gate Triggers	118
6.8	Series 10, Variable Gu	119
6.9	Series 11, Variable Gate Height	120
6.10	Series 12, Variable Gate Times	121
6.11	Efficiencies, Power Output and Cycle Times - Twin Chamber System	122
6.12	Series 22, Average Power Output and Efficiency	123
6.13	Series 22, Air Temperature and Net Heat Loss	124
6.14	Series 22, Instantaneous Power and Cycle Time	125
6.15	Series 23, Variable Gate Height	126
6.16	Series 24, Variable Gu	127
6.17	Series 26, Variable Gate Speed	128

CONTENTS (continued)

	Page
FIGURES (continued)	
7.1	Bankside PWE 156
7.2	Barrage With Bank Support 157
7.3	Free Standing PWE Barrage 158
7.4	Sheetpiled System 158
7.5	Sliding Forces 159
7.6	Overturning Forces 159
7.7	Worst Case - Interlock Tension 159
7.8	Active and Passive Pressures, Side Walls 159
7.9	General Layout of all Systems 160
7.10	Bank Protection 160
7.11	Gate Cover Detail 161
7.12	Gate Cover Detail (Section on B-B) 162
7.13	Gate Cover Detail (Section on A-A) 162
7.14	Temporary Cofferdams 163
7.15	Turbine Support Frame 164
7.16	Types of Sluice Gate 164
7.17	Structure Acting as Cofferdam 165
7.18	Precast Concrete System 166
7.19	Detail of Side Wall and Chamber Interface 166
7.20	In-Situ Concrete System (Cofferdam) 167
7.21	In-Situ Concrete System (Open Water) 167
7.22	Suggested Layout of Portadam 168
7.22	(continued) Cross Section of Portadam 169
7.23	Suggested Method of Grout Leak Protection 170
7.24	In-Situ Concrete Gate Cover 171
7.25	In-Situ Concrete Gate Cover (Section on A-A) 171
7.26	Possible Gate Design 172
7.27	Possible Trashrack Design 173
7.28	Alternative System Configuration 174
7.29	Suggested Gate Details 177
8.1	Unit Cost / Capital Cost 190
8.2	Variable Downtime 190
8.3	Variable Energy Value 191
8.4	Variable Capital Cost 191
8.5	Variable Maintenance Costs 192
8.6	Cost Projections 193

CONTENTS (continued)

	Page
FIGURES (continued)	
8.7	Cost Projections 194
9.1	The Articulated Plate 218
9.2	Flow Diagram for PWEVO 219
9.3	Mean Average Power Output 220
9.4	Standard Deviation 221
9.5.1	Generation 1 222
9.5.2	Generation 5 223
9.5.3	Generation 10 224
9.5.4	Generation 20 225
9.5.5	Generation 50 226
9.5.6	Generation 110 227
9.6	Idealized Air Space 228
9.7	Pressure Differentials 229
10.1	Chamber Shape 246
10.2	Shallow Water, Offshore Energy Barrage 247
PHOTOGRAPHIC PLATES	
1	Initial Truncated Model 42
2	Initial Model Under Test 43
3	Model 3.2 44
4	Model 3.2 Under Test 45
5	Non-circular Chambers 46

1.0 : INTRODUCTION

1.1 Overview

The construction of hydro-electric installations utilizing various types of conventional water turbine has become standard civil engineering practice using proven technology. Cost effective energy production has been possible at high and medium head sites for many years and steady improvements in both hydraulic design and turbine efficiency have enabled the head required to be progressively reduced. This, coupled with a greater demand for energy and a shortage of undeveloped high and medium head sites has directed attention towards the potential of low-head hydropower. One result is the development of chains of relatively low-head installations along such rivers as the Danube. Another is the development of tidal projects such as La Rance, Brittany (240 MW); Annapolis Royal, the Bay of Fundy, Canada (17.8 MW); and the ongoing interest in both the Severn and Mersey Barrages (7200 MW and 620 MW respectively).

Conventional turbines, however, still prove non-economic when considering differential heads in the two to three metre range. This is largely due to the high capital costs both of the large diameter turbines required to capture a significant amount of energy at a low head and of the extensive civil works necessary to house the turbines in a hydraulically efficient manner. Another factor is the slow speed/high torque characteristics of a low-head turbine and the related high bearing and maintenance costs.

The concept of the Pneumatic Water Engine (PWE) involves the replacement of the large, slow moving, water powered turbine with a high speed, small diameter, self-rectifying air turbine. This would be housed in a structure which would convert the water power of the differential head into air power. In its simplest form, the PWE achieves this in the manner shown in Figs. 1.1 and 1.2. The turbine is situated within an opening in the roof of a chamber which is, itself, an integral part of a river barrage across which the differential head is generated. Upstream and downstream gates alternately open and close creating an oscillating water column within the chamber which drives air to and from atmosphere through the self-rectifying turbine (Fig.1.2). Thus, the high cost of the large, water turbine is avoided and replaced by the much lower cost of the high speed air turbine. The air turbine has the added advantage of being sited above water level in an accessible position offering easy maintenance and replacement when necessary.

Systems such as the PWE, if proven to be economically viable, could realize the energy potential of a vast number of sites worldwide where head differentials of between one and six metres can be generated. Most of the world's assumed tidal power potential of 8,800,000 GWh/a falls within this category¹; indeed, within the

United Kingdom forty-nine attractive tidal sites of this type have been identified in Scotland² alone with a total potential of over 142 GWh/a. Turning to run-of-the-river situations, a survey of the Severn/Trent catchment areas recently completed for the Department of Energy³ has identified 71 sites with head differentials of between 1.5 m and 6.0 m and water power potentials of 100 kW or greater. This survey was restricted to sites where existing civil works such as sluices, weirs, and watermills might be adapted to accommodate a suitable low-head hydro system. These sites alone showed a potential of 155 GWh/a and an estimate of the total low-head energy potential of England extrapolated from the results of this survey lies in the range of 700 GWh/a to 1200 GWh/a.

Further investigation of the Severn/Trent study indicates that the area's potential is reduced to 132 GWh/a when only those sites with an available head of 3 m or less are considered. This suggests that the potential for ultra low-head run-of-the-river schemes in England is some 600 to 1000 GWh/a. A more recent study⁴ has investigated the economic aspects of ultra low-head potential in the UK as a whole. This study considers the use of commercially available conventional turbines at heads in the 2-3 m range producing electricity at 2.7p/kWh and providing an internal rate of return of 10% on the capital invested. An overall economic potential of less than 20 GWh/a was estimated. This illustrates the need for the development of hydropower devices that can be fabricated and installed at a lower cost than conventional turbine sets. In this manner a greater percentage of the technical potential of reference 3 can be exploited in a commercially attractive manner.

The economic viability of any small scale hydroelectric system, irrespective of available head, depends in the main upon two factors: the current cost of fossil fuels and the location of the system in relation to the consumer. Where electricity is readily available from an existing grid system then the economics of any alternative supply must compete with that of the existing supply. As the bulk of this supply will generally be provided by oil and coal fired power stations then the governing factors will be the cost of these fuels and the possible return on the initial capital investment. However, when dealing with an isolated community where either no national supply exists or connection to an existing grid system is either physically impossible or prohibitively expensive then competition in the main will be restricted to electricity supplied by diesel generator. Again, the actual cost of the fuel plays a part but in addition the availability of that fuel and the cost of transportation must be taken into account. Maintenance of the generating sets is also important and in some situations, particularly in the developing world, both the availability and cost of spare parts together with poor local knowledge of generator maintenance can lead to regular failure of the system. This can result in a large percentage of the generating sets standing idle. In such situations the

economic viability and practicality of an easily maintained Pneumatic Water Engine may prove to be attractive. Furthermore low-head hydro installations are generally located in lowland areas. This is where communities tend to be located often in close proximity to a river, estuary or irrigation scheme with the necessary potential to drive a PWE which could supply useful quantities of electricity.

The object of the present study, is to investigate the performance and economics of the P.W.E. and to finally ascertain the probable cost per kilowatt-hour of the power generated. This cost can then be compared to present day C.E.G.B. prices to ascertain its economic viability within the United Kingdom. Some estimate can then be made of the system's usefulness in the more remote areas of the British Isles such as small island communities. The design and construction of the system is kept as simple as possible both to minimise costs and to present few, if any, maintenance or construction problems in a third world situation.

1.2 History and Background

The earliest records of the extraction of water power date back to approximately 85 B.C. when very simple vertical axis waterwheels began to appear in parts of Greece⁵. The first large horizontal-axis machines were in use by the time of Christ although it was several centuries before this more efficient design became widely used and it was not until the end of the tenth century that they became established in Britain. From this point on the waterwheel continued to develop steadily throughout the British Isles and by the middle of the sixteenth century they were assisting in both the mining and fabrication of metals, in the making of paper and in fulling and tanning processes as well as in the production of flour.

It was due to the contributions of such engineers as Smeaton, Poncelet, Fairburn and Brunel that the waterwheel reached the peak of its efficiency in the mid-nineteenth century. However, by this time progress was being made in the development of the water turbine and it is the continued development of this technology that has resulted in the vast hydro-electric schemes of the present day.

1.2.1 Recent Developments

The waterwheel, in its many forms, can be considered to be the the first machine capable of extracting energy from low-head situations. However, due to its slow speed and low efficiency, it is not suited to economic production of electrical power. With the increased interest in low-head, hydro-electric generation in recent years, a variety of machines varying from refinements of the water turbine to new, novel systems have been developed.

Two conventional water turbines currently considered suitable for differential heads as low as three metres are the Straflo rim-generator turbine and the

Ossberger Crossflow turbine. In the Straflo turbine the rim around the turbine runner blades forms the generator rotor and carries the poles. The most significant advantages of this arrangement when compared to the more conventional bulb turbine are that its natural inertia is up to four times that of a bulb turbine of similar diameter and the removal of the bulb leads to arrangements of the water passage that are very much shorter and cheaper to construct⁶.

The Straflo turbine has been considered suitable for the proposed Mersey Barrage but is not the 'lead' machine for the Severn Barrage as concern has been expressed over the efficiency of the rim seals of a set with the necessary runner diameter of 7.5 m. However, a 7.5 m diameter Straflo turbine was installed in the Annapolis tidal power plant constructed in the Bay of Fundy, Nova Scotia and commissioned in August 1984⁷. This turbine has a rated operating head of 5.5 m at which it produces an output of 17.8 MW.

The Annapolis installation represents a pilot scheme for the possible future construction of a series of much larger tidal power plants. Its performance has been constantly monitored and a major inspection carried out in June, 1985 showed that the hydrostatic seals were in good condition and that there was no sign of corrosion or cavitation damage on the blades. Continued monitoring of this system could technically prove the reliability of this machine and ensure its inclusion in further low-head situations. However, it would appear that the Straflo is more suited to situations with a substantial flow rate and tidal situations in particular.

The Ossberger Crossflow turbine⁸ is a radial impulse turbine with partial admission. Its suitability to small-scale hydropower installations stems from the inclusion of two guide vanes which divide the stream of water at the inlet and direct it in such a manner that it smoothly enters the rotor. These two guide vanes can handle any flowrate in a range from 1/6 of the proposed full flow to the actual full flow with optimum efficiency. The guide vanes can be adjusted either manually or automatically to suit the prevailing flow conditions. Crossflow turbines are therefore, especially suitable for the efficient utilization of water flowrates subject to wide fluctuations; a situation most likely to be found at a low-head site with no upstream storage. Their mean overall efficiency under low-load conditions is guaranteed to be 80% and problems of cavitation are claimed to be overcome by various inherent design features irrespective of the working head. The economics of a system incorporating an Ossberger turbine operating under heads of around 3 metres, although competitive when compared to other conventional turbines, still cannot compete with the prices of electricity supplied by the CEGB.

The non-conventional systems include such devices as the Salford Transverse Oscillator (STO)² designed and developed by E.M. Wilson and G.N. Bullock at

Salford University (see Fig. 1.3). The device can operate under heads of between 0.5 and 3.0 m and laboratory testing of this device has shown that up to 45% of available water power can be extracted from the flow. The projected cost of electricity produced from a prototype has been estimated to be in the region of 7.5p/kWh falling to 4.7p/kWh with optimization of the system. However, a prototype has not yet been constructed.

The STO was developed in the early eighties at which time another device was being developed at Salford University namely the AUR water engine invented by Allister Ure Reid². This device is directly related to the Pneumatic Water Engine in that it incorporates an oscillating water column within an enclosed chamber although in this case power take-off is achieved via a float driven by the water column (Fig 1.4). A prototype has been constructed on a site in Sussex, England by AUR Hydropower Ltd. but no performance data concerning this prototype is available for publication.

In June 1982, Professor A.M. Gorlov of Boston University presented a paper at a conference entitled 'New Approaches to Tidal Power'⁹ held at the Bedford Institute of Oceanography, Dartmouth, Nova Scotia. This described a tidal power system incorporating oscillating water columns to drive air to and from atmosphere through an air turbine. A series of valves ensures that the flow passes through the turbine in one direction only. Rough cost estimates of the construction of such a tidal power system were in the region of 1530 \$/kW rated output at 1982 prices.

The oscillating water column (OWC) concept of both the AUR water engine and Gorlov's system is not new; the wave activated whistle buoy has used this concept for nearly a century and in the 1960's Commander Masuda¹⁰ used this principle to drive an air turbine which produced sufficient power to light a navigation buoy. Wave powered buoys have subsequently been used throughout the world. The use of rectifying valves to ensure unidirectional flow through a conventional air turbine was also included in the design of the Vickers Attenuator¹¹ and the National Engineering Laboratory's O.W.C. device¹², two proposed large scale, wave powered machines of the late seventies.

The introduction of the Wells' self rectifying turbine developed in the mid-seventies by Professor Wells of Belfast University¹³ means that pneumatic energy devices including those incorporating an oscillating water column can dispense with the complicated valve system formerly required for air flow rectification. This has prompted a number of new developments. Within the wave power field these range in size from the Whale wave activated buoy developed by Munster Simms Engineering (in conjunction with Queen's University, Belfast¹⁴) to the Kvaerner Brugs, 500 kW, wave actuated, oscillating water column device formerly situated at Toftestallen on the west coast of Norway¹⁵. Both these devices are now

commercial propositions. Another currently significant pneumatic wave power device is the circular Sea Clam¹⁶, a device developed by the Energy Systems Group of Coventry. The system consists of a series of air bags supported on a circular frame. The displacement of air to and from these bags drives a number of Wells turbines. The projected cost estimates for this device are in the region of 3.62p/kWh at 1986 prices. A shore based wave power machine incorporating an OWC has been developed by the Wave Energy Group of Belfast University. A prototype is currently under construction on the Scottish island of Islay¹⁵. Power take-off will be achieved via a 180 kW bi-plane Wells Turbine and it is estimated that 1 MW stations based on this scheme might achieve generating costs of 3-4.5p/kWh.

The development of pneumatic run-of-the-river and tidal schemes has also progressed since the introduction of the Wells Turbine. The Energy Systems Group of Coventry Polytechnic^{17,3} have developed a novel, two bag, water to air converter which consists of a flexible membrane with a dividing septum as shown in Fig. 1.5. Slugs of water entering the duct alternatively inflate and deflate the bags creating an oscillating air flow across the turbine as shown in the diagram. A demonstration system has been constructed at a former watermill site on the River Derwent in Derbyshire. This operates under a head of 2.8 metres and utilizes a 150 kW Wells Turbine with a diameter of one metre. The same organization has also been involved in the development and testing¹⁸ of a pneumatic box system very similar in design and operation to the Pneumatic Water Engine. Economic assessments of this device show a capital cost per installed kilowatt of between £800 (at 175 kW output) and £1800 (at 15 kW output) and a projected cost per kWh based on parametric model studies of between 1.75 and 1.85p.

Research into pneumatic run-of-the-river and tidal systems is also in progress at Queens University, Belfast and a prototype, pneumatic box system has been constructed at Benburb in Northern Ireland.

The oscillating water column concept and the resulting water to air power conversion has therefore been established for a number of years especially within the wavepower field. However, run-of-the-river devices are very much in their infancy and a considerable amount of research is still necessary before either their performance or economics can be determined. Problems associated with the hydraulic design and eventual construction of a PWE also remain to be solved.

1.3 **The Present Study**

Much of the work reported in this Thesis was carried out as part of an investigation into the performance and economics of a run-of-the-river PWE funded by The Energy Technology Support Unit (ETSU) of the Department of Energy. The

objectives of the study and the general progression of the research programme were broadly as follows:

- i) To develop a mathematical model to simulate the performance of various PWE designs.**
- ii) To investigate the concept of a PWE and establish relevant design criteria.**
- iii) To calibrate the mathematical model using both existing data and data obtained by means of small-scale hydraulic model tests. It was also planned to use the latter to indicate the suitability of any selected gate design.**
- iv) To predict attainable power output, system operational dynamics and control requirements by means of parametric studies using the mathematical model.**
- v) To produce outline designs of the system upon which reliable cost estimates could be based.**
- vi) To provide an economic analysis of the PWE based on the results of the Parametric Studies and the costing exercises.**

The above research has been carried out under the direction of and in collaboration with Dr. G. N. Bullock, Reader in Civil Engineering whose previous experience within the field of low-head hydropower includes the co-invention of the Salford Transverse Oscillator and the management of the research and development of the AUR Water Engine.

This Thesis follows the programme outlined above. At the time that the author joined the project (May '86) the basic form of the mathematical model had already been established by Dr. Bullock and its development was well under way. The author's initial involvement lay in the establishment of an acceptable design criteria and in the study of possible gate arrangements. This led to the design and implementation of the small-scale hydraulic model study and the subsequent development of the flow-actuated gates discussed in Chapter 3. A greater involvement in the mathematical modelling followed especially with regard to the simulation of the Wells Turbine and the modelling of the compressible airflow. The author was entirely responsible for the development of the off-line turbine models described in Chapter 5 and for the outline design, costing and economic analysis of the system. The latter utilized the results of a series of parametric tests.

The research described in the penultimate chapter of the thesis which concerns the evolutionary design and optimization of particular elements of the PWE system, was not funded by ETSU. It was funded by Polytechnic South West and undertaken independently by the author.

The Thesis concentrates upon those aspects of the research programme for which the author was largely responsible. An overview of the elements to which he made a lesser contribution, for example the thermodynamic modelling, are included to ensure continuity and facilitate a more complete understanding of the research process. A comprehensive presentation of the work not fully covered in the Thesis can be found in the relevant ETSU reports referred to in the text.

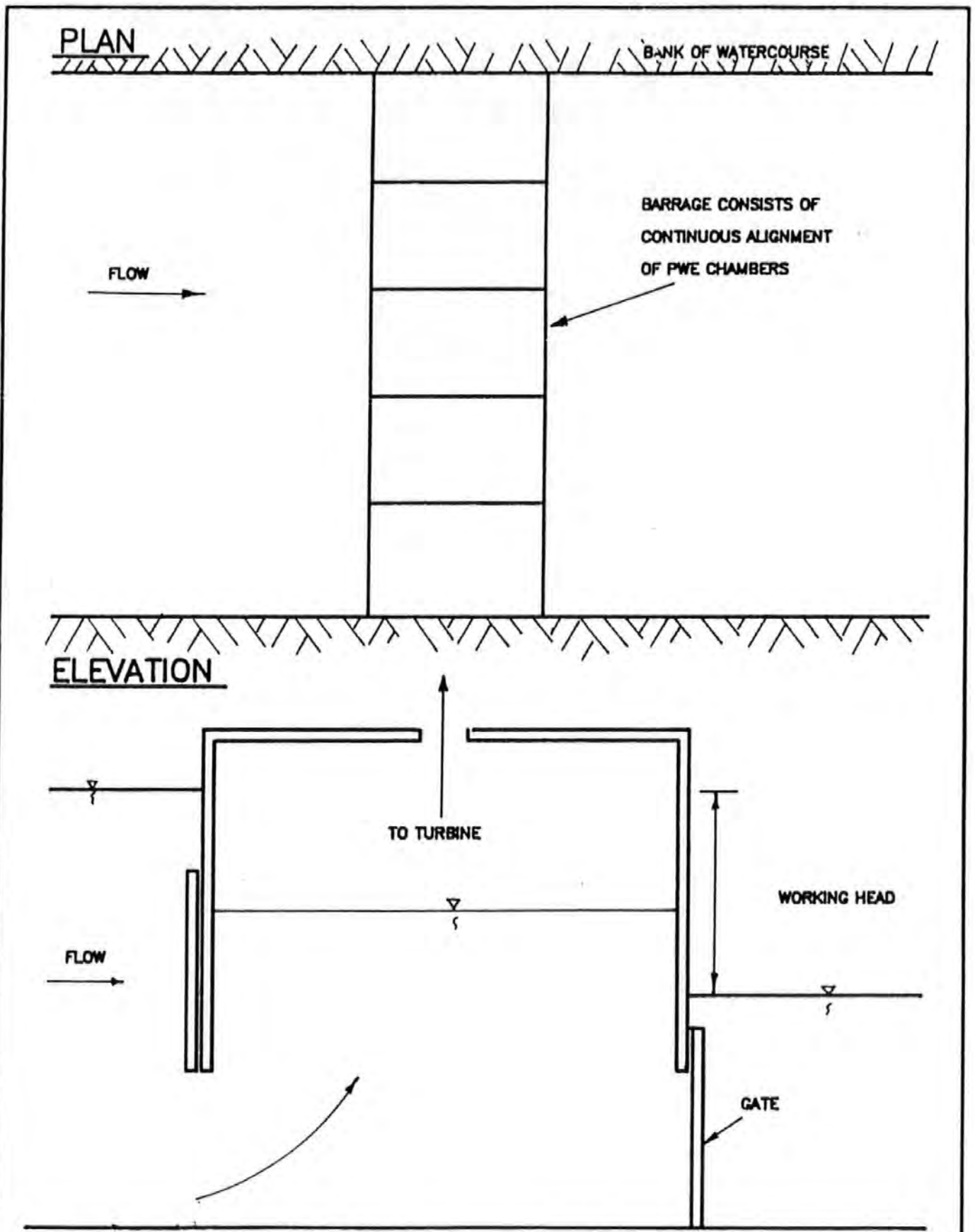
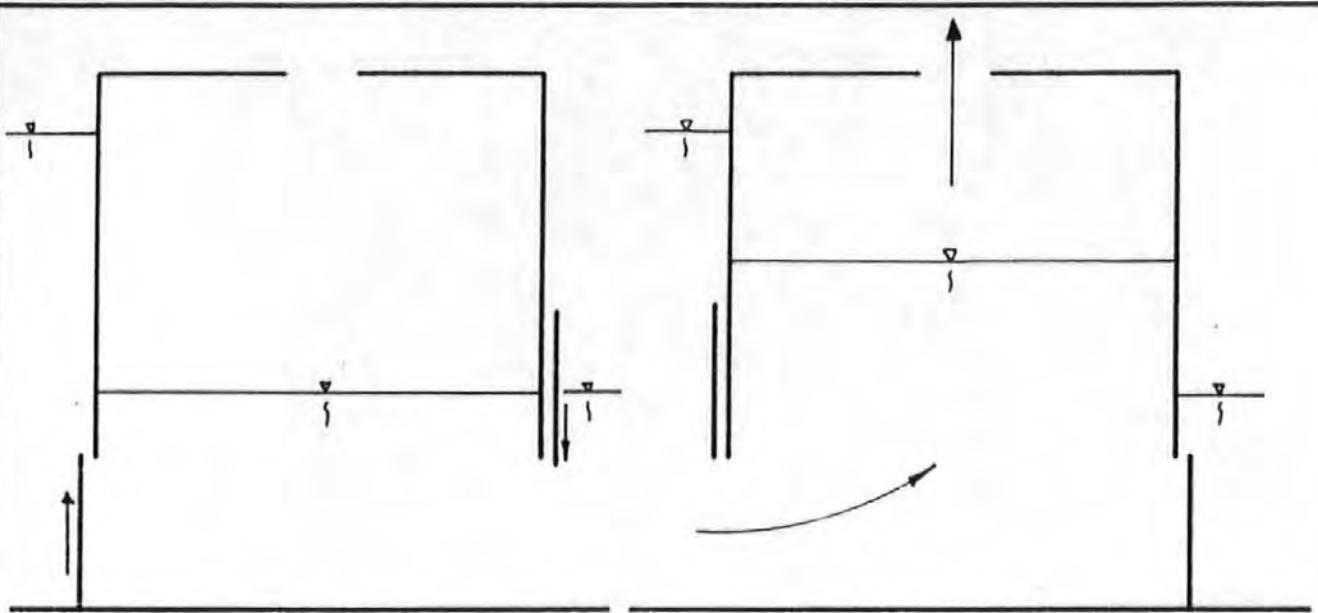
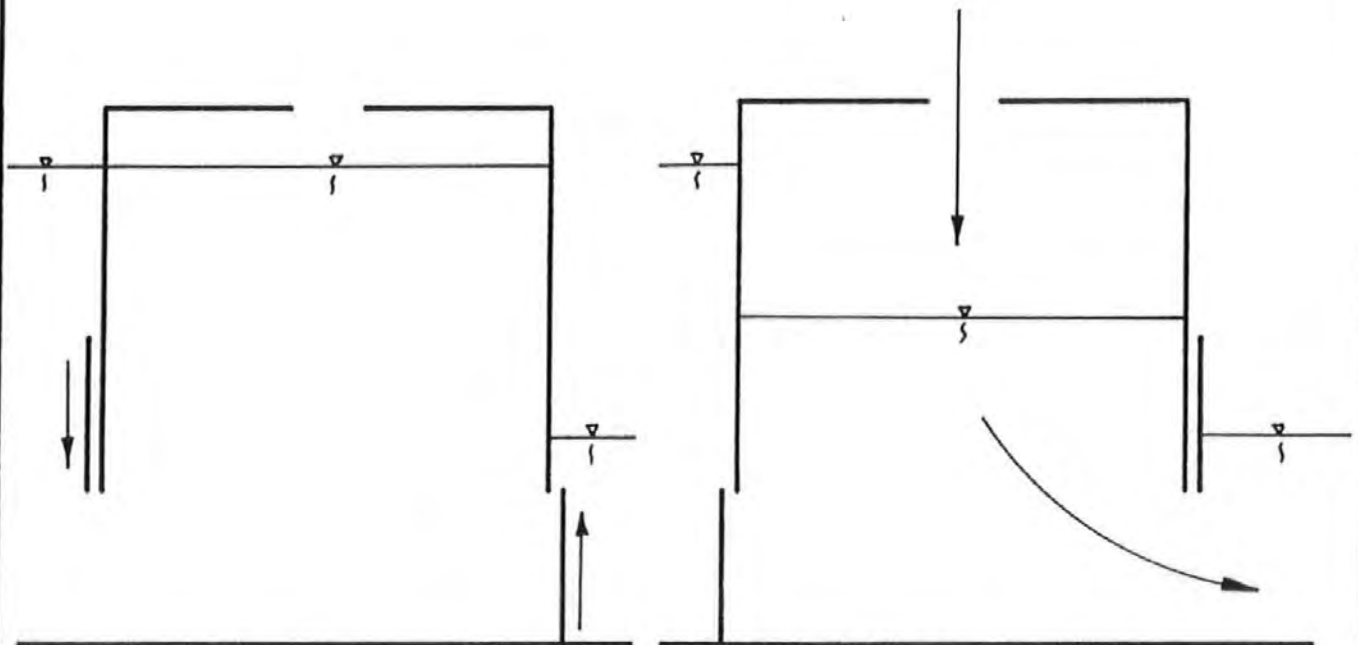


FIG. 1.1: REPRESENTATION OF A PWE BARRAGE



a) Close downstream gate and open upstream gate.

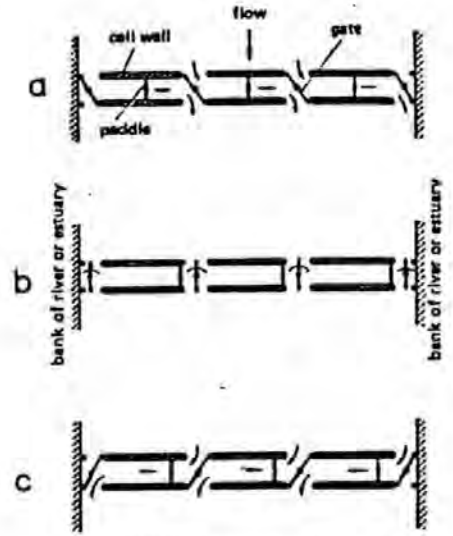
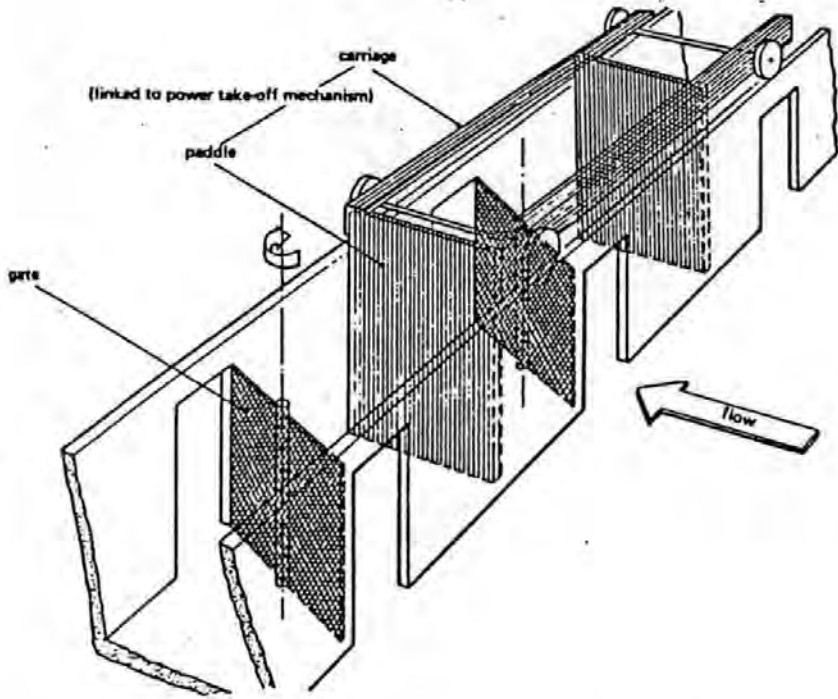
b) Air forced out of chamber through turbine.



c) Close upstream gate and open downstream gate.

d) Air drawn into chamber through turbine.

FIG. 1.2: TYPICAL MODE OF OPERATION.



DIAGRAMATIC REPRESENTATION:

- a) Flow forces paddles to the right.
- b) Paddles are at end of stroke and gates are changing position.
- c) Flow forces paddles to the left.

FIG. 1.3: PERSPECTIVE VIEW OF STO

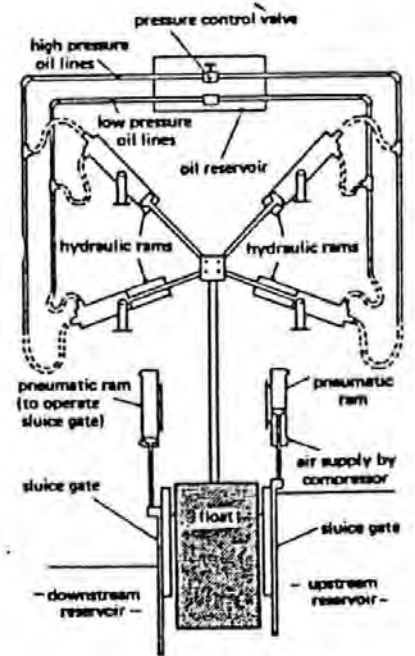
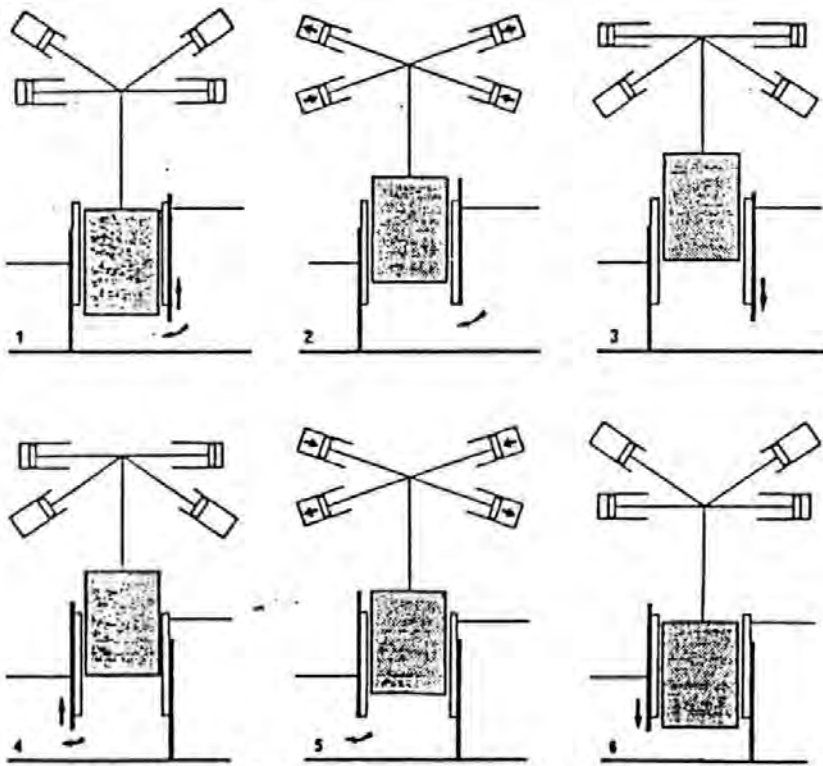


FIG. 1.4: THE AUR WATER ENGINE. — SEQUENCE OF OPERATION:

- 1) Float at bottom of stroke, upstream gate opening.
- 2) Float is halfway up and hydraulic rams are charged.
- 3) Float at top of stroke, upstream gate closing.
- 4) Float still at top of stroke, downstream gate closing.
- 5) Float halfway down.
- 6) Float at bottom of stroke, downstream gate closing.

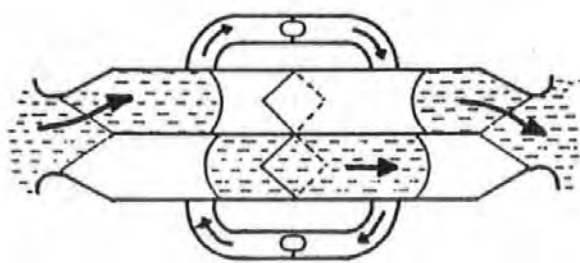
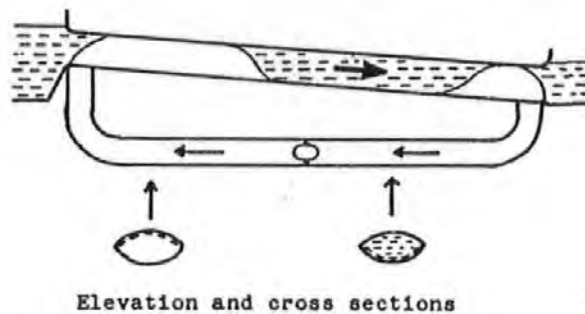
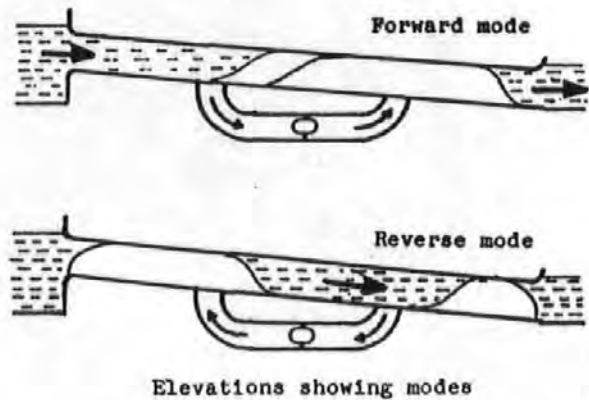
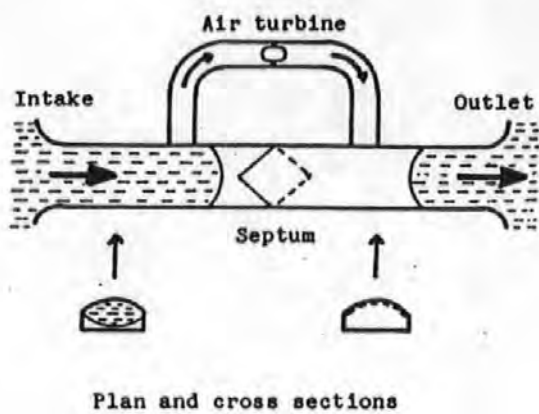


Figure 5. Twin duct arrangement

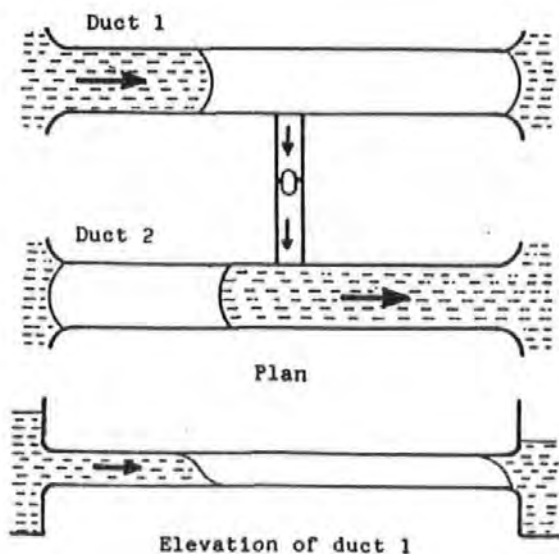


FIG 1.5: THE PNEUMATIC BAG DEVICE
(ENERGY SYSTEMS GROUP, COVENTRY POLYTECHNIC)

2.0 : THE DESIGN OF A PWE SYSTEM

2.1 Design Criteria

The configuration of the Pneumatic Water Engine in its simplest form has been described in Section 1.1. In practice this simple configuration is far from ideal. Any development of a PWE will depend solely upon the economic viability of the net energy produced and every effort must be made to ensure that the necessary, overall efficiency can be achieved whilst minimising construction, material and maintenance costs. The hydraulic efficiency of each of the simple sluice gates shown in Fig. 2.1 will be significantly reduced due to flow contraction and expansion. Friction between the gates and their supports would be greatly increased by the pressure generated from the head differentials ensuring that much energy would be required for successful gate operation. Factors such as these led to the formulation of the following basic design criteria:

- a) **Good Hydrodynamic and Aerodynamic Efficiency.**
- b) **Good Reliability;** ie a minimum of moving parts and a gate motion that is not prone to jamming by either silt or debris.
- c) **A Low Energy Gate System;** ie large hydrodynamic forces must not oppose the gate action; friction and inertia forces should be minimised.
- d) **Strength and Stability;** ie the structure must be able to resist sliding and overturning forces and seepage problems caused by the differential heads.
- e) **Low Construction Cost;** ie wherever possible continuous construction techniques based on proven civil engineering methods and 'off-the-shelf' components should be used.
- f) **Low Maintenance Cost;** ie easy access to gate, gate mechanism, turbine and generator.

2.2 Gate Design

Careful design of the gate system is an essential aspect of the overall design of the PWE. It is quite possible that the gate mechanism will absorb a significant proportion of the energy extracted. Steps must be taken to ensure that this plus the cost of the necessary control system for the gate do not render the energy output of the PWE uneconomic.

Many gate and chamber configurations have been considered. However only the following gate systems were thought to possess the required potential after taking account of the established criteria:

- 1) **Horizontal-axis radial gate** (Fig. 2.1).
- 2) **Vertical-axis radial gate** (Fig. 2.2).
- 3) **Vertical-axis butterfly gate** (Fig. 2.3).

Both radial and butterfly gates are traditional, well-proven designs. The circular arc of the radial gate ensures that the resultant hydrodynamic forces are transmitted directly to bearings at the gate axis thereby avoiding the large friction forces that are inherent in the sluice-type gate design. The lack of water resistance presented to the gate face as it moves within its own plane is an added advantage not shared by the butterfly gate. The butterfly gate moves in a direction normal to its face thereby presenting the possibility that its action could be opposed by large hydrodynamic forces. The overall dimensions of a butterfly gate could well be limited by the effect of these forces and by the added risk of damage due to shock loading.

The horizontal-axis radial gate would only be suitable for controlling the flow to and from a single chamber and could be so configured as to allow the closing gate to provide a significant percentage of the energy required by the opening gate as shown in Fig. 2.1. The vertical-axis radial gate could perform either a single or dual function, ie. two such gates could switch the flow between two chambers within a barrage configuration (see Fig. 2.4) or a single gate could service a single bankside chamber as shown in Fig. 2.5. The vertical-axis butterfly gate is primarily suited to twin circular chamber configurations as indicated in Fig. 2.3. The butterfly gate alternately directs flow into one of the two circular chambers whilst allowing the other chamber to discharge. It has the advantage over the other gate designs of providing a chamber/gate^{nb} ratio of 2:1 with the associated cost savings in fabrication, construction and subsequent maintenance.

An advantage inherent in all three gate systems is that there exists no point in their respective motions where two edges are required to pass one another, ie. all gate configurations involving a guillotine action have been avoided. In this way the possibility of serious damage when debris becomes trapped between the gate edges and the chamber walls is substantially reduced. In addition as the gate moves away from the chamber wall to complete its open/close cycle the debris would be released. This implies that the gate has a reasonable capacity for self-recovery after jamming. A simple trash screen would be necessary to further reduce the risk or at least the frequency of such incidents. However, the screen

nb A chamber/gate ratio of 2:1 indicates that one gate is required for the successful operation of two chambers.

must be of a sufficiently large gauge that significant hydraulic losses are not incurred across it. It is essential therefore that any chosen gate design must be capable of handling debris of a size likely to pass through such a trash screen.

2.3 Gate Size

The advantages and disadvantages of increasing gate size relative to chamber size are:

Advantages :

Increased volumetric flow rates both when filling and emptying the chamber.

Less time required to complete each fill and empty cycle once the gates are in the appropriate fully open and fully closed positions.

Larger differential air pressures can be established across the turbine.

Increased gross power can be harnessed.

Disadvantages :

Larger and heavier gates.

A fairly general increase in the magnitude of forces both upon the gate and within the structure as a whole.

More power required to move the gates, particularly if the potential advantages of a reduced cycle time are not to be lost due to a slower gate motion.

A more turbulent water flow leading to an increased risk of water striking the roof of the chamber or reaching the turbo-generator.

Increased costs.

The work described in Chapter 6.0 indicates that cycle times of nine to ten seconds are required to achieve maximum power output. A ten second cycle time would result in the gate components performing a reciprocating motion (in possibly silt laden water) 3,155,760 times per annum. The importance of ease of access to both the gate components (especially in the case of bearings and seals) and the operating mechanism becomes self-evident under these conditions.

2.4 Hydraulic Efficiency of Gate and Chamber Configuration

In order to capture a significant amount of energy from a low head flow it is essential that energy losses within the system are minimized. This implies that the

hydraulic efficiency of each chamber entrance and exit should be maximised to whatever extent that the situation and cost constraints allow.

It is envisaged that overall energy losses in the case of the Horizontal-axis Radial gate will be similar to those of a plane vertical sluice gate. The momentum of the flow into the chamber however will cause the water within the chamber to climb up the downstream wall. This surging within the chamber could result in an unacceptable loss of energy.

In the case of the Vertical-axis Radial gate, the gate system can be aligned with the chamber or chambers so as to achieve a reasonable inlet and outlet flow pattern thereby ensuring a correspondingly good hydraulic efficiency. For example, in the case of the single circular chamber of Fig. 2.5, it is envisaged that the flow into the chamber will form a vortex which will continue to rotate as the gate changes position and the chamber empties. Thus, to some extent, the flow will wind itself into the chamber and, with no change in direction of rotation, wind itself out again with little loss in momentum. A similar type of flow is likely to occur with the arrangement illustrated in Fig. 2.4 with the additional advantage that the gate system is arranged to take full advantage of the entry and exit configurations formed both by the curved faces of the radial gates and the curvature of the chambers' external walls. The hydraulic efficiency of these two systems is likely to be significantly better than that of systems incorporating a Horizontal-axis Radial gate.

Much the same principles of optimal flow patterns apply to the butterfly-gated configuration of Fig. 2.3. If the plane of the butterfly gate is approximately tangential to the walls of the two chambers when it is closed then a further improvement in the flow patterns can be achieved.

A further advantage of the arrangement shown in Fig. 2.3 is that the gate can be placed midway between closed positions to form a simple sluicing facility. This will enable the flow to pass straight through the system in times of flood or during maintenance periods which require a lowering of the upstream water level.

2.5 Gate Drive and Gate Access

A system of pneumatic or hydraulic rams pressurized by a suitable compressor would provide a comparatively low-maintenance gate drive mechanism with a minimum of moving parts. The pneumatic system would probably be the best choice due to its non-polluting characteristics and comparative cheapness. It is essential that a minimum of the power harnessed by the turbine is required by the compressor for successful gate operation. Hence the necessity for the development of a suitable low-inertia gate system.

It is apparent from the reciprocal motion calculation of Section 2.3 that another major factor in the selection of a suitable gate/chamber combination will be the ease with which the various gate components can be maintained or renewed.

Dewatering the gate area by placing stoplogs in appropriate positions and subsequent pumping, should present few problems with the majority of configurations so far considered. Suitable positions for stoplogs are indicated by points A and B in Fig. 2.4. The same positions would be appropriate for the butterfly-gated system. Ease of access however varies greatly depending upon whether the gate system is exterior to the chambers or actually housed within them.

In the case of those configurations incorporating a Horizontal-axis Radial gate, access for maintenance or renewal of minor parts such as bearings could be gained via a suitably sized hatch in the chamber roof. However, replacement of major components would invariably involve the removal of the turbine, ducting and a major part of the chamber roof. By comparison, in the case of those twin-chamber systems incorporating a Vertical-axis Radial gate or a Butterfly gate, the removal of all or part of the gate cover would be sufficient both for general maintenance and major renewal.

2.6 Multi-chamber Arrangements

The barrage alignment of Fig. 2.6 suggests the possibility of significant savings in both construction time and materials by use of common chamber walls plus a method of continuous construction suited to a multi-module arrangement.

Unfortunately, it would initially seem that the most suitable gate arrangement for such an alignment would be the Horizontal-axis Radial gate with its 1:1 chamber/gate ratio, comparatively low hydraulic efficiency and aforementioned maintenance problems. In a barrage situation these maintenance problems could be eased by the installation of an overhead crane running the entire length of the structure. A standardized maintenance procedure involving the temporary decommissioning of successive pairs of chambers could then be introduced. A similar procedure could be adopted for any barrage irrespective of gate type.

Fig. 2.2 shows the Vertical-axis Radial gate incorporated in a barrage which still retains some common chamber walls whilst allowing the gates to be exterior to the chambers themselves. Taking this one step further, the arrangement of Fig. 2.7 retains the common chamber walls to the same extent as that shown in Fig. 2.6. The Vertical-axis Radial gates in this case however still remain exterior to the chambers.

It would seem that twin circular chambers with a common butterfly gate can be included within a barrage only with the loss of the common chamber walls.

2.7 Conclusions

The interdependent nature of the relationship between the gate system, the shape of the chambers and the configuration of the barrage has been discussed in the preceding sections. Supplementary detail, if required, can be found in the final report prepared for the Energy Technology Support Unit¹⁹.

In order to concentrate research in the most promising areas, each of the above configurations was considered in the light of the design criteria listed in Section 2.1. The conclusions were as follows:

2.7.1 The Horizontal-axis Radial Gate

The Horizontal-axis Radial gate is suited primarily to the square or rectangular configurations of Figs. 2.1 and 2.6. The main advantages of this design are:

- 1) The radial gate is a well-proven design with wide ranging application.
- 2) Potential for large gate openings and hence increased energy production.
- 3) Ease of construction due to simple chamber shape and common walls.

However, restricted access to the gates will tend to increase maintenance costs. These costs, plus those linked to the procurement, installation and use of a gate drive system, will affect the financial gains associated with the above advantages. Furthermore an increase in gate size will only add to the problem of this gate's inherent high inertia. The 1:1 chamber : gate ratio must also be taken into consideration.

It would seem that savings or gains in one direction will invariably result in losses in another. Consequently it is highly questionable whether this gate system and the associated chamber configuration has any overall financial advantage over the alternatives.

2.7.2 The Vertical-axis Radial Gate

When used as shown in Fig. 2.4, it would seem possible to achieve a higher hydraulic efficiency with this gate than with the last. This potential is further enhanced by the gate's ability to open and close without any change in its elevation. The relatively low inertia of this gate system could result in faster operation and a low energy requirement.

The smaller gate openings of this system must be taken into account as must the 1:1 chamber : gate ratio. However the barrage configuration of Fig. 2.7 is considered to represent an improvement over those of Figs. 2.2 and 2.6.

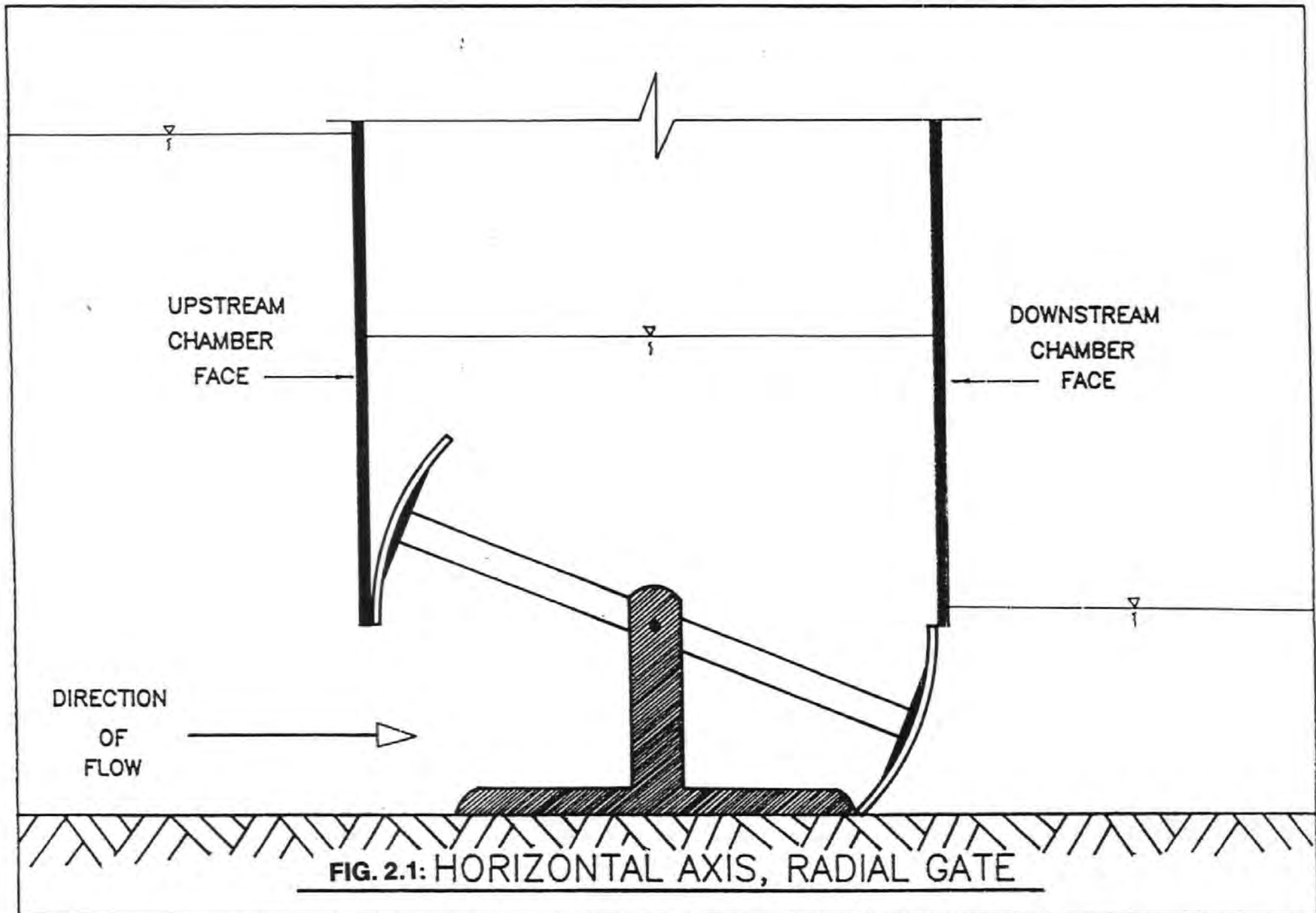
2.7.3 The Vertical-axis Butterfly Gate

It was decided that the vertical-axis butterfly gate situated as shown in Fig. 2.3 complies to the greatest extent with the initial design criteria. The main factors influencing this choice are as follows:

- 1) Overall simplicity.
- 2) A minimum of moving parts.
- 3) Good access to the gate mechanism.
- 4) Well shaped water passages.
- 5) Inherent strength of circular construction.
- 6) 2:1 chamber : gate ratio.

The loss of the common chamber walls and increased cost of the circular construction must be taken into account as must the possibility of the gate motion being opposed by significant hydrodynamic forces and the gate itself being subjected to excessive shock loadings. It was felt however that these forces and loadings could be avoided by development of the gate size and gate position. A further possibility was that such development could lead to these forces actually assisting the gate action.

In order to ascertain the feasibility of such a configuration and to both identify those problems likely to be incurred and to determine whether they could be overcome a series of small-scale hydraulic tests were embarked upon. The results, presented in the following Chapter, were very encouraging and more than justify the concentration of effort upon this one design.



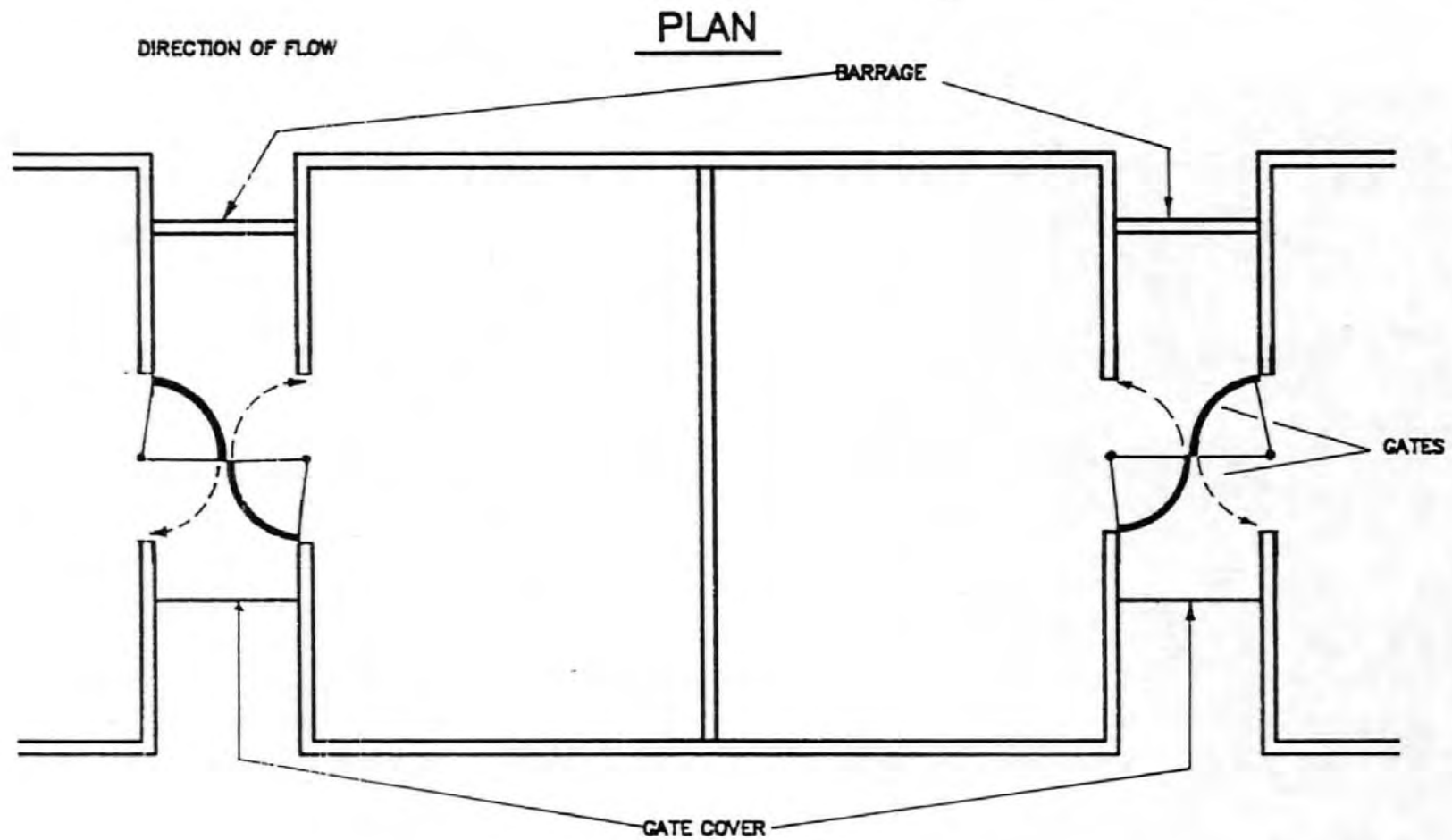


FIG. 2.2 : VERTICAL-AXIS, RADIAL GATE / RECTANGULAR CHAMBER

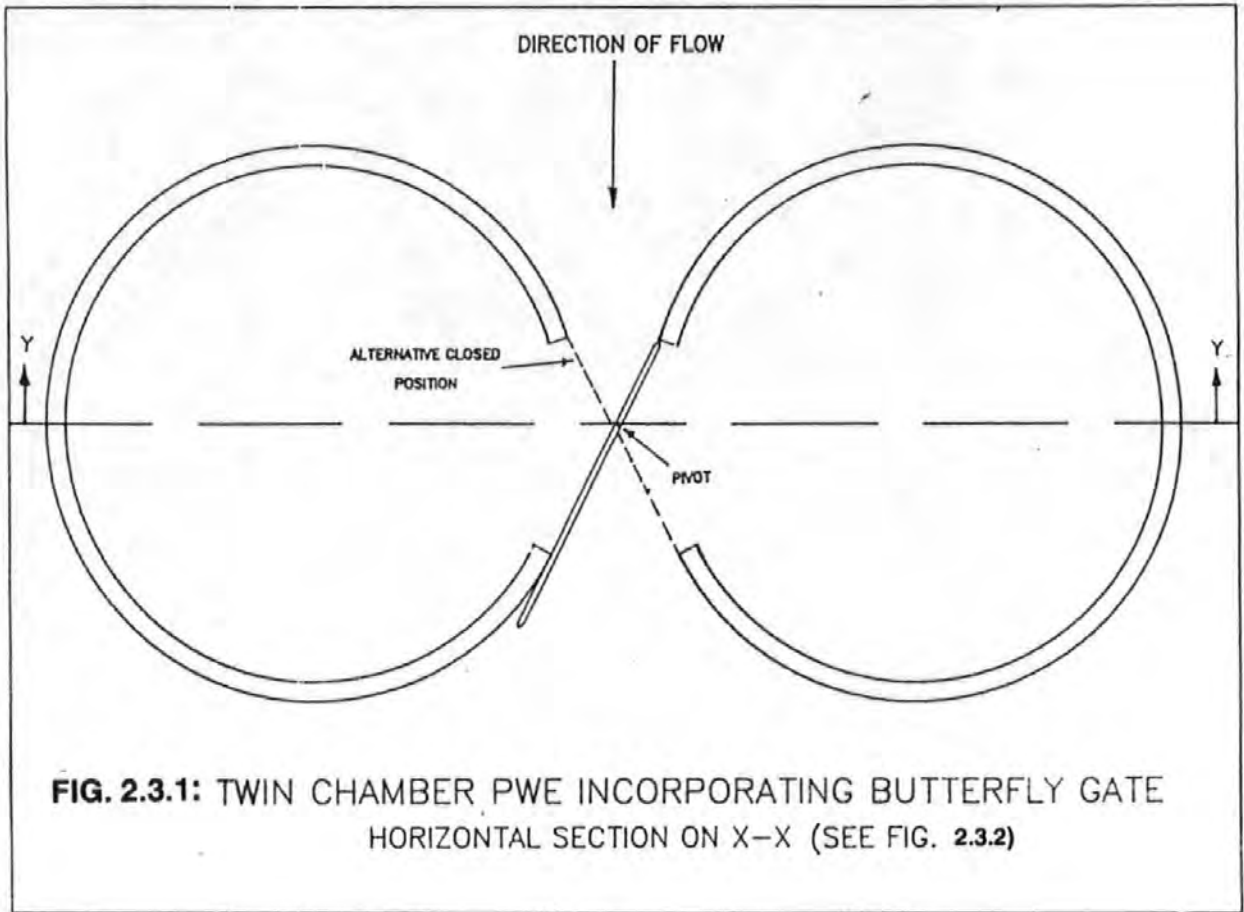


FIG. 2.3.1: TWIN CHAMBER PWE INCORPORATING BUTTERFLY GATE
HORIZONTAL SECTION ON X-X (SEE FIG. 2.3.2)

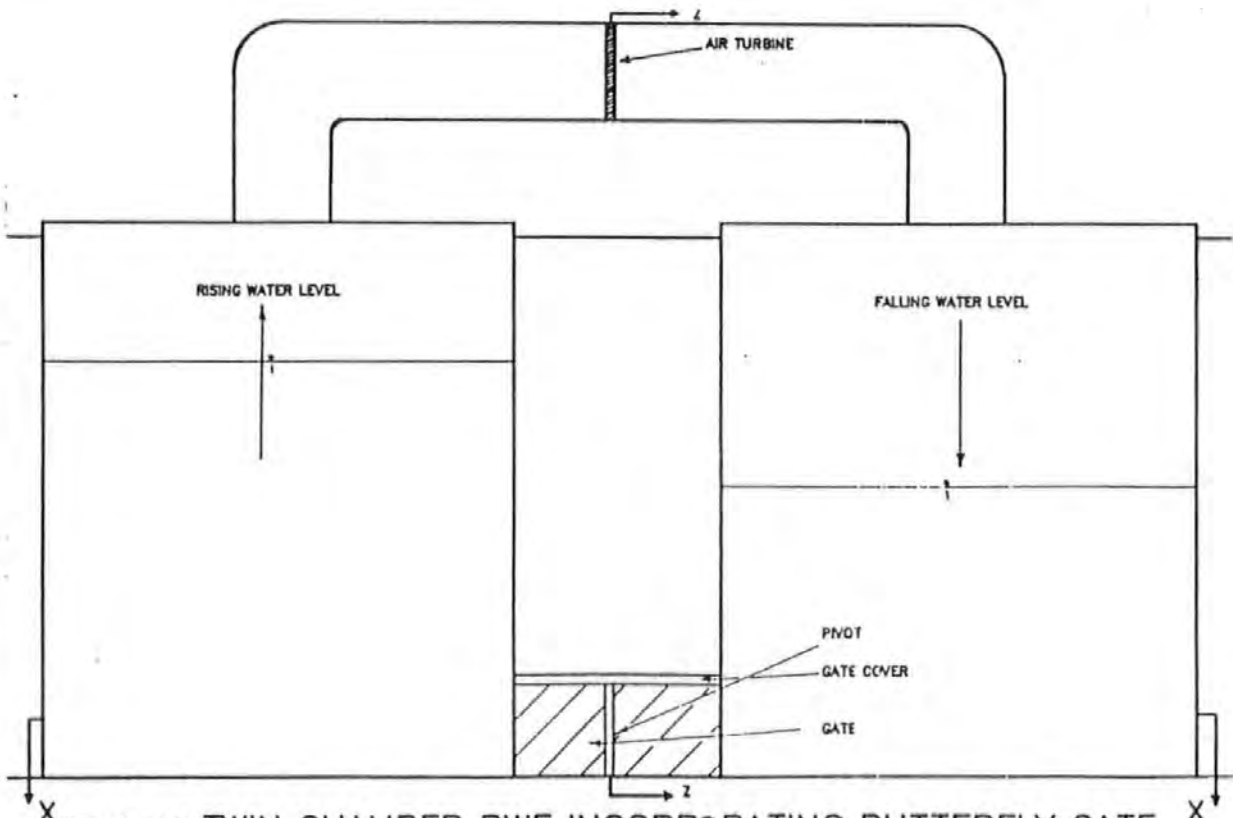


FIG. 2.3.2: TWIN CHAMBER PWE INCORPORATING BUTTERFLY GATE
VERTICAL SECTION ON Y-Y (SEE FIG. 2.3.1)

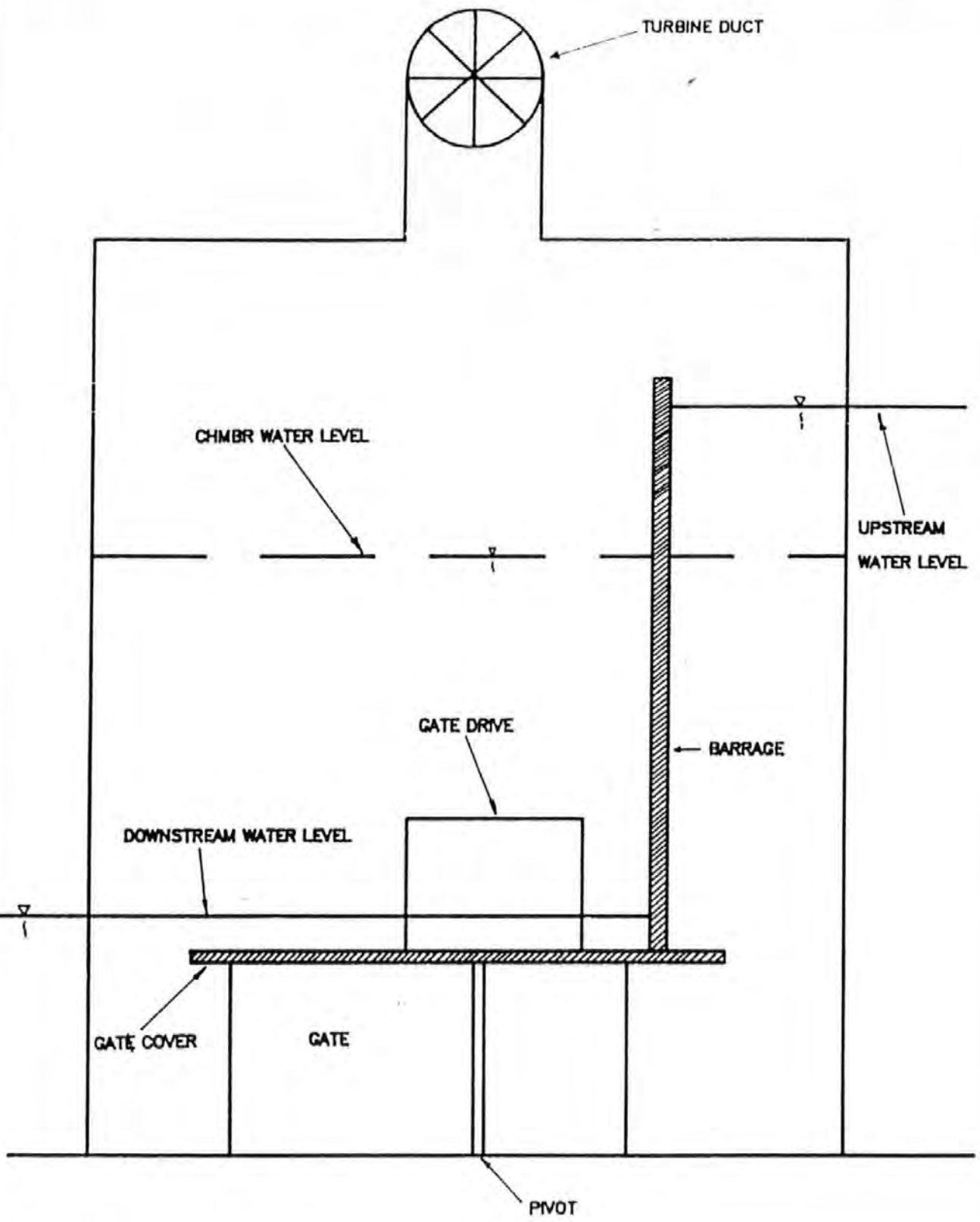


FIG. 2.3.3: TWIN CHAMBER PWE
VERTICAL SECTION ON Z-Z (SEE FIG 2.3.2)

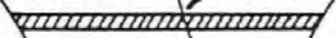
DIRECTION OF FLOW



A

A

BARRAGE



B

B

GATE COVER

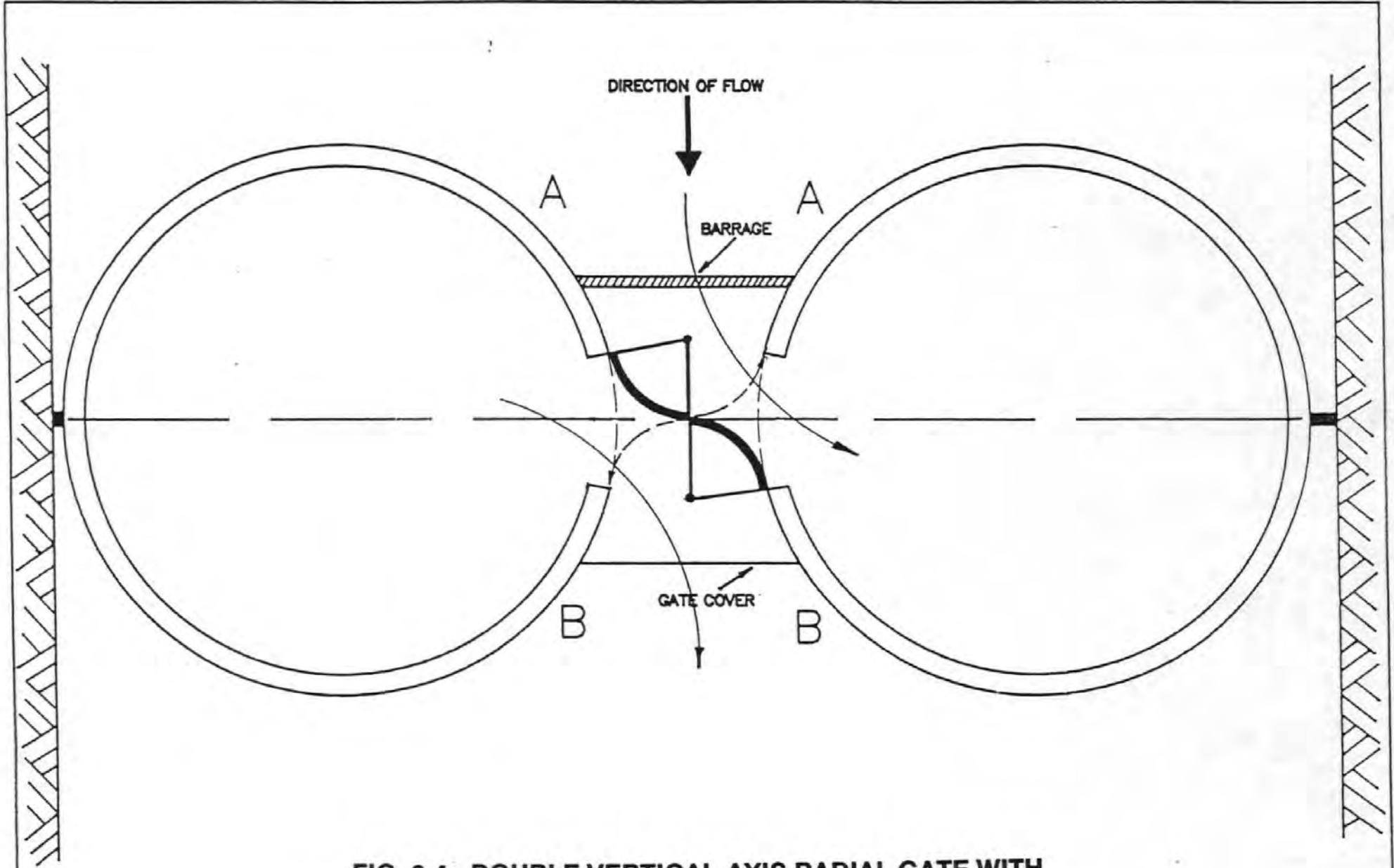
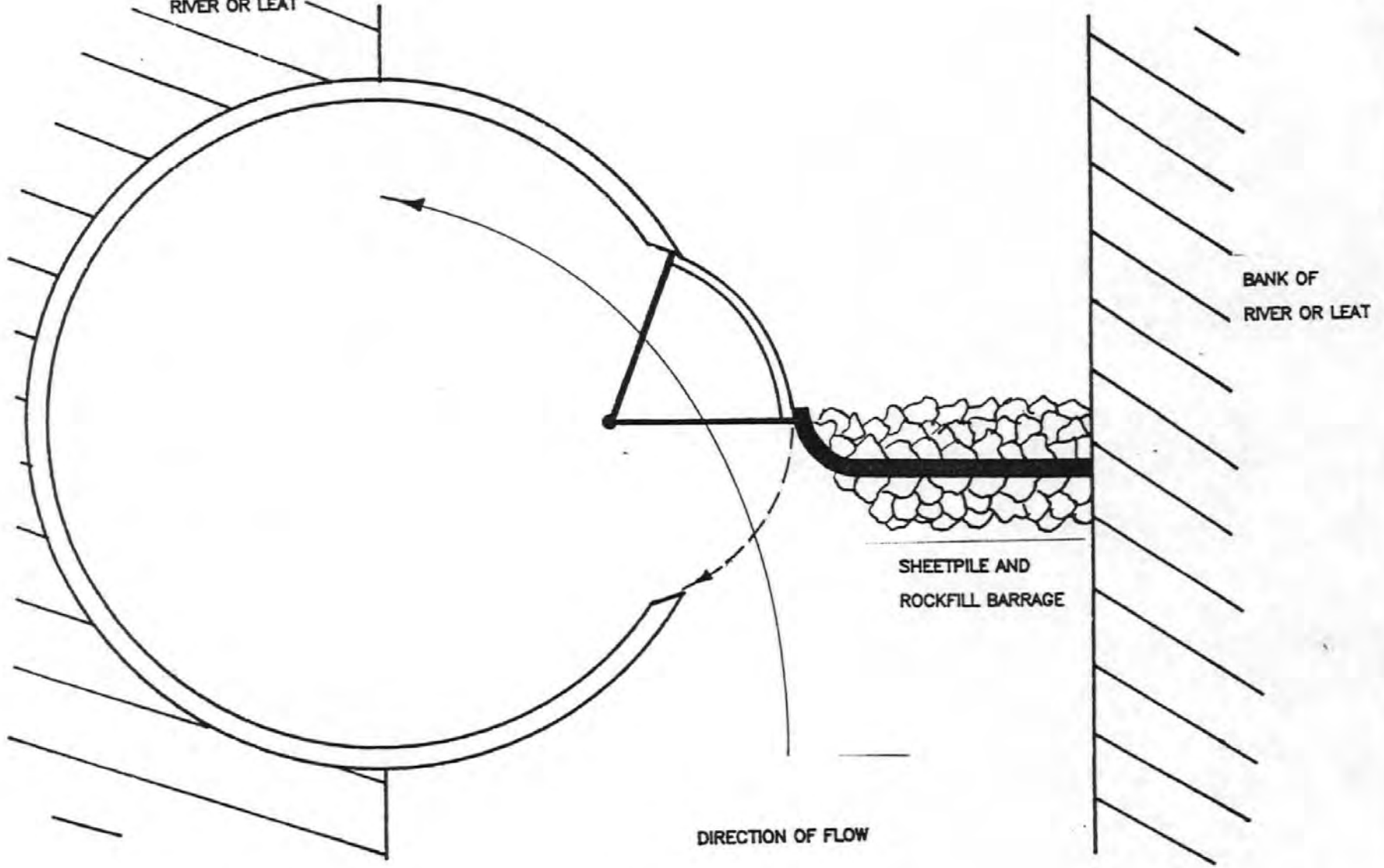


FIG. 2.4: DOUBLE VERTICAL-AXIS RADIAL GATE WITH TWIN CHAMBERS

BANK OF
RIVER OR LEAT



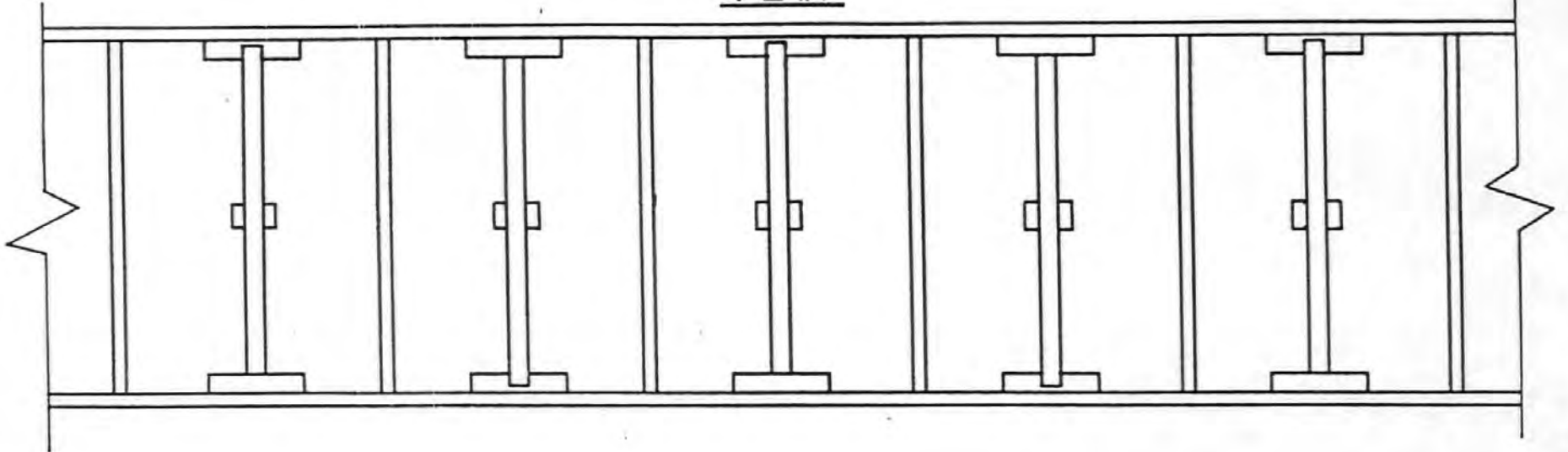
BANK OF
RIVER OR LEAT

SHEETPILE AND
ROCKFILL BARRAGE

DIRECTION OF FLOW

FIG. 2.5: VERTICAL-AXIS RADIAL GATE / SINGLE CIRCULAR CHAMBER

PLAN



ELEVATION (DOWNSTREAM)

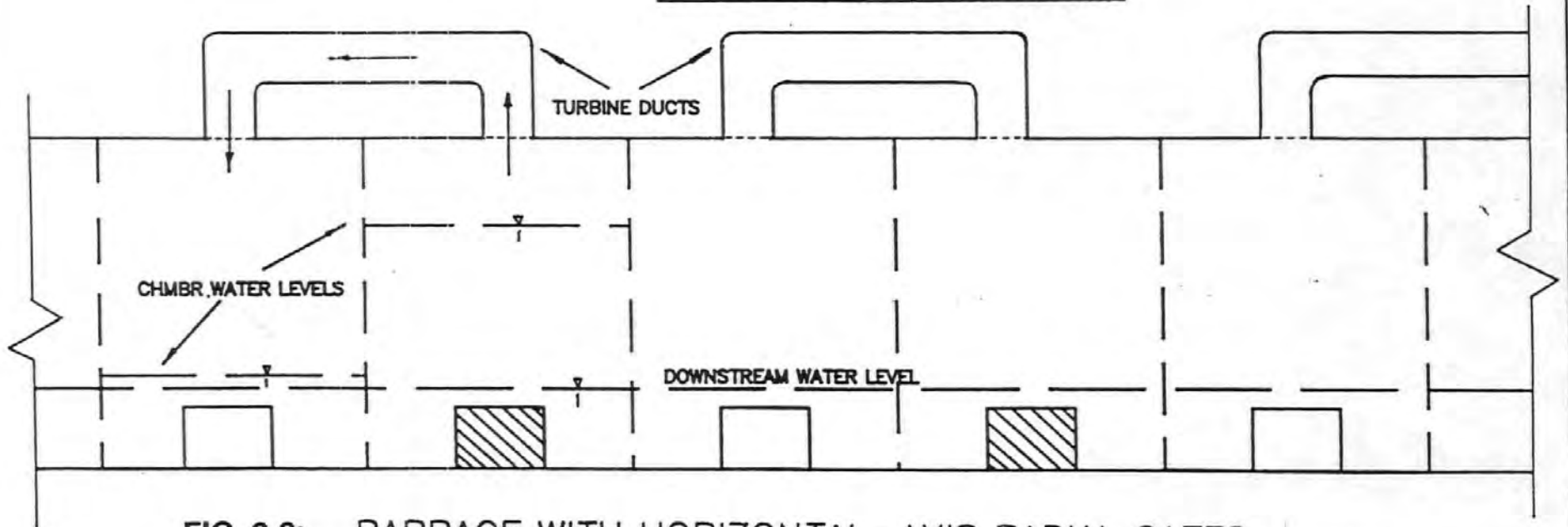
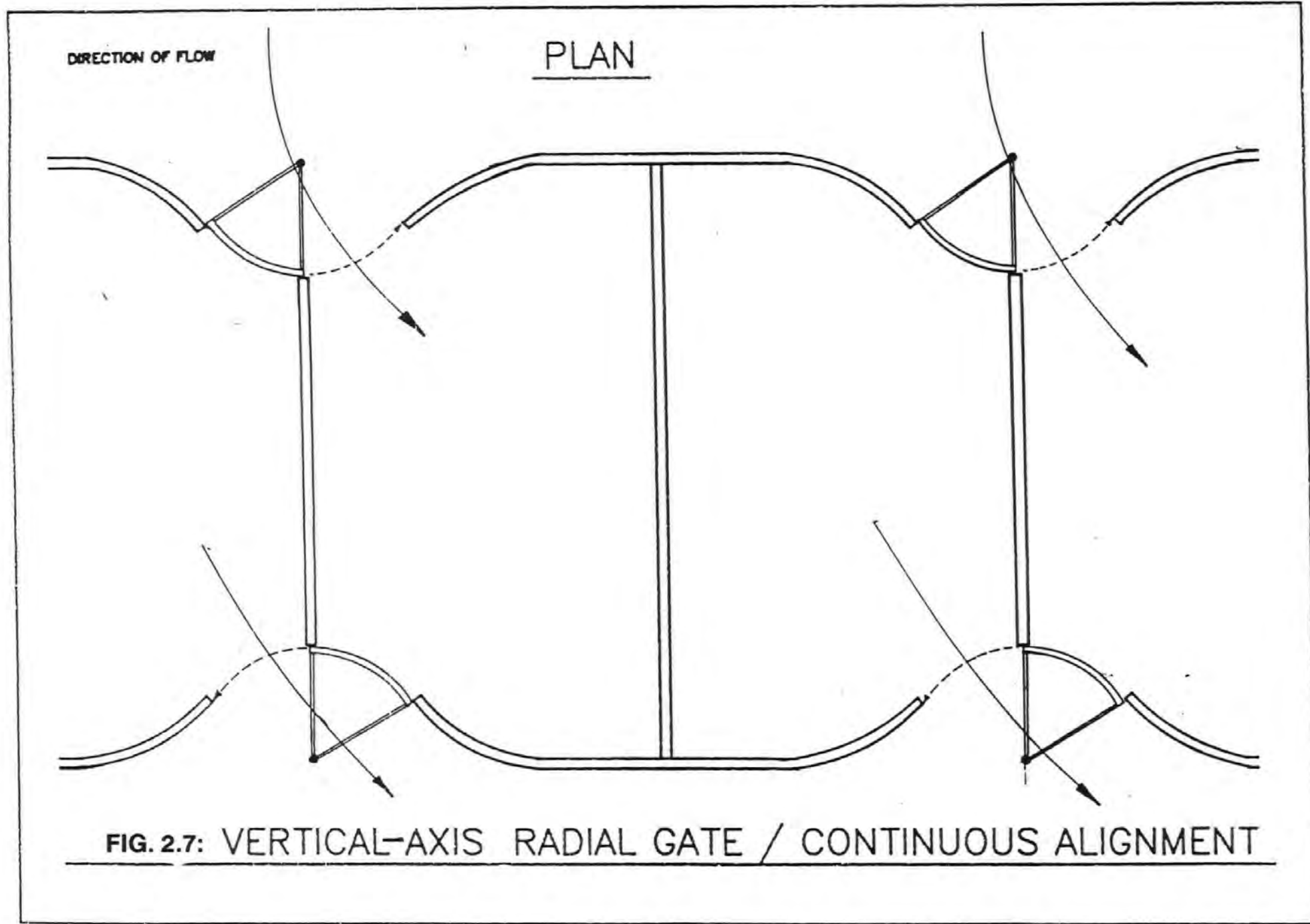


FIG. 2.6: BARRAGE WITH HORIZONTAL-AXIS RADIAL GATES.



3.0 : HYDRAULIC MODEL TESTS

3.1 Introduction

Once it was decided that the design criteria were most likely to be satisfied by the arrangement shown in Fig. 2.3, small scale model tests were conducted with the following objectives:

- 1) To assess whether large hydrodynamic forces would necessarily oppose the action of a butterfly gate.
- 2) To determine whether the flow could be induced to assist in moving the gate.

A flow assisted gate action would be very desirable as less of the energy harnessed by the turbine would be needed to operate the gate system. The optimum situation would be a totally flow actuated gate, possibly with the latching arrangement described in Section 3.3.5 providing an advantageous degree of control whilst absorbing very little energy.

3.2 Preliminary Tests (Series 1)

All the tests were carried out in a 3080 mm long by 610 mm wide recirculating channel. The chambers were constructed from 273 mm external diameter PVC pipe, and the gates, central barrage and baseplate from clear acrylic sheet. The initial model consisted of two truncated chambers, each 140 mm high (see Plates 1 and 2 and Fig. 3.1); the intention at this stage being to obtain a 'feel' for the problem before progressing to model chambers of a more practical height. Three, 80 mm high butterfly gates, each with a single pivot point were fabricated. The pivot itself consisted of a short length of 3 mm diameter brass rod which extended out of the baseplate, passed through the gate and finally located into the gate cover. Thin, stainless steel washers separated both the base plate and the gate cover from direct contact with the gate itself. The distance between the two chambers was such that the gate was required to turn through 65 degrees from one closed position to the other (Fig. 3.1). The first of the three gates was 195 mm long and was symmetrical about its pivot point. The second (250 mm long) and third (270 mm long) however, were the same length as the first upstream of their pivot points, but were longer downstream.

The symmetrical gate remained at the 'closed' position when water was passing through the model unless appreciable manual force was applied to it. An indication of the relative magnitude of this force is given in Table 1 of Appendix I. Furthermore, if the gate was held parallel to the approaching flow until the water levels in both chambers were equal, upon release it would turn to one of the

'closed' positions and remain there. This first test clearly illustrated the way the water flow can oppose the motion of a butterfly gate. However, when the size of the chamber openings was increased and their downstream walls chamfered (Fig. 3.2) to accommodate the longer tail of the 250 mm gate, the gate's performance was improved considerably and the final 270 mm gate was found to be entirely flow actuated. This was considered sufficiently encouraging to instigate a further series of tests with a more realistic PWE model.

3.3 Main Series of Tests

For all the main series of tests the height of the model was increased to 400 mm. The upstream water level was generally 280 mm and the downstream level 130 mm giving a differential head of 150 mm across the model. The model was therefore, a 1:20 scale equivalent of a PWE with twin, 5 m diameter chambers and a head differential of 3 m.

3.3.1 Test Series 2

The chambers of the second model were spaced so as to retain the 65 degree arc gate motion and the same size of the chamber openings as the initial model. It was expected that similar results to those of the truncated model would follow and that it may be possible to reduce the distance between the pivot and the downstream edge of the gate (see Gd, Fig. 3.3) without affecting flow actuation due to the influence of the increased hydrostatic head. A reduced overall gate size was desirable to avoid associated problems of large gates at full scale (see Section 2.2). However, as can be seen from Table 2.0, Appendix I, the initial results were disappointing in that the gates would invariably remain several millimetres away from the 'closed' position and a significant force was required to turn each gate through the central region of its 65 degree movement. Some improvement was gained by the addition of varying combinations of aerofoils at the upstream edge of the gate and fins at the downstream edge (see Fig. 3.4). Tables 2.1 and 2.2 illustrate this and the marked improvement in the gate action leading to the partial flow actuation evident in tests 2.9 and 2.91 stimulated the implementation of a series of modifications to the basic model design.

3.3.2 Test Series 3

The gates used in this next series of tests each possessed a number of pivot points along their length. This made it possible to fully investigate the effect upon the gate action of varying the ratio of the distance between the upstream leading edge of the gate and its pivot point (G_u) and the distance between the downstream trailing edge of the gate and its pivot point (G_d). In order to retain a proper alignment between the chamber openings and the upstream edge of the

gate in these tests, the model was designed so that the chambers could be rotated upon their baseplate into a position suited to the particular gate in use before being firmly clamped in position (see Fig. 3.5).

To simulate the envisaged design of a full scale PWE, clear, removable acrylic covers were attached to the tops of the chambers. Central openings in each of the covers were then connected by a length of flexible, plastic hose thereby creating a sealed, twin chamber system (see Plates 3 and 4). The turbine duct was represented by a hose so that the throttling effect of the turbine could be simulated by a simple clamp at its mid-point. The volume of entrapped air was adjusted by means of a screw-down valve in the chamber covers.

Three models were constructed to this modified design each with a different chamber spacing and therefore a different arc of gate movement. To reduce the overall length of the gate, the chambers of two of the models were set closer together than in Test Series 2. This change also reduced the maximum widths of both chamber entrances and exits. The final three models were as follows:

Model 3.1: 65 degree gate movement.

Model 3.2: 55 degree gate movement.

Model 3.3: 45 degree gate movement.

The height of the chambers and their openings were as Model No.2.

Model 3.3 was the first to be tested and a selection of the results and observations can be found in Tables 3.0 to 3.4 (Appendix I). Upstream and downstream heads were similar to those of Test Series 2 and details of the various gates tested and their respective pivot points can be found in Fig. 3.6. Again, various combinations of aerofoils and fins were introduced. It soon became apparent that the larger the gate and the lower the $G_u:G_d$ ratio the more promising the gate action. Full flow actuation was eventually achieved with the largest of the gates (155 mm) using the minimum G_u value (30 mm) plus various configurations of fins and aerofoils (see Table 3.2).

At this stage it seemed that flow actuation could be duplicated with other gate sizes by setting the $G_u:G_d$ ratio to that of the successful 155 mm gate and introducing the necessary fins and aerofoils. However, as Tables 3.3 and 3.4 show, all attempts to achieve this with the 140 mm gate failed. An additional factor for successful flow actuation was now becoming apparent. If the dimension of the downstream portion of the chamber opening (see L_d , Fig. 3.3) was too great, the hydrostatic force and the hydrodynamic force on the gate developed by the flow leaving a chamber prevented the gate from reaching the 'closed' position. Adjustable cowls were therefore fashioned and attached to the downstream edge of the gate openings (Fig. 3.3). This made it possible to first rotate the chambers

to suit the G_u dimension of the gate under test and then to adjust the flow through the downstream chamber openings until flow actuation was achieved. The additional flexibility provided by the cowls enabled flow actuation to be achieved with a wide variety of gate sizes and configurations during the remainder of the research period. Although unrestricted changes in chamber geometry were still far from possible it had been proved that the action of a butterfly gate need not necessarily be opposed by excessive hydrostatic or dynamic forces and could in fact be assisted by these forces.

3.3.3 Details of Test Series 3

Initially, the following five gates were found to operate satisfactorily when installed in the final version of Model 3.3:

Gate Length	G_u	G_d	L_u	L_d
155	40	115	33	70
140	40	100	35	70
130	40	90	35	65
130	30	100	25	63
120	30	90	33	60

A rapid oscillation of the gates at the 'closed' position was evident to a greater or lesser extent with most of these configurations, ie upon reaching the chamber sides the gate would repeatedly move away a small distance before returning. This produced a rapid 'chattering' noise as the gate repeatedly hit the chamber walls. Clearly, an oscillation of this sort would be far from satisfactory in a full scale system.

All attempts to trace the streamlines adjacent to the gate and hence deduce the pressure distribution were frustrated by the rapidly varying velocities and elevations of the non-steady flows. The installation of either piezometer tappings or pressure transducers to investigate the pressure differentials along the gate's surfaces was considered impractical due to the sizes of the gates involved.

It was expected that the third series of tests, as well as fully endorsing the feasibility of flow actuation, would provide further insight into the complex hydrodynamics of the system and quantify various physical characteristics. The planned format of the tests consisted of the recording of the ten cycle time (ie the time taken for a chamber to fill and empty ten times) and the maximum and minimum chamber heads achieved during the ten cycles. The readings were taken for the following three configurations of the models for each gate:

- i) Covers removed.
- ii) Covers in position.

iii) Covers in position and connected by the plastic hose.

In this way the throttling effect of both discharge to atmosphere and connected chambers could be studied. Whilst recording the cycle times a video recording of the gate action was taken with a stopwatch in-frame. Subsequent play-back of these recordings revealed the timing of the gate motion.

The results obtained with the first few gates indicated that there was a lack of consistency from one cycle to the next. In part it was caused by the rapid oscillation of the gates in the closed position. When the gate moved away from the 'closed' position the resulting leakage from the chamber halted or slowed the rise of the water column within it, the rise only being fully resumed when the gate had returned to the 'closed' position. This spasmodic rise resulted in the air being expelled from the chamber in a series of short spurts as opposed to a steady stream.

In order to solve the problem of gate chatter, it was necessary to develop at least a partial understanding of the mechanism causing it. Referring to Fig. 3.7 the combined dynamic and hydrostatic forces are the motivators which cause the gate to move away from the side of the chamber. As this happens the high velocity leakage through the resulting opening creates a low pressure area between the chamber sides and that part of the gate that extends beyond the chamber opening. This low pressure area, assisted by the high pressure flow from the emptying chamber acting on the opposite side of the gate causes the gate to return to the 'closed' position where the process is repeated. Initially, the motivating force pushing the gate away from the chamber sides is mainly dynamic and so the oscillations are high frequency due to the small distance through which the gate travels. However, as the chamber fills, an increasing hydrostatic force is added and the oscillations increase in magnitude and decrease in frequency (this was noticeable on the video recordings and also evident from the changing tone of the gate 'chatter' as the chambers filled). The larger oscillations also reduce the effectiveness of the low pressure area and this, coupled with the constantly lessening dynamic forces from the emptying chamber, results in the gate finally breaking free and swinging across to the opposite 'closed' position.

The first attempt to remedy this was to attach fins to the downstream edge of the gate. This had the detrimental effect of reducing the dynamic forces from the emptying chamber as shown in Fig. 3.8, thereby causing the gate to stand off from the relevant 'closed' position allowing substantial leakage from the chamber and drastically reducing the maximum potential chamber head.

A partial answer to the problem lay in an increase of the dynamic forces of the flow from the emptying chamber. It was necessary to create a high pressure area at the extreme downstream tail of the gate on the side adjacent to the emptying

chamber's flow in order to keep the gate firmly closed. This was achieved by adding a flange as shown in Fig. 3.9.

This solution was very effective when the model being tested was without covers, the oscillations being completely eliminated. However, when covers were attached the oscillations returned although much reduced in magnitude and in some cases, barely discernible. This suggested that the prime motivating force causing the oscillation was the increasing hydrostatic force of the filling chamber. With the covers in place the air pressure above the rising water column was contributing to the hydrostatic force, thereby initiating the renewal of the gate oscillation. This theory is further strengthened by the fact that these renewed oscillations did not commence until the water level in the rising chamber was at its mid-point at which time there existed both a significant hydrostatic head plus an appreciable air pressure. Before the introduction of the flanges the oscillations had occurred throughout the cycle.

The varying duration of the gate movements when observed over a number of cycles was also a cause of concern. This behaviour was most likely caused by the small mass of the gates, leakage around them, friction at the gate pivot plus the movement and play within both the gate system and the adjustable cowls and even within the rotating chambers themselves. It was evident that high precision could not be achieved when operating at such a small scale with the materials available. However, the results from this series of tests demonstrated the operation of both the flow actuated gate and the system as a whole and the experience gained will prove extremely useful in the design of any subsequent model at a larger scale.

With this in mind, the planned series of tests continued and flanges were introduced to the 130 mm gates to minimize the gate oscillation. The efficacy of these flanges is evident from the representative set of results and observations presented in Tables 4 and 5 of Appendix 1. The larger gates (170 mm to 190 mm) could not be accommodated in the 45 degree model and proved to be far less effective than their smaller counterparts when installed in the 55 degree model. Indeed, in the main, the smaller the gate, the more positive the gate action. The larger gates (170 to 190 mm) proved to be more successful when installed in the 65 degree model. However, the flow actuation achieved with these gates when installed in the 65 degree model was at best erratic and stalling at various points of the gate's movement was not uncommon. The irregularities of the gate's movement made the timing of ten consecutive cycles impossible and so further recorded testing of model 3.1 was abandoned. Subsequent experimentation with this model showed that a satisfactory gate motion could be achieved by reverting to the use of the 250 and 270 mm gates. However, these gates are rather large and their mass will tend to be excessive at full scale.

3.3.4 Flow Within the Chambers

The flow within the chambers was observed closely throughout the tests and proved to be quite complex. At shallow depths it sometimes took on the characteristics of a forced vortex while at greater depth it had the superficial characteristics of a free vortex. Much of the behaviour can probably be explained in terms of the conservation of angular momentum as the flow spirals upwards and inwards as it fills a chamber. There is reason to suppose that this momentum is recovered as the chamber empties. In a sense, the flow winds itself into a chamber, and having wound itself in, without stopping or changing direction, then winds itself out. Very little energy would seem to be lost in the process and inertia forces should also be small.

3.3.5 Gate Tuning and Latching

For each of the Series 3 tests the downstream, adjustable cowl had been positioned to present the minimum L_d measurement possible whilst still retaining satisfactory flow actuation. By increasing the magnitude of L_d it was possible to reduce the period of time that the gate remained at the 'closed' position and thereby decrease the maximum achievable head within the filling chamber, shortening the cycle time and increasing gate frequency. This was due to an increase of gate area being exposed to the motivating forces within the chamber. A certain amount of gate 'tuning' using the adjustable cowls was therefore possible. This reduction in cycle time could also be induced by tightening the clamp on the plastic hose to restrict the air flow and hence increase air pressure above the rising water column thus instigating an early gate movement. This could be counteracted by decreasing L_d via the downstream cowls.

This 'tuning' of the rise and fall characteristics would provide a useful control mechanism in a full-scale device. Alternatively, control of the gate system and related stroke volume could be achieved using pneumatic or hydraulic latches. This would enable the downstream chamber opening dimension, L_d , to be fixed at a value which would normally cause the gate to move away from the 'closed' position well before the required maximum chamber water level was reached. Premature motion would be prevented by holding the gate in position by a latch which would be automatically released when the rising water column reached the required level. This would result in a more positive and a more rapid gate movement to the opposite 'closed' position where it would again be held by a latch. Apart from this improvement in gate action the latch would eliminate any residual gate 'chatter' whilst requiring a minimum of power for its operation.

3.3.6 Linked Chambers

It was evident from the tests with linked chambers, that the tendency for the flowrate out of a chamber to be greater than the flowrate into a chamber generally lowered the air pressure above the rising water column in the filling chamber. Thus, all times in the linked chambers were greater than those with the link removed and air pressures within the linked chambers could be assumed to be sub-atmospheric throughout much of the cycle.

The imbalance of the flowrates into and out of the chambers can be accredited in part to the downstream gate opening being wider than the upstream opening. It is also caused, to some degree, by the pressure differential across the chamber vortices (see Sections 3.3.4 and 3.5.3). The increased pressure at the periphery of the vortex in the filling chamber restricts the flow in through the upstream opening whilst this same pressure differential in the emptying chamber assists the flow out through the downstream opening.

3.3.7 Further Refinements

A further refinement to the models was introduced subsequent to the Series 3 tests. In the series 3 tests, the downstream edge of the gate opening was approximately perpendicular to the flow within the chamber and this gave rise to a high pressure area which tended to open a closed gate. This high pressure area was eliminated by bevelling the downstream cowls as shown in Fig. 3.10. This, together with the action of the flanges mentioned earlier, caused a high pressure area to be created on the gate's outer face together with a relatively low pressure area on the gate's inner face. Further tests involving all the models and the various gate sizes showed that this eliminated the 'chatter' problem. Unfortunately, the time was not available to repeat all the measurements of Test Series 3 with this further refinement.

3.4 Non-Circular Chambers

The main disadvantages of the circular chamber, butterfly gated system are the relatively high cost of constructing a circular structure and the lack of common walls in a barrage situation. A non-circular model (model 3.4) was therefore fabricated to investigate whether the effect of these disadvantages could be lessened whilst still retaining the advantages of a flow actuated gate system. As can be seen from Plate 5 and Fig. 3.11 the hydraulically efficient characteristics of the circular model's entrance and exit configurations were duplicated in model 3.4, whilst an elongation of the chamber sides allowed a common wall to be included. The common walls were represented in the model either by the channel sides or

by moveable partitions that could be slotted into positions one to four within the chambers.

The chambers were spaced to provide a 50 degree gate movement and a 155 mm gate with a G_u measurement of 40 mm was used in each of the tests. The two plane, vertical partitions could be placed in any of the four positions shown in each chamber and a further configuration could be achieved by removing them entirely. In all cases the non-circular shape of the chambers had no apparent effect upon the flow actuation of the gate. Thus, with appropriate adjustment of the downstream cowls it was found that irrespective of partition position a satisfactory flow actuated gate action could be achieved. However, it was noted that as the partitions were moved progressively towards position four, the vortices within the foreshortened chambers became more distorted and turbulent and the flow tended to climb up the partition walls.

To what degree this non-circularity could be taken before the flow actuation is destroyed is not known but model 3.4 would seem a reasonable compromise between the constructional advantages of a rectangular chamber and the operational advantages of the circular chamber.

3.5 Calibration Data

For reasons previously discussed, the results obtained from Test Series 3 were not considered to be of a particularly high precision. A series of tests using a simple, rectangular chamber with a more easily controlled gate system could have been devised to provide more precise data. However, the significance of establishing the feasibility of flow actuation was considered of primary importance especially as excellent rise and fall data was available from other sources. This approach was more than justified by the successful conclusion of the model tests and the subsequent patenting of the flow actuated gate system by the Department of Energy.

The Series 3 models provided much valuable data, however. Recorded leakage through the system plus gate timings were of considerable use to the mathematical model. In addition, measurements of the surface profile and angular velocity of the vortices within the chambers were used in the calibration of the modelling of the flow into and out of the system and the resulting conservation of momentum of the flow.

3.5.1 Discharge Estimates

A series of tests were initiated using model 3.2 in order to ascertain the proportions of flow which were:

- i) Passing through the system whilst the gate was moving.
- ii) Leaking past a 'closed' gate. Such leakage could occur between the upstream and downstream edges of the chamber openings and the gate and between the top and bottom of the gate and the gate cover and baseplate respectively.
- iii) Passing via the chambers and therefore contributing to the rise and fall of the water levels within the chambers.

For these tests the underside of the baseplate was thickly coated with mastic to minimize leakage beneath the model. Both the 150 mm long and the 170 mm long gates were used with $G_u=40$ and 50 mm respectively. Flowrates were recorded initially with the gate being flow actuated, then with the gate fixed at the central position and finally with the gate held at one 'closed' position and then at the other. An upstream depth of flow of 300 mm was maintained during the flow actuated mode and during the final mode but was allowed to vary when the gate was held at the central position. The downstream depth of flow was approximately 150 mm for all three configurations.

The following results were obtained:

	<u>Gate Size</u>	
	<u>155 mm</u>	<u>170 mm</u>
	$G_u=40$ mm	$G_u=50$ mm
Discharge during flow actuation:	0.00305m ³ /s	0.00360m ³ /s
Discharge due to leakage:	<u>0.00120</u>	<u>0.00160</u>
Difference:	0.00185	0.00200
Flow into and out of chambers:	<u>0.00117</u>	<u>0.00107</u>
Flow not entering chambers: (ie passing straight through the system)	0.00068m ³ /s	0.00093m ³ /s

The greater the value of G_u , the greater the width of the upstream opening and, as would be expected, the larger the volume of flow passing straight through the system whilst the gate was in motion. The potential for increased leakage above and below the 170 mm gate due to its greater length has also been exploited.

These figures show that a massive 40% of the flow leaked through the system whilst the gates were at the 'closed' position and that 20 - 25% passed through the system without contributing to the rise and fall of the water columns within the chambers. Only 30 - 35% of the overall flow through the system contributed to the actual rise and fall of the columns.

The 40% 'closed' leakage was mainly caused by the low tolerances of the model's gate system; a necessity at this scale to reduce friction and thereby facilitate flow actuation. It is also suspected that the application of mastic to the baseplate did not restrict flow beneath the model to a satisfactory extent and that significant leakage was therefore occurring between the baseplate and the channel bottom. It is not envisaged that leakage in a well-designed, full scale PWE will be of the magnitude of that in the model. The 20 - 25% of the flow which passes straight through the system, however, is possible irrespective of scale. The parameters responsible for this aspect of the overall flow are as follows:

- i) The gate size and the velocity of its movement.
- ii) The spacing of the chambers and therefore the angle through which the gate must travel.
- iii) The volume of the water column stroke and therefore the cycle time of the system.

The complex interaction between all of these parameters became clearer during the parametric testing carried out via the mathematical model. The overall impression at this stage however was of a system possessing a relatively low hydraulic efficiency.

The discharge results obtained by holding the gate at the central position were used to determine a coefficient of discharge of the system (C_d). The maximum cross-sectional area of the water passage, the resulting flow rates and the head differential across the model gave a coefficient of discharge of 0.71 using the usual discharge equation:

$$Q = C_d \cdot A \sqrt{2gh}$$

3.5.2 Gate Velocity

When the video recordings of the gate action with a stopwatch in frame were studied in slow motion, it was seen that the gate action could vary considerably even between consecutive cycles (the reasons for this have already been suggested in Section 3.3.3). It was evident (from the recordings) that the gate's swing started very slowly and it was not until after the gate had reached the mid point that its velocity appreciably increased. This slow initial start would be avoided with the use of gate latches as an increased hydrostatic head within the filling chamber could be brought to bear upon the downstream element of the gate as soon as the latch was released (see Section 3.3.5). The fully flow actuated gate movement from one closed position to the other was timed at between 0.5

and 0.9 seconds. It should be noted that friction effects at full scale will be relatively less and so it would be expected that the scaled-up values (2.23 - 4.02 secs at an assumed scale of 1:20) of these times could be significantly improved upon. The importance of the velocity of the gate action will become apparent in Chapter 6.

3.5.3 Classification of the Vortices

Observation of the flow within the chambers led to the conclusion that in order to mathematically model the hydrodynamics of the system successfully the pressure distributions and momentum characteristics of the vortices formed within the chambers must be taken into account.

The chamber vortices were never completely destroyed by the changeover from the emptying half-cycle to the filling half-cycle. The vortex in the filling chamber, although distorted during the changeover, rapidly recovered and increased in strength with the rise of water level. With the chamber completely open to the atmosphere a pronounced superelevation of water level was produced around the walls during this fill stroke with well-defined water surface slopes falling into a significant central depression. This would suggest that the pressure distribution within the bodies of water increased with radius. It therefore follows that the higher peripheral pressures would inhibit flow into the chambers whilst assisting flow out. The strength of the vortex invariably decreased with the falling water levels of the emptying half-cycle.

A significant flattening of the vortex superelevation was evident when the chamber covers were in position and the throttling effect of the connecting duct caused a decrease in flow rate both into and out of the chambers.

In order to model fully the non-steady, three dimensional flow of the vortices with the inherent variations in water levels and momentum flux it would be necessary to take into account both boundary layer formation at the chamber walls and viscous effects at the central core. This was considered too ambitious for inclusion into the existing mathematical model. Instead, a series of tests were carried out in order to ascertain the characteristics of the vortices which could subsequently be modelled using a lumped-mass approach.

A video recorder was again utilised to record the rise of the water column in a filling chamber with its cover removed. A stopwatch was placed in frame and a weak soap solution introduced to the chamber. Playback of the recording using freeze-frame and slow-motion facilities allowed the variation of the water surface velocity at the top of the stroke to be ascertained using the rotating soap bubbles as markers. The results of this test are shown in Fig. 3.12.

The surface profile of the vortex at the top of the stroke was obtained by taking a series of measurements across the diameter of the chamber normal to the direction of the channel flow. Several readings were taken at each point over a number of cycles and an average then taken. The results are shown in Fig. 3.13 from which it is interesting to note that the maximum water level is greater on the bank side of the chamber, presumably due to the momentum flux through the gate. Throughout these tests the cycle time of the rise and fall of the water columns was 5.2 secs.

The surface profile results have been plotted alongside profiles typical of a number of vortex types in Fig. 3.13. Using this comparison plus the surface velocity information, the following vortices have been disregarded:

- 1) **Constant Momentum:** ie velocity is constant with radius. This does not conform with the measured velocities.
- 2) **Free or Irrotational Vortex:** ie velocity decreases with radius. Again this is at variance with the test results except near the chamber walls.
- 3) **Forced Vortex:** ie velocity increases in direct proportion to the radius. Although the velocity profile is in good agreement with the test results at small radii the corresponding surface profile is not considered a good match.

The following vortices were considered to be most suitable:

- 4) **Forced Vortex plus boundary layer:** This could possibly provide the 'best fit' solution but its development would have to depend upon better data than is available at the present model scale.
- 5) **Uniform Surface Slope:** This is considered a reasonable approximation to both the surface elevation profile and the velocity profile.

Taking into consideration the data available from the existing physical models it was decided that the mathematical model should reproduce the relatively simple characteristics of the Uniform Surface Slope vortex. This could be refined at a later stage if more sophisticated physical models with a larger scale are to be developed.

3.6 Introduction of the 'Stepped Gate'

One of the disadvantages of the flow-actuated butterfly gate is the restricted width of the chamber entrances caused by the offset pivot and the reduced length (L_d) of the upstream portion of the gate. If the size of the entrance could be increased it would almost certainly result in a significant increase in average power output

(see Section 6.4). However, the two methods of achieving this that immediately come to mind are an increase in overall gate length or an increase in the turning angle of the gate. The former is undesirable for reasons previously discussed and the latter will result in increased gate inertia and longer transit times thereby potentially reducing average power output.

This leaves only one dimension that could be satisfactorily increased whilst still retaining flow-actuation, ie the gate height. Unfortunately, in order to prevent air escaping from the chambers, this dimension is restricted by the combination of downstream water level and the minimum water level within the chambers. The downstream portion of the gate must remain submerged at all times. It is possible that the gate could be recessed into the channel bed but the additional expense incurred and the possibilities of excessive siltation could prove severely limiting.

However, the height of that portion of the gate that lies upstream of the pivot point is only restricted by the minimum water level expected within the chambers. A 'stepped gate' such as that shown in Fig. 3.14 could therefore be installed. Careful design of the chamber openings may then result in satisfactory flow actuation. If this proved possible, average power output would be improved whilst minimising any increase in gate inertia and possibly increasing the speed of the gate movement.

A modified form of model 3.2 incorporating stepped chamber openings and a more complex gate cover to prevent leakage was fabricated and a range of gates with upstream 'steps' increasing in magnitude as shown in Fig. 3.14 were tested. The results exceeded all expectations. Very positive and therefore faster gate movements were achieved with all the sizes tested. This resulted in shorter rise and fall periods with favourable indications of increased power output.

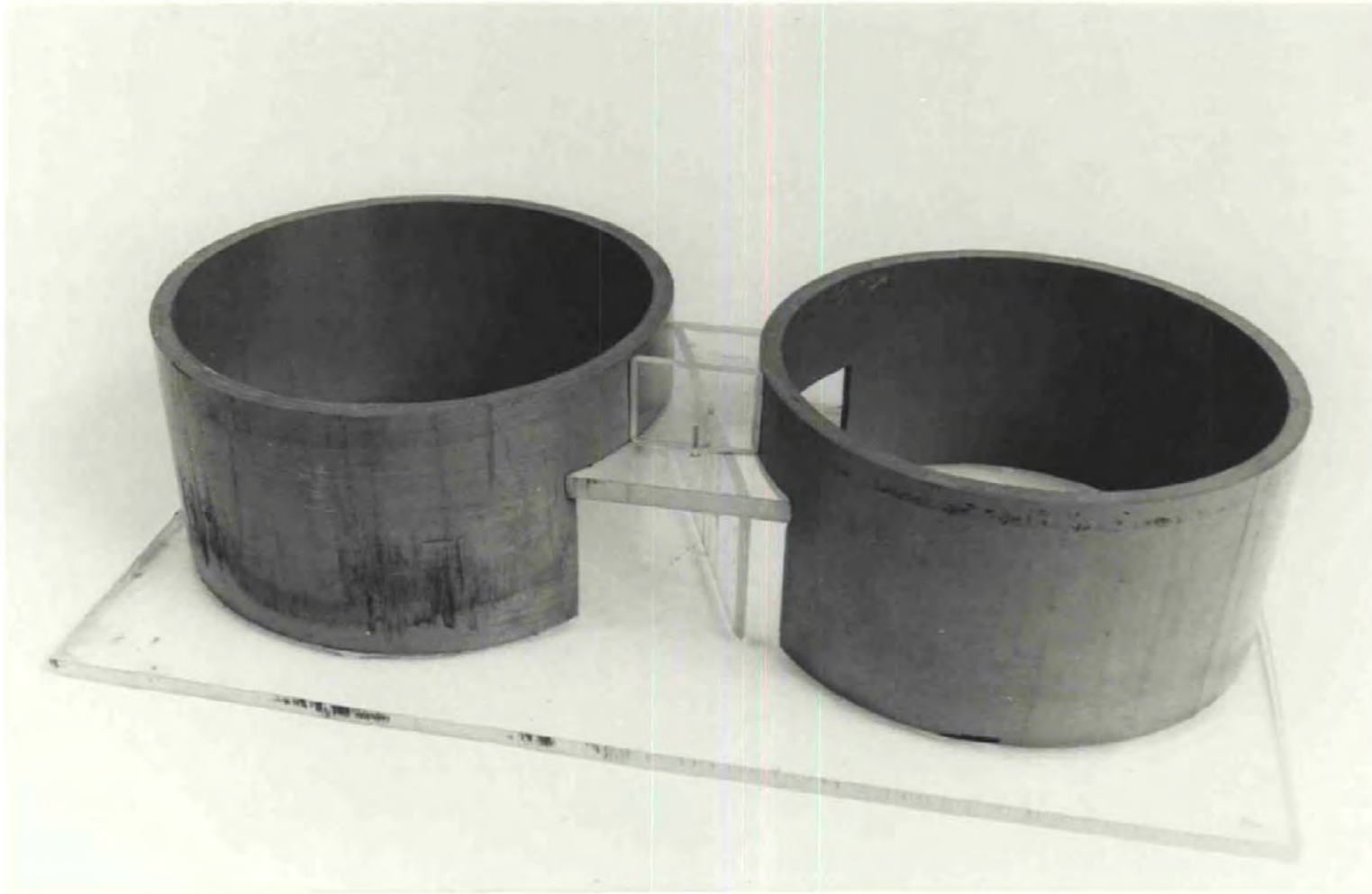


**PLATE 1: INITIAL TRUNCATED MODEL
(SERIES 1)**



**PLATE 2: INITIAL MODEL UNDER TEST
IN RECIRCULATING CHANNEL**



PLATE 3: MODEL 3.2 - 55° GATE MOVEMENT



**PLATE 4: MODEL 3.2 UNDER TEST IN
RECIRCULATING CHANNEL**

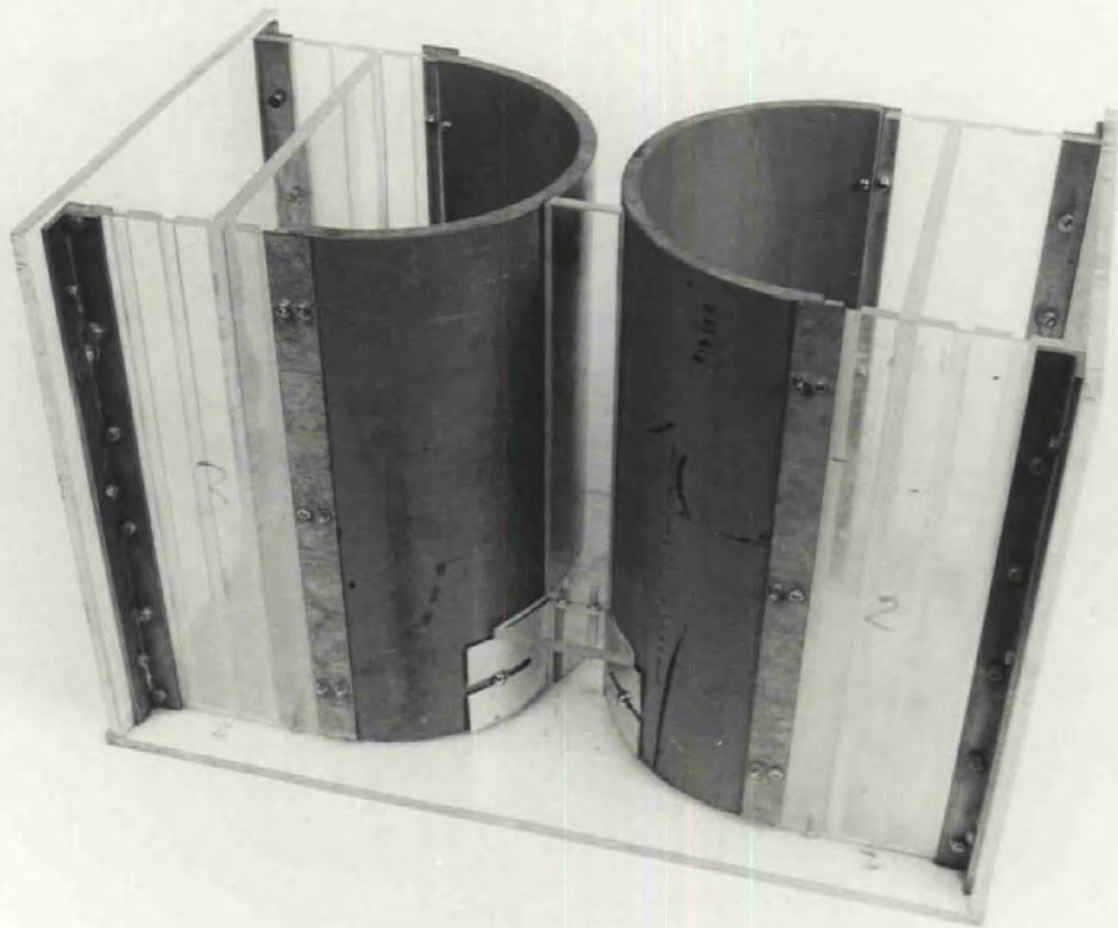


PLATE 5: NON-CIRCULAR CHAMBERS

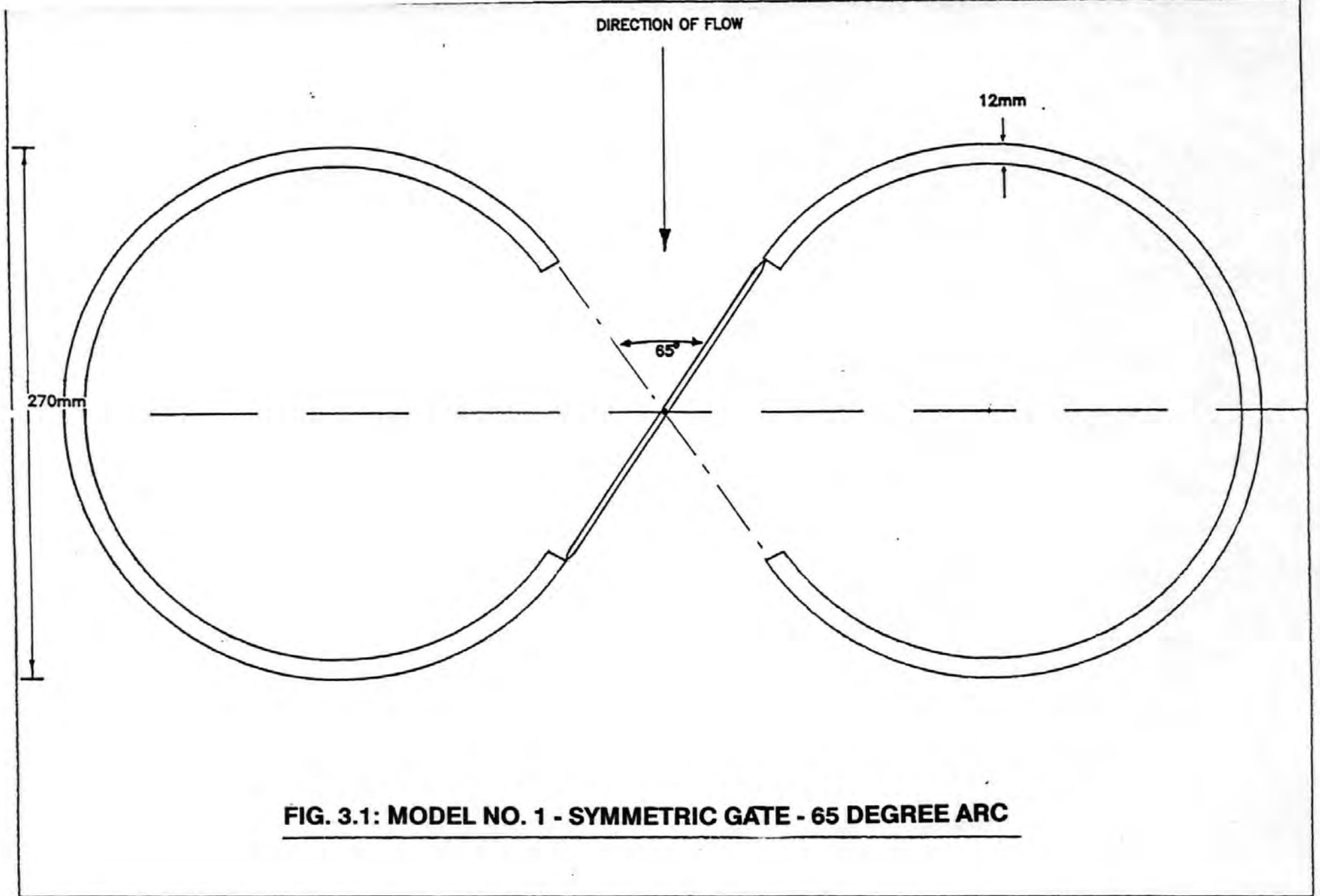


FIG. 3.1: MODEL NO. 1 - SYMMETRIC GATE - 65 DEGREE ARC

DIRECTION OF FLOW

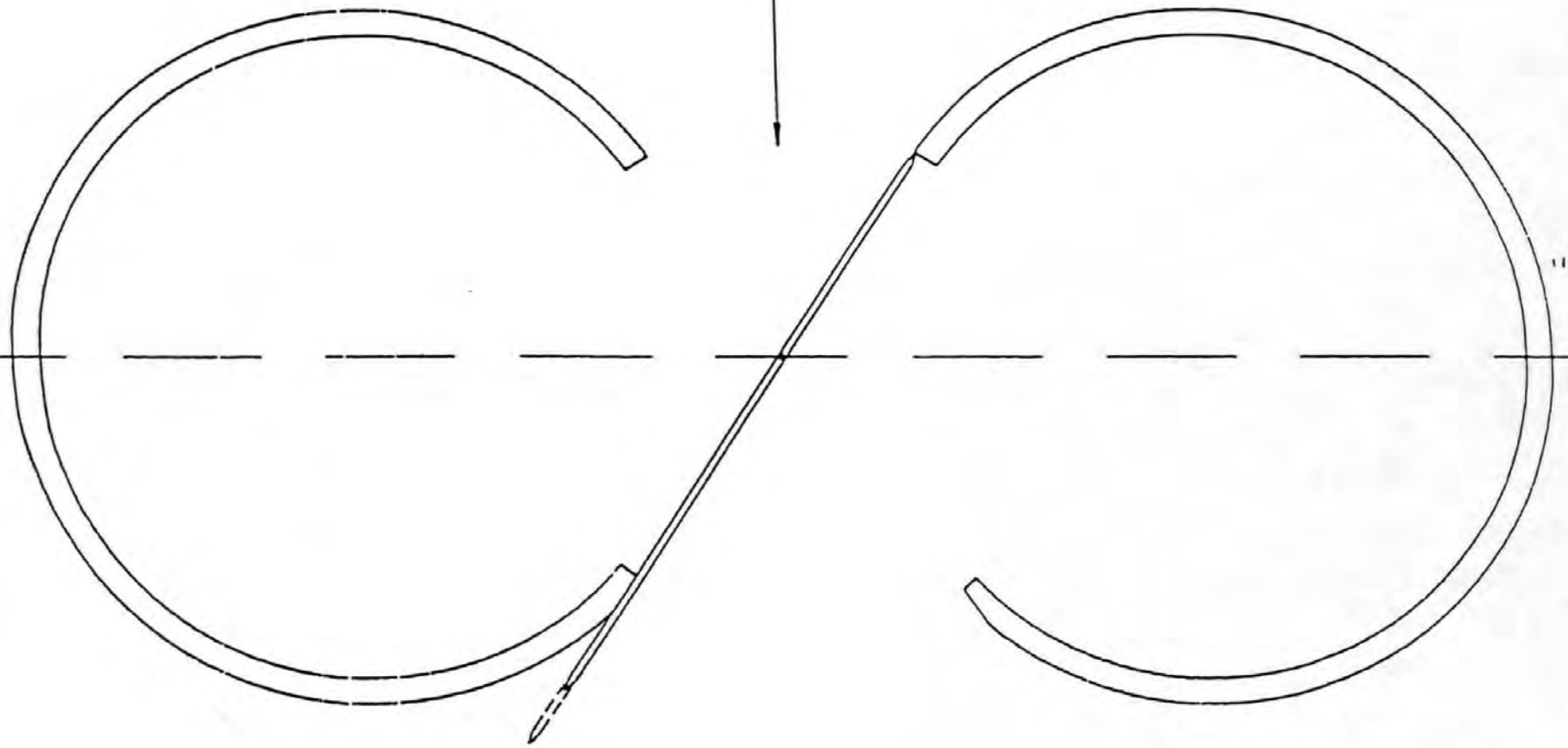
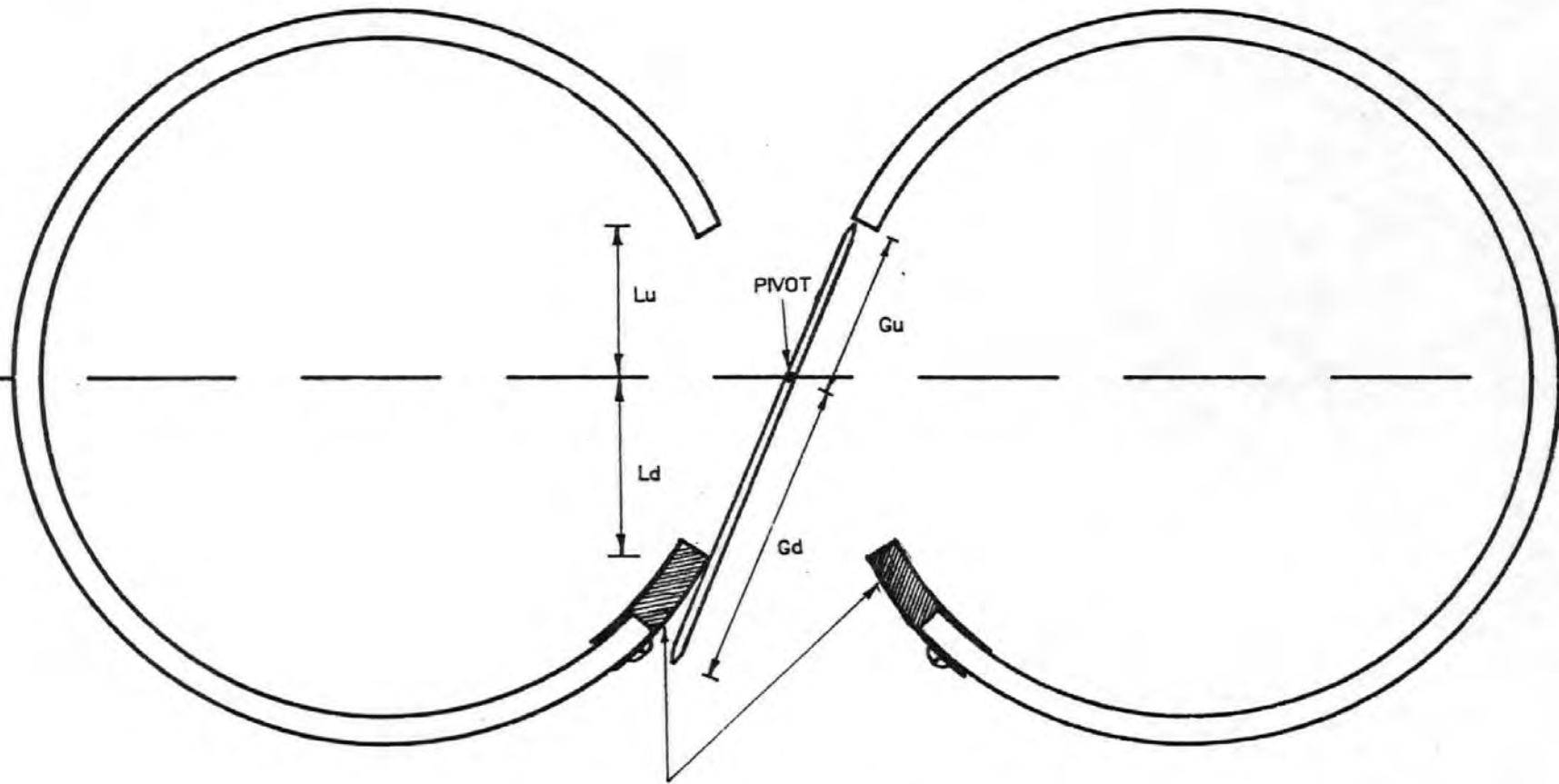


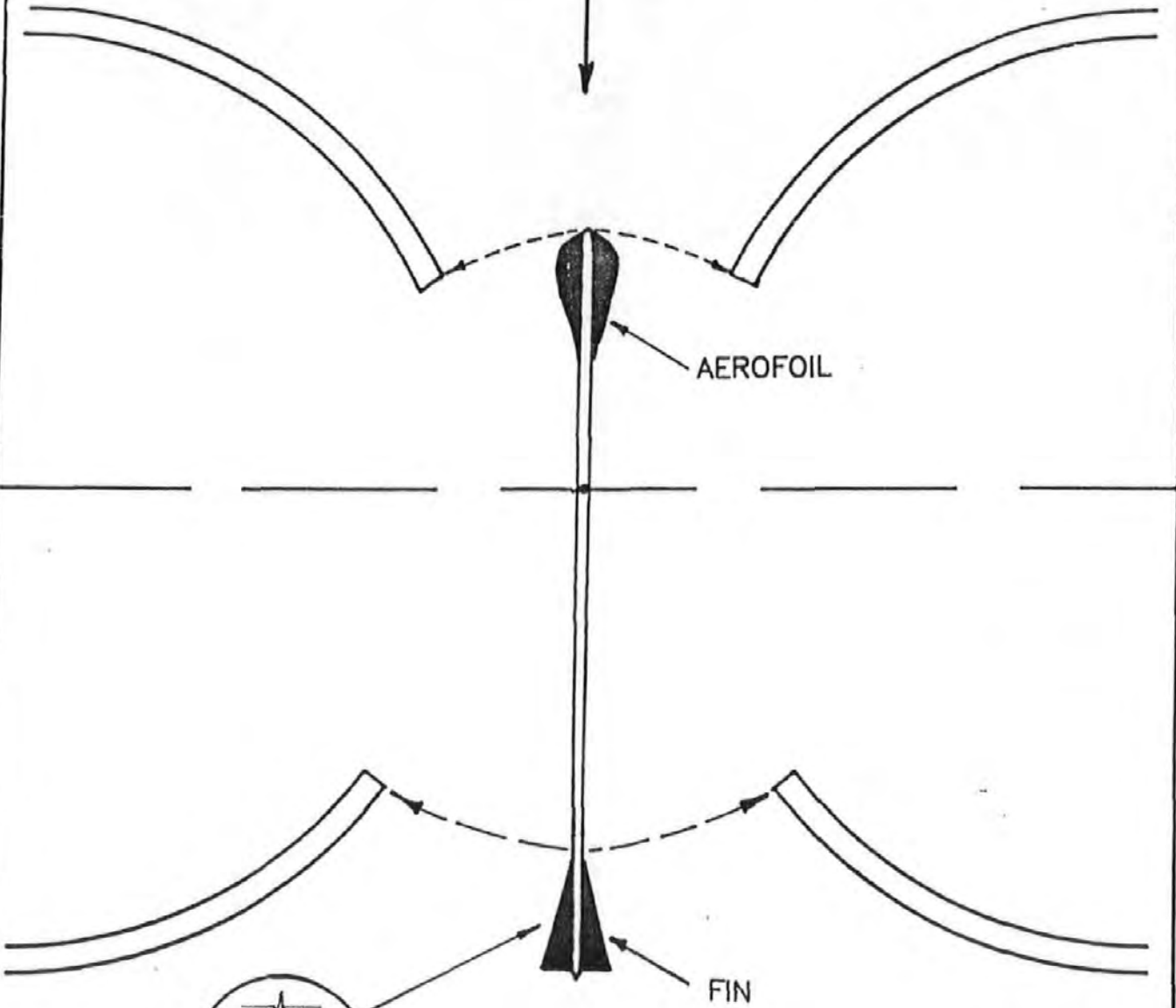
FIG. 3.2: MODEL NO.1 - NON SYMMETRIC GATE - 65 DEGREE ARC



ADJUSTABLE DOWNSTREAM OPENINGS

FIG. 3.3: MODEL NO.3.3 : DEFINITION DRAWING.

DIRECTION OF FLOW



ALTERNATIVE T-SHAPED
FIN DESIGN.

FIG. 3.4 :GENERAL ARRANGEMENT: AEROFOIL + FINS

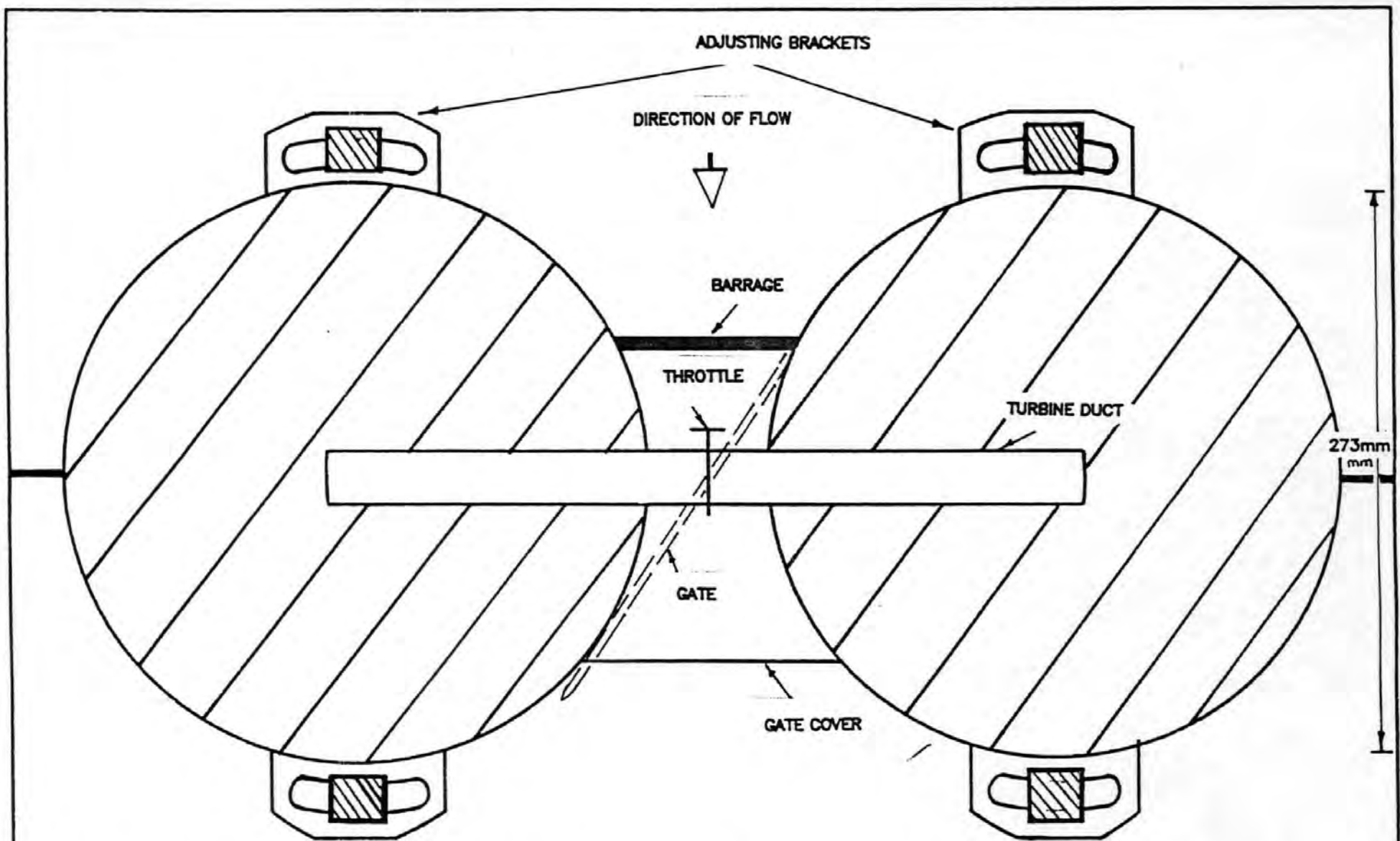


FIG 3.5: FINAL CONFIGURATION (PLAN) FOR MODELS 3:1, 3:2 AND 3:3
(65°, 55° AND 45° ARC RESPECTIVELY)

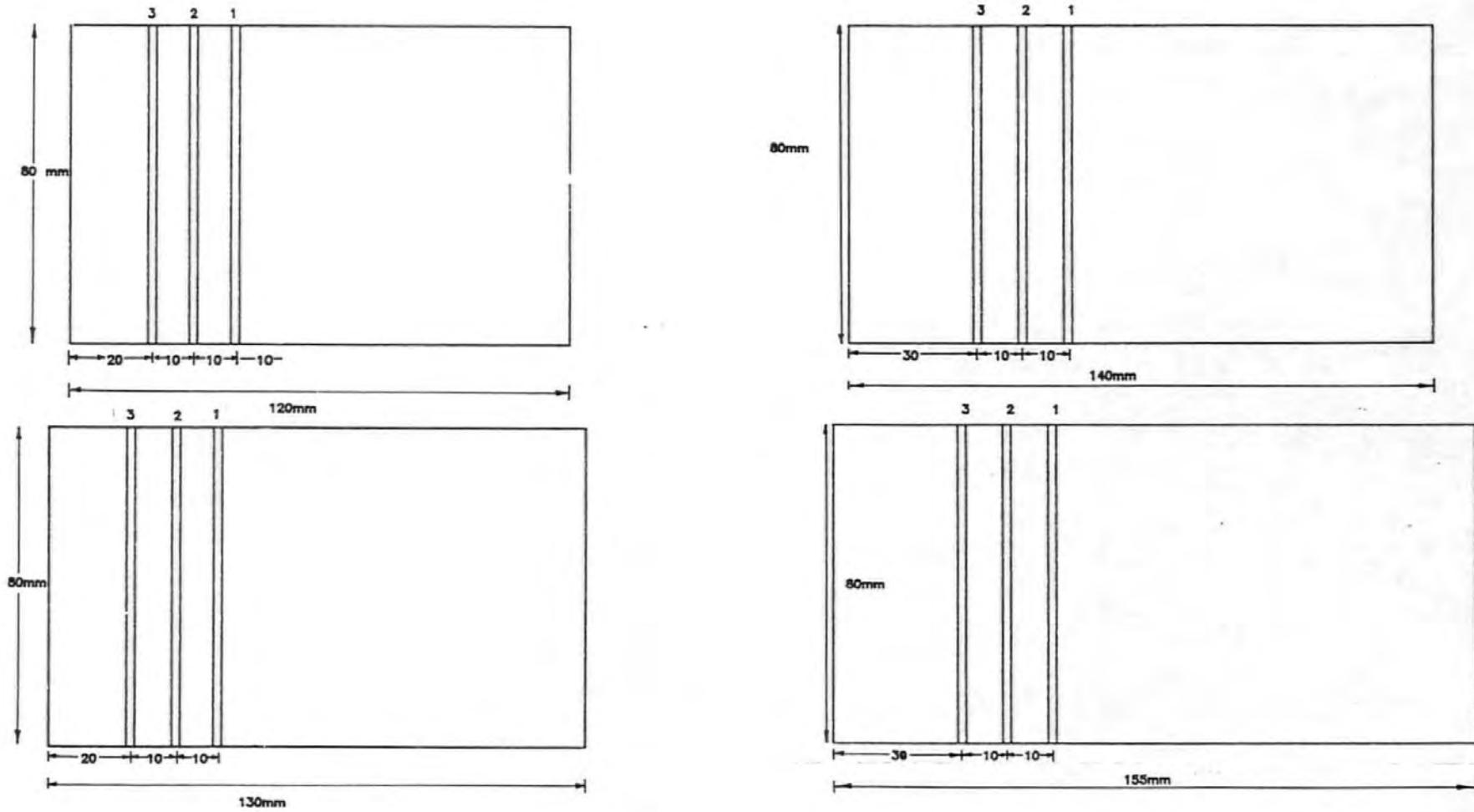


FIG. 3.6: ADJUSTABLE PIVOT GATES FOR MODEL 3.3

FIG. 3.7: STREAMLINES AS GATE COMMENCES TO OPEN

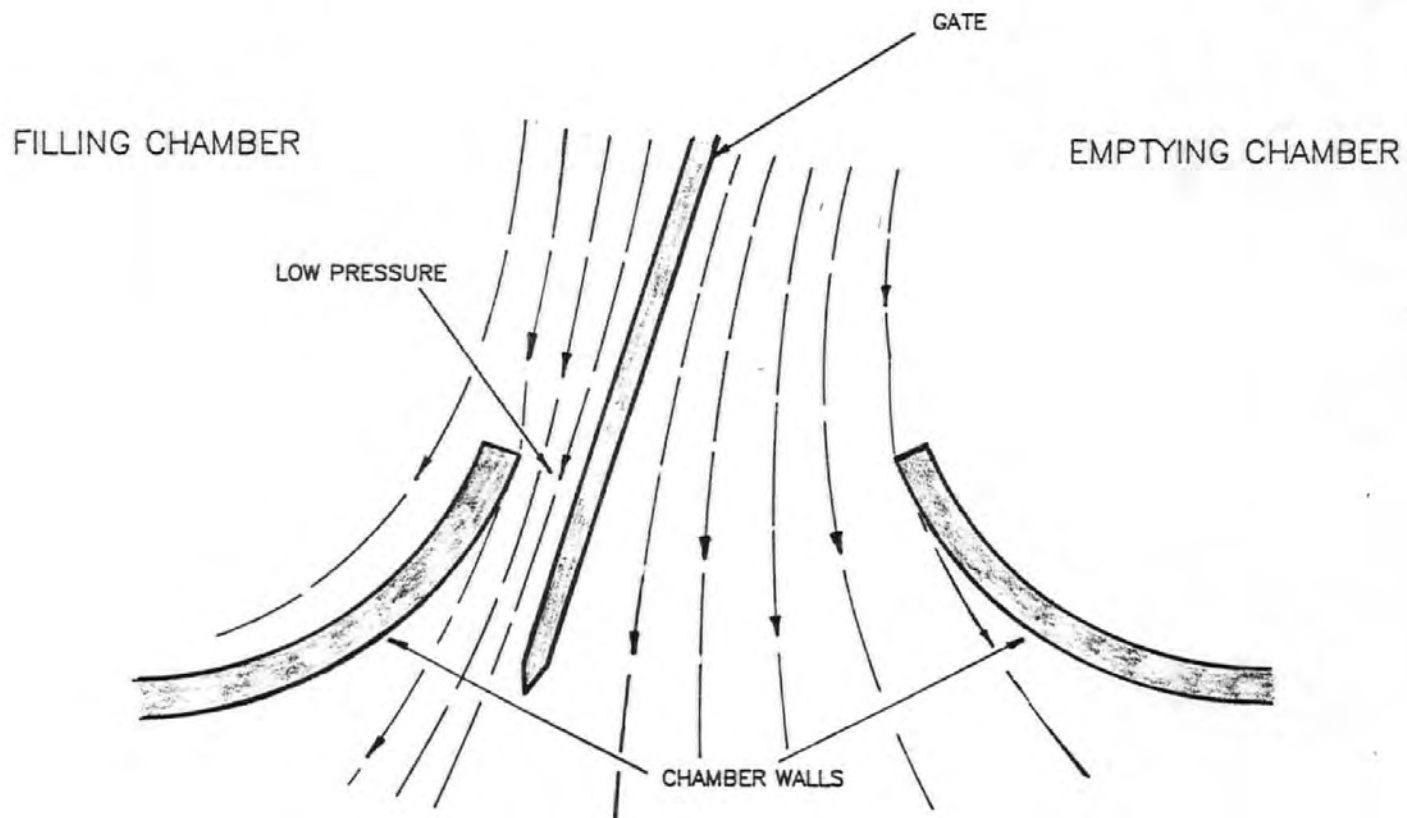


FIG. 3.8: INTRODUCTION OF CONVENTIONAL FIN

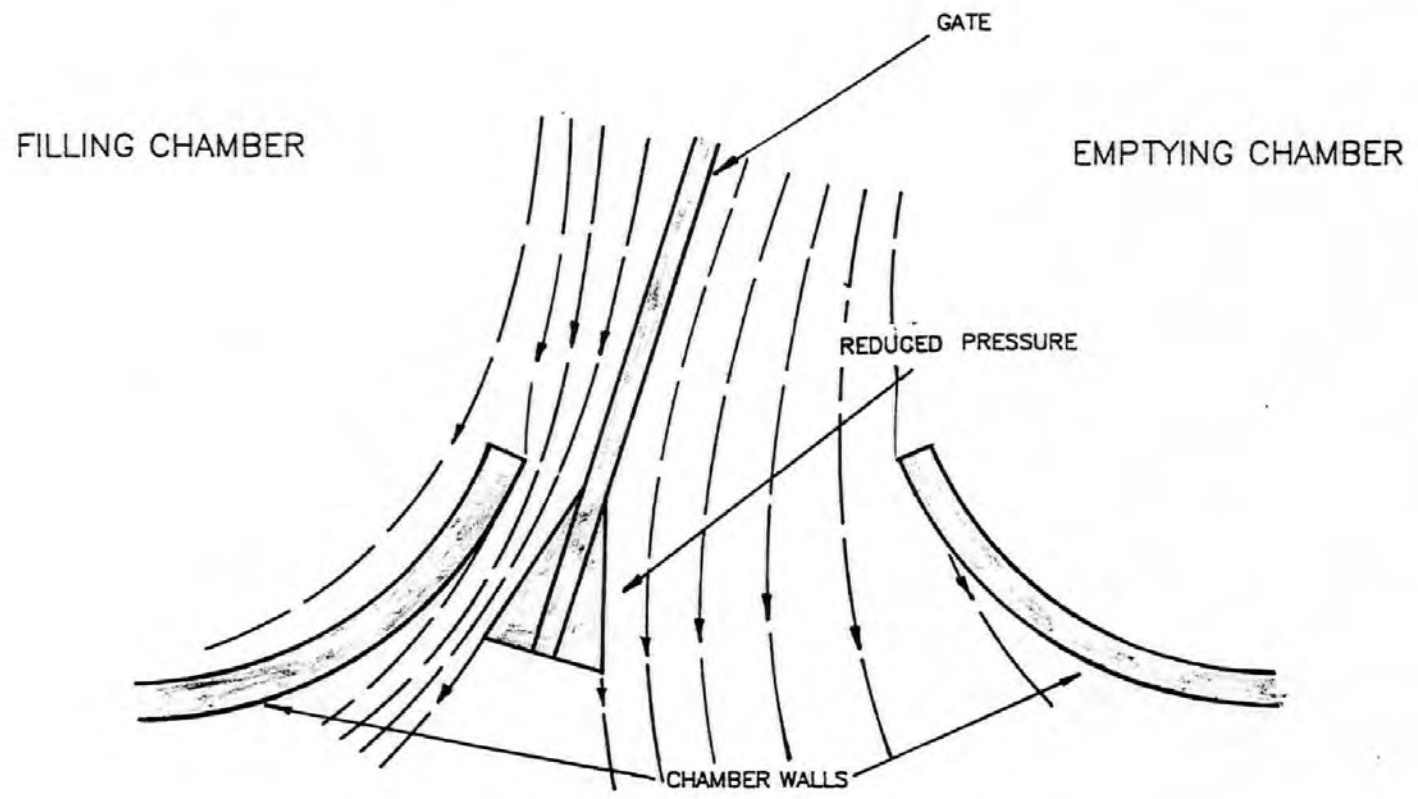


FIG. 3.9: INTRODUCTION OF T-SHAPED FLANGE

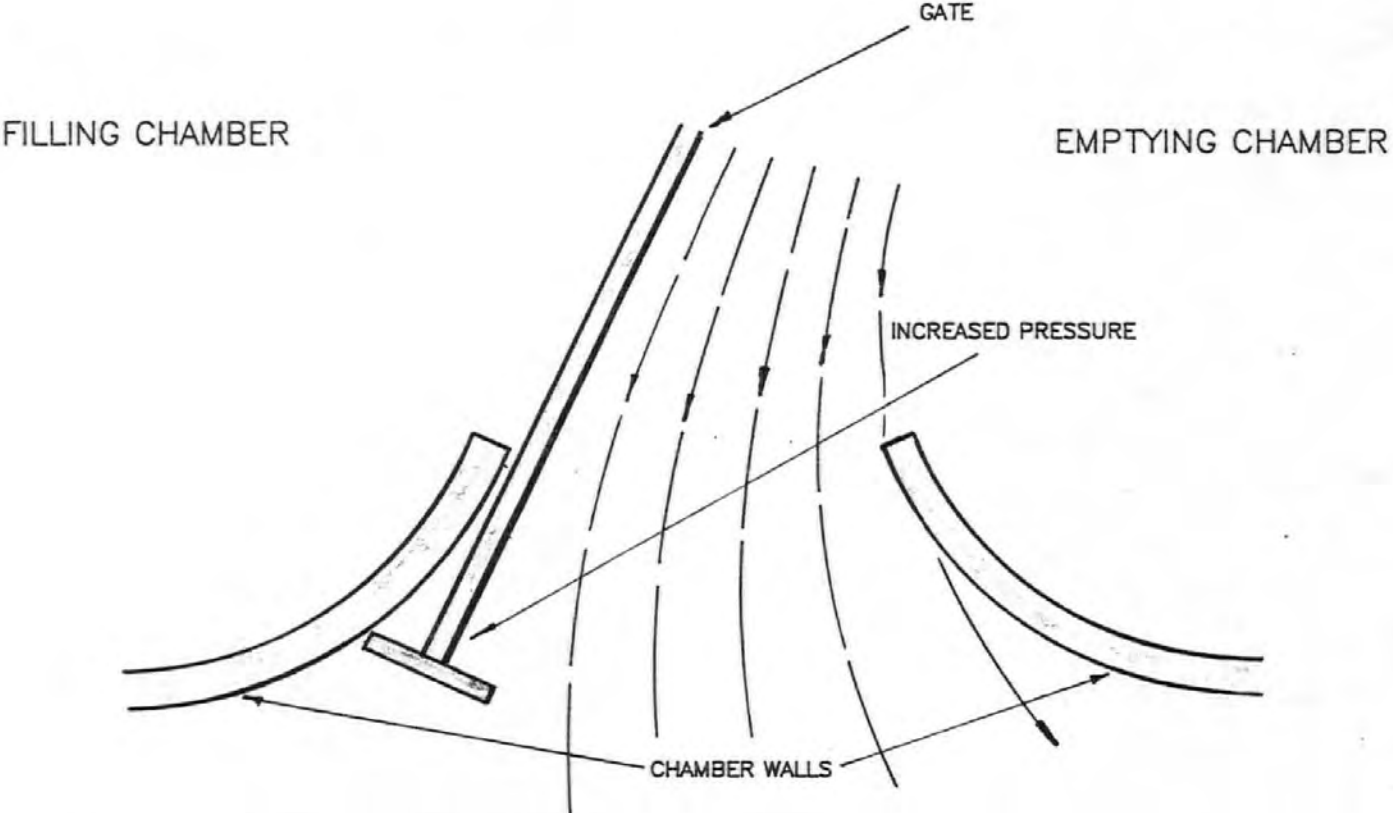


FIG. 3.10: INTRODUCTION OF SHAPED DOWNSTREAM EDGES

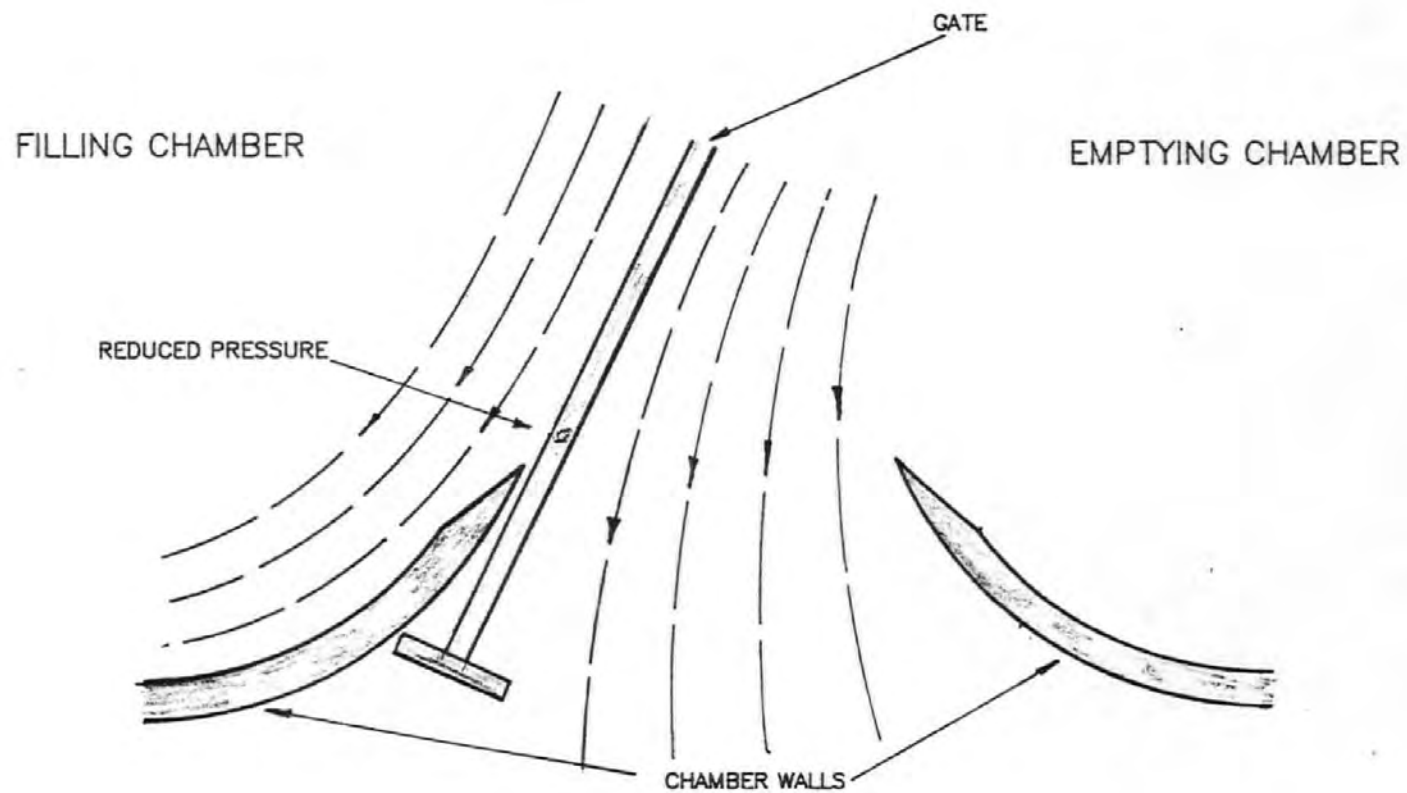


FIG. 3.12: SURFACE VELOCITY OF VORTICES
(AT TOP OF STROKE)

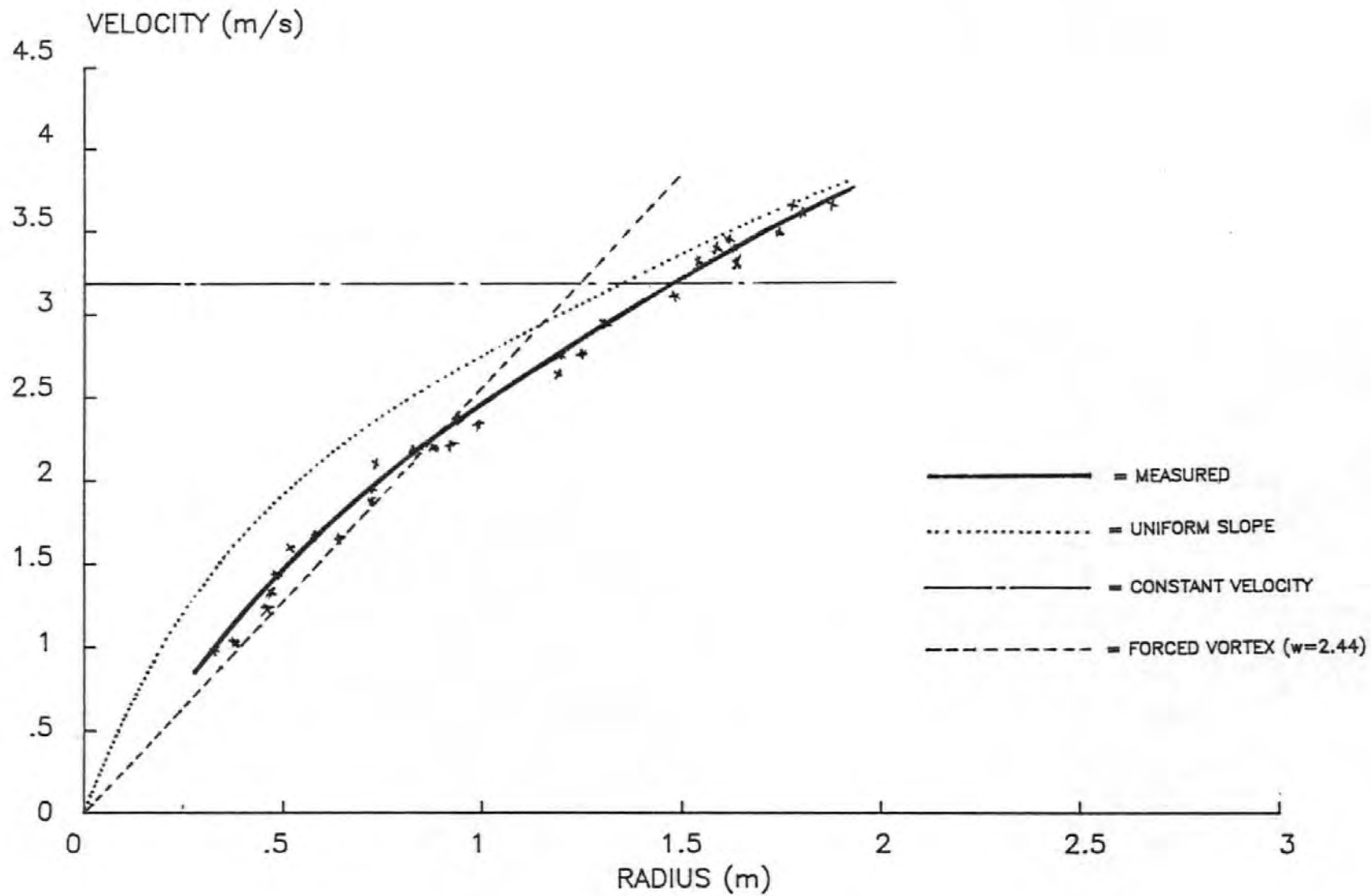
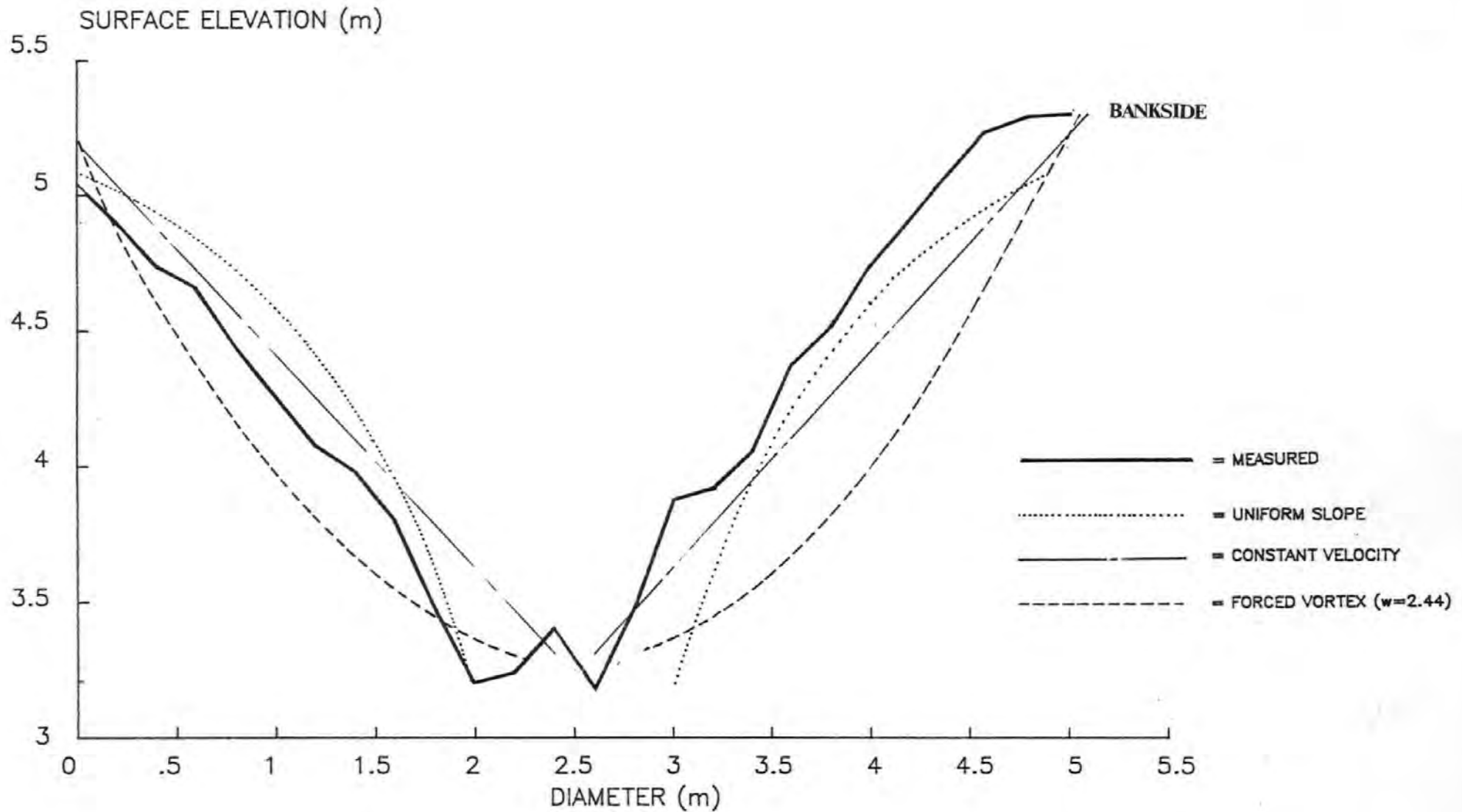


FIG. 3.13: SURFACE PROFILE OF VORTICES
(AT TOP OF STROKE)



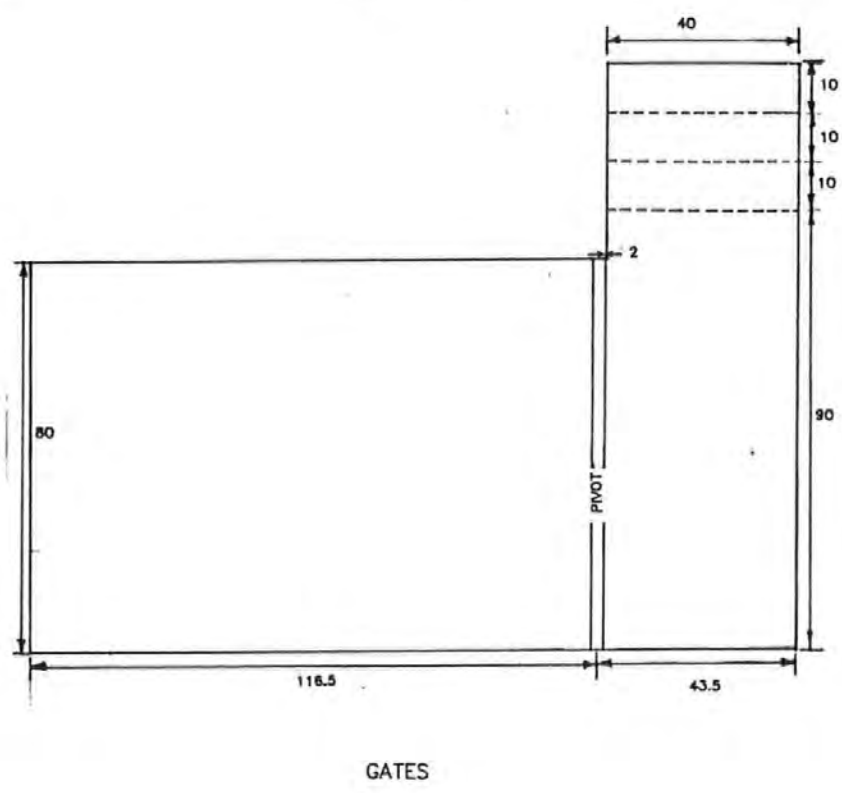
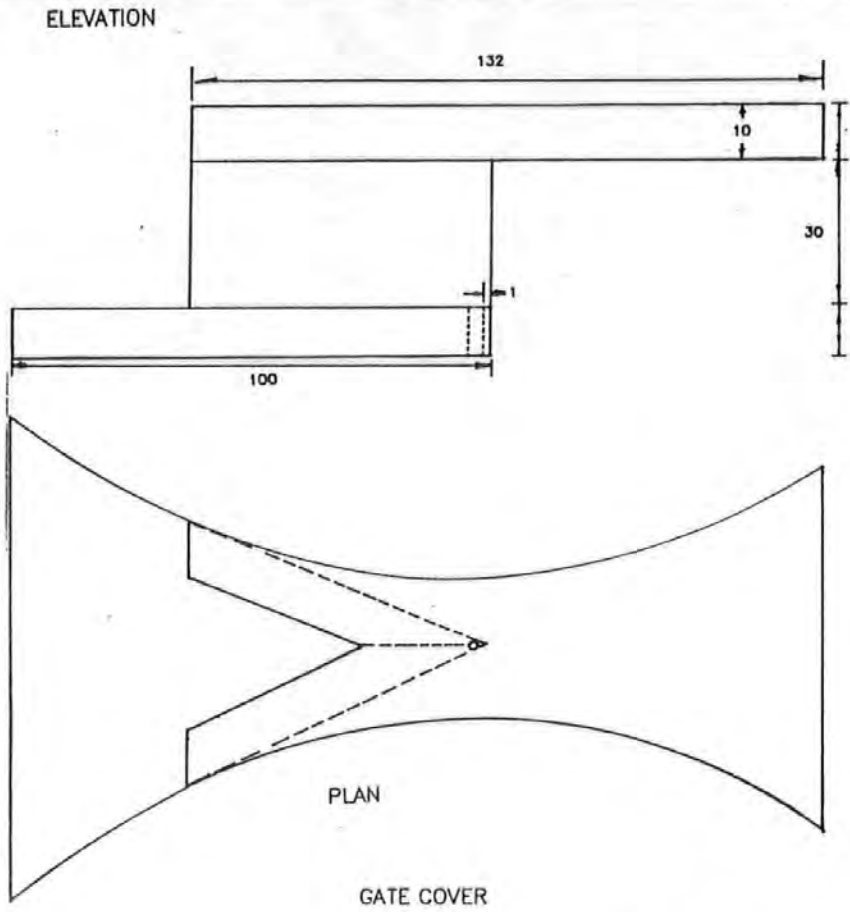


FIG. 3.14: STEPPED GATE DESIGNS.

4.0 : OVERVIEW OF THE MATHEMATICAL MODEL

4.1 Introduction

As has been previously explained in Section 1.3 it is not intended to reproduce a detailed analysis of the Mathematical Model. An overview of this analysis is presented in the following sections in order that the reader may understand the hydraulic, pneumatic and thermodynamic aspects of the model and appreciate the degree of flexibility inherent within its final structure.

This approach should serve as an introduction to the concept of a comprehensive, flexible mathematical model being utilized as a useful design tool in subsequent parametric and optimization studies.

4.2 Initial Approach

4.2.1 The Open Chamber Model

A lumped-mass approach to the hydrodynamics of the system is adopted in which the simplified motion of various masses of water are considered as a whole. Initially a model was developed for a single, rectangular chamber with one upstream gate and one downstream gate. In the model the three lumped masses of water considered at any one instant in time were:

- (a) The mass of water in the chamber above the centre of the gate opening.
- (b) The added mass of water upstream of the downstream gate.
- (c) The added mass of water downstream of the downstream gate.

The Inertias of these three masses are assumed to be linked in a dynamic system which is controlled by opening and closing the gates to the chamber. This approach is similar to that previously used to simulate the behaviour of the AUR Water Engine.² No turbine was included at the initial stage and the chamber was considered to be open to the atmosphere, the object being to attain a good approximation to the water flow. The required programme was written in Fortran 77 in segmented form suitable for use on an IBM AT personal computer. Solutions are obtained by stepping forward in the time domain using a variable-step Runge-Kutta routine based on a pair of fourth- and fifth- order methods attributable to Fehlberg.²¹ Both absolute and relative error criteria are taken into account when selecting the magnitude of the timestep, DT. Throughout the parametric testing of this thesis:

$$DT = 1/(2^{NDT}) \quad (4.1)$$

with $6 < NDT < 15$ so that DT lies between approximately 0.01563s and 0.00003s. By introducing this variable timestep continuity (see Section 4.5.1) can be maintained during those periods of the PWE cycle when absolute and relative error are at their greatest. This is most likely to occur at the water column turning points when there is an increased potential for instability as water surface accelerations and velocities tend to zero.

Further details of this initial programme can be found in the second part of Reference 19.

4.2.2 Calibration of the Initial Model

The initial "open chamber" model was calibrated against data obtained from the early physical tests for the AUR Water Engine²⁰ project. These tests involved the timing of the rise and fall of water within a square, sluice-gated chamber with a plan area of 0.51 m².

In a "Rise" test a known differential head was established across the chamber and the time taken for the rising water column to reach a maximum elevation recorded as the upstream gate was opened. The time taken for the gate to open was also recorded.

In a "Fall" test a known differential was established between the chamber water level and the downstream channel water level and the time of the fall of the water column recorded.

In both cases the water column exhibited a damped oscillatory motion about the respective upper and lower bounds of the stroke. (A water column stroke being defined as that distance between the mean minimum chamber water level and the mean maximum chamber water level). This oscillatory action was caused by the inherent inertia of the rising or falling water columns and its magnitude was recorded.

The results obtained from the initial mathematical model (PWEONE) are compared to those of the AUR physical tests in Figs. 4.1, 4.2 and 4.3. The same oscillatory action was predicted by PWEONE as was observed in the physical tests. These results were considered to represent a satisfactory level of agreement between the predictions of the mathematical model and the behaviour of the physical model. When making this comparison it must be remembered that the physical model test results cannot be considered error free as the turbulence and surging within the chambers can make it extremely difficult to select a

representative elevation for the upper and lower bounds of the water column strokes. Another factor which would introduce discrepancy is the lack of information concerning the variation of the gate velocity during opening and closing. The PWEONE tests assumed that this velocity remained constant over the known period of the gate action.

4.3 Further Development

Further development of the mathematical model and subsequent refining of the programme was constantly taking place throughout the project. The inclusion of a turbine model within the single chamber programme (PWEONE) was of primary importance as was the development of a twin chamber programme (PWETWO). The alternate passage of the airflow from one chamber to the other via the air turbine is simulated within PWETWO.

These developments also include a more precise approach to the modelling of the gate action. This became necessary in order to take into account those periods when both gates are open and also to allow for some leakage past a closed gate. In addition, the compressible and thermodynamic aspects of the airflow within the PWE are now modelled and the airflow can be assumed to be either isentropic or non-isentropic. The varying efficiency of the turbine during a cycle is also included in the manner described in Section 5.3.

In order to accommodate these changes it became necessary to consider the following masses of both air and water:

- (a) The added mass of water upstream of the upstream gate or gates.
- (b) The mass of water in the upper part of the chamber which is associated with flow through the upstream gate.
- (c) The mass of water in the upper part of a chamber which is associated with flow through the downstream gate.
- (d) The mass of water in the lower part of a chamber which is associated with flow through the upstream gate and which passes directly to the downstream gate.
- (e) The added mass of water downstream of the downstream gate or gates.
- (f) The mass of air in the chamber.

4.4 **Model Flexibility**

There are several physical features of the PWE in the final versions of the mathematical model that can be easily altered via an EDIT routine. This inherent flexibility allowed the parametric studies of Chapter 6 to be carried out with relative ease. These studies concentrated mainly upon the twin-chamber model (PWETWO) for which the following options are available:

Upstream and Downstream Channels: Both upstream and downstream heads and mass coefficients can be varied as can the physical dimensions of the channel.

Chamber Shape: The chambers can be either rectangular or circular in plan with vertical walls and variable dimensions.

Flow Control Gates: The gates are assumed to lie within the upstream and downstream walls of a rectangular chamber. If twin circular chambers are selected a single butterfly gate is assumed and the formation of the vortices detailed in Section 3.5.3 is simulated.

The gates can be set to operate:

- (i) independently as the water level within a chamber reaches specified elevations;
- (ii) linked, i.e. the upstream gate starts to open and the downstream gate starts to close in one chamber as the upstream gate starts to close and the downstream gate starts to open in the other chamber;
- (iii) as a single butterfly gate.

All dimensions of the gates can be altered as can the contraction coefficients, closure times and water elevations controlling the gate actions. A minimum opening equal to 0.5% of the maximum opening is always assumed to simulate leakage through imperfect gate seals.

Turbine: The turbine efficiency can either be set at 100% throughout the cycle or can vary with the differential pressure across the turbine. Turbine scale and Design Pressures are variable.

Thermodynamics: Air flow processes can be assumed to be isentropic or non-isentropic.

4.5 Governing Equations

The mathematical representation of a number of processes involving the various lumped masses of air and water are presented in this section. It is not intended to reproduce all the variations of these equations which take into account direction of flow, gate position etc. Neither is it intended to illustrate their derivation. Such detail, if required, can be found in Reference 19.

The basic notation for the mathematical model is illustrated in Fig. 4.4, whilst a complete listing can be found in Appendix II.

4.5.1 Continuity

Hydraulics: The flow of water within each chamber of a PWE must satisfy the relationship:

$$\dot{Y}A_p = Q_{UG} - Q_{DG} \quad (4.2)$$

where:

\dot{Y} = vertical velocity of the free surface of the water within a chamber.

A_p = cross-sectional area of the chamber.

Q_{UG} and Q_{DG} = Discharges through upstream and downstream gates

Airflow: Taking into account compressibility and assuming the process is both adiabatic and isentropic the absolute pressure (PA) and density (ρ) of the air can be related by the expression:

$$PA / \rho^{1.4} = \text{Constant} \quad (4.3)$$

However, this isentropic assumption implies that the isentropic efficiency of the turbine is 100%, whereas in reality the isentropic efficiency of a small air turbine could be as low as 60% with an increase in the entropy of the air as it passes through the turbine and a subsequent increase in the temperature of the air downstream. In the twin chamber system this will produce an increase in mean temperature until a thermodynamic equilibrium is established with a net loss of heat through the various boundaries of the system.

In this non-isentropic case the following relationship is used:

$$\frac{P_A}{\rho^{1.4}} = \frac{P_{Ar}}{\rho r^{1.4}} \exp \left[\frac{SS - SS_r}{CV} \right] \quad (4.4)$$

The mass-flow equation for a particular chamber is:

$$\frac{d}{dt} (\rho VOL) = \rho \dot{VOL} + \rho \dot{VOL} = - QT \quad (4.5)$$

This equation is applicable to both single and twin chamber PWE's.

4.5.2 Flow through an Upstream Gate

An extended form of the Bernoulli equation is applied to model flow both into and out of the chamber via the upstream gate. Although generally the flow through this gate will be into the chamber, this situation is reversed when the inertia of the flow has caused the water within the chamber to rise above the water level in the upstream channel. Flow into the chamber through this gate is considered positive and outward flow negative.

-Into the Chamber (ie QUG > 0):

$$D_{UC} + \frac{V_{UC}^2}{2g} + Z_{UC} = Z_{UC} + \frac{P_{UG}}{\rho g} + \frac{VJ_{IUG}^2}{2g} + \frac{CM_{UC}(D_{UC} + Z_{UC} - Z_{UG})}{g} \dot{V}_{UC} \quad (4.6)$$

Flow out of the chamber (i.e. QUG < 0) is modelled in a similar manner.

4.5.3 Flow through the Downstream Gate

Again an extended form of Bernoulli's equation is used and although flow will be, in the main, out of the chamber (flow considered positive) the opposite will be the case when inertia effects cause the water level within the chamber to be less than that in the downstream channel.

$$\begin{aligned}
Z_{DG} + P_{DG} + \frac{v_{IDG}^2}{2g} = D_{DC} + Z_{DC} + \frac{v_{DC}^2}{2g} + \frac{K_{ODG} V_{ODG}^2}{2g} \\
+ \frac{C M_{DC} (D_{DC} + Z_{DC} - Z_{DG}) \dot{V}_{DC}}{g} \quad (4.7)
\end{aligned}$$

Flow into the chamber via the downstream gate is considered to be negative and is modelled in a similar manner.

4.5.4 Flow of Water Within a Chamber

Where a circular chamber is being considered a special feature is taken into account. If the water enters in a tangential direction the angular momentum of the flow is considered to be conserved. This momentum is then passed to the outlet flow as it is subsequently discharged in a complementary tangential direction. In this situation, the resultant velocity at the air/water interface is estimated from:

$$\dot{Y}_R = (\dot{Y}^2 + V_T^2)^{0.5} \quad (4.8)$$

In non-circular chambers $V_T = 0$ so that $\dot{Y}_R = \dot{Y}$

(The full analysis of the vortices based upon the empirical data obtained from the testing of Section 3.5.3 can be found in Ref. 19).

In order to model all the possible flow regimes within the chambers the following combinations of flow through the upstream and downstream gate must be taken into account:

- (i) chamber water level rising, flow in through both the upstream and downstream gates;
- (ii) chamber water level rising, flow in through the upstream gate; flow out through the downstream gate;
- (iii) chamber level falling, flow out through both the upstream and downstream gates
- (iv) chamber water level falling, flow out through the downstream gate; flow in through the upstream gate.

Taking condition (ii) as an example, applying Bernoulli's equation between the upstream gate and the surface of the water within the chamber yields:

$$Z_{UG} + \frac{P_G}{\rho g} + \frac{V_{J_{IUG}}^2}{2g} = Y + \frac{P_A}{\rho g} + \frac{\dot{Y}_R^2}{2g} + \frac{C_{M_{UP}}(Y - Z_G) \dot{Y}}{g} + K_{IUG} \frac{V_{J_{IUG}}^2}{2g} \quad (4.9)$$

However, as only part of the jet from the upstream gate must expand to fill the whole chamber the remainder of the jet from the upstream gate is assumed to supply the flow out of the downstream gate. Application of Bernoulli's equation between the two gates yields:

$$Z_{UG} + \frac{P_{UG}}{\rho g} + \frac{V_{J_{IUG}}^2}{2g} = Z_{DG} + \frac{P_{DG}}{\rho g} + \frac{V_{IDG}^2}{2g} + \frac{C_{M_{UDP}} L \dot{V}_{IDG}}{g} + K_{UDP} \frac{V_{J_{IUG}}^2}{2g} \quad (4.10)$$

4.6 The Air Turbine

The development of the Wells Self Rectifying Air Turbine and the effect of its utilization within Oscillating Water Column devices has been discussed in Section 1.2.1. The apparent advantages of this method of power take-off have led to the inclusion of its characteristics within the mathematical model.

The operation of the Wells Turbine is more fully investigated in Chapter 5. The mathematical model utilizes the linear relationship between the pressure differential (P_D) across the turbine and the air flow rate (Q_A) through the turbine:

$$Q_A = K_T P_D \quad (4.11)$$

where K_T is a constant.

Performance tests on a 0.4 m diameter, single stage Wells Turbine carried out by the Central Electricity Generating Board²² have provided pressure/flow rate data from which an average value of K_T equal to $0.0005 \text{ m}^5/\text{Ns}^2$ has been determined. This value of K_T appears elsewhere in the literature²³ and is used as a reference value within the mathematical model such that:

$$K_T = S_T 0.0005 \text{ m}^5/\text{Ns}^2 \quad (4.12)$$

where ST is a dimensionless scale factor allowing the scale of the turbine to be altered within the programme. The significance of this scale factor is further investigated in Section 5.2.

4.7 Thermodynamics of the Airflow

The modelling of the thermodynamics of the compressible airflow takes into account both the convective entropy transfer which occurs as the airflow passes through the turbine and the entropy transfer with heat that occurs at the various boundaries of the sealed system. This concept is illustrated in Fig. 4.5.

4.7.1 Convective Entropy Transfer

The air within the chamber is assumed to be a uniformly mixed, ideal or perfect gas with constant specific heats. It is also assumed that the losses within the turbine duct can be neglected and the airflow through the turbine is adiabatic with no significant changes to its kinetic and potential energy.

The specific entropy of air entering the chamber downstream of the turbine is calculated from:

$$SS_2 = SS_1 + CP \ln \left[\frac{TEMPK_2}{TEMPK_1} \right] - RGC \ln \left[\frac{P_{A2}}{P_{A1}} \right] \quad (4.13)$$

the temporal rate of change of entropy can then be found from:

$$-S = SS(-QMA) \quad (4.14)$$

4.7.2 Entropy Transfer with Heat

A relatively simple heat transfer model is used in PWETWO. The build up of heat caused by the increase in entropy described in the previous section is balanced by a net heat transfer through the water, chamber walls and chamber roof. This model neglects thermal inertia; assumes that at any instant of time, the temperature is uniform throughout the air within a chamber and that evaporation and condensation can be neglected. The heat transfer rate (QH) at any boundary is represented by:

$$QH = (T_1 - T_2) CH \quad (4.15)$$

where $(T_1 - T_2)$ is the temperature difference across the boundary and CH is its overall thermal conductance.

The chamber air temperature is calculated using:

$$\text{TEMPK}_1 = P_{A1}/(r_1 \text{RGC}) \quad (4.16)$$

and the ambient temperature of the air and water outside the chamber is set at 13.96°C. The walls of the chamber are assumed to be steel and the roof concrete.

The rate of entropy outflow is calculated from:

$$S = QH/\text{TEMPK} \quad (4.17)$$

where TEMPK is the absolute temperature inside the chamber.

Having determined the net rate of entropy transfer from equations 4.14 and 4.17 the total entropy of the air in the chamber is estimated via the Runge Kutta technique and the specific entropy can then be calculated and air pressure determined from equation 4.4.

4.8 The Calibration of PWETWO

The data collected for the classification of the chamber vortices (see Section 3.5.3) was also used for the calibration of the twin, circular chamber option of PWETWO.

Assuming a model scale of 1:20 the period of a full-scale PWE cycle based on the data from the physical model tests of Section 3.5.3 is approximately 23 seconds and the mean water surface elevation at the top of the water column stroke is about 4.8 m. Upstream and downstream water surface elevations are equal to 6 m and 3 m respectively.

In order to simulate these tests using PWETWO the initial mean water surface elevations of chamber 1 and chamber 2 were set equal to the downstream and upstream water levels respectively. Although most of these parameters can be easily set within the PWETWO model a certain amount of trial and error is necessary before a suitable upper gate trigger level can be ascertained. This trigger level must result in a similar mean water surface elevation at the top of the water column stroke to that observed in the physical model tests. The trigger level eventually chosen was 4.6 m. The results from the first nine cycles of PWETWO operation are as follows:

Cycle No.	Period (s)	Y _{max} (m)		Y _{min} (m)		V _{Tmax} * (s)	V _{Tmin} * (s)	T _{fall} *
		1	2	(m/s) 1	(m/s) 2			
1	17.2	4.8	4.8	2.8	3.0	3.4	9.9	7.3
2	17.8	4.8	4.8	2.8	2.8	4.4	10.4	7.4
3	19.4	4.6	4.8	2.6	2.7	4.9	12.0	7.4
4	20.8	4.7	4.7	2.7	2.6	5.0	13.5	7.3
5	19.6	4.6	4.7	2.6	2.6	4.9	12.3	7.4
6	21.1	4.7	4.6	2.7	2.6	4.9	13.7	7.3
7	19.8	4.6	4.7	2.7	2.6	4.9	12.4	7.4
8	20.9	4.7	4.7	2.7	2.6	4.9	13.5	7.3
9	19.9	4.7	4.7	2.7	2.6	4.9	12.6	7.4

* = Chamber 1 Values

Comparing the ninth cycle results with the corresponding values from the hydraulic model:

	PWETWO	Hyd. Model
Cycle period	19.9s	23.0s
Y _{max}	4.7m	4.8m
Tangential velocity (VT max)	4.9m/s	4.5m/s

If the gate trigger level was slightly increased the PWETWO values could be brought closer to those of the hydraulic model tests. However, considering the accuracy of the laboratory data this was not considered worthwhile and the agreement between the two sets of data was considered to be sufficient to validate the mathematical model.

4.9 The Computer Program

At present there are two versions of the computer program, namely PWEONE and PWETWO covering the single chamber and twin chamber PWE respectively. There follows a brief description of each of the subroutines which should be read in conjunction with the flow chart for PWETWO shown in Fig. 4.6.

4.9.1 PWEONE and PWETWO

These are the master subroutines which provide much of the operational control for the programme. Their main functions are listed below:

- (a) Presets dimensions of the scheme.
- (b) Asks whether printout is required from subroutines.
- (c) Calculates initial values.
- (d) Adjusts the timestep value.
- (e) Calculates the turbine variables.
- (f) Updates the values.

4.9.2 EDIT and TEDIT

These subroutines provide an edit facility for changing the preset dimensions of a PWE.

4.9.3 GATE and TGATE

These subroutines calculate the variable dimension of both the upstream and downstream gate openings at time T for each of the three types of gate described in Section 2.2.

4.9.4 RKF2 and TRKF2

These subroutines carry out the Runge-Kutta, numerical solution of the governing differential equations. Error estimates EST are also calculated within these routines.

4.9.5 AIR and TAIR

These subroutines calculate both the gauge pressure and the rate of change in density for the air in the chamber.

4.9.6 WATER and TWATER

The water accelerations within the chamber and at the upstream and downstream gates are calculated here; for the twin chamber the six unknowns are evaluated by Gaussian elimination using partial pivoting.

4.9.7 CHECK and TCHECK

These subroutines check for continuity and adjust the water velocities if necessary.

4.9.8 GAMCAL and TGAMCAL

These subroutines calculate the error parameters for the dynamic variables and instigate a reduction in the timestep if the necessary criteria are not satisfied.

FIG. 4.1: PWEONE/AUR RISE TIMES
SLOW GATE

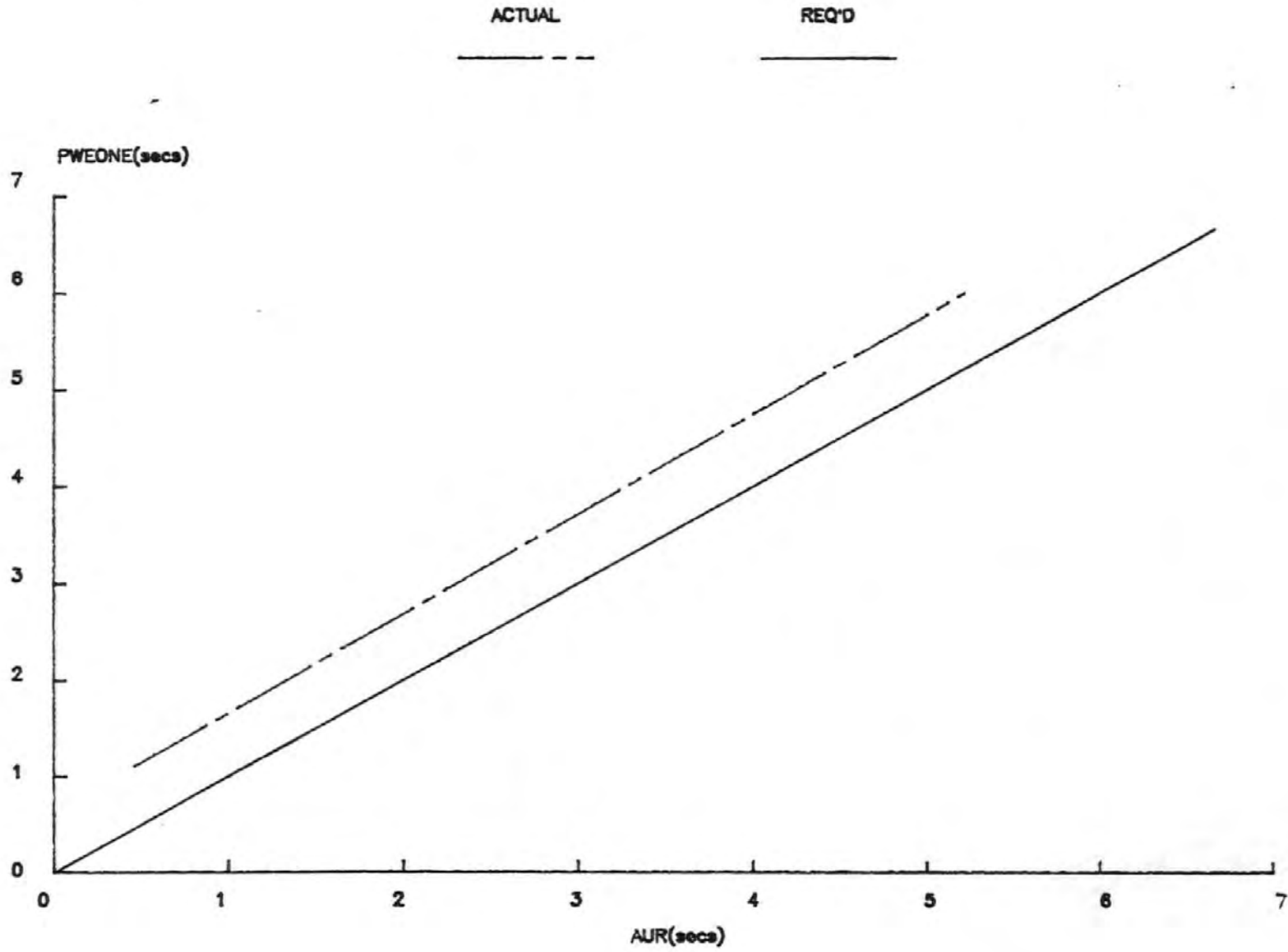
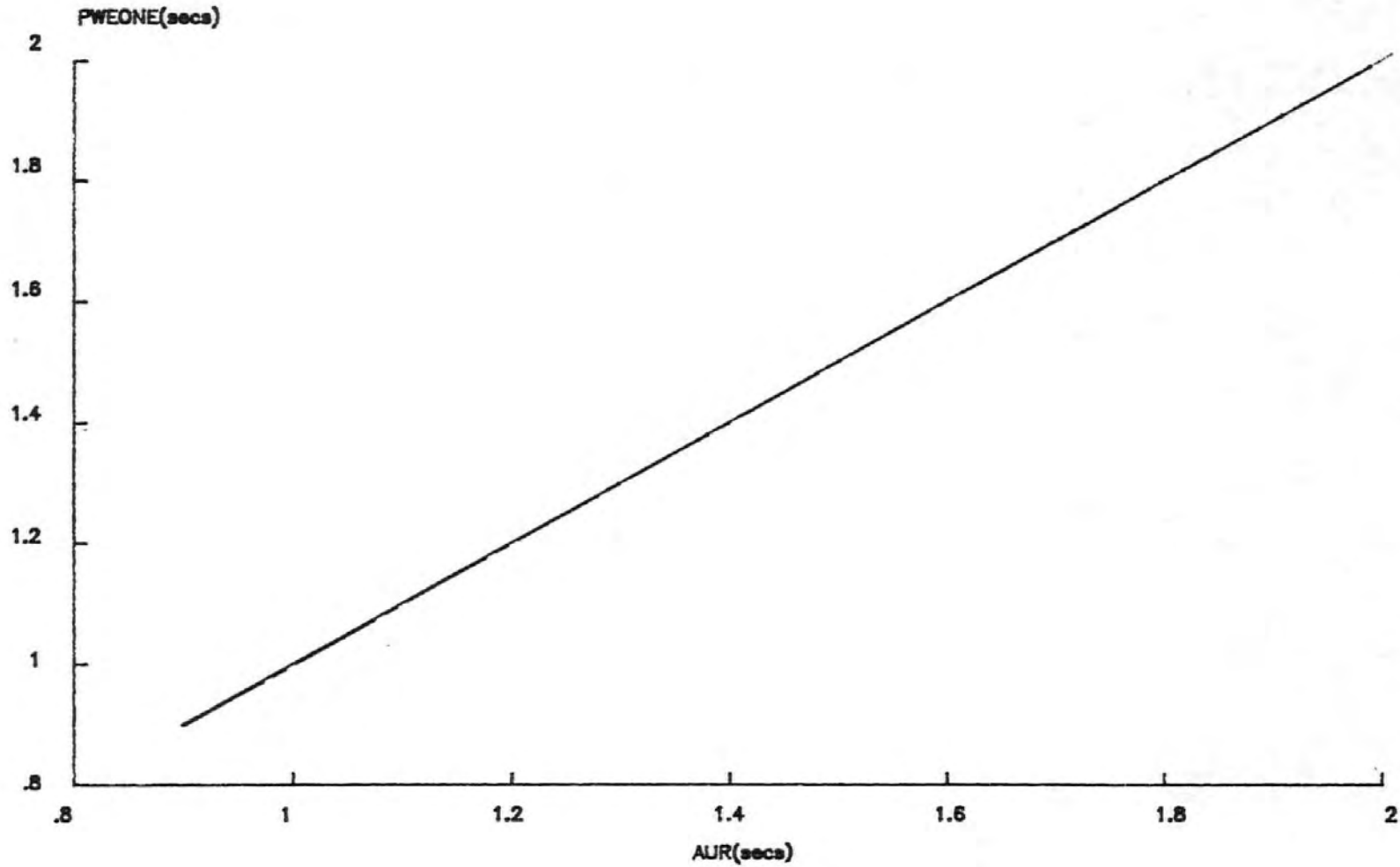


FIG. 4.2: PWEONE/AUR RISE TIMES
FAST GATE

ACTUAL REQ'D

----- _____



75

FIG. 4.3: PWEONE/AUR FALL TIMES

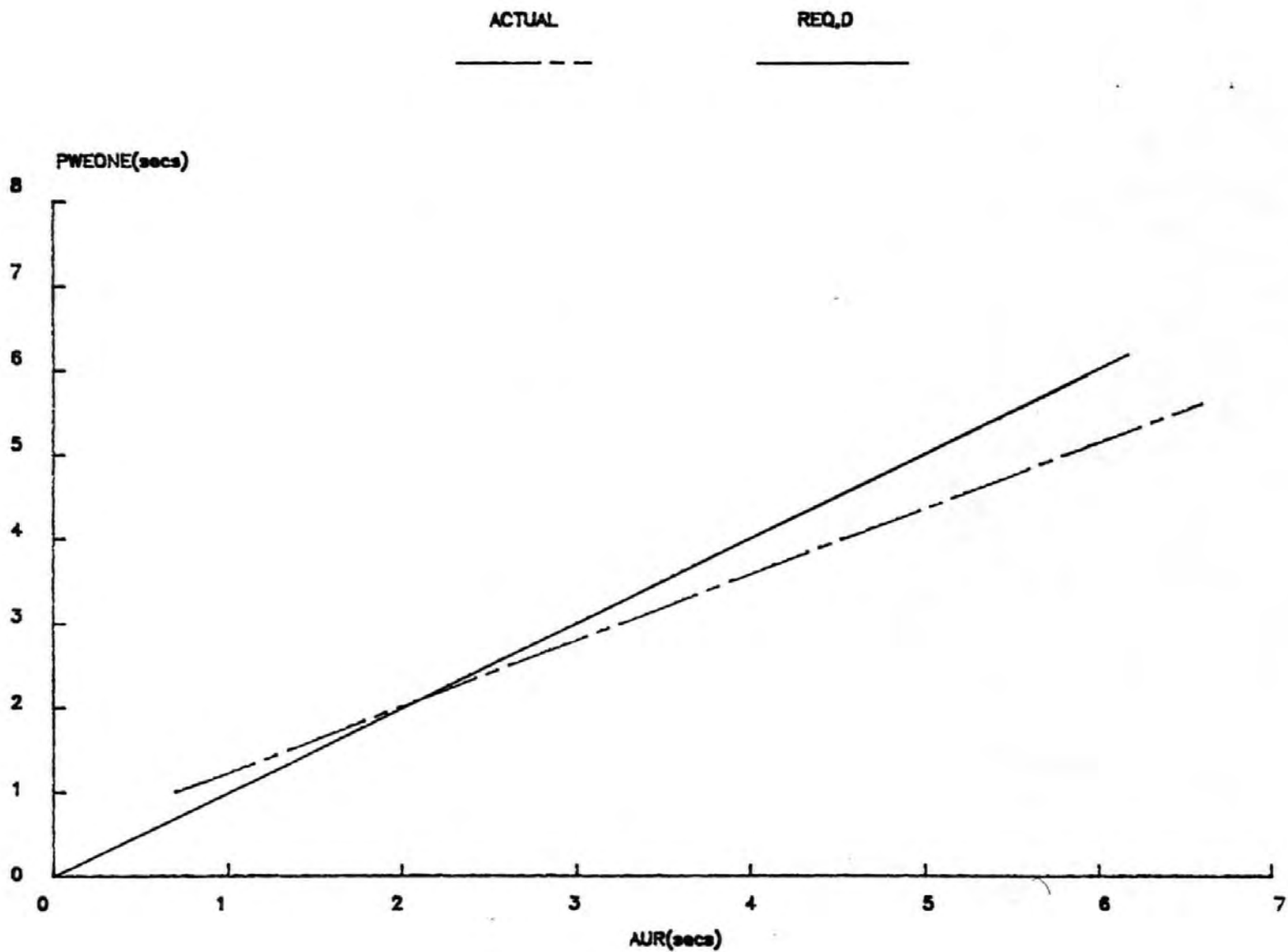
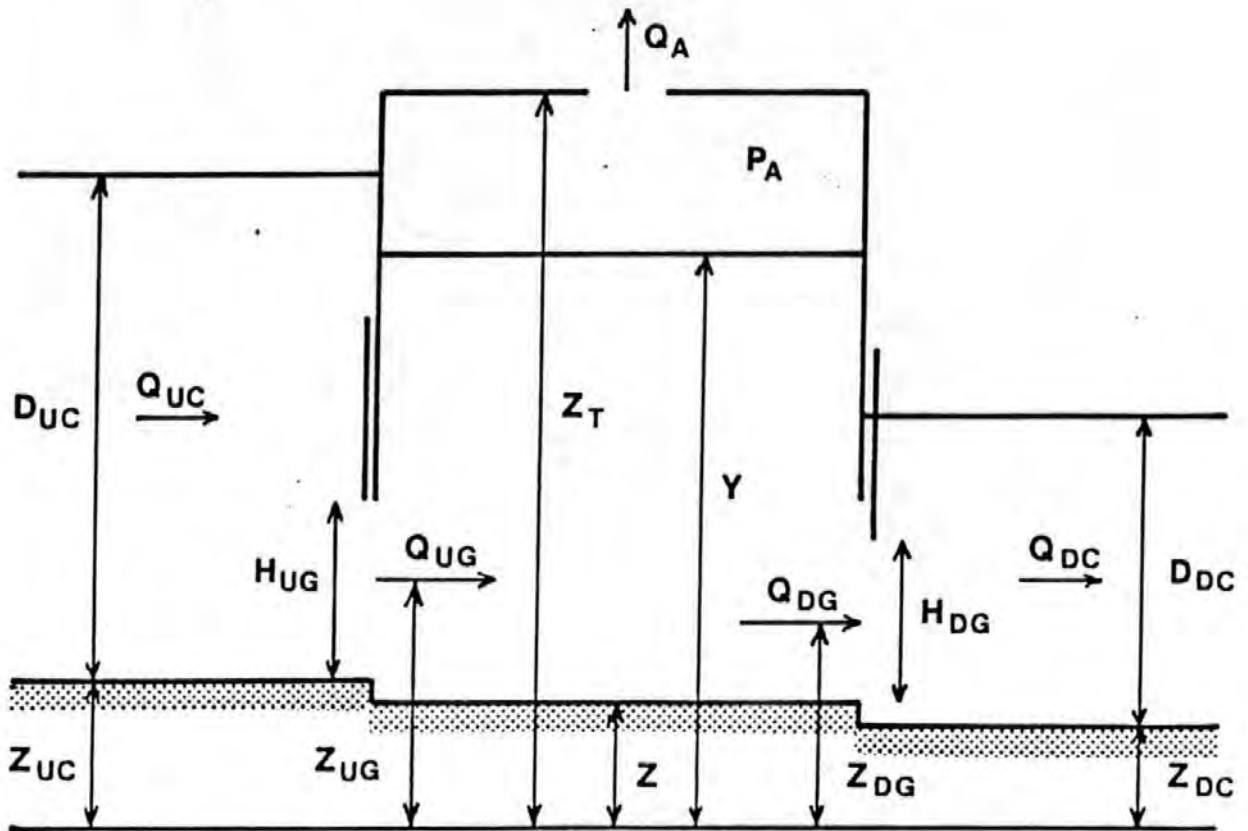
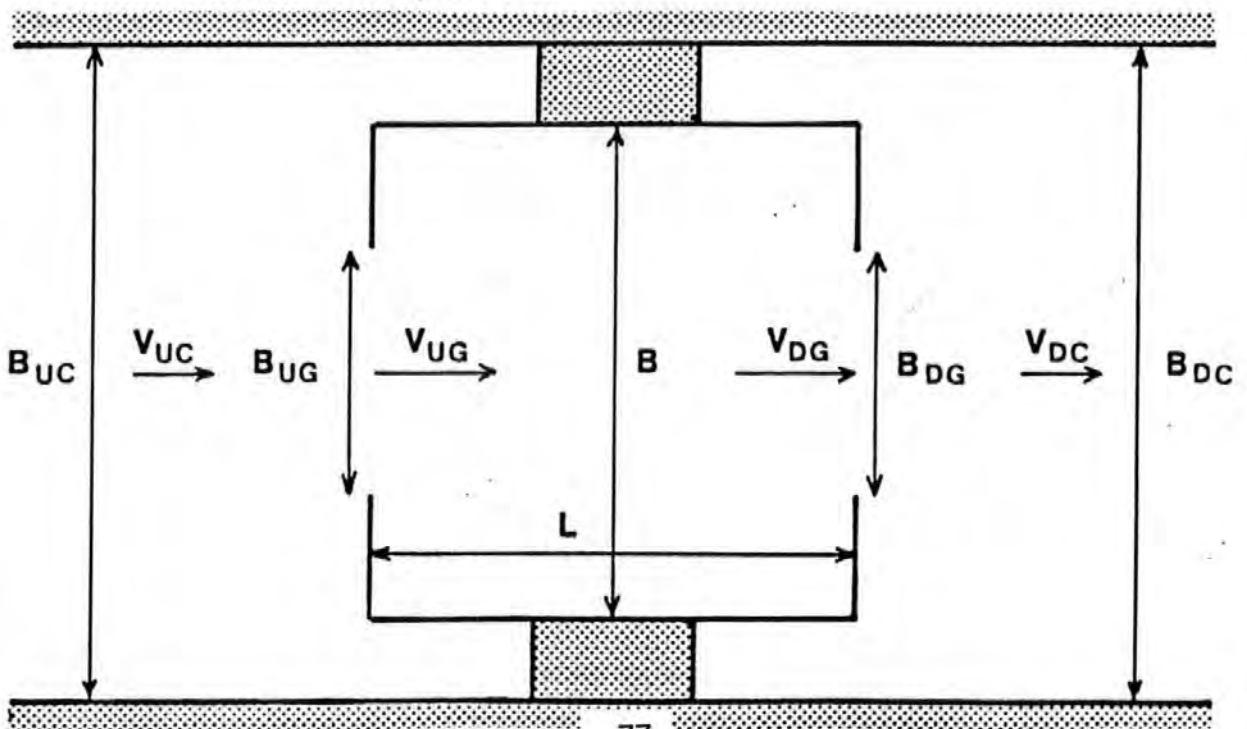


FIG. 4.4: BASIC NOTATION

ELEVATION



PLAN



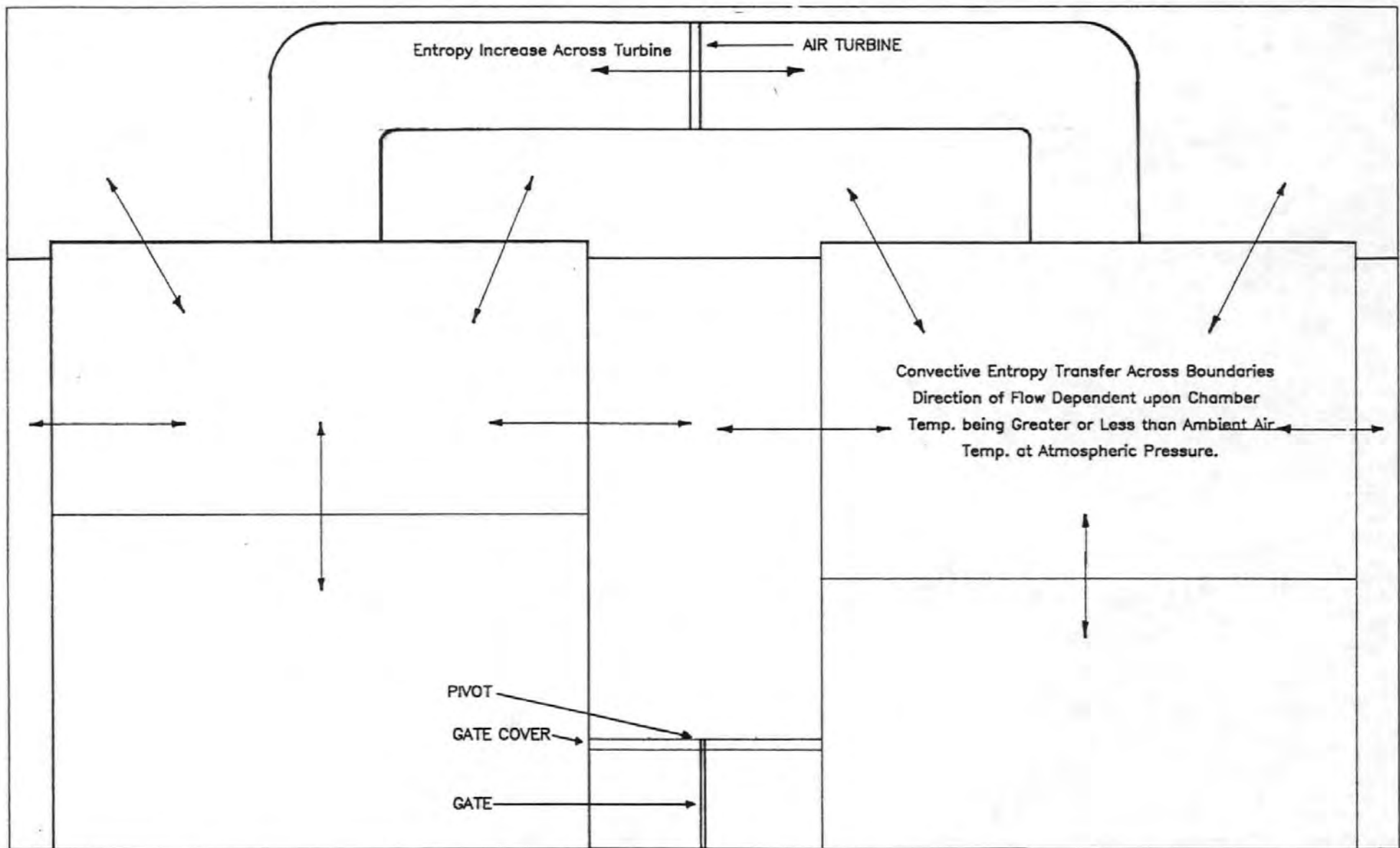


FIG. 4.5: TWIN CHAMBER PWE – THERMODYNAMIC ASPECTS

FIG. 4.6 FLOW DIAGRAM FOR 'PWETWO'

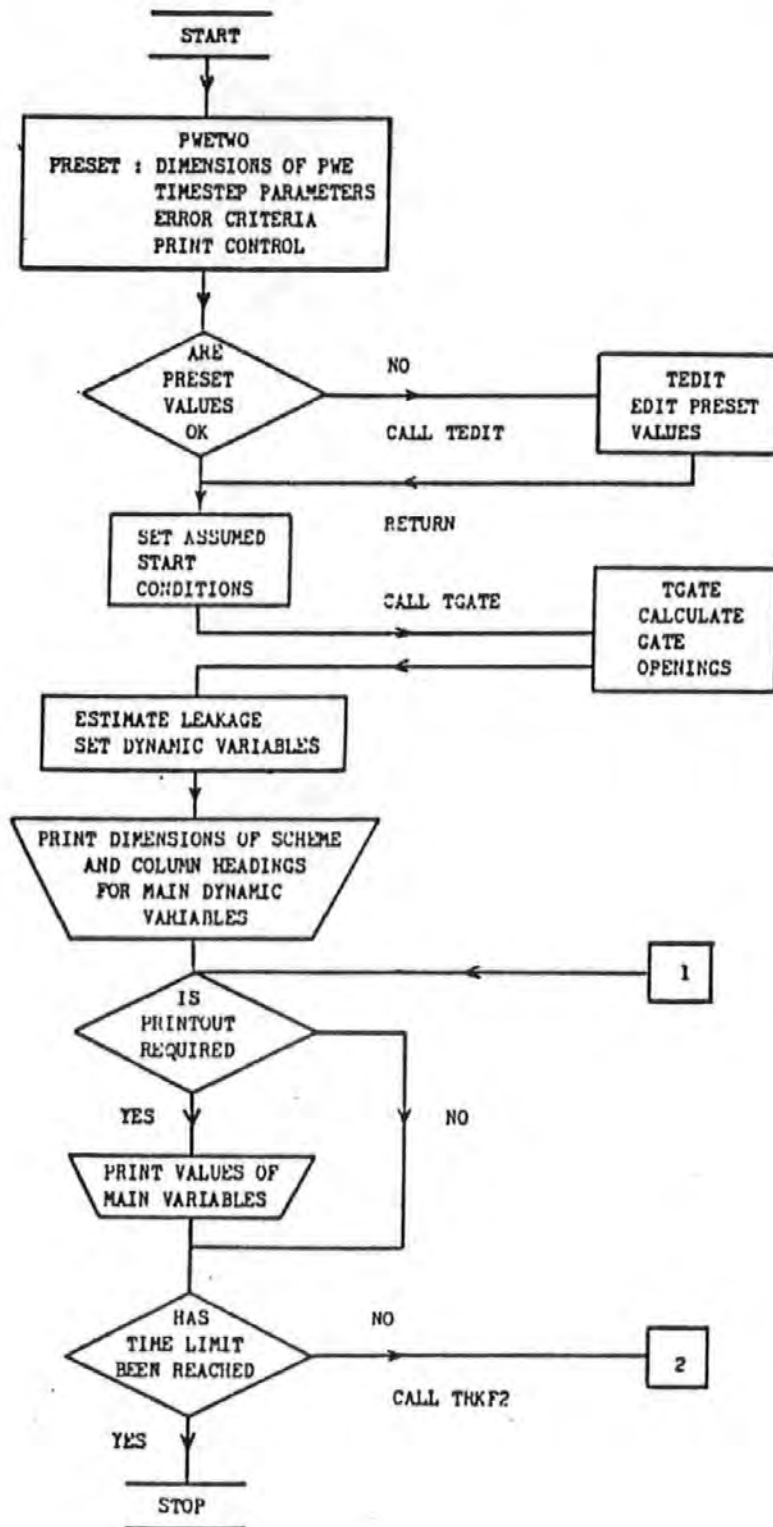
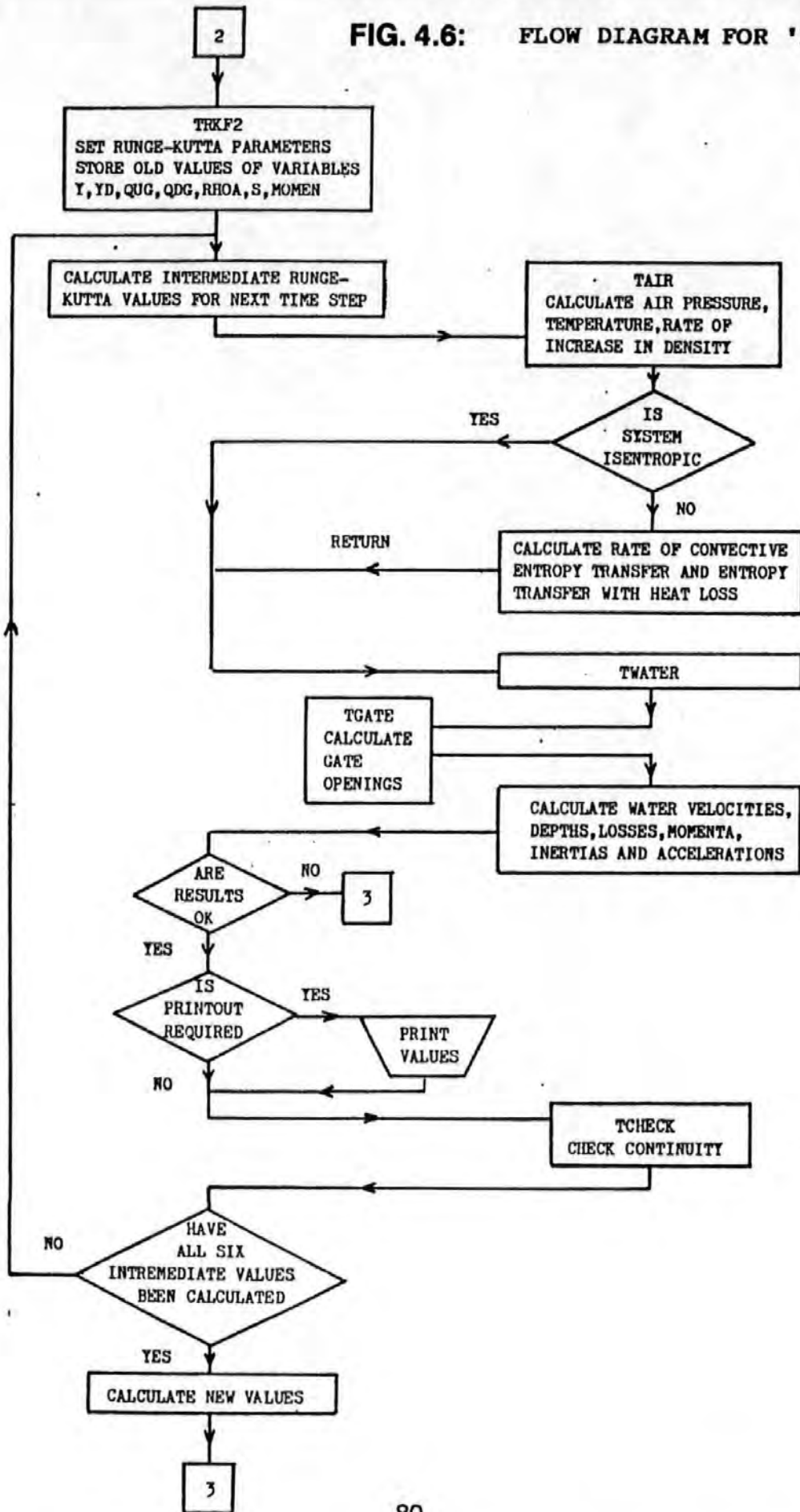




FIG. 4.6: FLOW DIAGRAM FOR 'PWETWO'



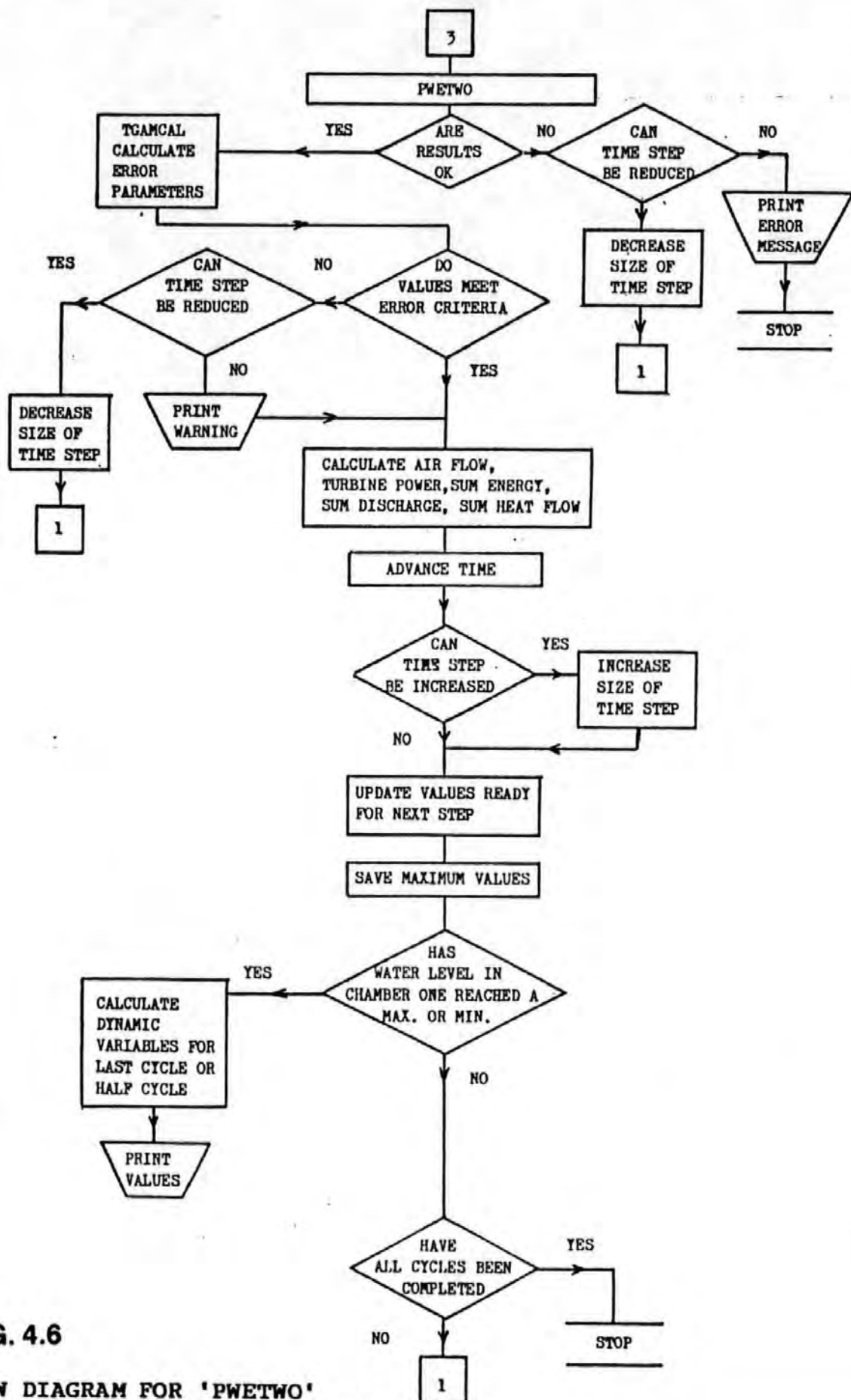


FIG. 4.6

FLOW DIAGRAM FOR 'PWETWO'

5.0 : THE WELLS TURBINE

5.1 Introduction

The Wells turbine was invented by Professor A. Wells of Queens University, Belfast¹³. It is a self-rectifying axial flow turbine suitable for extracting energy from reversed cyclic air flows. Even though such a cyclic airflow produces oscillating axial forces on the aerofoil blades the tangential force is always in the same direction (see Fig. 5.1) causing the rotor to rotate without the need for complex rectifying flap valves. It is essentially a high speed system which can therefore be coupled to a conventional electrical generator.

The tangential force F_t and the normal force F_x on an element of length of an isolated aerofoil can be expressed as:

$$F_t = L \sin \alpha - D \cos \alpha \quad (5.1)$$

$$F_x = L \cos \alpha + D \sin \alpha \quad (5.2)$$

where:

L = Lift force

D = Drag force

If the angular velocity of the rotor is w and the axial velocity of the airflow is V_x , the relative velocity (w) is at an angle α as shown in Fig. 5.1, resulting in a power output $F_t w r$ at a radius r . Any variation in V_x will result in variations of power output unless the rotor possesses sufficient inertia to overcome such fluctuations.

5.2 The Scale Factor

Tests carried out by the Central Electricity Generating Board²² have confirmed that the Wells Turbine acts as a linear orifice and that the air flow rate through the turbine (Q_A) is therefore a linear function of the pressure drop (P_D) across the turbine.

$$\text{i.e. } Q_A = K_T P_D \quad (5.3)$$

where K_T is a constant. Deviations from a perfectly linear relationship do occur, but these are generally small and are not easy to predict in the absence of empirical data. Consequently, a linear discharge relationship is assumed.

Performance tests^{22,23} on a 0.4 m diameter, single stage Wells Turbine operating at constant speed suggest an average value of K_T of about $0.0005 \text{ m}^5/\text{Ns}^2$. This value is used as a reference value within the mathematical model such that:

$$K_T = S_T 0.0005 \text{ m}^5/\text{Ns}^2 \quad (5.4)$$

Inclusion of the scale factor S_T enables the scale of the turbine to be altered within the programme. The power output from the turbine is assumed to be a simple function of the air flow rate (Q_A) and the pressure drop.

Once the value of S_T has been set, it remains constant throughout each PWE cycle in both PWEONE and PWETWO. This implies that the turbine is running at a constant speed. In practice a near constant speed could be achieved by connecting the turbine to the local grid via an induction motor/generator. During any PWE cycle the turbine would therefore be either supplying power to the local grid or would be driven by the motor at a near synchronous speed during periods when the mass flowrate through the turbine was not sufficient for that speed to be attained. This mode of connection was adopted in the Norwegian wave energy device at Toffestallen¹⁵. It has been found, however, that a suitable flywheel attached to the turbine shaft is also necessary to smooth turbine speed fluctuations during an oscillating water column (OWC) cycle. This will be an additional feature of the two 500kW OWC devices being installed by Kvaerner Brug on the island of Tonga²⁴, Fiji.

It is envisaged that this mode of operation would be most suitable in UK type situations where local supply is generally available. In a developing country however it would be necessary to operate the turbine at variable speed in the majority of situations. Unfortunately the varying torque data necessary for the successful modelling of the dynamics of the turbine operating in this mode is unavailable.

Having established the air flowrate through the turbine the power output (POWT) can be calculated from:

$$\text{POWT} = \text{EFFT } Q_A P_D \quad (5.5)$$

The efficiency (EFFT) of the turbine can be set at 100% or a variable efficiency can be selected. This variable efficiency is derived in the manner described in the following section.

5.3 The Design Pressure Differential

Dr. T. Whittaker of Queen's University, Belfast has supplied an efficiency curve (Fig. 5.2) that can be considered suitable for a turbine operating under the differential pressure regime of a twin chamber PWE with a 3 m head differential.

Extensive tests on the Wells Turbine carried out at Queens University, Belfast²⁵ indicate that it is reasonable to assume that:

$$P^* / \phi = \epsilon \quad (5.6)$$

Where: $P^* = \frac{P_D}{4 \cdot \rho_{\text{atmos}} \cdot U_T^2} =$ non-dimensional pressure drop across the turbine

$$\phi = \frac{V_x}{U_T} = \tan \alpha$$

ϵ = constant for a particular design of turbine.

U_T = tangential velocity at tip of turbine rotor.

ρ_{atmos} = density of air at normal atmospheric pressure (kg/m^3).

Assuming the axial velocity of the airflow is constant with annulus radius the discharge Q_A through a turbine of diameter D_T is given by:

$$Q_A = \frac{\pi (D_T^2 - D_H^2) \cdot V_x}{4} \quad (5.7)$$

or, using pressure/flowrate data:

$$Q_A = S_T K_T P_D \quad (5.8)$$

Therefore:

$$V_x = \frac{4 Q_A}{\pi (D_T^2 - D_H^2)} \quad (5.9)$$

or:

$$V_x = \frac{4 S_T K P_D}{\pi (D_T^2 - D_H^2)} \quad (5.10)$$

Therefore:

$$\tan \alpha = \frac{4 Q_A}{\pi (D_T^2 - D_H^2) U_T} = \frac{4 S_T K_T P_D}{\pi (D_T^2 - D_H^2) U_T} \quad (5.11)$$

The efficiency curve of Fig. 5.2 shows that maximum efficiency is achieved at $\tan \alpha = 0.15$. If the area of the annulus and the turbine speed were so selected that:

$$\tan \alpha = \frac{4 Q_{AD}}{\pi (D_T^2 - D_H^2) U_T} = \frac{4 S_T K_T P_{DD}}{\pi (D_T^2 - D_H^2) U_T} = 0.15 \quad (5.12)$$

where Q_{AD} and P_{DD} are the 'design' values of the flow rate through the turbine and the pressure differential respectively, then it is possible to replot the efficiency curve of Fig. 5.2 in terms of Q_A/Q_{AD} and P_D/P_{DD} using:

$$\tan \alpha = \frac{0.15 Q_A}{Q_{AD}} = \frac{0.15 P_D}{P_{DD}} \quad (5.13)$$

as shown in Fig. 5.3.

This means that for any turbine of given dimensions operated at a particular constant speed there exists a 'design' pressure differential at which maximum *overall* turbine efficiency is achieved, i.e. average output over a complete oscillating water column cycle is optimised.

This situation is analogous to the 'design point' of a conventional water turbine at which, under a defined set of conditions, the hydropower installation is required to achieve maximum efficiency.

A PWE differs from a conventional hydropower installation in that the pressure differential and hence the flow through the turbine is constantly varying. At any instant of time the ratio of flow rate or pressure differential to the design values has been termed the Off-Design Ratio (ODR). An off-line program (ODRAT) has been written, again in Fortran 77, to determine the optimum design pressure using pressure differential data from PWETWO. In order to achieve this the following iterative sequence must be carried out:

- (i) Several cycles of PWETWO are run with the efficiency option set to 100% and all variables selected as required. After a set number of cycles,

pressure data from one complete cycle is read to an internal file. The number of cycles run before data is collected depends upon how long it takes for the cycles to become stable. This in turn depends upon whether the isentropic or non-isentropic version has been selected (see Section 4.3).

- (ii) The off-line programme, ODRAT, can now be set in motion. A design pressure differential thought to be suitable is input via the keyboard and the programme then calculates power output at each timestep using the idealized efficiency curve of Fig. 5.3 and the pressure differential data from PWETWO. Average power output over the cycle is calculated.
- (iii) This process is repeated until an optimum design pressure differential is found which maximises average power output over the cycle.
- (iv) This optimal design pressure differential can now be input to PWETWO using the variable efficiency option.

This method of optimizing P_{DD} although time consuming, proved to be adequate for the initial parametric studies described in Chapter 6. Subsequently a more sophisticated and efficient methodology for the optimization of this and several other parameters has been devised and is fully described in Chapter 9.

5.3.1 The Optimisation of the Turbine Output via the Design Pressure Differential

Fig. 5.4 shows typical examples of the temporal variation in output from the turbine over one half cycle of operation of a twin chamber PWE for different values of P_{DD} (a half cycle is the period of time taken for the surface elevation of a water column to pass between its upper and lower bounds). The reduction in power output shown in curve B and to an even greater extent by curve C is due to the turbine design (as defined by the scale factor and the design pressure differential) being unable to cope with the excessive axial velocities created by the differential pressures. The resulting high values of angle of incidence cause the turbine to stall until the pressure differential decreases and brings the axial velocity down with it. When the turbine again operates within the bounds of the efficiency curve the power output recovers. An increase in P_{DD} results in a turbine with either increased annulus area or increased operating speed or a combination of the two. This can have the effect of either reducing the pressure differential by reducing the throttling effect of the turbine or altering the relationship between the axial velocity and the tangential speed or, again, a combination of the two. This results in a reduction in angle of incidence allowing the turbine to operate within the bounds of the efficiency curve for a longer period during the half cycle. When the optimum design is achieved via the selection of an appropriate P_{DD} the depression in the

curve disappears, the turbine operates within the bounds of the efficiency curve throughout the half cycle and the average power output is at an optimum. This situation is illustrated by curve A in Fig. 5.4.

5.4 The Off-Line Turbine Model

In order to gain a more thorough understanding of the behaviour of the Wells Turbine an investigation into those aspects of aerofoil theory that significantly affect power output was embarked upon. Various published methods^{26,27} for predicting turbine power output were used during this investigation. These methods rely heavily upon empirical aerofoil data.

An off-line turbine model (TURB4) utilizing pressure data from PWETWO and using the methodology described in References 26 and 27 was subsequently developed. The results from this model provided a very interesting and useful insight into the aerodynamic theory of the self-rectifying turbine.

The following two approaches to the modelling of the airflow through the turbine are taken in the off-line turbine model:

(1) Variable Velocity Approach

In this approach the axial velocity (V_x) of the airflow at the turbine inlet is assumed to vary linearly with radius²⁷.

$$QA = \int_{rh}^{rt} V_x 2\pi r \, dr \quad (5.14)$$

where:

rt = radius at turbine tip

rh = radius at turbine hub

It follows that, as $\tan \alpha = V_x/U_t$, the angle of incidence must remain constant with radius.

$$\begin{aligned} \text{Now } V_x &= C_{vx} r \\ &= \text{Constant} \times \text{radius} \end{aligned} \quad (5.15)$$

Substituting equation 5.15 into equation 5.14 and integrating across the turbine annulus:

$$Q_A = \left[C_{vx} 2\pi \left[\frac{r^3}{3} \right] \right]_{rh}^{rt} \quad (5.16)$$

giving:

$$C_{vx} = 12Q_A / \pi (D_T^3 - D_H^3) \quad (5.17)$$

(2) The Constant Velocity Approach

In this case axial velocity is assumed constant across the turbine inlet²⁷. This causes the angle of incidence to vary along the turbine blade ie:

$$\begin{aligned} \tan \alpha h &= V_x / \omega r h \\ \tan \alpha &= V_x / \omega r \end{aligned} \quad (5.18)$$

therefore:

$$\tan \alpha = \tan \alpha h \cdot r h / r \quad (5.19)$$

In both cases the turbine parameters were initially set to those of the CEGB test turbine,²² ie:

Turbine tip diameter, (D_T)	= 0.4 m
Turbine hub diameter, (D_H)	= 0.2 m
Turbine speed	= 6000 rpm
Blade chord length, (CH)	= 0.055 m
Number of blades, (N)	= 8
Aerofoil section	= NACA 0015
Pressure/flowrate gradient, (K_T)	= 0.00043

This allowed the turbine model, TURB4, to be calibrated against the CEGB results (see Fig. 5.7). TURB4 utilizes pressure data from a complete cycle of PWETWO with turbine efficiency set at 100%. At each timestep the air flowrate is calculated using the above K_T factor and equation 5.3. In the case of the Variable Velocity Approach the axial velocity of the airflow at the turbine tip and the corresponding value of the angle of incidence are calculated from equations 5.18 and 5.19 and power both into and out of the turbine is calculated from the following equations of Reference 13:

$$POW_{Tin} = \frac{C_T}{128} \frac{\rho a C_H N}{\cos^2 \alpha} \tan \alpha w^3 D_T^4 (1-h^4) \quad (5.20)$$

$$POW_{Tout} = \frac{C_X}{128} \frac{\rho a C_H N}{\cos^2 \alpha} w^3 D_T^4 (1-h^4) \quad (5.21)$$

$$EFFT = \frac{POW_{Tout}}{POW_{Tin}} \quad (5.22)$$

where:

- POW_{Tin} = the power input (watts)
- C_T = Tangential force coefficient
- C_X = Axial force coefficient
- ρ a = Air density at that timestep
- h = rh/rt

In the case of the Constant Velocity approach V_x is calculated from equation 5.15 and the angle of incidence at the turbine hub from equation 5.18. The power input and output is then calculated by the integration of the non-dimensional forms of equations 5.20 and 5.21 along the turbine blade using equation 5.19 to calculate the relevant value of the angle of incidence. (The non-dimensional forms of the power equations can be found in Reference 27).

5.4.1 Generation of Force Coefficients

Both the Constant and the Variable velocity approaches use the following sequence which closely follows that recommended by Raghunathan²⁷ to determine the axial and tangential force coefficients C_X and C_T .

For each timestep and/or point on the turbine blade:

- (i) Coefficients of Lift and Drag, C_L and C_D , are estimated for the relevant angle of incidence from the graphs of Fig. 5.5 and Fig. 5.6. These graphs are linearized forms of those to be found in Reference 29 which are based on performance data from wind tunnel tests on an isolated NACA 0015 aerofoil.
- (ii) The angle of incidence must be adjusted in order that the same local velocity distribution is produced over the upper surfaces of both the isolated aerofoil providing the initial drag and lift data and that same

aerofoil when arranged in cascade (ie when it is one of a number of aerofoils in the runner of a turbine). The relevant factor depends upon the solidity of the turbine and the necessary graphical data required for its generation was kindly supplied by Dr. Raghunathan of Queens University, Belfast.

- (iii) The effect of air compressibility on the Lift coefficient in subsonic flow is taken into account by the use of the Prandtl-Glauert rule²⁹:

$$C_{Lc} = \frac{C_{Lin}}{\sqrt{1-M^2}} \quad (5.22)$$

where:

C_{Lc} = Coefficient of Lift (compressible flow)
 C_{Lin} = Coefficient of Lift (Incompressible flow)
 M = The Mach Number of the flow

- (iv) The tangential and axial force coefficients are calculated from:

$$C_T = C_L \sin \alpha - C_D \cos \alpha \quad (6.23)$$

$$C_X = C_L \cos \alpha + C_D \sin \alpha \quad (6.24)$$

- (v) These force coefficients must be adjusted to allow for the relationship between isolated aerofoil performance and the performance of aerofoils in cascade. The necessary factors are solidity dependent (ie dependent upon the relationship between the size and number of turbine blades and the mean circumference of the turbine annulus) and were obtained from Reference 28.
- (vi) Power output and Input plus turbine efficiency are calculated from either equations 5.20, 5.21 and 5.22 or via their non-dimensional equivalents.

The results from typical runs of TURB4 using both approaches are shown in Fig. 5.7 alongside the CEGB test data and PWETWO output. The TURB4 outputs have been calculated using C_L and C_D data for Reynolds Numbers of 331,000 and 655,000. The Reynolds Number of a turbine with a chord length of 0.055 m operating within the pressure regime relevant to the flow rates shown reaches a maximum of approximately 470,000 at the turbine tip. Unfortunately the corresponding lift and drag data at this Reynolds number were not readily

available. The power outputs achieved using C_L and C_D values generated from the $Re = 331,000$ curves are considered to be sufficiently representative for present purposes.

The PWETWO curve being based on a specific turbine design and an efficiency curve relevant to a far higher pressure regime soon breaks away from the CEGB curve whereas the TURB4 curves show satisfactory agreement. The efficiency curve (Fig. 5.8) generated from the same TURB4 data shows similar characteristics both to the curve supplied by Queens University and other published efficiency data.

Having established the validity of TURB4 the next logical step would be to estimate the turbine parameters for a particular optimized design pressure using equation 5.12. An average value of Tangential Velocity (U_T) of 150 m/s could be used and a tip diameter easily generated. By trial and error hub diameter, chord length and number of blades could be determined to give a solidity that minimized the extent of the stall region thereby preventing turbine crawling as described in the literature. This data could then be utilized by TURB4 to match the ODR curve using varying aerofoil and solidity data. Unfortunately, in order to achieve this TURB4 would require a far more extensive databank of empirical data. As such models no doubt exist in other institutions it is not intended to reproduce such work here.

5.5 Summary

The work described in the preceding sections has led to a greater understanding of the main characteristics of the Wells Turbine and to an appreciation of its likely performance throughout a typical PWE cycle.

The development of the TURB4 programme has illustrated the impracticality of the inclusion of such a turbine model within the PWEONE or PWETWO programmes due to its inherent dependence upon empirical aerofoil data. This problem has been overcome within PWETWO by the introduction of the scaling factor, S_T , to the pressure/flowrate characteristics of the CEGB test results.

The concept of a Design Pressure Differential, P_{DD} , has been developed by combining a pressure/flowrate model of the turbine with the turbine theory developed at the Queen's University, Belfast. This concept provides an efficiency curve that is easily utilized by the turbine model of PWETWO.

The average power output curves generated via the ODRAT routine and illustrated in Fig. 5.4 clearly exhibit a rapid initial rise followed by a sudden fall when a sub-optimum design pressure differential has been introduced to the programme.

This initial rise and fall is directly comparable to that of the curves generated by TURB4 and the CEGB test results shown in Fig. 5.7.

Closer study of the TURB4 results reveals a steady increase in axial velocity with flow rate. This finally results in an angle of incidence which induces turbine stall. The stall is primarily caused by a rapid increase in drag coefficient, C_D , and can only be avoided by altering the solidity of the turbine and/or altering the turbine operating speed. A change in solidity would involve a re-design of the turbine as suggested in Section 5.3.1. It is apparent therefore that the turbine model of PWETWO behaves in a manner directly comparable to that of TURB4. This, plus the favourable comparison of the TURB4 results and the empirical data of the CEGB tests, would suggest that the PWETWO approach to the modelling of the turbine provides a valid representation of likely turbine performance. An additional advantage of the PWETWO approach is the indication of an optimal turbine design provided by the design pressure differential, P_{DD} , and the turbine scale factor, S_T , via equations 5.10 and 5.12.

With this further validation of its performance (see Sections 4.2.2 and 4.8), the PWETWO programme could now be considered to represent an extremely useful design tool. This aspect has been fully exploited in the following parametric studies of Chapter 6 and the final optimization of the system described in Chapter 9.

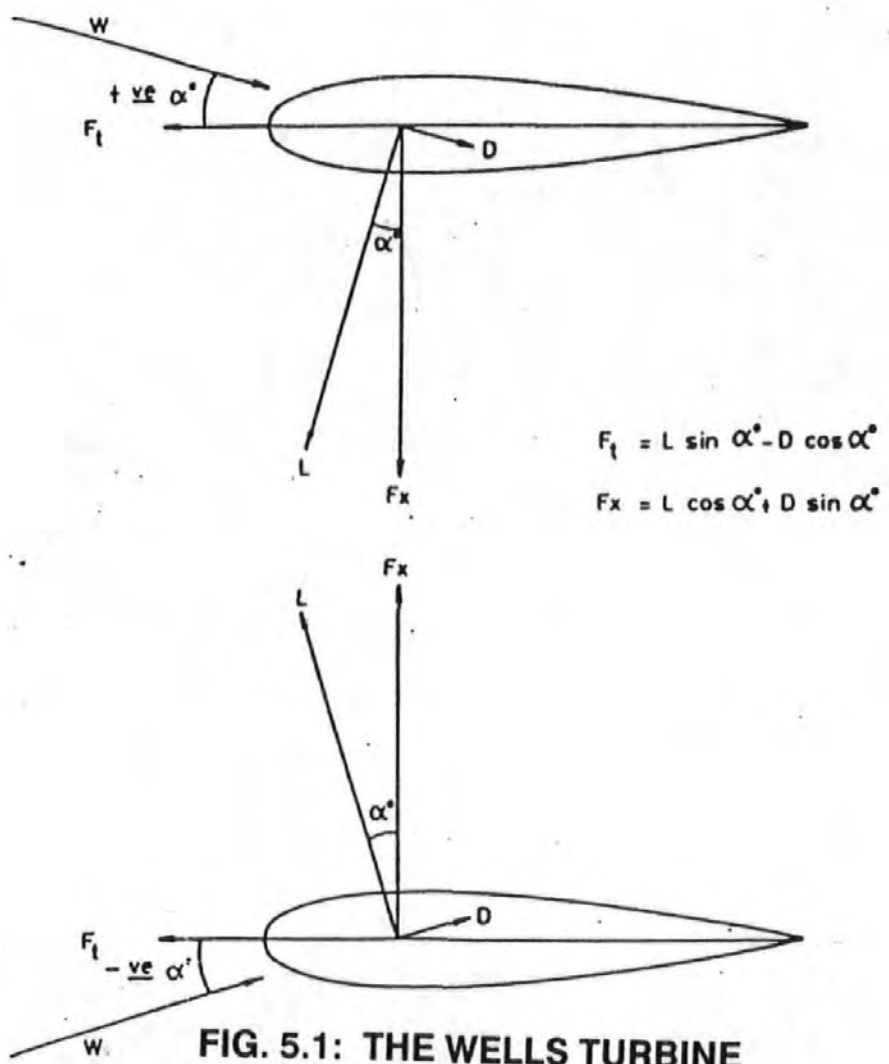
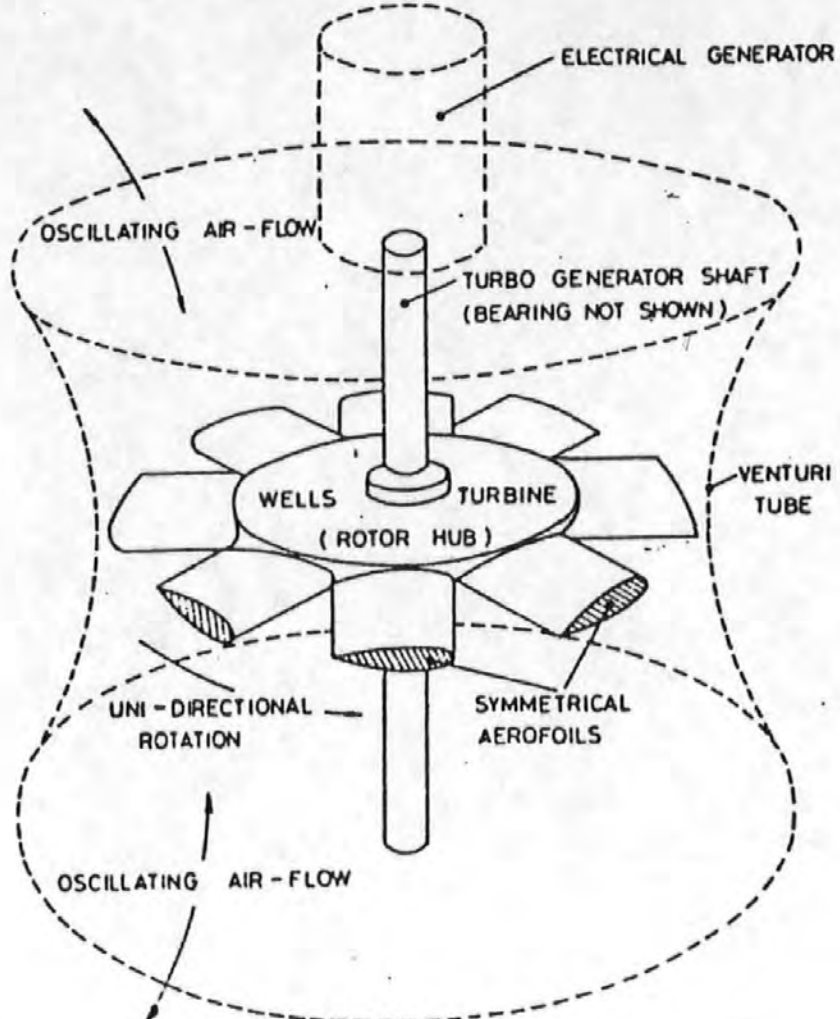


FIG. 5.1: THE WELLS TURBINE

FIG. 5.2: TURBINE EFFICIENCY

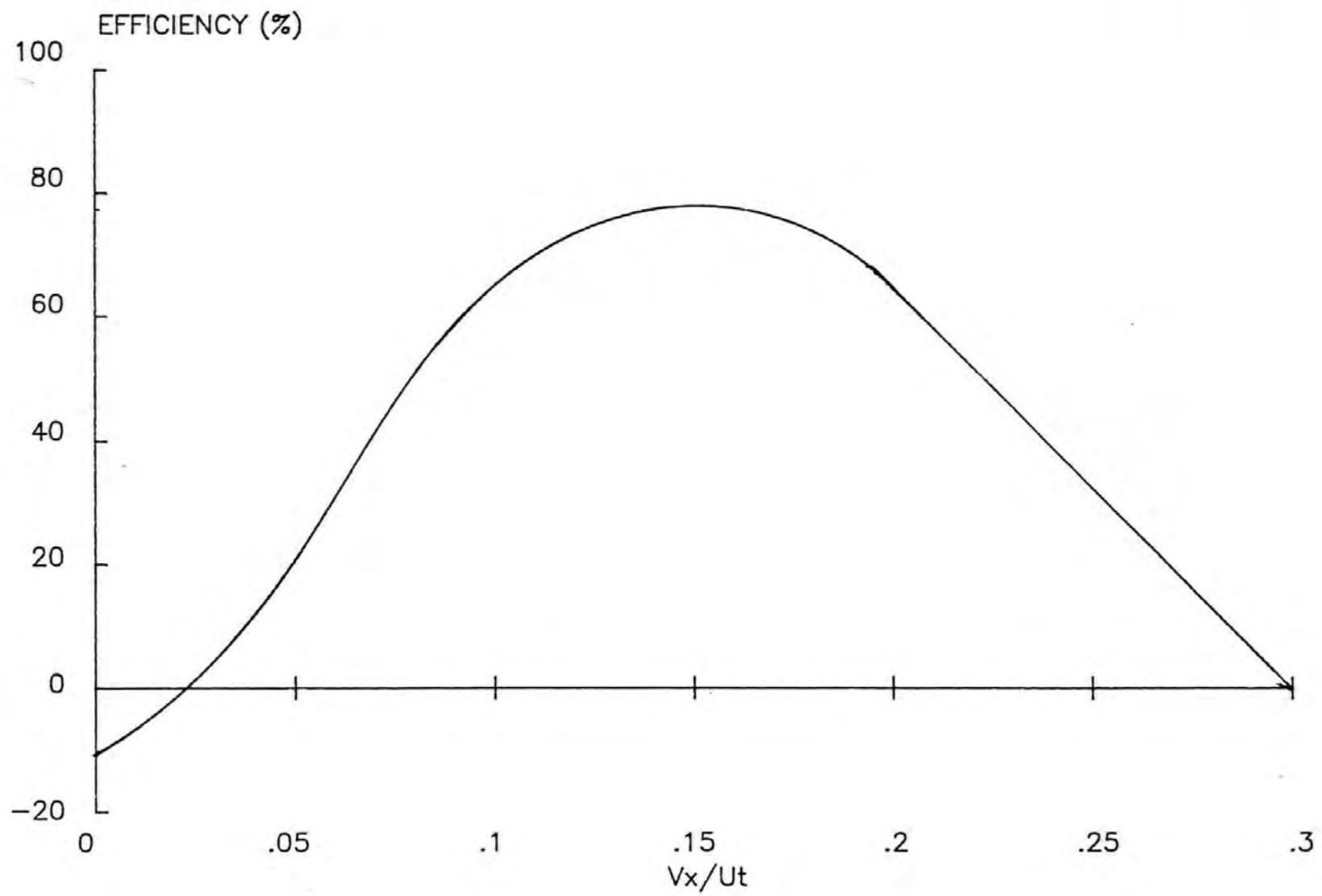


FIG. 5.3: OFF-DESIGN RATIO

95

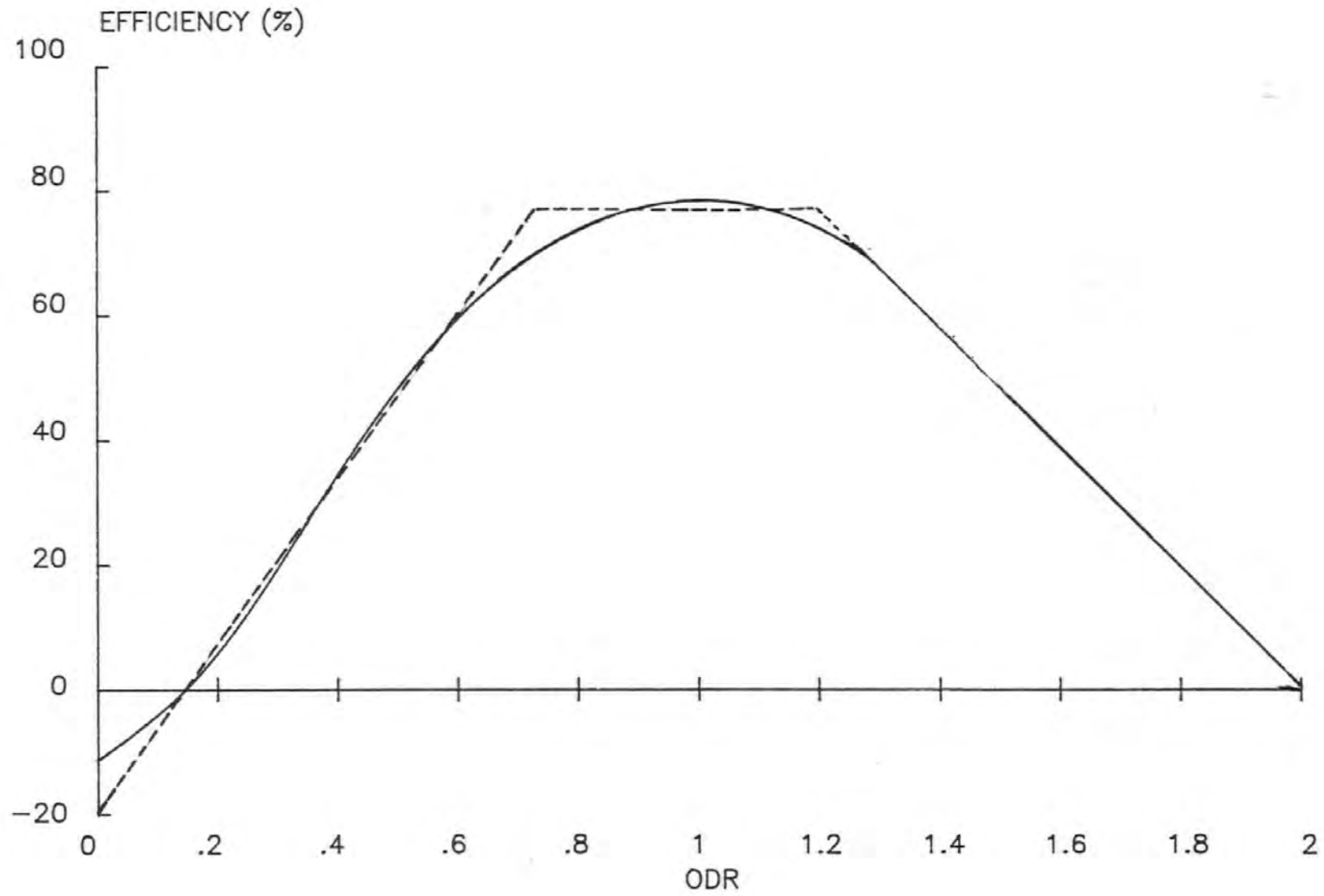


FIG: 5.4: OPTIMIZATION OF THE DESIGN PRESSURE

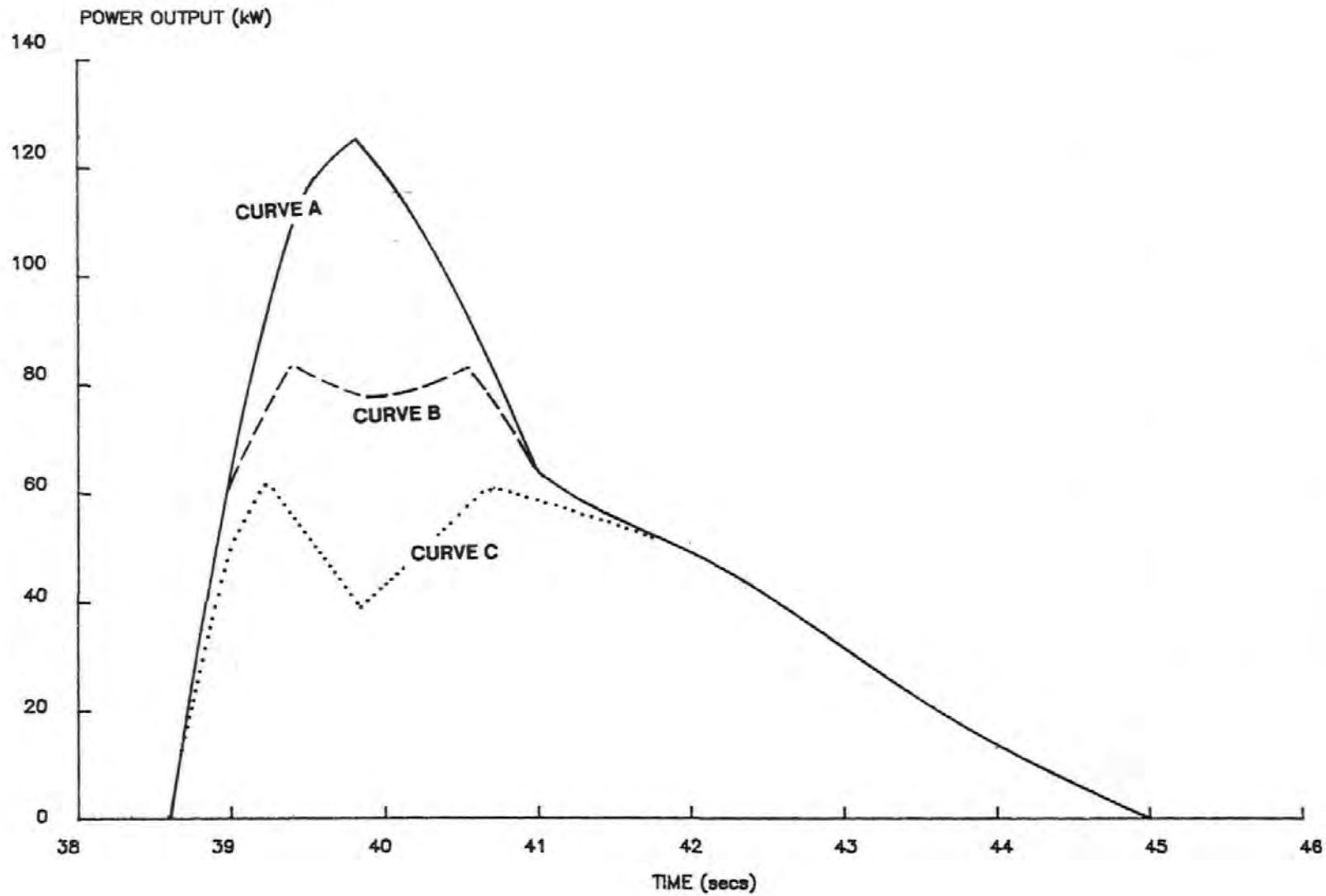


FIG. 5.5: IDEALIZED DRAG DATA

--- RE = 655,000; RE = 331,000

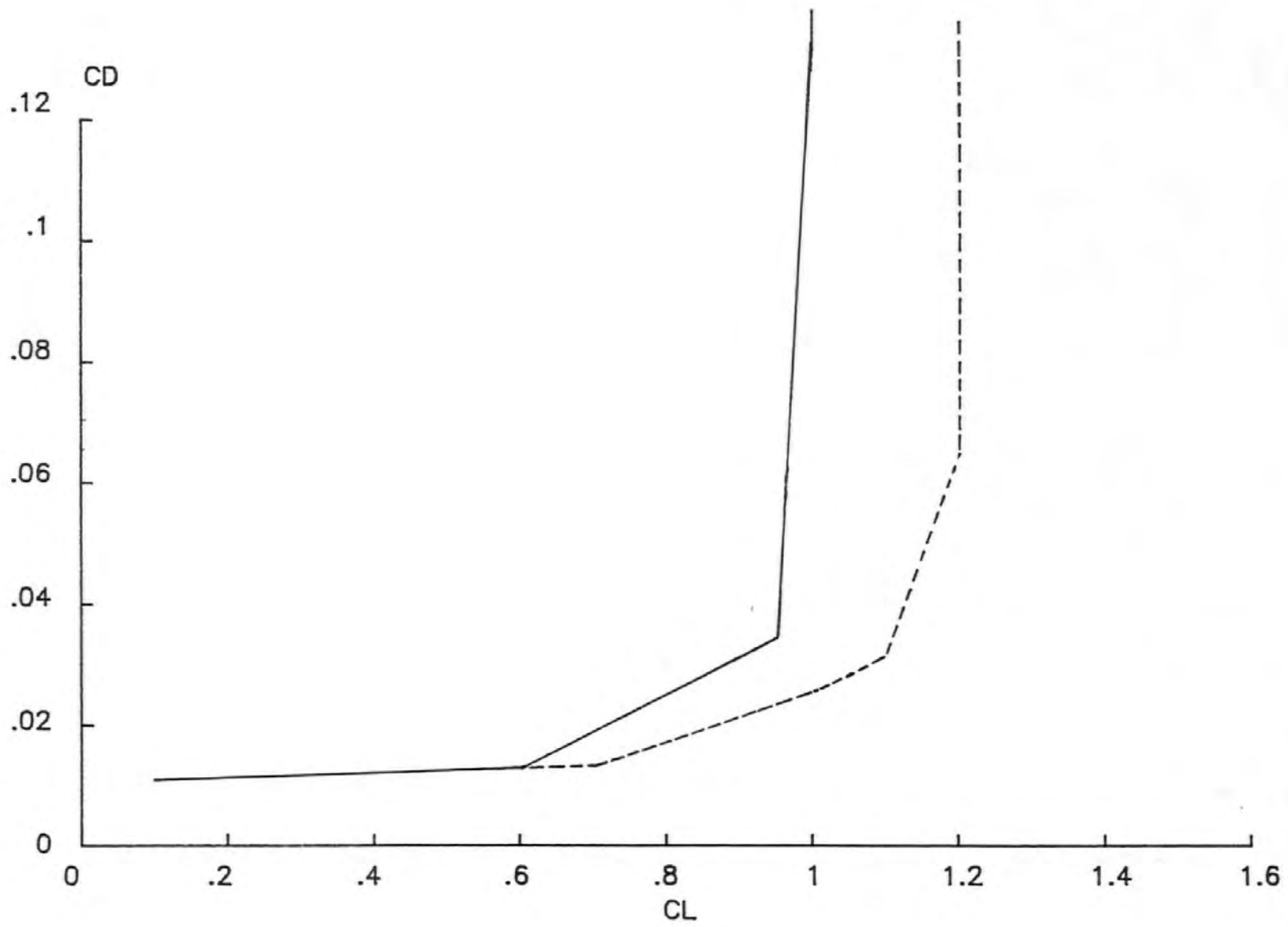


FIG. 5.6: IDEALIZED LIFT DATA

--- RE = 655,000 - - - - - RE = 331,000

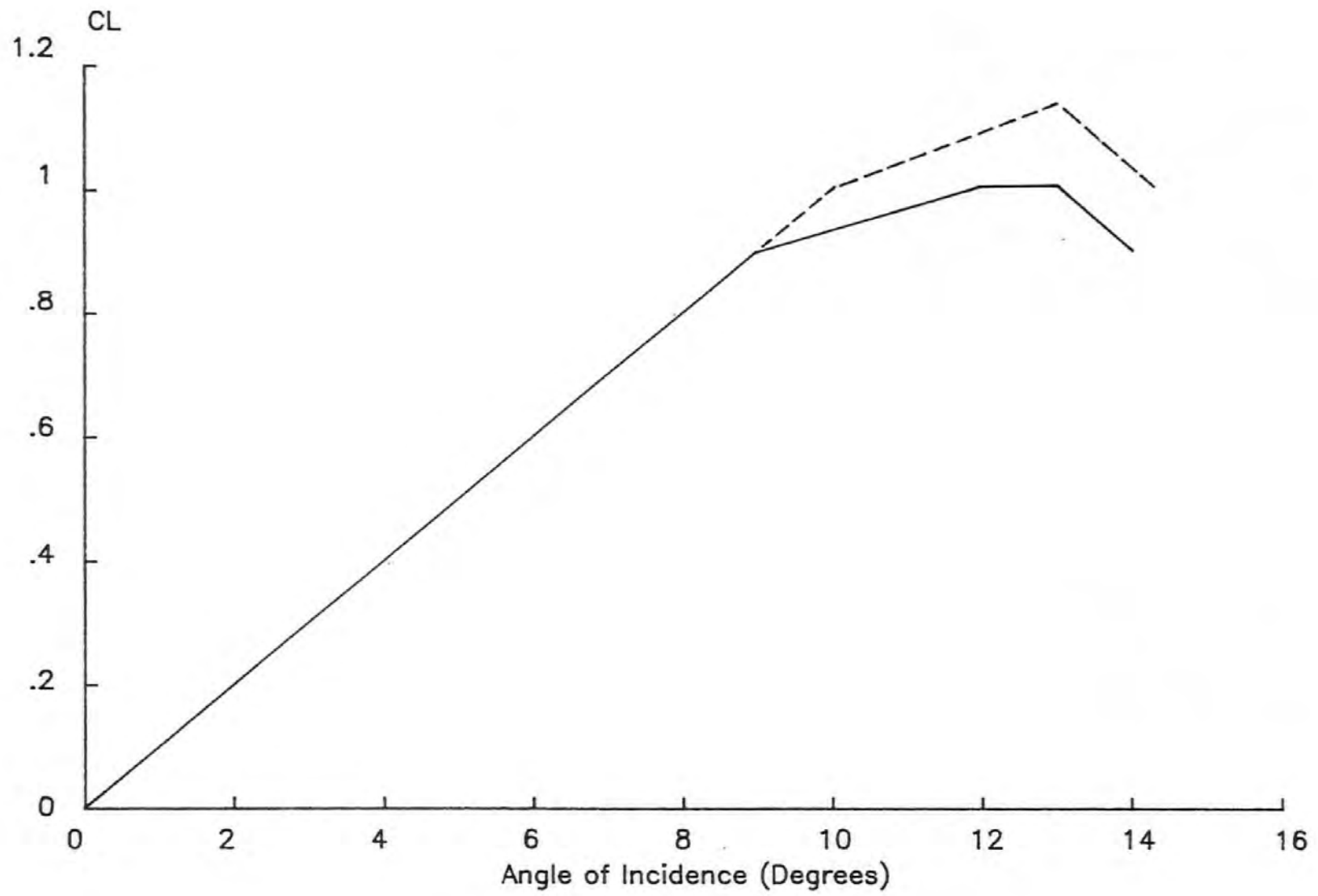


FIG. 5.7: POWER OUTPUTS FROM CEGB TEST,
PWETWO AND TURB4

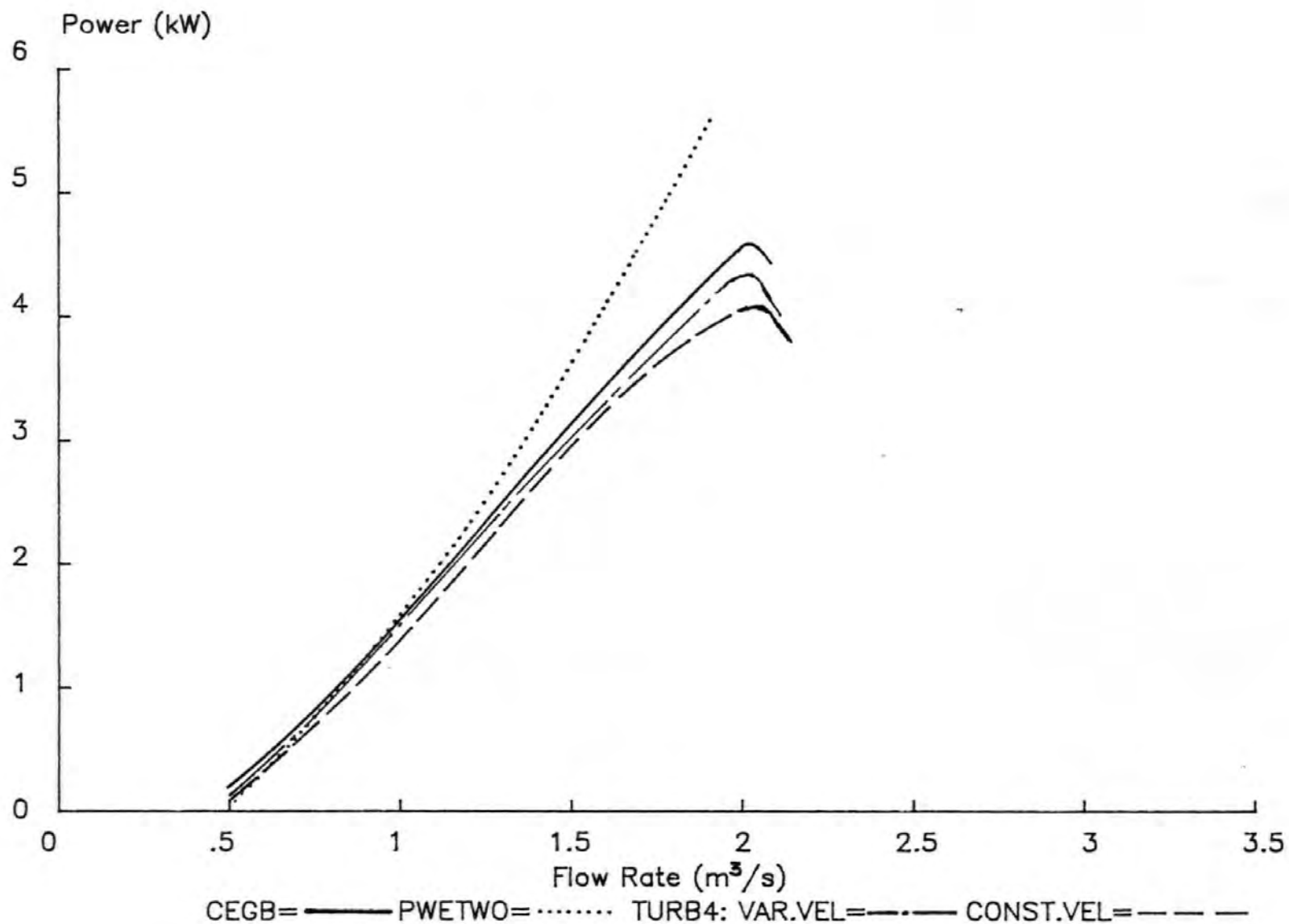
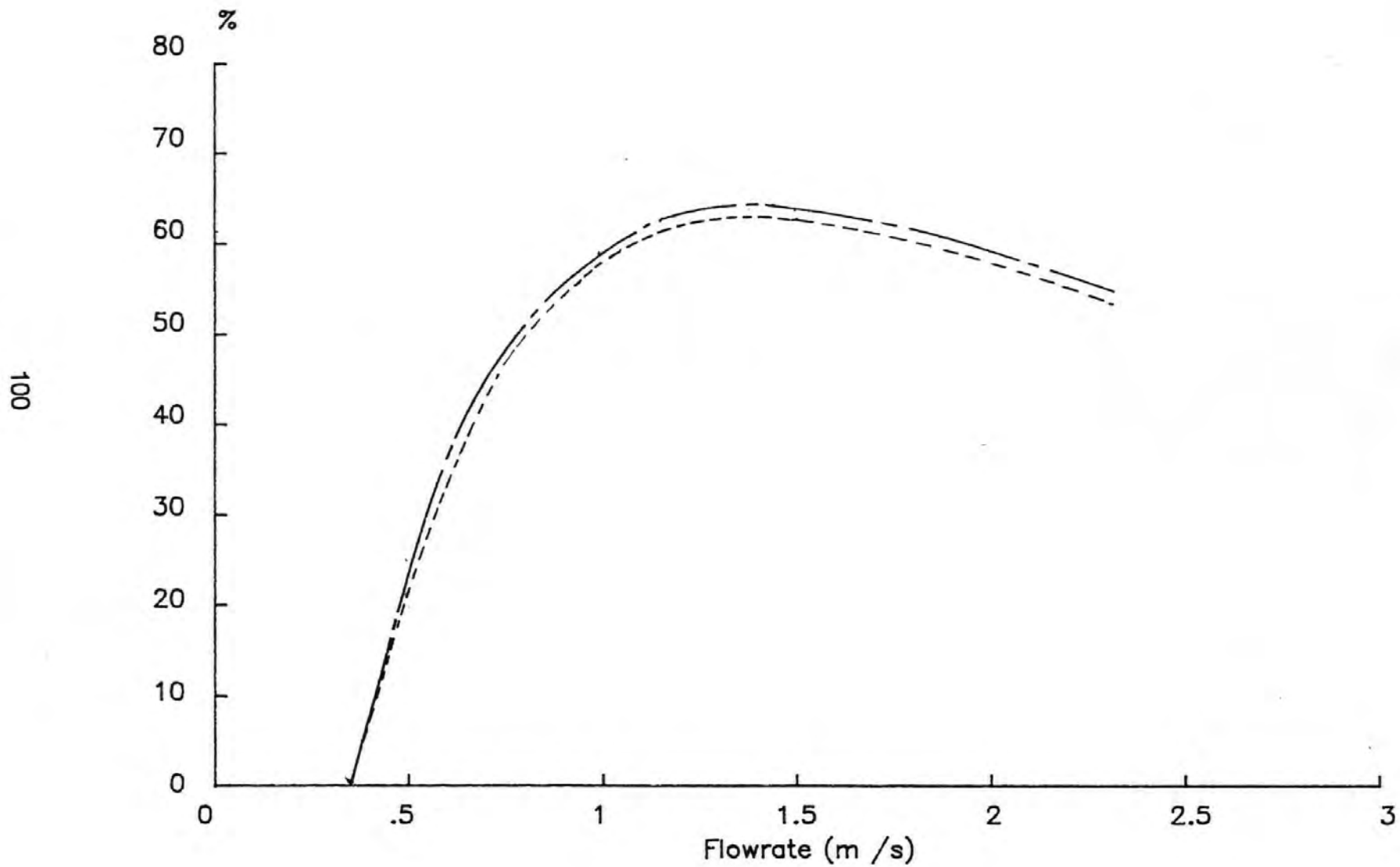


FIG. 5.8: EFFICIENCY CURVE GENERATED BY TURB4

VAR.VEL = ——— CONST.VEL = - - - -



6.0 : PARAMETRIC TESTING

6.1 Introduction

Parametric testing using both PWEONE and PWETWO was carried out at various stages of the development of the mathematical model. An initial indication of the parameters that tended to have the greatest effect upon the overall performance of the system was obtained from observation of the PWE cycle during the physical model tests.

The primary object of the parametric tests was to optimize the average power output. A realistic economic assessment of the PWE's potential could be based upon this output. In addition it was expected that the results of such tests, when considered alongside the physical model observations, would lead to a more complete understanding of the complex interactive nature of various elements of the PWE system.

On the basis of the physical model tests, the following two parameters were selected as the initial variables for the parametric study:

- i) Gate trigger levels.
- ii) Turbine scale factor.

The reasons for this choice are outlined in the following sections. It was expected that the information and experience gained from their variation would subsequently lead to further parameter selection.

6.2 Energy Test 1

6.2.1 Parameter Selection

Gate Trigger Levels

Manipulation of the butterfly gates during the physical model tests clearly illustrated the disproportionate amount of time taken for the rising or falling water columns to pass through the final ten to twenty millimetres at the extremities of their maximum stroke (a water column stroke being defined as the distance between the minimum and maximum chamber levels likely to be achieved under a given set of conditions).

This slowing of the water column's rise or fall is due in part to the minimal differential heads driving the water columns during these particular periods. Also the differential heads across the gate ensure that the magnitude of the leakage

both into the falling chamber and out of the rising chamber reaches a maximum as the chamber water levels approach their upper and lower bounds and this further reduces the velocities of the already slow-moving water columns.

It is reasonable to assume that in order to maximise average power output from the PWE it is necessary to ensure that a high average air pressure differential is maintained across the turbine over a complete PWE cycle. The disproportionate periods (when compared with overall cycle time) of low water column velocities described above are not compatible with this assumption.

In the case of the physical model appropriate 'tuning' of the gate (see Section 3.3.5) reduced the magnitude of the water column stroke thus ensuring that the maximum and minimum chamber water levels were always significantly below and above the respective upstream and downstream water levels. Elimination of the final few centimetres at the top or bottom of the water column stroke resulted in a substantial reduction in cycle time. It is envisaged that the same result could be achieved with a full-scale, butterfly-gated PWE by use of the 'latching' system described in Section 3.3.5, the latches being pneumatically controlled and activated when the water surface elevations within the chambers reach the optimum gate trigger level. In the case of an externally powered gate system, such as the Horizontal-axis Radial gate, the hydraulic/pneumatic drive would be controlled in a similar manner.

The determination of the appropriate gate trigger levels must therefore be considered essential in any overall optimization programme.

Turbine Scale Factor

The value of the turbine scale factor (S_T) determines the extent of the throttling effect of the turbine on the chamber airflow as indicated by equations 5.3 and 5.4. Variation of the airflow capacity either between twin chambers or between a single chamber and the atmosphere directly affects the chamber air pressure regime over the complete PWE cycle. Any change in this regime instigates corresponding changes in the air density and the air temperature. In addition, significant changes in water column velocities are induced.

Some of these effects were very apparent during the Series 3 tests described in Section 3.3.2. The removal of either the chamber covers, the connecting hose or both during the tests resulted in marked variation in cycle time and in the magnitude of the water column strokes. Such variation could also be induced by appropriate adjustment of the simple clamp situated at the mid-point of the connecting hose (Fig. 3.5).

It is therefore evident that any change in gate trigger levels must be investigated at various turbine scale factors to study the combined effect upon the overall pressure regime and upon the average power output of the PWE.

6.2.2 System Configuration

The initial series of tests involved either single or twin, square chambers each with a plan area of 20m². The gating arrangement consisted of independently controlled gates which could be considered as either the simple sluice gates of Fig. 1.1 or the horizontal-axis radial gates of Fig 2.6. The gates extended the full widths of the upstream and downstream faces of the chamber and were assumed to open or close at a constant, preset velocity. Gate opening or closing was initiated when the water within a chamber reached a trigger level as described below:

ZHCUG: The upper control level for the upstream gate. When the chamber water level reaches this point the upstream gate, currently open, commences to close.

ZHCDG: The upper control level for the downstream gate. When the chamber water level reaches this point the downstream gate, currently closed, commences to open.

ZLCUG: The lower control level for the upstream gate. When the chamber water level falls to this point the upstream gate, currently closed, commences to open.

ZLCDG: The lower control level, downstream gate; when the chamber level falls to this point the downstream gate, currently open, commences to close.

6.2.3 Test Format

The Series 1 format involved the gradual reduction of the upper gate trigger levels (ZHCG) in 50 mm steps whilst increasing the lower gate trigger levels (ZLCG) by the same increment. At each step, two complete cycles of the programme were run for turbine scale factors of 0.5 to 5.0 at 0.5 increments. This allowed a comparison of different water column strokes whilst also illustrating the effect of turbine damping on the air and water flow. These initial tests were carried out before the introduction of the ODR parameter described in the previous chapter. Consequently the turbine was assumed to be operating at 100% efficiency throughout. A typical set of results for both the single (S1.0 - S1.7) and twin (T1.0 - T1.7) chamber programmes are shown in Appendix III. Initial dimensions and starting values are also included.

6.2.4 Test Series 1: Results and Discussion

The curves shown in Figs. 6.2 to 6.7 reveal the complex manner in which the various parameters interact to affect overall PWE performance. Fig. 6.3, for example, illustrates the effects of increasing the turbine scale factor, S_T , whilst the upper and lower trigger levels remain fixed at the values of test S1.4. As the scale factor increases up to 3.0 there is a rapid lessening of the cycle time due to the decrease in the damping of the airflow through the turbine. This decrease in damping also allows the rising water column to achieve a higher maximum level and, conversely, the falling water column to achieve a lower minimum level. This increases the water flow rate through the system and causes a steep rise of the Average Power Dissipated curve. The Average Power Dissipated (APD) is the average power available to the system taking into account the three metre head differential across the chambers and the average flowrate through the system over a complete cycle. As the damping effects become less marked with increasing S_T so the slopes of the Cycle Time and the APD curves flatten.

A further effect of a reduced cycle time is a decrease in leakage due to imperfect gate closure. This causes the Overall Efficiency curve and the 'No Leakage' Efficiency curve to converge as S_T increases. The 'No Leakage Efficiency' is the efficiency of the system when only the volume of water that contributes to the oscillating water columns is taken into account. Only this water contributes directly to producing the average power output. An increase in leakage is evident when S_T is less than 1.0 and cycle times become excessive. The Overall Efficiency curve begins to flatten out in this region whereas the slope of the 'No Leakage' curve remains constant.

This divergence of the two efficiency curves at low S_T could be attributed to an increased chamber air pressure during the initial rise of the water column. It is during this initial period that the upstream and downstream gates of the chamber are simultaneously open. An increased air pressure above the water column inhibits flow into the chamber and thus causes a greater volume to pass straight through the system without contributing to the rising water column as illustrated in Fig. 6.1.

A similar situation exists as the chamber commences to empty. Sub-atmospheric air pressure above the falling water column retards its fall rate allowing a greater volume of water to enter the chamber through the upstream gate and again pass straight through the system.

By referring again to Fig. 6.1, it can be seen that the air pressure regime at higher values of S_T causes a lesser volume of water to be lost in straight through leakage. However if the magnitude of the water column stroke is reduced by bringing

together the upper and lower gate trigger levels, the swept volume of the chambers must also be reduced. Straight through leakage then represents a higher percentage of the overall flow through the system during a complete cycle. This explains why the significant increase in average power output illustrated by test S1.7 in Fig. 6.2 is not accompanied by a similar increase in overall efficiency.

As the instantaneous power output is dependent upon the pressure differential across the turbine, the highest instantaneous power outputs occur at the lower values of S_T . However, the average power output over the complete PWE cycle is reduced by the long cycle times caused by such S_T values. This is illustrated clearly by the steep decline of the Average Power curve as S_T tends to zero. The S_T value which proves to be the optimum, therefore, is that at which the cycle time and instantaneous power outputs are so balanced as to produce an optimum average power output over a complete cycle. This was achieved with an S_T of around 3.0. As the slope of the cycle time curve starts to level out at this point, the average power output for values of S_T greater than 3.0 becomes mainly dependent on the instantaneous power outputs. However these outputs are decaying due to a reduction in differential pressures across the turbine caused by a reduction in the air damping effect. This results in a gradual decline in the Average Power curve as S_T exceeds 3.0.

The same parameters illustrated graphically in Fig. 6.3 are again represented in Fig. 6.4.^{nb} However in this case S_T remains constant at 2.5 whilst the upper and lower trigger levels are adjusted in increments of 50mm. The beneficial effect on both cycle time and average power output of lowering the upper gate trigger levels and raising the lower gate trigger levels (see A3.1 to A3.7) is evident from the gradient of the Average Power Output curve between tests S1.0 and S1.2.

Figs. 6.5 and 6.6 show the relationship between chamber water level, air pressure and instantaneous turbine power output for the single and twin chamber configurations. As the upstream gate opens the large differential head ensures that there is a rapid rise in water level and chamber air pressure. This results in a corresponding rise in instantaneous power output as the air within the remaining volume of the chamber is compressed and the pressure differential across the turbine increases. In the case of the twin chamber configuration the sub-atmospheric air pressure above the falling water column increases the magnitude of the pressure differential. There then follows a much steadier fall in both power and pressure as the head differential decreases. The duration of this part of the cycle is dependent upon the settings of the upper and lower trigger levels and illustrates how length of stroke can adversely affect average power output.

^{nb}

and Fig. 6.11

6.3 Test Series 9-12

6.3.1 System Configuration

Both the chamber shape and butterfly gate options were included within PWETWO for this series of tests. The opening and closing of the butterfly gate was initiated when the water within a chamber reached an upper gate trigger level, ZHCG (see Section 4.4).

PWETWO also included the vortex model described in Sections 3.5.3 and 4.5.4. Consequently the momentum of the flow within the chambers was conserved.

Test Series 9 to 12 therefore concentrated solely upon a simulation of the twin chamber, butterfly-gated configuration considered in the Series 3 physical model tests of Section 3.3.2. The basic dimensions of the PWE for this series of parametric tests were as follows:

Chamber diameter	=	5.04 m	Chamber height	=	5.5 m
Angle of gate arc	=	55 degrees	Length of gate	=	3.1 m
Height of gate	=	2.0 m	Upstream head	=	5.0 m
Downstream head	=	2.0 m			

These dimensions correspond at a scale of 1:20 to the 55 degree laboratory model of Section 3.3.2 (model 3.2). A 155 mm long gate was found to flow-actuate in a most satisfactory manner when installed within this model, hence the inclusion of a similar sized gate here. Further details of initial dimensions and starting values can be found in Appendix III along with the relevant tables of results (see A3.8 to A3.13).

Because of the increased complexity of the mathematical model, it was now necessary to run PWETWO through three complete cycles to obtain stable results. Programme stability is further discussed in Section 6.4.2.

6.3.2 Parameter Selection

The Series 9 tests involved similar variations of S_T and ZHCG as those considered in Section 6.2. The one different aspect was the use of the single gate trigger level as opposed to the upper and lower gate trigger levels of the Series 1 tests.

The results of Test Series 9 indicated that the maximum average power output could be achieved with a ZHCG setting of 4.0m. This value was therefore utilized by the following three series.

Test Series 10

Series 10 tests involved the variation of G_u , ie the length of that part of the butterfly gate which is upstream of the pivot point (see Fig. 3.3). Any adjustment in the magnitude of G_u results in a corresponding variation in the width of both the upstream and downstream chamber entrances. The decision to vary this particular parameter was based upon the assumption that the resulting increase in chamber entrance and exit widths would lead to a significant increase in mass flow rate both into and out of the chambers. This could prove especially beneficial during the initial rapid rise and fall of the water columns when optimum energy capture takes place. The necessary three cycles of PWETWO at turbine scale factors varying from 0.2 to 1.0 were run for the G_u dimensions (in metres) shown in Fig. 6.8.

This attempt to increase mass flow rate was continued in Test Series 11 and 12 by respectively increasing gate height and gate speed. Gate height, B_G , was increased in 40 mm increments from 2.0 to 2.2m in Series 11 whereas the time taken for the gate to traverse the 55 degree arc, T_G , was reduced from 2.8 seconds to 2.4 seconds in 0.2 second increments in Series 12.

In both cases similar turbine scale factors as those used in Series 10 were incorporated. The results are presented in Figs. 6.9 and 6.10.

6.3.3 Results and Discussion

As was expected increased gate size and gate speed resulted in significant increases in average power output. It is not feasible however to continue increasing G_u above the limits imposed in the Series 10 test. An overall gate size resulting from further increase would prove excessive for the reasons outlined in Section 2.3. It is assumed that the increase in gate height of Series 11 could be accommodated by recessing the gate area into the channel bed as suggested in Section 3.6. However an overall gate height of 2.2 m is considered to represent an upper limit to this parameter variation.

The physical model test measurements of Section 3.5.2 suggest a possible range of gate movement times of between 2.3 and 4.02 seconds for model 3.2. The selection of a gate movement time of 2.4 seconds is therefore considered to be a conservative lower bound.

The optimum average power curve of Fig 6.10 represents a combination of the four optimum gate parameters defined by Test Series 9 to 12 ie $Z_{HCG} = 4.0\text{m}$; $G_u = 1.2\text{m}$; $B_G = 2.2\text{m}$ and $T_G = 2.4$ secs. The resulting average power output is equal to 72 kW. However this assumes that the turbogenerator set is 100% efficient. If it is assumed that such a set would have an average efficiency over a

PWE cycle of approximately 70%, the average power output would be in the region of 50 kW.

It is interesting to note that in each of these series of tests the chamber air pressure tends to be sub-atmospheric throughout most of the cycle. This is due to the following two factors:

- i) The configuration of the flow-actuated gate is such that the chamber exits are greater in width than the entrances. In a twin chamber system not connected by a turbine duct this would result in a greater flow rate leaving the emptying chamber than that entering the filling chamber.
- ii) The high periphery pressures of the chamber vortices inhibit flow into a chamber but assist flow out of a chamber.

If the two chambers were not connected by a turbine duct the fall times of the water columns would always be less than the rise times. However rise and fall times within a connected system must always be approximately the same. In order for this to be possible the falling water column in one chamber must assist in drawing water into the other. This can only occur when sub-atmospheric pressures exist in both chambers.

6.4 Final Developments

6.4.1 Introduction

The inclusion of two further refinements within PWETWO contributed to the final generation of an optimum average power output. These two refinements provided the following additional options:

- i) The inclusion of variable efficiency over the PWE cycle using the Design Pressure Differential as described in Section 5.3.
- ii) The introduction of the non-isentropic process outlined in Section 4.6.

Test Series 22 to 26 utilize these final two developments and can therefore be regarded as the most representative of the parametric tests. The final optimum average power output achieved during these series was considered to be suitable for inclusion within the economic assessment of Chapter 8.

The magnitudes of the various set parameters of these tests are identical to those of Series 12.

6.4.2 Test Series 22

The following three PWETWO options were fully investigated in Series 22:

- i) A 100% efficient turbine and an isentropic process.
- ii) Variable turbine efficiency and an isentropic process. An optimum design pressure differential of 15696 N/m^2 was determined from the pressure data generated from condition (i) using the off-line programme ODRAT.
- iii) Variable turbine efficiency with the design pressure differential again equal to 15696 N/m^2 but with the non-isentropic factors described in Section 4.7 now taken into account. The initial ambient air temperature in the chambers was set at 13.96°C , this being considered to represent an average daily temperature in the UK.

As has already been mentioned, it was necessary to run a number of cycles for each of the parametric tests in order that initial transients could die out and to allow the programme operation to stabilize. The inclusion of the vortex model increased the time required to reach stability due to the progressive formation of the vortices over the initial cycles. Fig. 6.12 shows the number of cycles necessary for near identical results to be obtained from successive cycles for the three modes of operation outlined above. It is evident from this figure that the non-isentropic approach requires a substantial number of cycles before an acceptable degree of repeatability is achieved. This is due to the progressive increase in mean air temperature.

Referring again to Fig. 6.12, the change from 100% efficiency to the variable efficiency defined by Fig. 5.3 (in which the maximum efficiency is 78%) inevitably reduced both the average power output and the overall efficiency in cases B and C. The thermodynamic aspects of case C further reduced the output by approximately 4 kW. The overall efficiency in these latter two cases however, remained the same. Further study of the results from case C revealed that a combination of an increase in both energy harnessed per cycle and in cycle time plus a decrease in percentage leakage produced an overall efficiency comparable to that of the isentropic process of case B.

Curves A and B of Fig. 6.13 show the variation in chamber air temperature for the isentropic processes at both 100% and variable efficiencies. The development of the chamber vortices results in a progressive reduction in chamber air pressures. This pressure reduction is responsible for the initial drop in air temperature evident in both curves. As the vortices become fully formed so the chamber air pressures

stabilize producing a maximum of -2943 N/m^2 and the maximum and minimum chamber air temperatures become constant.

The non-isentropic approach produces the rising maximum and minimum air temperature curves, a and b. The variation in net heat loss per cycle from the air in a particular chamber is represented by curve H.

Fig. 6.14 concentrates on the maximum instantaneous power from the turbine in the three cases outlined. Again, a severe reduction is evident upon the introduction of variable efficiency although in percentage terms this is not as severe as the corresponding reduction in average power output of Fig. 6.12. Instantaneous power output is unaffected by the introduction of the non-isentropic process as illustrated by curves B and C signifying that maximum pressure differential across the turbine must also be comparable for these two cases and that therefore the optimum design pressure differential must also be similar.

6.5 Primary Optimization for Costing and Financial Analysis

Having fully investigated the operating characteristics of the twin circular chambered, butterfly gated system via the preceding parametric studies it was necessary to establish an optimum average power output that could be considered achievable under 'typical' operating conditions and upon which a cost per kilowatt-hour could be based.

It is evident from Test Series 10 to 12 that significant improvements in average power output can be achieved by increasing the vertical dimensions of the gate (BG), the upstream dimensions of the gate (G_u) and its speed of motion (TG). Care had been taken to ensure that the height of the gate did not exceed the downstream water level thereby allowing the possible escape of air from the chambers at the bottom of their respective water column strokes. However, it has become apparent from the parametric tests that the minimum mean water level in the chambers could be as high as 2.33 m. This indicates that the minimum water level at the periphery of the chambers was even higher due to the super-elevation across the vortices. As this would effectively seal the chambers preventing either the escape or ingress of air a further series of tests with increased gate height was embarked upon (Series 23). The results of this series are presented in graphical form in Fig. 6.15.

Figs. 6.16 and 6.17 show the effect of increasing G_u and the gate speed respectively. Series 23, 24 and 25 were carried out under the 'case (i)' conditions of Section 6.4.2 with an optimum upper gate trigger level (ZHCG) of 3.6m and can be considered to be logical extensions of Series 10 to 12. The minimum value of

TG corresponds to a model value of 0.56s and still lies therefore within the boundaries of the physical model testing of Section 3.5.2.

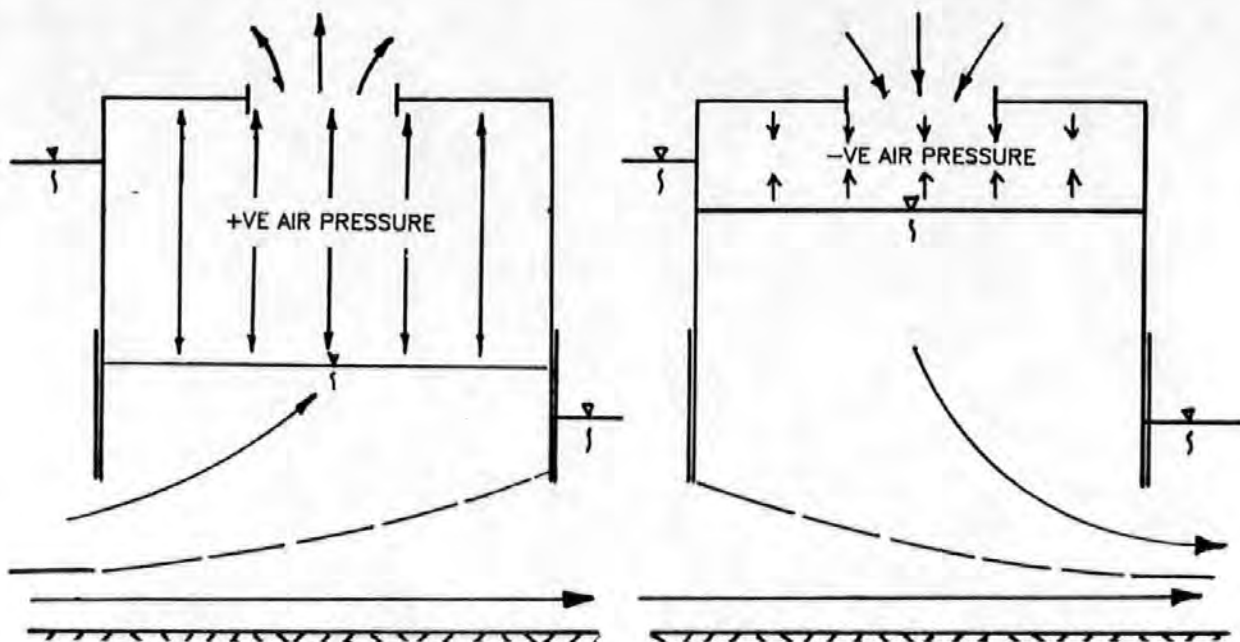
By taking the best conditions of these three Series (23 to 25) ie Gate height = 2.2m, $G_u = 1.2$ m and $T_G = 2.5$ s, and running PWETWO under non-isentropic conditions with variable efficiency and a design pressure differential of 15696 N/m², a maximum average power of 63.8 kW was achieved at an overall efficiency of 24.9%. S_T was equal to 1.0 resulting in a cycle time of 10.6s with a maximum instantaneous power of 130 kW. An average of some 25 kW was lost as heat.

The design pressure differential was subsequently validated via ODRAT for this non-isentropic case and a further series of tests with varying ZHCG values was undertaken to ascertain the new optimum value of ZHCG. A maximum average power output of 71.6 kW was achieved with a ZHCG of 3.5m at an efficiency of 26.8%, a cycle time of 8.93s and a maximum instantaneous power output of 128.3 kW. The iterative cycle of changes to S_T , ZHCG and Design pressure differential could have been continued to further 'fine-tune' the system and achieve an even greater output. However, this was not considered worthwhile due to the time-consuming runs of the non-isentropic version of PWETWO. Thus, the average output of the PWE operating under a 3m head differential was assumed to be 72 kW for the purpose of the financial assessment of Chapter 8.

6.6 **Twin Rectangular Chamber PWE with Horizontal-axis Radial Gates**

A similar but less extensive optimization procedure was carried out in order to ascertain the possible maximum average power output of the Rectangular chamber configuration of Fig. 2.1. As can be seen from Fig. 7.28 the widths of the chambers have been extended in order to gain some support for the structure from the channel banks. The lengths of the chambers have been reduced in order to lessen the required torque necessary for the gate's movement whilst still retaining a realistic gate area.

Using the dimensions stipulated in Section 7.11 with a gate movement time of 2.0s, the non-isentropic version of PWETWO with variable efficiency provided a maximum average power output of 90 kW.

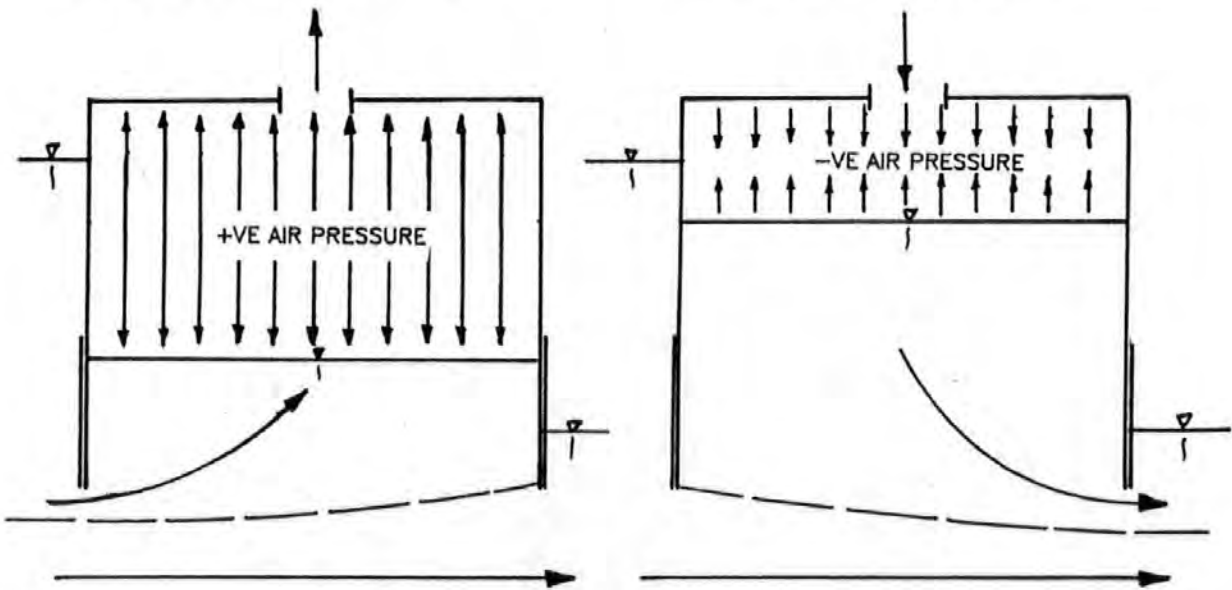


1) CHAMBER FILLING/LARGE TURBINE:

Low +ve air pressures allow greater volume of flow to enter the chamber. Straight-through leakage correspondingly decreased.

2) EMPTYING CHAMBER/LARGE TURBINE:

High -ve air pressures allow greater volume of flow to leave the chamber. Straight-through leakage correspondingly decreased.



3) FILLING CHAMBER/SMALL TURBINE:

High +ve air pressures restrict flow into the chamber. Straight-through leakage correspondingly increased.

4) EMPTYING CHAMBER/SMALL TURBINE:

Low -ve air pressures restrict flow out of the chamber. Straight-through leakage correspondingly increased.

FIG. 6.1: DIAGRAMATIC REPRESENTATION OF RELATIONSHIP BETWEEN TURBINE SCALE AND LEAKAGE THROUGH THE SYSTEM



FIG. 6.2: ENERGY TESTS S1.0 - S1.7

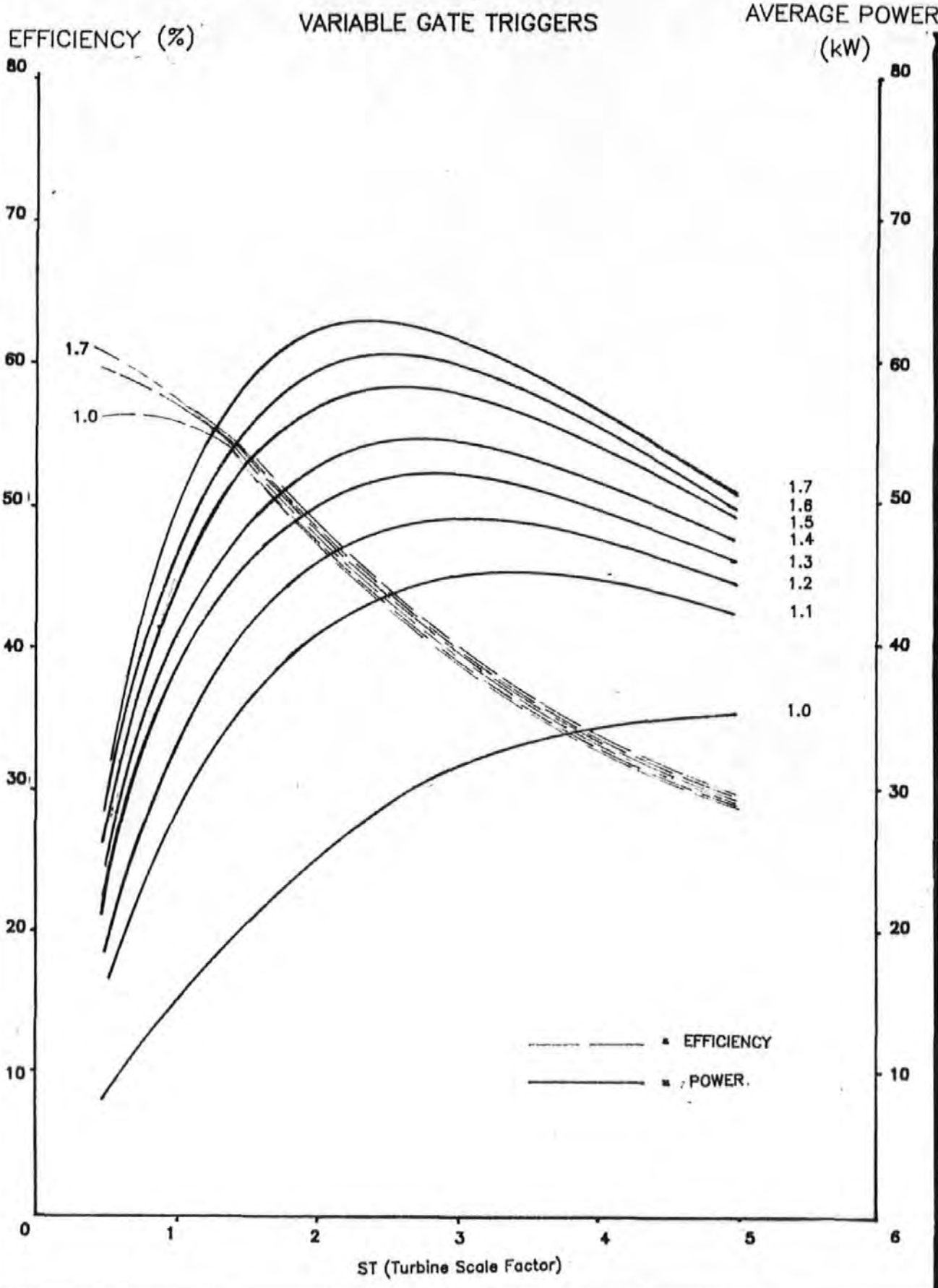


FIG. 6.3: POWER OUTPUT AND EFFICIENCIES (E.T. S1.4)

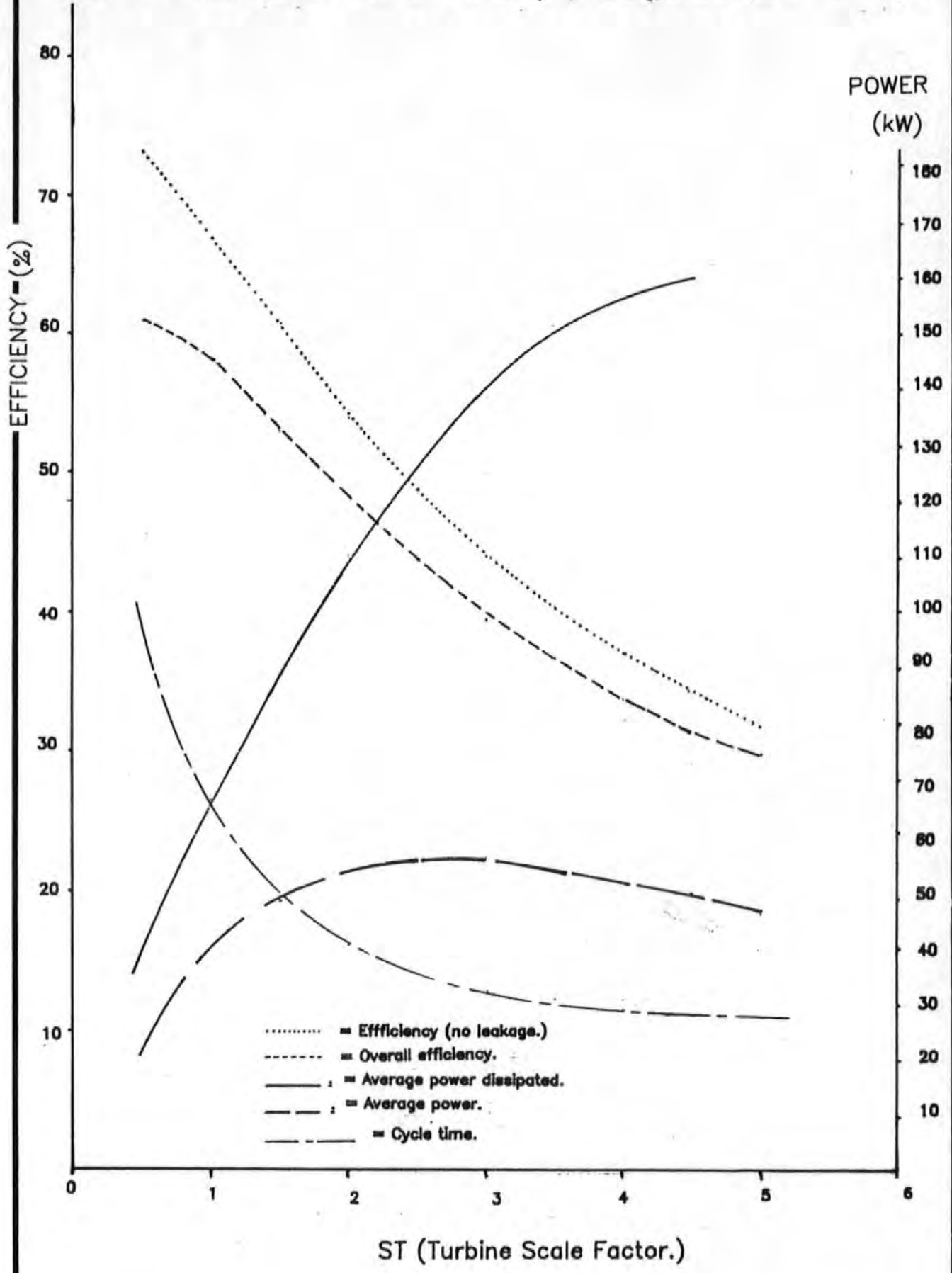




FIG. 6.4: POWER OUTPUT AND CYCLE TIME

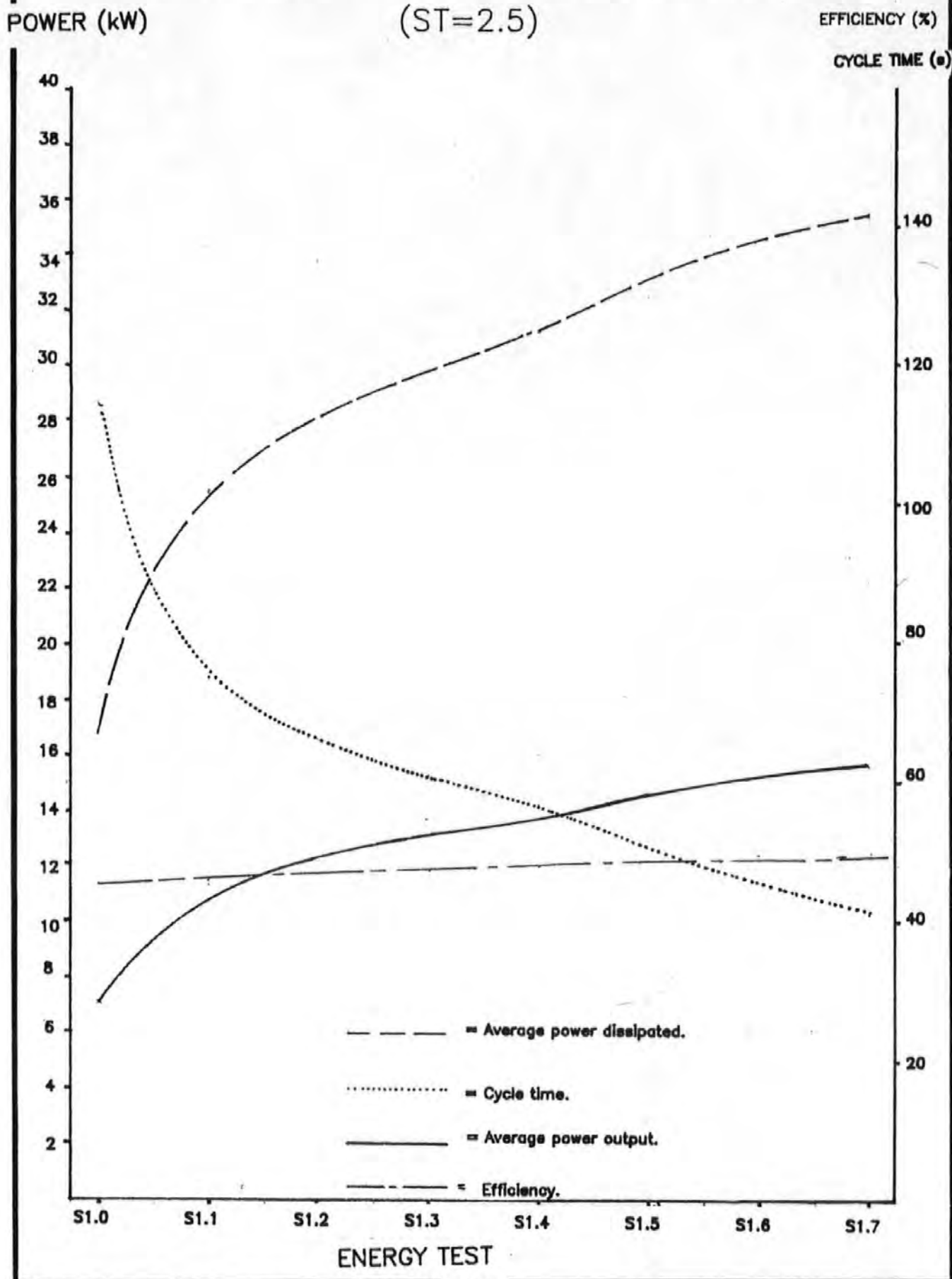


FIG. 6.5: ENERGY TEST S1.4; ST=2.5

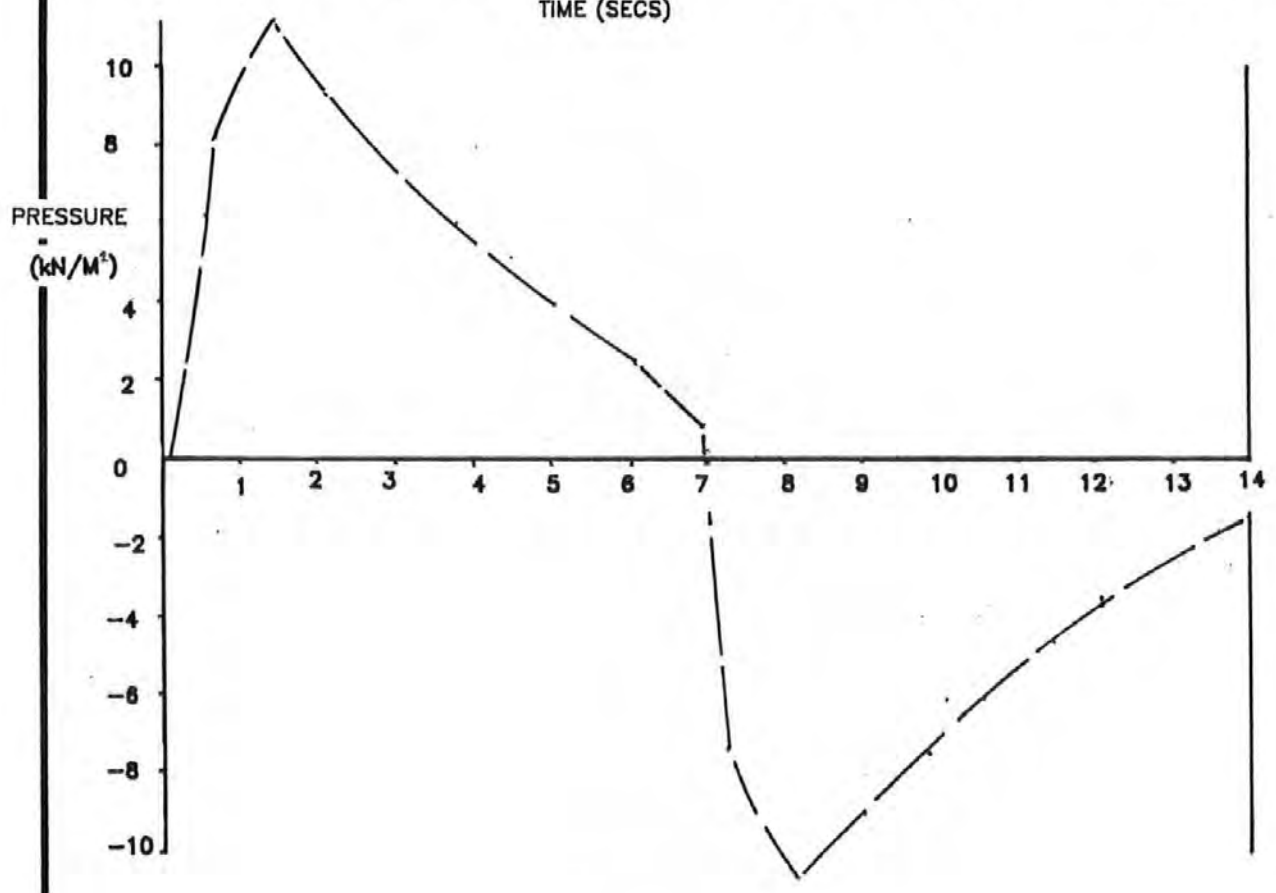
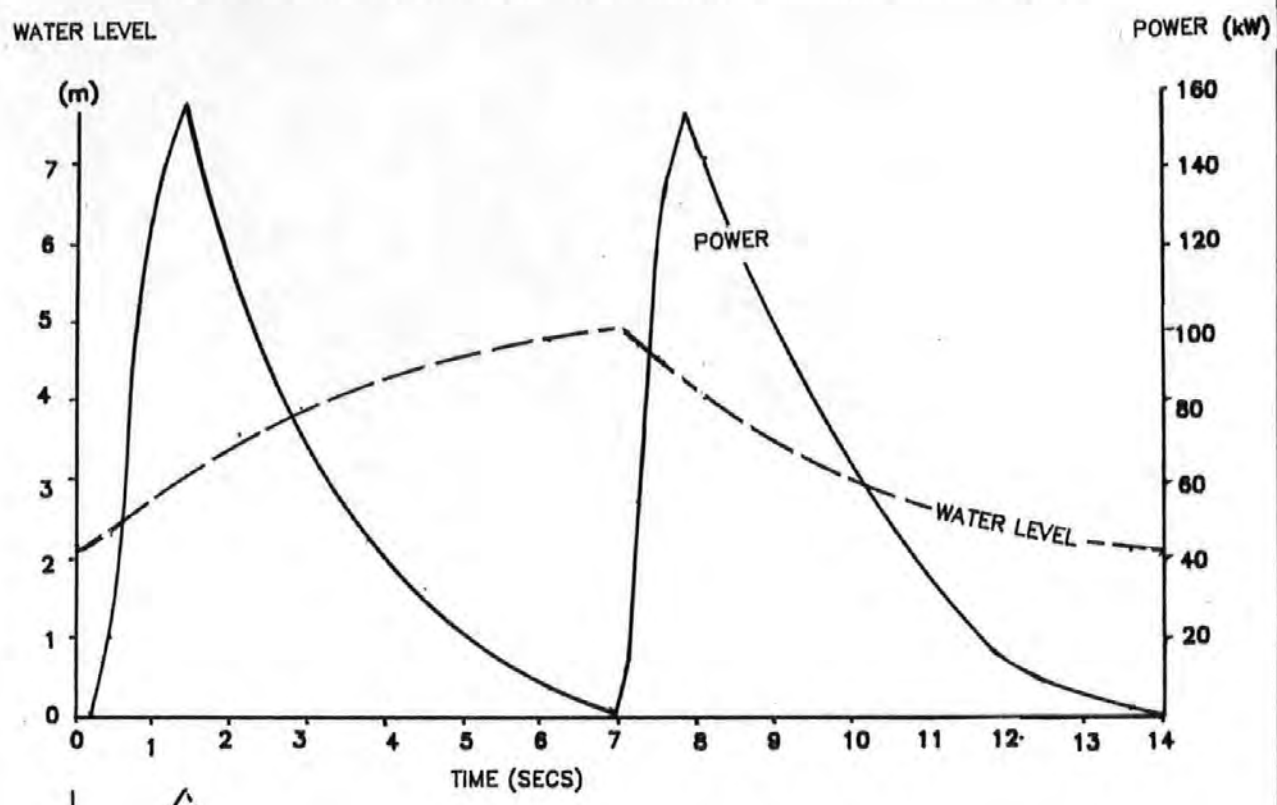




FIG. 6.6: ENERGY TEST T1.4; ST = 1.5

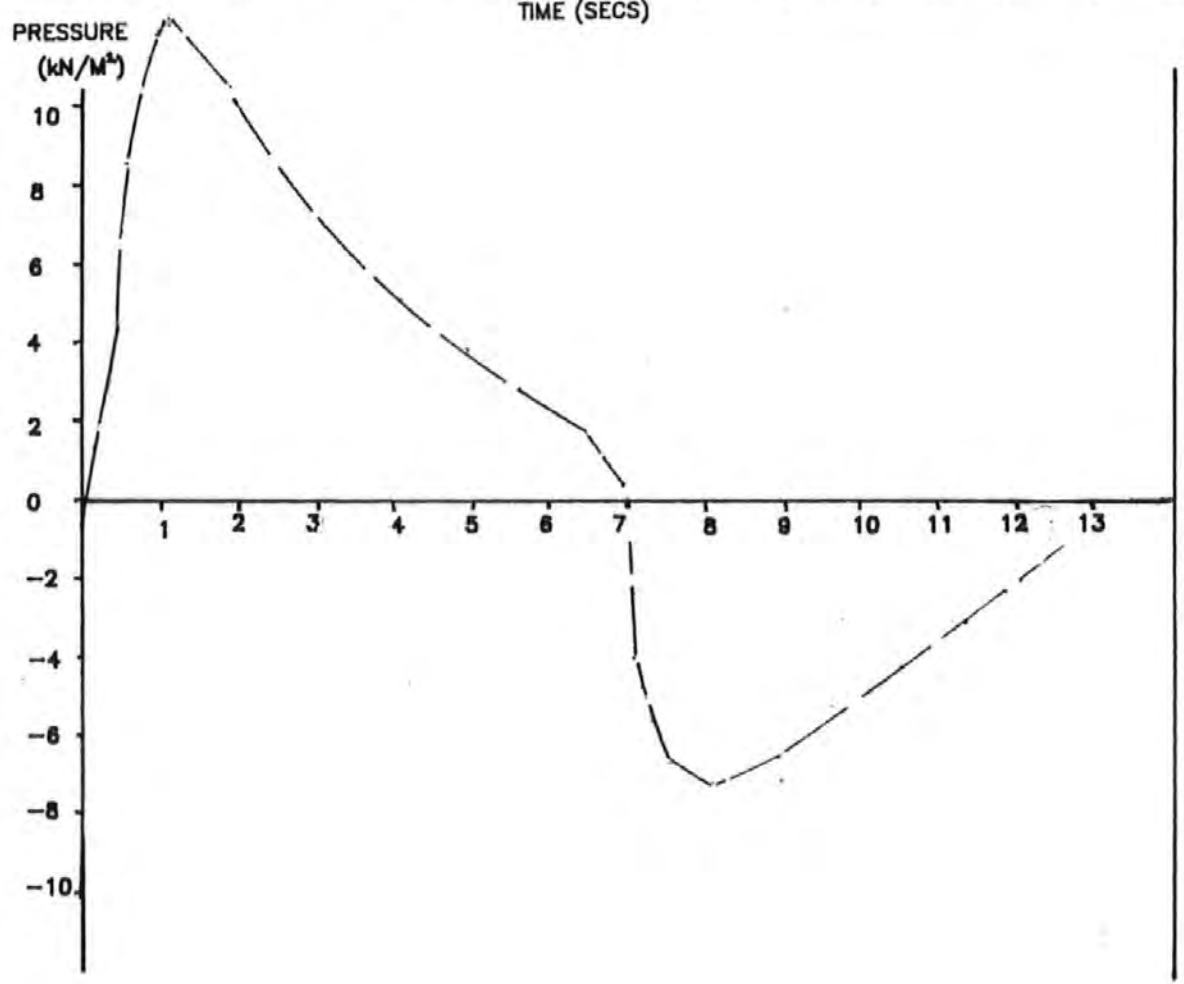
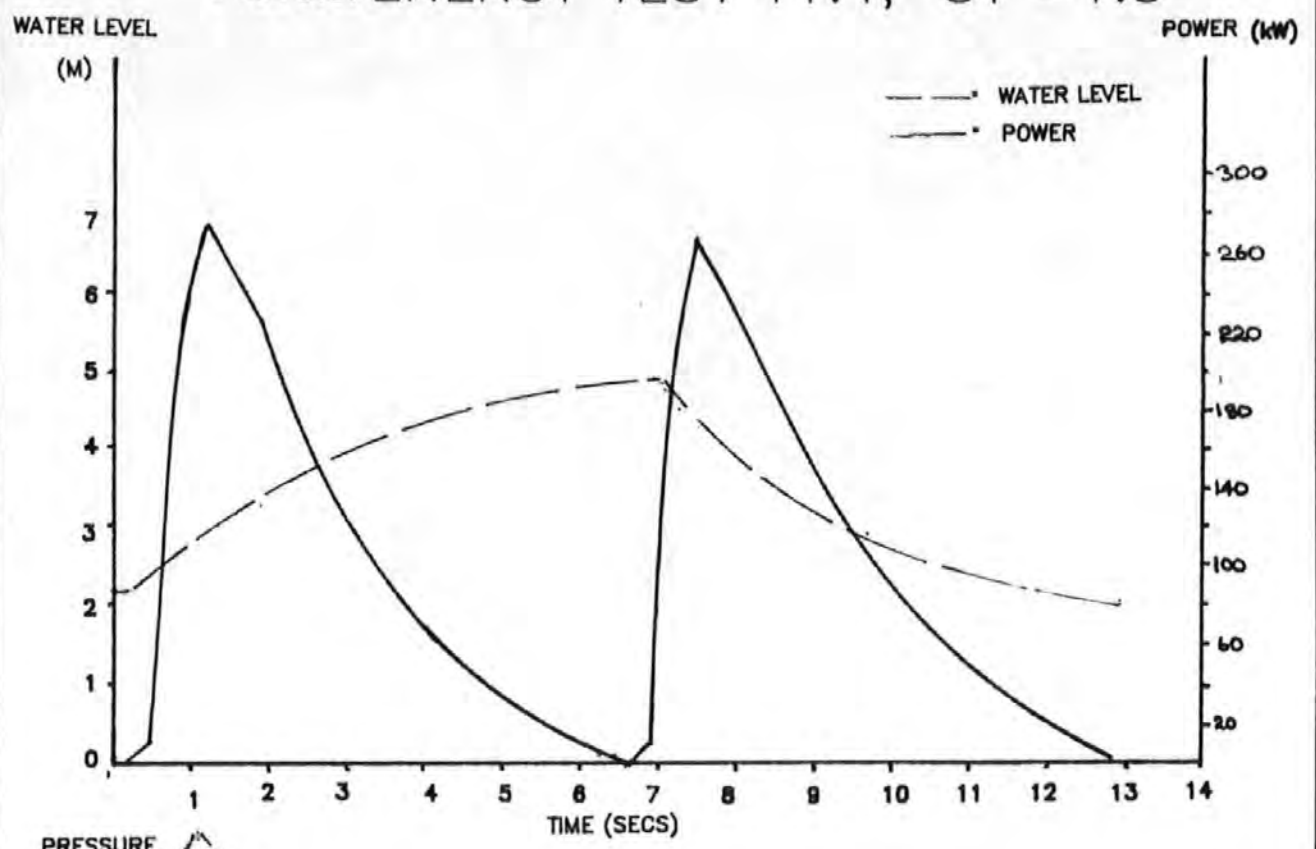


FIG. 6.7: ENERGY TESTS T1.0 – T1.7
(VARYING GATE TRIGGERS)

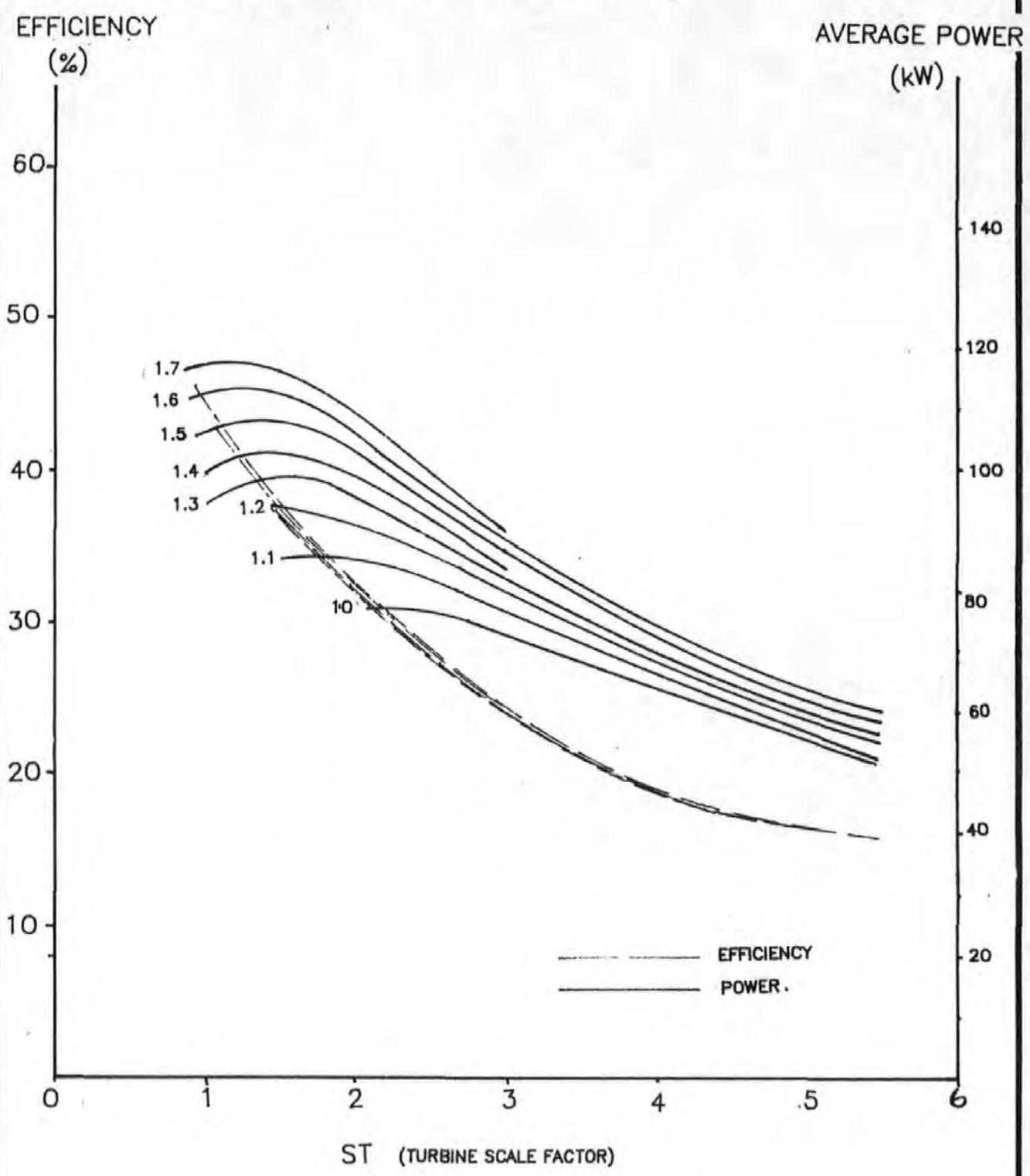


FIG. 6.8: SERIES 10

Variable Gu

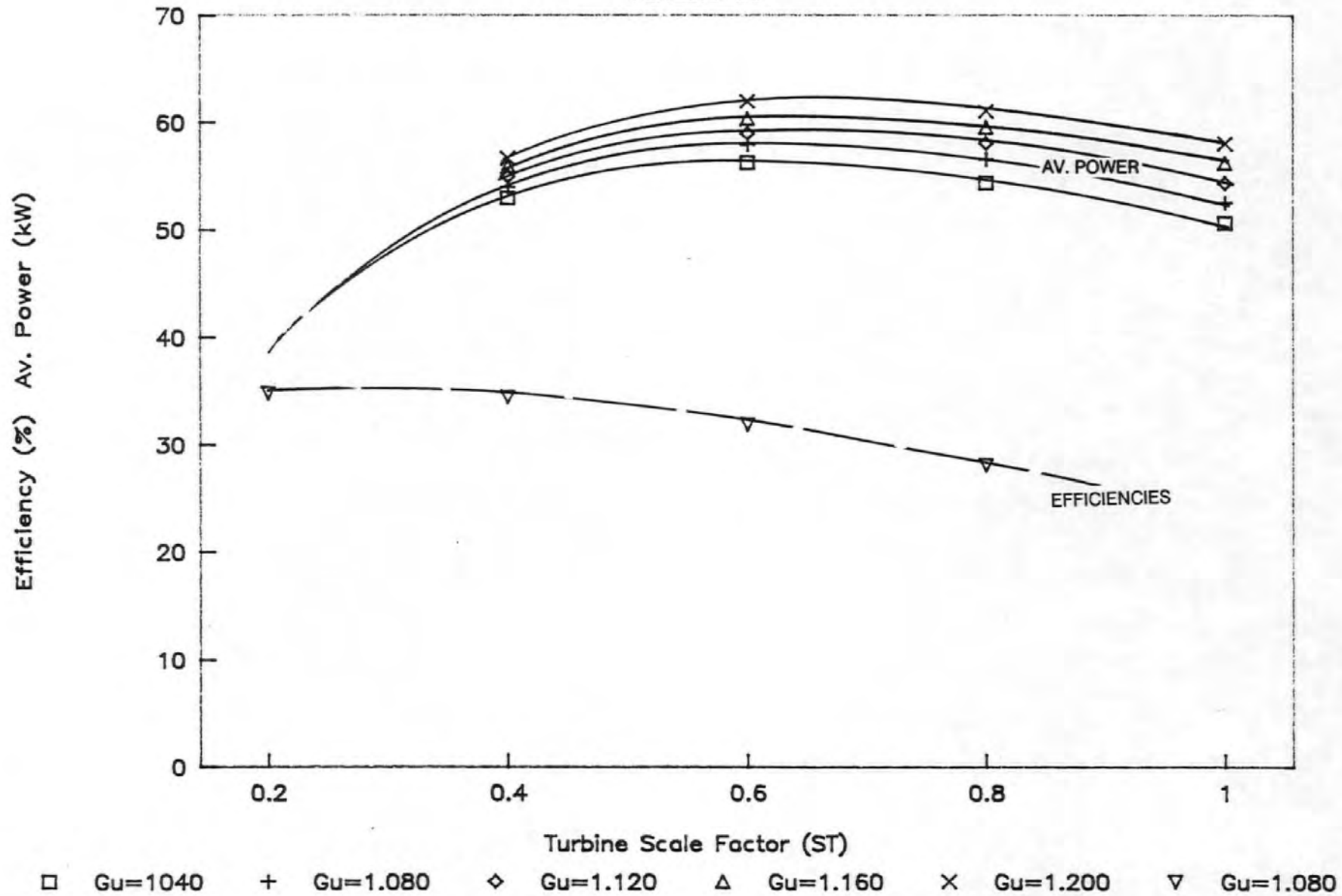
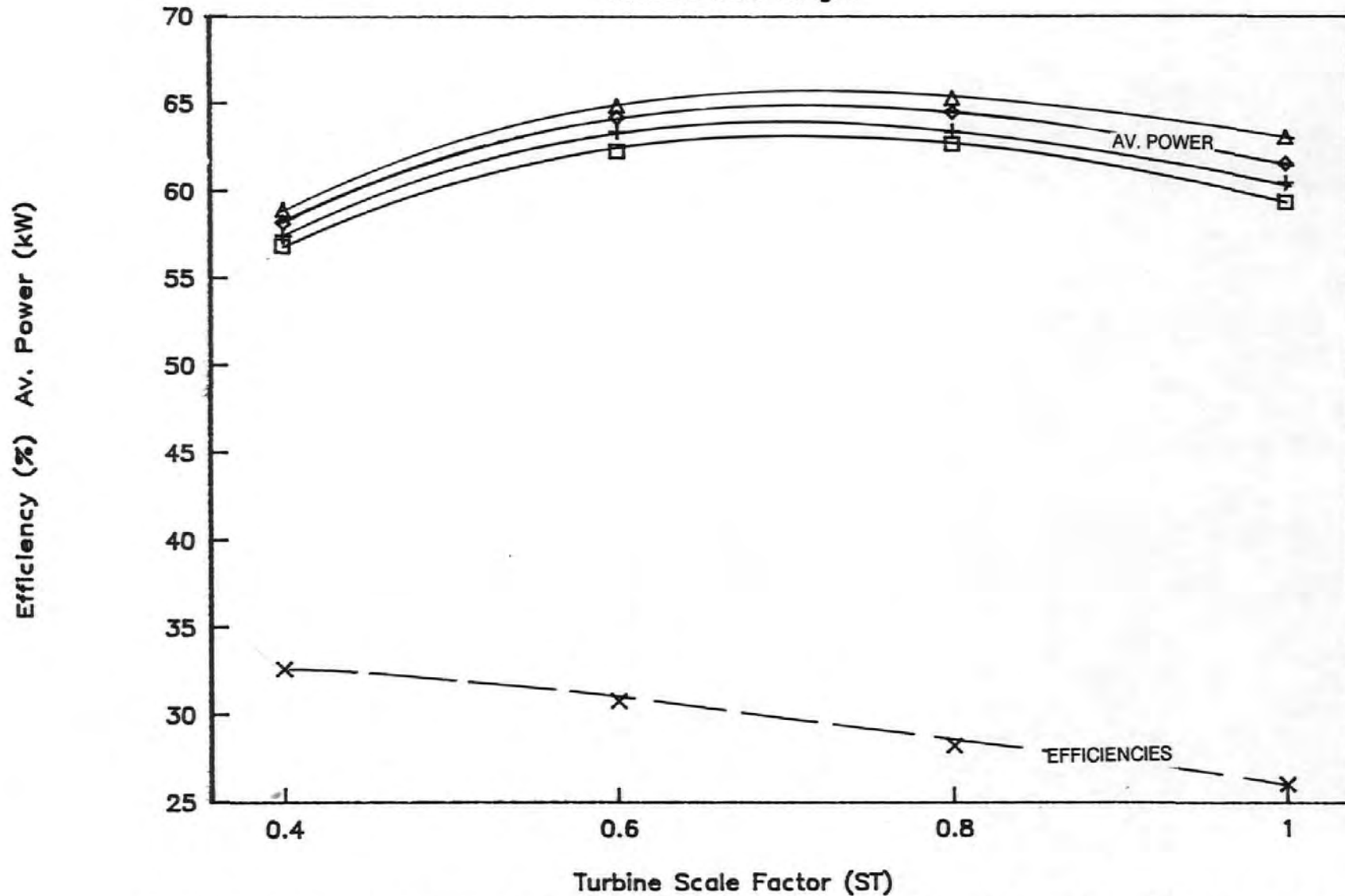


FIG. 6.9: SERIES 11
Variable Gate Height



□ BG=2.050 + BG=2.100 ◇ BG=2.150 △ BG=2.200 × BG=2.0 - 2.2

FIG. 6.10:

SERIES 12

Variable Gate Times

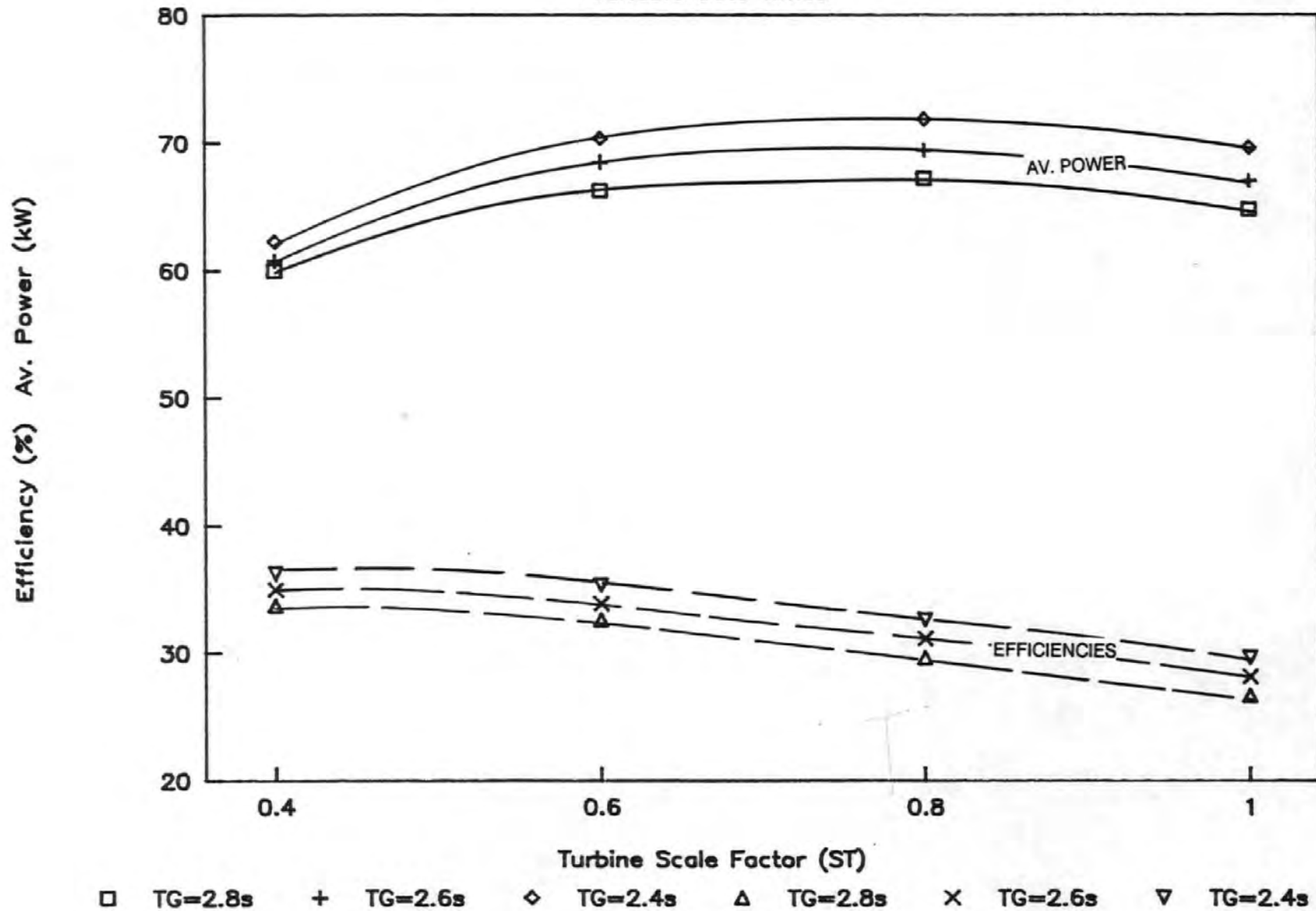
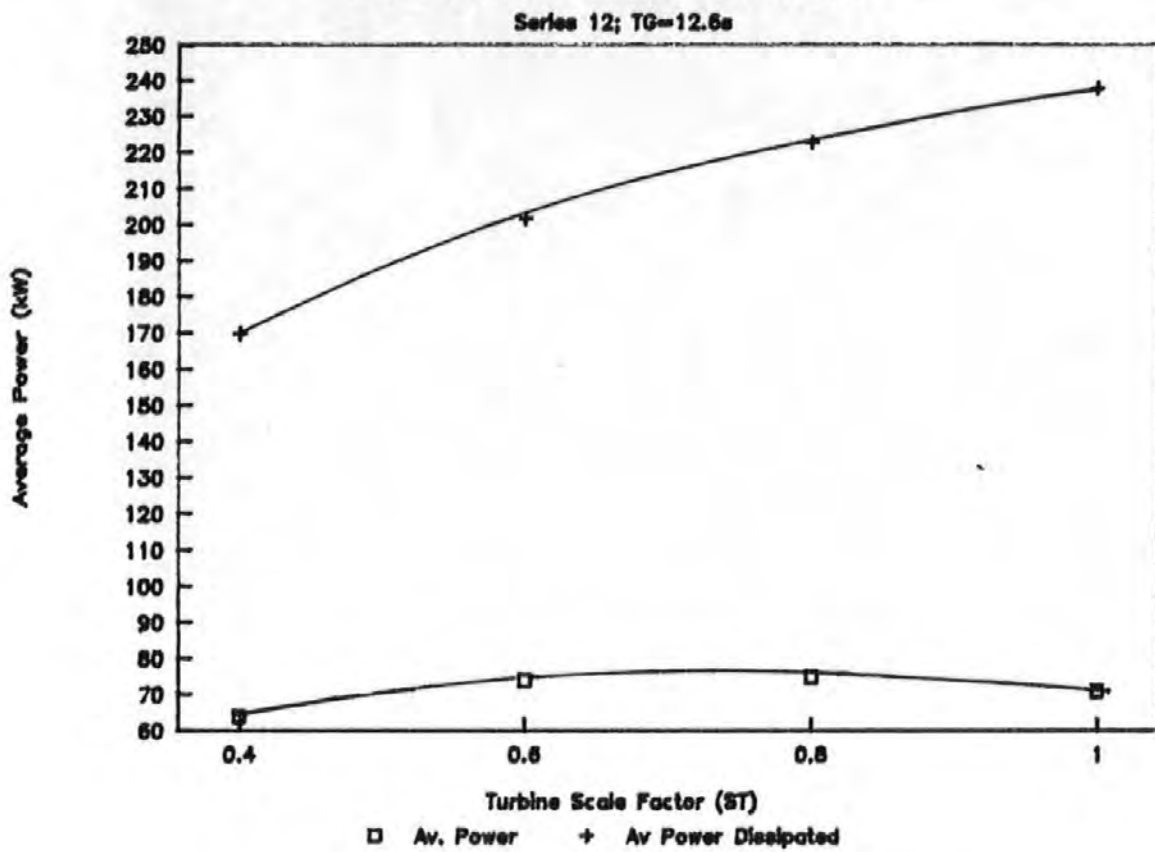
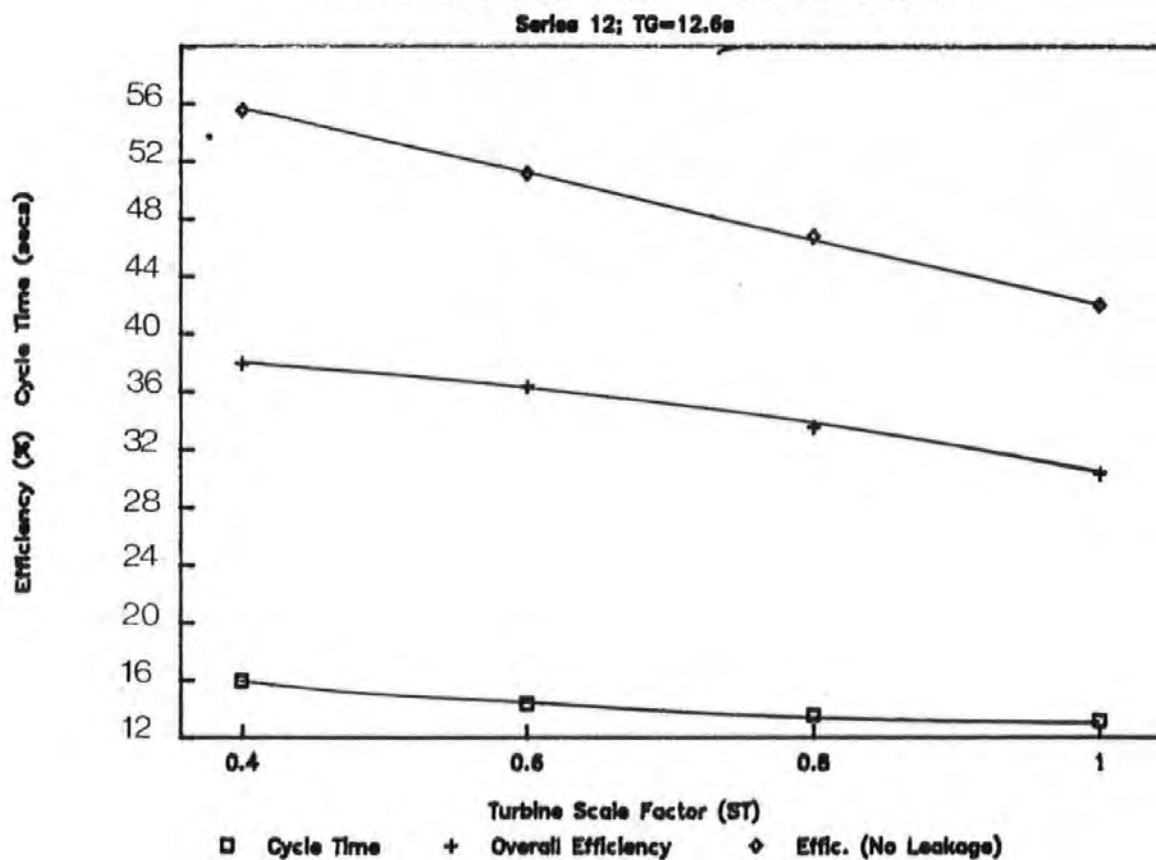


FIG. 6.11: EFFICIENCIES, POWER OUTPUT AND CYCLE TIMES
TWIN CHAMBER SYSTEM

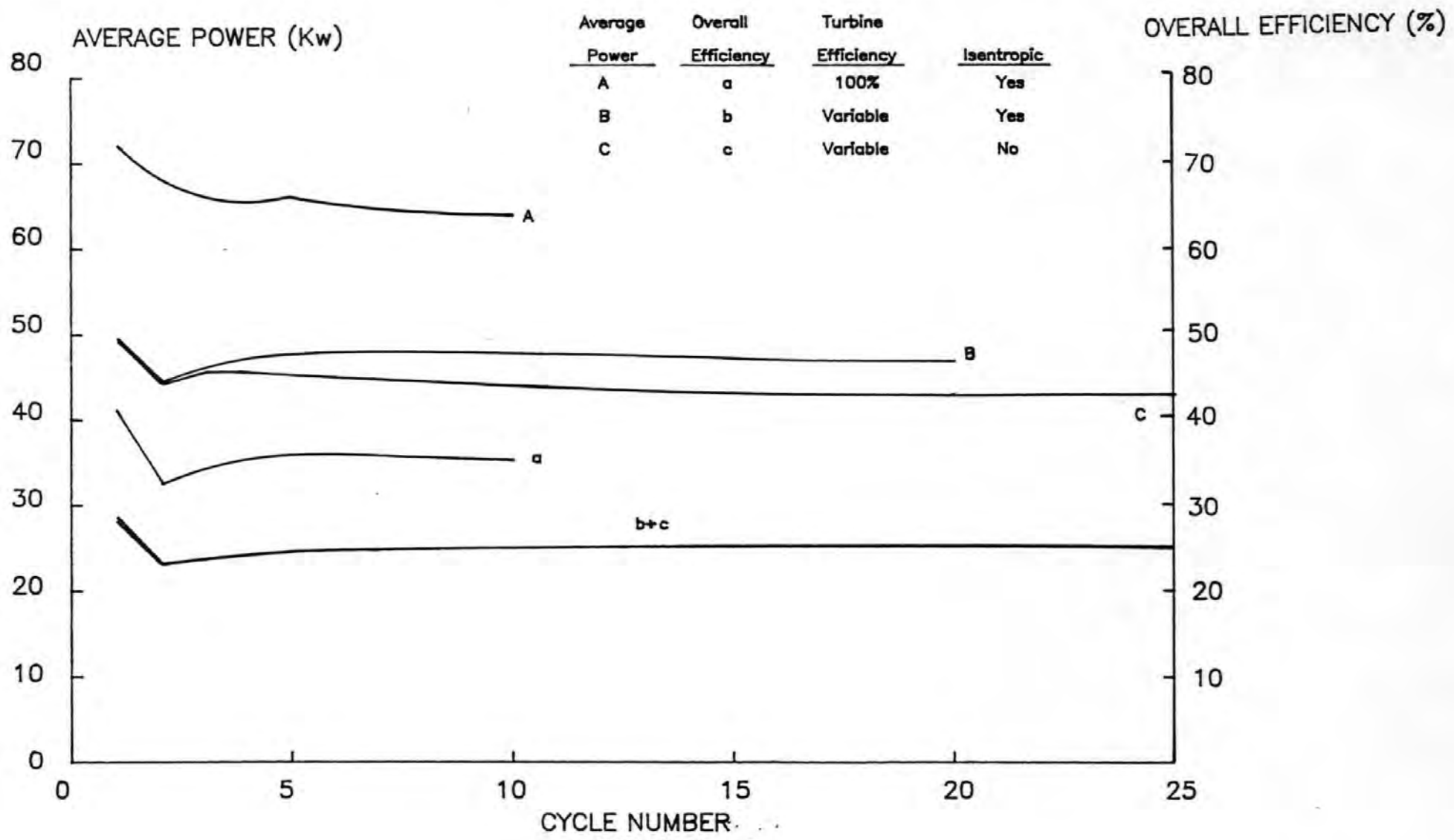
AVERAGE POWER OUTPUT



EFFICIENCIES AND CYCLE TIME



TEST SERIES 22 – AVERAGE POWER OUTPUT
AND EFFICIENCY.



123

FIG. 6.12

TEST SERIES 22 – AIR TEMPERATURE AND
NET HEAT LOSS

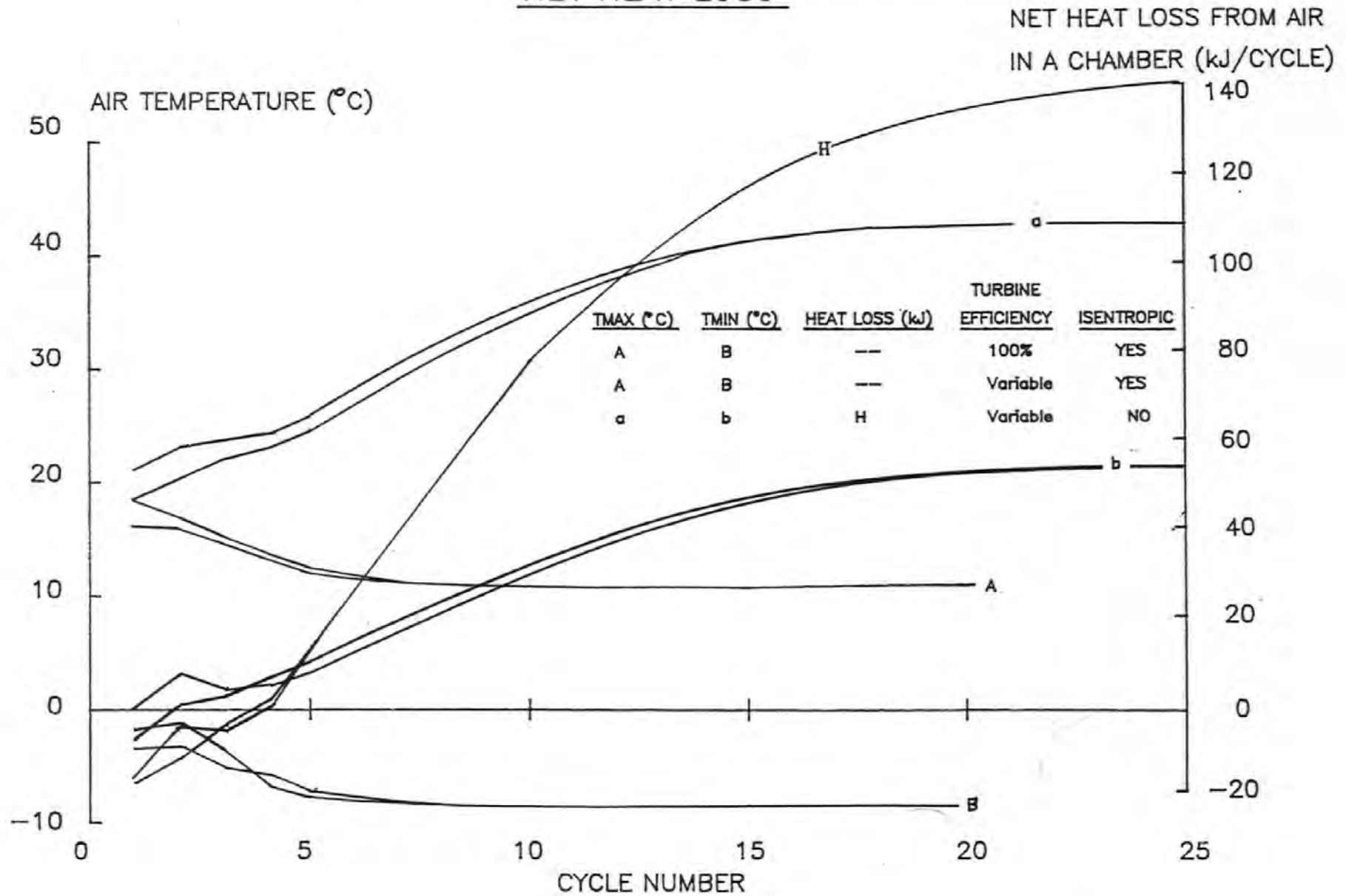
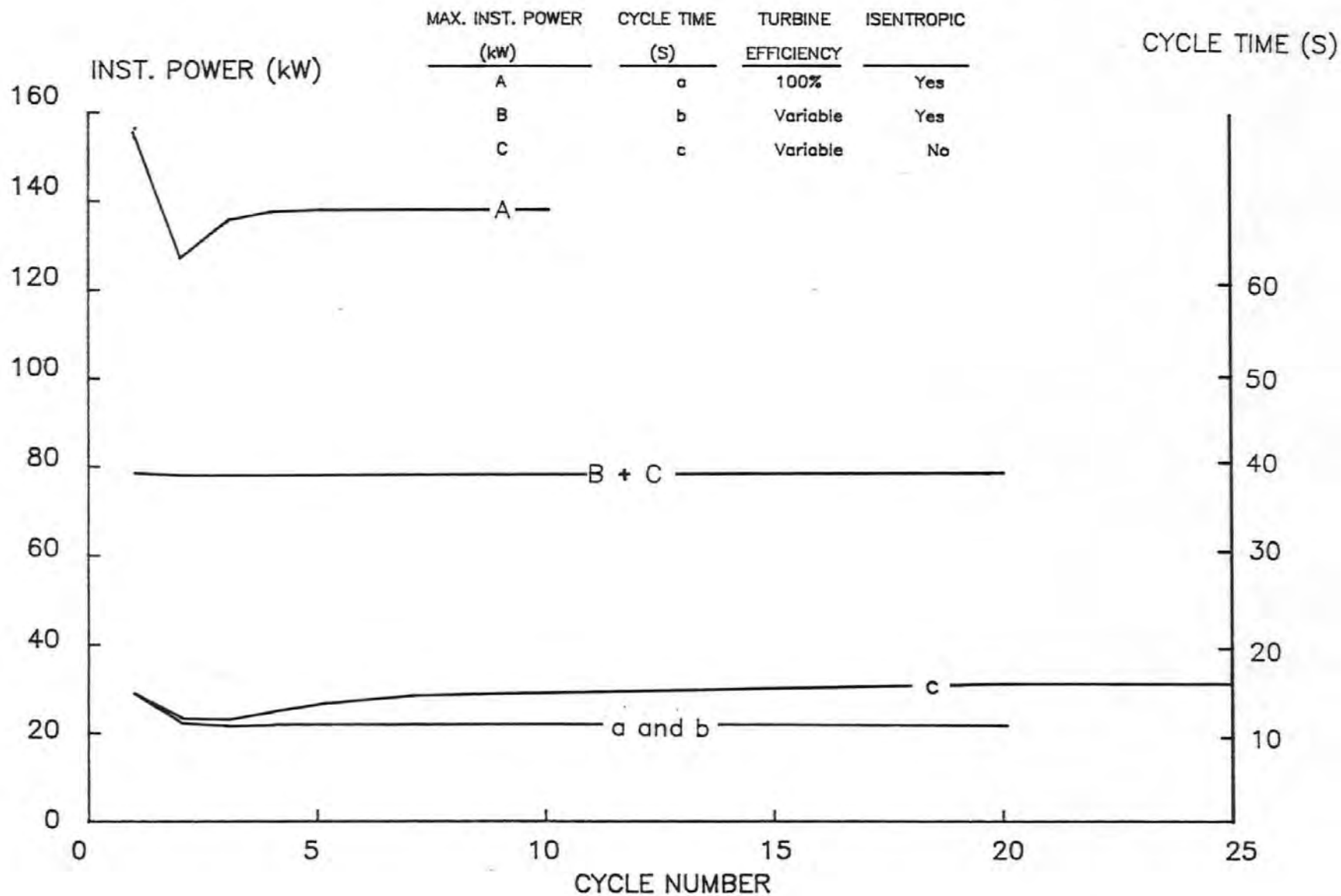


FIG. 6.13

TEST SERIES 22 – INSTANTANEOUS POWER AND CYCLE TIME



TEST SERIES 23 – VARIABLE GATE HEIGHT

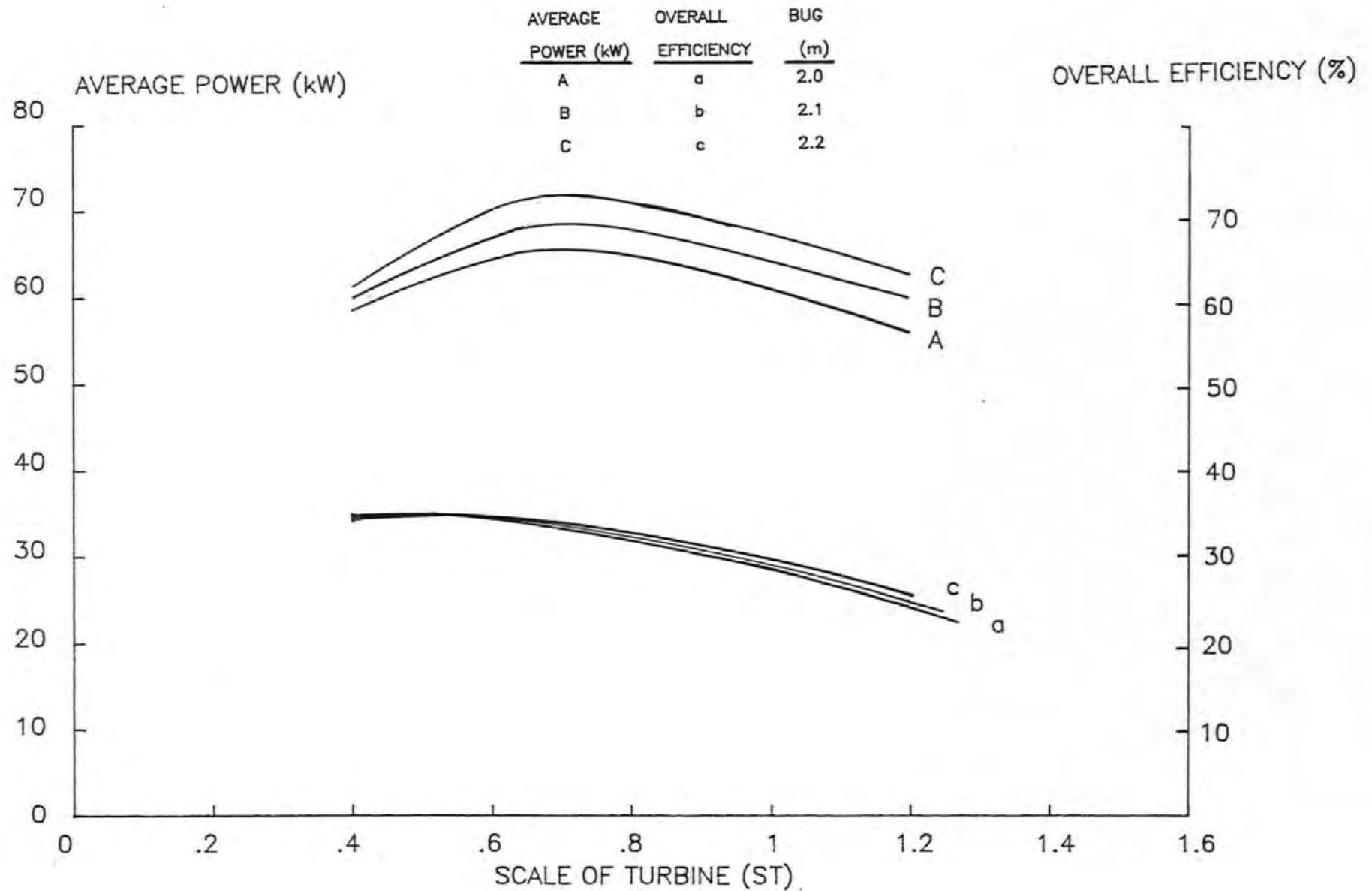


FIG. 6.15

TEST SERIES 24 - VARIABLE GU

AVERAGE POWER (kW)	OVERALL EFFICIENCY	GU (m)
A	a	1.0
B	b	1.1
C	c	1.2

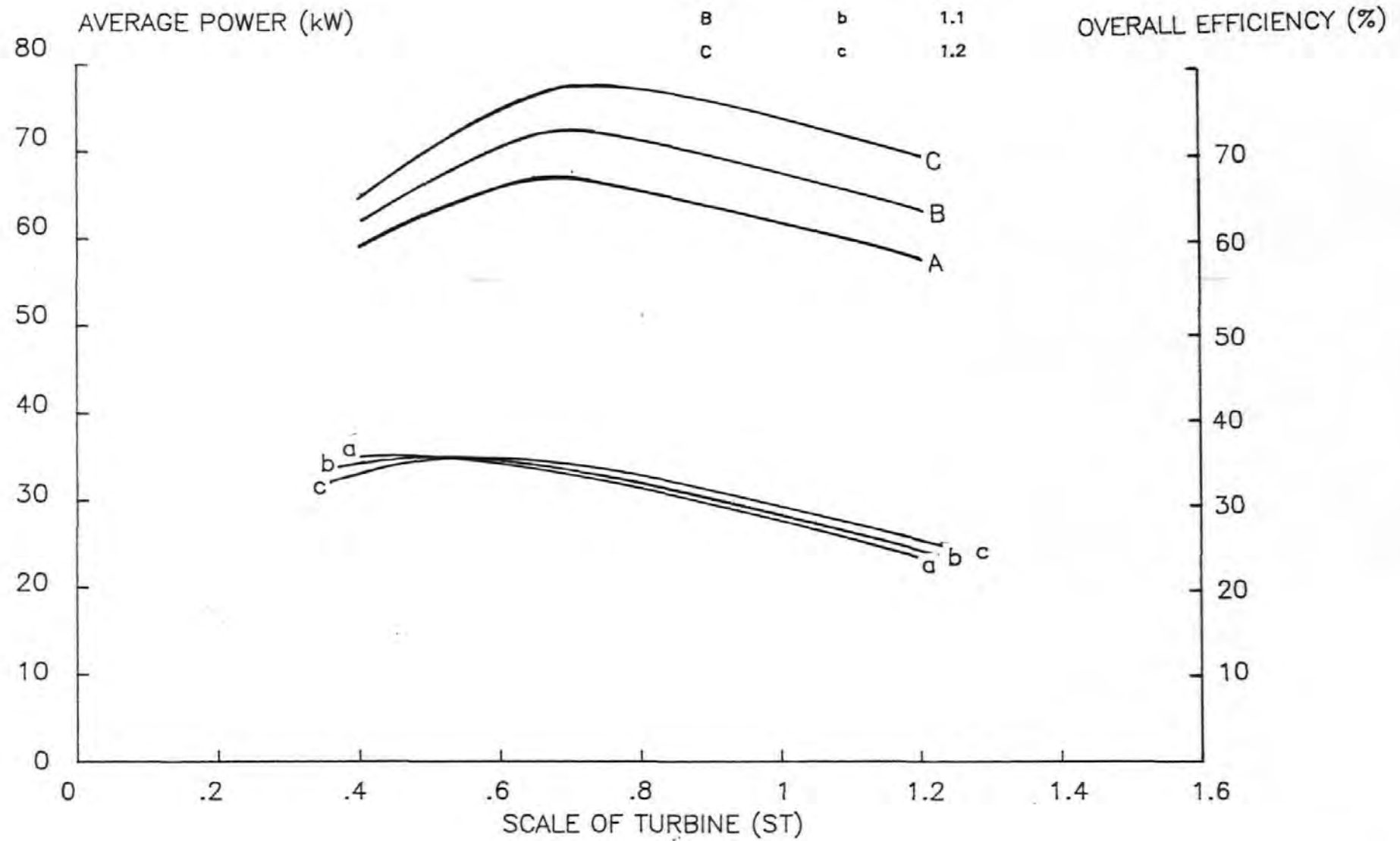


FIG. 6.16

TEST SERIES 26 – VARIABLE GATE SPEED

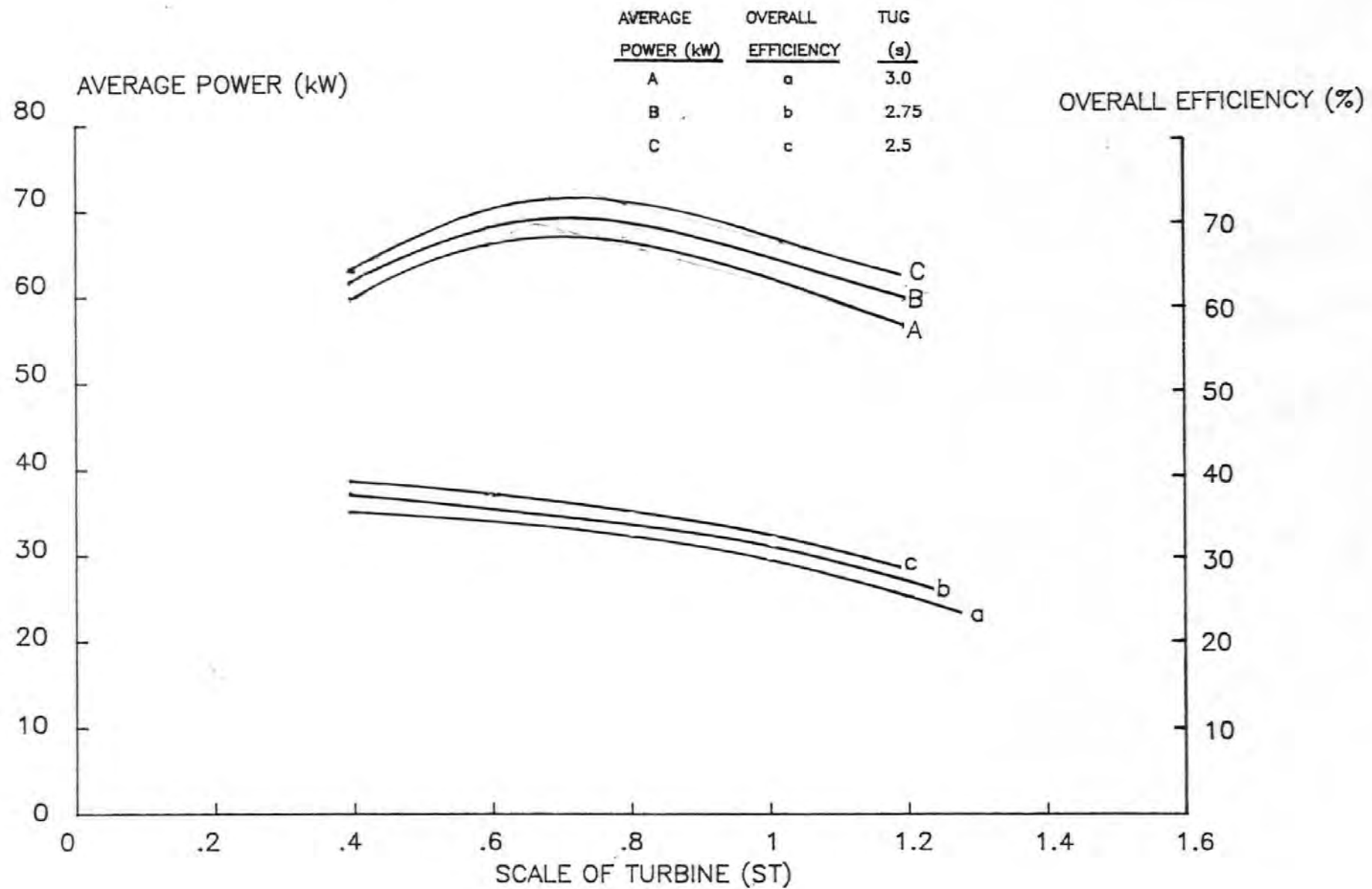


FIG. 6.17

7.0 : OUTLINE DESIGN AND COSTING

7.1 Initial Concepts

Both the physical and the mathematical model studies suggest that the design criteria set out in Section 2.1 are most likely to be satisfied by a twin, circular chamber PWE incorporating a flow-assisted butterfly gate. Consequently the following outline design and costing exercise concentrates on this particular configuration. A less rigorous appraisal of the rectangular chamber system incorporating a horizontal-axis radial gate is included.

Once suitable system configurations have been selected it becomes necessary to decide how these configurations can best be sited in a river channel. A number of possibilities are discussed in the following section before a 'typical' PWE layout is chosen for the purposes of this study. It must be remembered that the objective is to obtain an estimate of the final, overall cost of the system not to produce a detailed design. Thus, various assumptions and compromises are made to compensate for the lack of detailed knowledge of a specific site. In some cases section sizes and member thicknesses are assumed in order to avoid lengthy, iterative design procedures.

It should be stressed at this point that the following outline designs are for the purpose of investigating the feasibility of each scheme and of establishing a basis for a reasonable cost estimate. Consequently, in no way should the present proposals be considered as detailed designs nor the drawings as working drawings.

7.2 Position

As far as the Twin chambered, butterfly-gated system is concerned, three situations would seem most appropriate:

1) Within the channel bank, as shown in Fig. 7.1

With this arrangement a separate weir-type structure would be necessary in order to generate the required head. Consequently, the suitability of this arrangement would depend upon the river topography and the configuration of any existing weirs, millpools etc. A local example of such a site is Totnes Weir on the River Dart in Devon. Here, the river turns through approximately ninety degrees as it passes over the weir, which produces a head of between 1.4 and 3.6 metres depending upon the state of the tide on the downstream side.

One of the advantages of this type of site is that by commencing excavation and construction from the downstream side the site could be self-draining to a certain extent. The driving of a temporary sheet pile wall along the upstream bank or better still, the placing of a much cheaper fabric Portadam may prove necessary as may the installation of pumping equipment. Upon completion, ninety per cent of the structure would be below ground level and would therefore have a minimum effect on the surrounding landscape.

The structure would not significantly affect the river flow in times of flood. In fact it could be utilized as an extra sluicing facility by moving the gate to the central position. Losses will be incurred at either end of the culvert which could impair the system's performance. Careful design of both the entrance and exit configurations would be necessary to minimize such losses.

2) Partially within the bank whilst still spanning the channel, as shown in Fig. 7.2

Entrance and exit losses would be significantly reduced in this arrangement and the structure itself provides the means to generate the required head. If a large percentage of the chambers were set within the channel banks as shown, the banks would provide some of the necessary support to withstand the sliding and overturning forces generated by the differential head across the chambers. Although this reduces the need for deep foundations some form of cut-off wall beneath the structure would prove necessary where granular, non-cohesive soils were in evidence to prevent piping and scour. The construction of a bypass waterway may also be required in order to cope with large discharges in flood conditions and to prevent extensive upstream flooding. Model testing has shown that the system is quite capable of operating when flow is passing over the chamber roofs. A certain degree of flood alleviation could therefore be achieved by allowing this configuration to operate in an overtopping mode when necessary.

3) Free-standing, across the river channel, as shown in Fig. 7.3

Again the structure also acts as the barrage, the chambers being connected to the banks via short, barrage walls. This would allow for the installation of sidewall sluices to reduce the upstream head both during construction and also in times of flood. The elevation of these side walls would be equal to that of the upstream water level. They would therefore

act as side weirs, and provide a control for the upstream water level which could possibly obviate the need for permanent sluices.

By taking away the bank support, however, the structure is now subjected to the full sliding and overturning forces of the differential head and a much deeper foundation would be required.

To summarize, the bankside system would require a separate water retaining structure such as a weir and is very site specific although in an appropriate situation it could prove to be the most viable option of the three. The second system's stability is greatly assisted by the surrounding banks. However, due to its lack of side walls and sluices, it may have to be designed to overtop during periods of flood. Its construction could also involve the added costs of a separate waterway in order to prevent extensive flooding upstream. The third option, although possessing the necessary side walls and/or sluices to help prevent flooding, may prove more costly to construct due to its deeper foundation.

Each one of these options could prove to be most suitable given a certain set of circumstances. It is felt, however, that the third option provides the solution most likely to suit the majority of situations and it is this option upon which the following outline design and costing exercise was based.

7.3 The Structure

For the purposes of the outline design, the structure has been kept as simple as possible. It consists of two circular chambers surmounted by flat roofs from which the connecting turbine ducting protrudes as shown in Fig. 2.3. The butterfly gate is situated between the two chambers and the entrance and exit ducts are formed by the gate cover and the adjacent chamber walls. The two side walls connect the chambers to the bank and the remaining central span is closed by an intermediate wall. The final, costed designs are based upon model no. 3.2 of Section 3.3.2 which has a 55° gate movement. The satisfactory performance of this model when coupled with the 155 mm gate led to its inclusion at full scale within the parametric tests of Section 6.5 and provided the final, optimum average power output.

The design philosophy has been to treat the structure as three separate units, ie chambers, side walls and intermediate wall plus gate system. This is to allow a construction sequence in which the structure acts as its own coffer dam thereby introducing significant savings in cost. This is described in more detail in the following sections. Those materials thought most suitable for the project are steel sheet piling, steelplate, prefabricated concrete, in-situ concrete and plastic/fibreglass laminate. Each system investigated in the following sections consist either wholly of one of these materials or from a combination of several of

them. The outline design of the main structural elements of the system takes account of the engineering capabilities of those soils most likely to be encountered in practice. This has enabled drive depths and the appropriate sizes of relevant sections to be determined. Quantities have been estimated in accordance with the Civil Engineering Standard Method of Measurement, 2nd Edition³⁰, and corresponding rates were applied to these estimates either from the Wessex Database for Civil Engineering³¹ or from information obtained from various suppliers³². Any costs not considered current were suitably adjusted to 1988 prices using relevant construction indices³³. In this way, a reliable, overall UK cost estimate for the major elements of the system, including their construction, has been built up and used as a basis on which to derive a cost for the energy produced.

Unfortunately, due to the extensive nature of these costing studies it is not possible to include them in their entirety. It is intended therefore to present the complete steel sheet pile study followed by summaries of the other options. This should sufficiently illustrate the extent of the outline design. Further detail can be obtained from Part 3 of Reference 19.

A summary of the outline designs and costings for the proposed configuration of the structure using a number of combinations of materials and construction methods that would seem most appropriate and cost effective for the scheme in question is therefore presented. A summary of the outline design and costing of a rectangular chamber system is also included for comparative purposes.

7.4 Steel Sheet Pile Construction

7.4.1 Introduction

It would be quite feasible to construct the chambers, the side walls and the intermediate wall from interlocking, steel sheet piles. The design and construction methodology would be similar to that for circular, sheet piled cofferdams the installation of which is established civil engineering practice. The chambers of the PWE for the purpose of the outline design, can be considered as circular cofferdams containing an oscillating water column instead of the more usual granular fill material. This in itself, however, presents several unique design problems which will be discussed subsequently. As pile design is based on the prevailing ground conditions of a specific site, both cohesive and granular soils are considered here and the case of an underlying rock strata is also discussed.

7.4.2 Design Considerations

For the purpose of the following outline designs the chambers are assumed to act as rigid gravity structures, their rigidity being supplied by the reinforced concrete roof and floor slabs plus the intermediate, circular wallings shown in Fig. 7.4. This assumption is based on the cellular cofferdam design method of Terzaghi³⁴. The structure therefore must be stable against sliding on the base, overturning, excessive interlock tension and uplift due to buoyancy. In addition, chambers on sand must be stable against failure from the effects of underseepage, while those on clay must be stable against bearing capacity failure. A problem which is possibly unique to a structure housing an oscillating water column is the pumping effect of the constantly changing mass within it on the supporting soil; a condition which could effect both underseepage and bearing capacity if not contained.

The barrage side walls are treated as independent units and drive depth is calculated using the Free Earth Support method and Rankine theory.

7.4.3 Chamber Design

It is proposed that Frodingham straight web sections would be most suitable for the chamber walls. The interlocks of these sections are designed to transmit the circumferential tension between adjacent piles and at the same time permit sufficient angular deviation between adjacent piles to allow chambers of the required diameter to be formed. Neither 'Z' nor 'U' sections are designed to withstand lateral tension forces. The straight web sections, however, will not support significant axial loading and so a 219 mm diameter, hollow steel section has been included to transmit the weight of both the roof and turbine into the base slab as shown in Fig. 7.4. It is envisaged that a high degree of accuracy in the forming of the circular chambers will be unnecessary although accurate positioning will be required to allow correct installation of the gate system.

7.4.4 Ground Conditions

The following assumptions have been made concerning the properties of the underlying soils:

<u>Sand</u>	γ sat	=	20.0 kN/m ³
	ϕ	=	35°
	Ka	=	0.27
	Kp	=	3.7
<u>Clay</u>	γ sat	=	18.0 kN/m ³
	Cu	=	45.0 kN/m ²
	Ka	=	Kp = 1.0

where:

- γ_{sat} = saturated unit weight of soil
- ϕ = angle of internal friction
- K_a = coefficient of active earth pressure
- K_p = coefficient of passive earth pressure
- C_u = cohesive strength

These assumptions are based upon borehole data collected during the construction of the M5 crossing of the flood plain of the River Exe. As a non-specific site is under consideration it would seem reasonable to adopt such values and to consider them representative of a typical lowland situation.

7.4.5 Sliding

Fig. 7.5 shows the principle forces to be taken into account when determining the required depth of drive (d) to prevent failure by sliding. For no sliding, $F_a = F_p$, however, Lacroix et al³⁴ recommend a factor of safety of between 1.25 and 1.5 based upon the ratio of the product of the overall weight of the structure and a friction factor, and the difference in total forces acting in the upstream and downstream directions, i.e.

$$F_s = \frac{W'\lambda}{PL-PU} = 1.25$$

- where:
- W' = effective weight of chamber and fill
 - λ = frictional resistance of the chamber fill ($\tan \phi$)
 - PL = horizontal total force on the upstream side
 - PU = horizontal total force on the downstream side

sand

$$F_{a1} = 5.5^2 \times 10.0 \times 0.5 = 151.25 \text{ kN/m}^2$$

$$F_{a2} = 0.27 \times 5.5 \times 10.0 \times d = 14.9d$$

$$F_{a3} = 0.27 \times 10.0d^2 \times 0.5 = 1.35d^2$$

$$F_{p1} = 2.0^2 \times 10.0 \times 0.5 = 20.0 \text{ kN/m}^2$$

$$F_{p2} = 3.7 \times 20.0 \times d = 74.0d$$

$$F_{p3} = 3.7 \times 10.0 \times 0.5d^2 = 18.5d^2$$

therefore:

$$\begin{aligned} \text{PL-PU} &= 7.85 (1.35d^2 - 18.5d^2 + 14.9d - 74.0d + 151.25 - 20.0) \\ &= 134.62d^2 + 463.94d - 1030.3 \end{aligned}$$

and:

$$\begin{aligned} W' \lambda &= 0.7 (P_{\text{roof}} + P_{\text{turb.}} + P_{\text{head}} + P_{\text{floor}}) \\ &= 46.99 + 12.25 + 274.82 + 179.03 \\ &= 513.1 \text{ kN} \end{aligned}$$

therefore:

$$168.28d^2 + 579.93d - 1800.98 = 0$$

by trial and error: $d = 2.0 \text{ m}$

The depth of drive must also be sufficient to prevent further penetration of the piles on the downstream side. The resistance to further penetration depends upon the shear resistance between the pile walls and the soil. Terzaghi recommends a minimum drive depth of $2H/3$ to ensure that further penetration does not take place; the drive depth, therefore, should be increased to 2.3 m.

<u>Clay</u>	$F_{a1} = 5.5^2 \times 10.0 \times 0.5 = 151.25 \text{ kN}$
	$F_{a2} = (55.0 - (2 \times 45.0)) \times d = -35.0d$
	$F_{a3} = (18d - (2 \times 45.0)) \times 0.5d = 9.0d^2 - 45.0d$
	$F_{p1} = 2.0^2 \times 10.0 \times 0.5 = 20.0 \text{ kN}$
	$F_{p2} = (20.0 + (2.0 \times 45.0/1.35)) \times d = 86.67d$
	$F_{p3} = (18.0d + (2.0 \times 45.0/1.35)) \times 0.5d = 9.0d^2 + 33.3d$

therefore: $\text{PL-PU} = 7.85 (200.57d - 131.25) = 1574.5d - 1030.31$

In the case of a cohesive soil where $\lambda = 0$:

$$F_s = \frac{C_u \cdot A_{ch}}{\text{PL-PU}} = 1.25$$

where: C_u = cohesive strength of soil

A_{ch} = c.s. area of chamber

therefore:

$$1574.5d - 1913.71 = 0$$

$$\underline{d = 1.22 \text{ m}}$$

7.4.6 Overturning

The forces taken into account when considering overturning of the structure are shown in Fig. 7.6. The forces exerted by the concrete sections, contained water and buoyancy are for unit width. Lacroix et al. recommend a factor of safety of at least 3.0, based upon the ratio of resisting moment to overturning moment, i.e.:

$$F_s = \frac{M_r}{M_o} = 3.0$$

sand

$$F_{a1} = 5.5^2 \times 10.0 \times 0.5 = 151.3 \text{ kN/m}$$
$$F_{a2} = 0.27 \times 2.0 \times 10.0 \times d = 5.4d$$
$$F_{a3} = 0.27 \times d^2 \times 10.0 \times 0.5 = 1.35d^2$$

$$F_{p1} = 2.0^2 \times 10.0 \times 0.5 = 20.0 \text{ kN/m}$$
$$F_{p2} = 3.7 \times 5.5 \times 10.0 \times d = 203.5d$$
$$F_{p3} = 3.7 \times d^2 \times 10.0 \times 0.5 = 18.5d^2$$

$$M_r = 2.5(F_r + F_t + F_h + F_f + F_c + F_s) + 0.67F_{p1} - (0.5d \times F_{p2}) + (0.67d \times F_{p3})$$
$$= 12.4d^3 + 101.75d^2 + 250.0d + 419.29$$

$$M_o = 1.83F_{a1} + (0.5d \times F_{a2}) + (0.67d \times F_{p3}) + 3.75F_b$$
$$= 1.01d^3 + 2.7d^2 + 604.91$$

therefore:

$$9.37d^3 + 93.65d^2 + 250.0d - 1395.44 = 0$$

by trial and error:

$$\underline{d = 2.60 \text{ m}}$$

Clay

$$Fa1 = 5.5^2 \times 10.0 \times 0.5 = 151.25 \text{ kN/m}$$

$$Fa2 = (20.0 - (2.0 \times 45.0))d = -70.0d$$

$$Fa3 = (18.0d - (2.0 \times 45.0)) \times 0.5d = 9.0d^2 - 45.0d$$

$$Fp1 = 2.0^2 \times 10.0 \times 0.5 = 20.0 \text{ kN/m}$$

$$Fp2 = (55.0 + (2.0 \times 45.0))d = 145.0d$$

$$Fp3 = (18.0d + (2.0 \times 45.0)) \times 0.5d = 9.0d^2 + 45.0d$$

$$Mr = 6.03d^3 + 42.35d^2 + 250d + 432.7$$

$$Mo = 6.03d^3 - 65.15d^2 + 1261.16$$

therefore: $12.06d^3 - 237.8d^2 - 250d + 828.46 = 0$

$$\underline{d = 1.5 \text{ m}}$$

7.4.7 Interlock Tension

The "worst case" situation producing maximum lateral tensile force is shown in Fig. 7.7. This will act along the downstream face of the structure (a distance equal to half the circumference).

$$t_{\max} = P_{\max} \times L$$

where:

t = tensile force

P = horizontal stress

L = πr

$$\begin{aligned} t_{\max} &= 3.5^2 \times 10.0 \times 0.5 \times 7.85 \\ &= \underline{480.80 \text{ kN/m}} \end{aligned}$$

Lacroix et al. recommend a safety factor of 1.5 to 2.0. This corresponds to the ratio of t_{\max} to the minimum ultimate strength of the interlock.

$$F.S. = \frac{2795}{480.8} = 5.80$$

This would indicate that a circular waling situated as shown in Fig. 7.4 would be superfluous. However, in a cofferdam situation, initial filling with a granular material could cause 'barrelling out' of the coffer, i.e. a bulging of the walls of up to 150 mm. As we are dealing with a cyclical load in this case, any repeated movement could cause wear at the interlocks leading to leakage and eventual failure. The required rigidity of the structure must also be taken into account.

Bearing this in mind it is suggested that, for the purpose of this design, the intermediate waling should be retained.

7.4.8 Side Walls

If the width of the channel necessitates side walls then these should be of a 'U' or 'Z' section³⁵. A simplified design procedure has been carried out treating the pile as a simply supported beam with a loading equivalent to a 5.5 m head of water:

$$\begin{aligned} BM_{\max} &= \frac{Pab}{L} \\ &= \frac{5.5^2 \times 10.0 \times 0.5 \times 1.17 \times 2.3}{5.5} \\ BM_{\max} &= \underline{74.0 \text{ kN/m}} \end{aligned}$$

Assume Grade 43 steel, $p_{bc} = 165 \text{ N/mm}^2$:

$$\begin{aligned} M &= fz = 165z \\ z &= 6.06M_{\max} \\ &= \underline{448.5 \text{ cm}^3} \end{aligned}$$

Deflection:

$$\begin{aligned} y &= \frac{PL^3}{48EI} \left[\frac{3a}{L} - 4 \left[\frac{a}{L} \right] \right] \neq \frac{L}{360} \\ &= \underline{14,976 \text{ cm}^4} \end{aligned}$$

As the loading did not take the downstream water level into account, it would be reasonable to assume that a 2N Larsen section with a moment of inertia of $14,855 \text{ cm}^4$ would be adequate. Therefore, costing will be based upon a section modulus of 1000 cm^3 .

Fig. 7.8 shows the active and passive forces to be taken into account to determine drive depth. Again, the free earth support method is used:

$$\begin{aligned} \text{sand} \quad Fa1 &= 5.5^2 \times 10.0 \times 0.5 = 151.3 \text{ kN/m}^2 \\ Fa2 &= 0.27 \times 5.5 \times 10.0d = 14.85d \\ Fa3 &= 0.27 \times 10.0 \times 0.5d^2 = 1.35d^2 \\ \\ Fp1 &= 2.0^2 \times 10.0 \times 0.5 = 20.0 \text{ kN/m}^2 \\ Fp2 &= 3.7 \times 0.5 \times 20.0d = 37.0d \\ Fp3 &= 3.7 \times 0.5 \times 10.0d^2 = 18.5d^2 \end{aligned}$$

T.M.A."A":

$$(151.25 \times (1.83 + d)) + (14.85d \times 0.5d) + (1.35d^2 \times 0.33d) \\ - (20.0 \times (0.67 + d)) - (37.0d \times 0.5d) - (18.5d^2 \times 0.33d) = 0$$

therefore:

$$5.66d^3 + 11.10d^2 - 131.25d - 271.1 = 0$$

by trial and error:

$$d = 4.9 \text{ m}$$

Adding 20% for the passive force not included in the calculation:

$$\underline{d = 5.9 \text{ m}}$$

Clay

$$Fa1 = 5.5^2 \times 10.0 \times 0.5 = 151.25 \text{ kN/m}^2$$

$$Fa2 = (55.0 - (2.0 \times 45.0))d = -35.0d$$

$$Fa3 = (18.0d - (2.0 \times 45.0)) \times 0.5d = 9.0d^2 - 45.0d$$

$$Fp1 = 2.0^2 \times 10.0 \times 0.5 = 20.0 \text{ kN/m}^2$$

$$Fp2 = (10.0 + (2.0 \times 45.0))d = 110.0d$$

$$Fp3 = (9.0d + (2.0 \times 45.0)) \times 0.5d = 4.5d^2 + 45.0d$$

T.M.A."A":

$$(151.25 \times (1.83 + d)) - (35.0d \times 0.5d) + ((9.0d^2 - 45.0d) \times 0.33d) \\ - (20.0 \times (0.67 + d)) - (110.0d \times 0.5d) - ((4.5d^2 + 45.0d) \times 0.33d) = 0$$

therefore: $1.5d^3 - 102.3d^2 + 131.3d + 263.4 = 0$

by trial and error: $d = 2.4 \text{ m}$

Adding 20% for the passive force not included in the calculation:

$$\underline{d = 2.9 \text{ m}}$$

Connection to the chamber can be achieved via a straight web connecting sheet pile driven as part of the chamber wall. To form a sufficiently watertight seal at the

bank/wall interface, the final sheetpile should be set into the concrete abutment to a depth equal to half its width (see Fig. 7.10).

7.4.9 Intermediate Wall

The loading on the section of wall between the two chambers will have to be carried (via connecting sheet piles and the gate cover) by the chamber walls. It may prove necessary to introduce additional piling and walings in order to spread this load around the immediate wall perimeter. No attempt has been made to ascertain the extent of this extra loading. However, additional walings spanning a quarter of each chamber's circumference and sited adjacent to the gate area, have been included in the costing. It is also assumed that the intermediate wall is fabricated from the same Fordingham straight web piles as the chamber walls. The connection between chamber wall and intermediate wall can be achieved using a connecting straight web pile driven as part of the chamber walls. The connecting flange, however, must not continue below the level of the gate cover as it would interfere with the flow into the chamber and could possibly mar the gate action (see Figs. 7.11 to 7.13).

7.4.10 Temporary Cofferdams

Upstream and downstream temporary cofferdams are necessary in order to achieve the dewatering of the chambers during the pouring of the concrete floor slabs and the installation of the trashrack and gate system. They would also be used periodically during maintenance procedures and during gate removal operations. It is proposed that they would be constructed in the main from plywood curved to a suitable radius around similar walings to those proposed for the main structure (see Fig. 7.14). A straight web pile would be bolted to each side of the coffer and these would locate into connecting sheet piles driven in the appropriate places as part of the chamber walls. A steel plate would also be attached along the bottom edge of the coffer in order that the coffer can be driven a small distance into the riverbed. It is envisaged that the coffer could be driven into position by hand or by small hand held pneumatic tools and, if necessary, the interlocking joints could be eased to facilitate this operation.

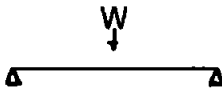
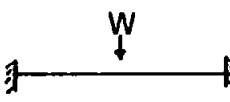

7.4.11 Turbine Frame

The turbine support frame is designed to carry the weight of the reinforced concrete roof slabs, the turbine/ generator and the turbine ducting (see Fig. 7.15). The combined weight of the turbine generator and ducting has been estimated to be in the region of 3.5 to 4.0 tonnes. A simplified design procedure has been carried out to estimate the required steel sections. It should be stressed that the

only function of these simplified procedures is to obtain approximate tonnages of steel which can be appropriately priced.

Beam

Approximate Maximum Bending Moment:

S.S.:		$M = \frac{WL}{4.0} = 57.0 \text{ kNm}$
Fixed:		$M = \frac{WL}{8.0} = 28.5 \text{ kNm}$
BMD:		28.5 28.5

Therefore, assume $BM_{max.} = \underline{28.5 \text{ kNm}}$

Grade 43 steel:

$$f_{bc} \triangleright P_{bc} \triangleright 165 \text{ N/mm}^2$$

$$M = fz = 165.0z$$

$$\begin{aligned} \text{Therefore, } z &= 6.06M \\ &= 6.06 \times 28.5 = \underline{172.7 \text{ cm}^3} \end{aligned}$$

Deflection:

$$\text{S.S.: } y = \frac{WL^3}{48EI} \triangleright \frac{L}{360}$$

Therefore, $y_{max} = 0.016 \text{ mm}$

$$\begin{aligned} I &= \frac{40.0 \times 570.0^3}{1.6 \times 21000 \times 48.0} \\ &= \underline{4641.4 \text{ cm}^4} \end{aligned}$$

Therefore, try 2 x 203 x 102 joists (25.33 kg/m)

Column

Try 219.0 mm diameter, circular, hollow section:

$$\begin{aligned} t &= 10.0 \text{ mm} \\ A &= 65.7 \text{ cm}^2 \\ \text{mass} &= 51.6 \text{ kg/m} \end{aligned}$$

$$l/r_y = \frac{0.85 \times 550}{7.4} = 63.17$$

Therefore:

$$P_c = 123.0 \text{ N/mm}^2$$

$$P_{bc} = 165.0 \text{ N/mm}^2$$

$$f_c = \frac{F}{A} = \frac{76000}{6570.0} = 11.56 \text{ N/mm}^2$$

$$P_c = \frac{M}{Z} = \frac{28500000}{328000} = 86.89 \text{ N/mm}^2$$

Therefore:

$$\frac{f_c}{P_c} + \frac{f_{bc}}{P_{bc}} = \frac{11.56}{123.0} + \frac{86.89}{165.0} = 0.62$$

Therefore, section is adequate

7.4.12 Gate Section

A suggested design for the gate cover, chamber opening frame and the overall gate section is shown in Figs. 7.11 to 7.13. A feature of this design is the removable gate cover which is held in place by transverse T-sections bolted to the chamber walls via the chamber opening frame. This cover would be removed and the gate lifted into the dry in order to carry out any necessary maintenance or bearing renewal. The transverse joists of the turbine frame could be utilised as suitable lifting points.

The section sizes shown are assumed to be adequate as a sufficient design procedure for this area is felt to be beyond the scope of the report brief. Indeed, until further studies of the gate system and its operation are carried out it is impossible to ascertain the forces that will be in evidence. Quantities of steel have been taken from the suggested design in order to estimate a probable cost of this section.

7.4.13 Wallings

It is not intended to carry out design procedures for the various wallings, it is merely assumed that Grade 43, 127 x 64 curved, steel channels would be satisfactory. Four complete rings would be necessary for the chambers themselves, with an additional four sections each equal to one quarter of the chamber circumference for strengthening the chamber walls in the gate area. Three curved sections would be needed to strengthen the intermediate wall and eight further curved sections would be necessary to fabricate the upstream and downstream, temporary cofferdams. Finally, eight straight sections would be necessary for the side walls.

7.4.14 Sluices

The installation of sluices in the side walls would prove advantageous during construction and times of flood. It is intended that the height of the side walls would equal the upstream water elevation so that overtopping would also occur at times of increased flow rate thereby controlling the upstream water level. A further method of passing increased volumes of water through the system would be to turn the gate to its central position thereby creating an additional sluicing facility albeit at the cost of lost energy production.

Possible sluice designs are shown in Fig. 7.16. These are very simple, easily fabricated systems recommended by the British Steel Corporation for integration into Larsen and Frodingham sheet piled systems. Discussion with the Technical Department of BSC has resulted in an estimated cost for their fabrication and installation of approximately £600.00 each provided the installation was carried out in the dry. It is envisaged that their simplicity would allow them to be fabricated on site by the contractor or local sub contractor.

Increased sophistication of the sluice system will obviously result in increased capital and possibly maintenance costs and it is not intended to develop any further ideas here. However, a figure of £1500.00 has been included in the costing to cover the two side wall sluices.

7.4.15 Rock Foundation

Where a rock strata exists below a layer of sand or clay, care must be taken that the reduced friction factors between the soil and the rock at the interface do not significantly decrease the structure's resistance to sliding. Conversely, if the rock is sufficiently weak to allow the piles to be driven to any appreciable depth then the structure's resistance to sliding could be significantly increased and seepage problems eradicated. This situation is so site specific that no attempt at an outline design is to be made here.

7.4.16 Summary

Based on the preceding calculations it is intended to base the costing of the piling works on the following sections and drive depths:

		Sand	Clay
CHAMBERS:	Straight Web	2.60m	1.50m
SIDE WALLS:	Larsen/2N	6.00m	3.00m

7.5 Construction Sequence for Sheet-piled Chambers

7.5.1 Introduction

The construction sequence for the sheet-piled system is such that the individual chambers plus two temporary, intermediate walls form a watertight enclosure within which the pouring of in-situ concrete floor slabs, and the installation of the gating system and trash screen can be carried out in dry conditions. This obviates the need for an independent cofferdam thereby saving significantly in overall construction costs.

7.5.2 Programme of Works

The initial task will be the preparation of the channel banks, installation of bank protection and removal of any unsuitable material from the channel bed. It is envisaged that this removal can be achieved by dragline using the same plant that will subsequently be required for the pile driving operation. This bankside work will include the necessary excavation and subsequent construction of the concrete abutments. The positioning of the temporary frames for the driving of the chamber piles will follow. It should only prove necessary to fabricate one circular driving frame which can be moved to facilitate the driving of both chambers (this being a standard practice in circular cofferdam construction in order to maximise re-use of materials and minimise cost). The driving of the chamber piles would then be carried out to the extent shown in Fig 7.17. The two circular wallings shown in Fig. 7.4 should be fitted at this point to provide the necessary rigidity to the structure.

The two temporary ply cofferdams can now be placed in position and driven down to just below channel bed level. The structure will then be dewatered to allow further construction to proceed in the dry. It may prove necessary to add temporary wallings to the chambers to improve the structure's stability until the floor and roof slabs are completed.

Once the gate frames have been bolted/welded into position it will prove to be a straightforward operation to place the necessary reinforcement for the floor slabs for both the gate area and the chambers. Frames supporting the holding down bolts for both the column support pads and the trash screen will be fixed in position as will the support frame for the gate pivot. Concrete could then be either skipped or pumped to the required areas.

Once the floors have reached a sufficient strength the trashrack, gate and gate cover can be installed and the intermediate wall constructed. Erection of the turbine frame will follow after which the in-situ concrete roof slabs can be shuttered

and poured. This completes the main chamber construction allowing the area to be flooded and the downstream temporary cofferdam to be removed.

It is expected that there will be sufficiently slack water immediately downstream of the gate area to allow the placing of the apron shutters and a reinforcement cage and also to allow the subsequent placing of the concrete via a tremie. Once this has sufficiently hardened the upstream coffer will be removed and the gate held at its central position in order that water can freely pass through the system. This will reduce the flow velocities between the banks and chamber sides and facilitate the placing of the temporary cofferdam for the driving of each side wall. The function of the cofferdam here, will be to merely divert the flow. Once one side has been completed, the cofferdam can be removed and the integral sluice gate of the side wall will be opened. Work can now commence on the opposite side. This only leaves the careful placing of the loose rock scour protection around the downstream perimeter of the barrage.

The construction of the barrage and chamber system will now be complete leaving only the installation of the turbine ducting, the turbine and the generator and the subsequent connection to the bankside switching facility. The gate will remain in the central position and the sluice gates will remain open until operation of the system commences. In times of severe flood or when maintenance is required they could be returned to this position to reduce the upstream head. The two joists supporting the turbine and ducting will have a secondary role during gate maintenance in that they could provide a gantry for the lifting of the gate through the gate cover opening into the dry.

7.6 Precast Concrete Construction

An equally viable method of construction involves the use of precast concrete caissons to form the circular chambers. The caissons would be sunk into the channel bed to a sufficient depth to provide structural stability whilst restricting seepage beneath the structure as shown in Fig. 7.18.

The design philosophy in this case is to utilize 'off the shelf' components in order to minimize costs. A suitable contender for the circular concrete caissons would be the Charcon One Pass smooth bore shaft linings manufactured by the Costain group of companies. These units can be supplied in 5.0 m diameter rings each of a depth of 600 mm and a wall thickness of 150 mm. A minimum of fourteen rings would be required for each chamber in order to achieve both the necessary depth of drive and the required height of chamber. The use of these units provides two advantages over the steel sheet pile system; the weight of the chambers (50 tonnes each) will assist the structural stability of the barrage whilst the shaft walls would be capable of supporting the chamber roofs, ducting and turbogenerator

thereby negating the need for the central supporting column of the sheet pile chambers. Calculations show that the integral weight of the structure alone is sufficient to prevent sliding although a depth of drive of 2.3 m would be required to resist the overturning moment.

Side and intermediate walls would again consist of Larsen sheet piles. These could be connected to the chambers via a suitable connecting sheet pile bolted to the chamber walls as shown in Fig. 7.19. Again the programme of works could be such that the precast chambers plus temporary stoplogs would provide their own cofferdam within which the necessary excavation for the sinking of the caisson and the gate installation could take place.

7.7 In-situ Concrete Construction

In order for this form of construction to be economically viable it is essential to minimize the cost of any cofferdam required to facilitate the placement of concrete. Preferably the need for a cofferdam should be eliminated. With this in mind two different design approaches have been formulated depending upon whether the system is to be constructed 'in the dry' or 'in the wet'. The first approach (Fig. 7.20), where a dry enclosure would be formed by the installation of a fabric portadam, would involve the siting of the chamber foundation at a sufficient depth to provide both a shear key and a cut-off wall to cope with those problems already identified in previous sections. In the second approach where no cofferdam is intended, the structure itself would be founded at bed level (Fig. 7.21). The driving of both shear-key piles and a sheet-pile cut-off wall would therefore be necessary.

The installation of a traditional sheet piled, temporary cofferdam to provide a dry enclosure would prove non-economic. It is therefore suggested that construction 'in the dry' would only be feasible if lightweight, fabric cofferdams could be utilized.

Discussion with Leigh Flexible Structures of Walsall has indicated that, if average, existing water levels in the river/leat channel are in the region of 1.0 to 1.5 metres and water velocities do not exceed 1.0 m/sec., their fabric portable cofferdams would prove adequate for the formation of the dry enclosure. These structures have been used successfully for many years in the U.K., Europe, North America and Africa to dam rivers, canals and lakes. They are flexible systems especially suited to sites where access is difficult as even the largest frames can be manhandled if necessary, and no special or heavy equipment is normally required. Fig. 7.22 show the general principle. However, maintaining a water velocity of below 1.0 m/sec. as construction proceeds and the cross-sectional

area of the channel decreases may only prove possible in situations where an existing river control system is in operation and bypass channels exist.

In order to construct in an open river situation (ie 'in the wet') a piling frame will be necessary to enable the accurate siting of the shear key piles and the sheet-piled, cut-off walls. The costing exercise has assumed timber formwork placed over the shear key piles which would act as both guides and supports. However, the hire of a prefabricated, metal pan formwork system may prove more economic and more suitable to the formation of the required radii. Some form of suspended fabric skirt would be necessary around the lower perimeter of the shutters to minimize grout loss. This could take the form of a continuous tube which, when in position, could be pumped full of either water or a bentonite solution to form a seal to the channel bed (see Fig. 7.23).

It is suggested that the chambers would be constructed one at a time, thereby allowing re-use of temporary works. Once the chambers are complete and have reached sufficient strength then central ply cofferdams can be positioned in order to allow the construction of the intermediate wall and the installation of the gate system. In order to construct the side walls and their sluices temporary cofferdams such as those used at the central position may prove necessary. The side walls would be constructed one at a time and during their construction the gate would be placed at its central position and any existing sluices would be opened in order to minimize upstream pressures.

7.8 Steel Chamber Construction

A further possibility for chamber construction is to preform the circular chambers from steel plate and to use the same form of construction as was proposed for the pre-cast concrete system, ie material would be excavated from within the chambers allowing them to sink to the required depth in the same way a steel or concrete caisson would be sunk into a river bed. Again, the chambers would act as their own cofferdams and seepage under the structure would be minimised by that portion of the chamber walls that lie below the channel bed level.

Factory gate prices for the steel plate and the forming of the necessary sections have been supplied by Barnshaw Section Benders Ltd. of Warley, West Midlands. The individual chambers would consist of four rings, each two metres deep and each consisting of three segments. The rings would be assembled on site to the required depth. It is envisaged that the construction sequence would then closely follow that of the pre-cast concrete system using the wall and gate cover elements outlined in Section 7.4.12.

7.9 **Plastic and Glass-reinforced Plastic Construction**

The final alternative for chamber construction is the use of pre-formed, plastic/G.R.P. chamber sections that would be placed in the river channel in a similar way to the pre-cast concrete and pre-formed steel sections.

Two plastics firms were contacted: Plastic Installations of Glencoed, Mid-Glamorgan and Gendall Rainford Products of Redruth, Cornwall. Details of the internal and external predicted pressure differentials and the required dimensions were supplied to them. Plastic Installations suggested that the chamber walls should consist of a fibreglass outer and inner wall with polypropelene sandwiched between. This would provide the necessary strength to withstand the varying differential pressures on both the internal and external, upstream and downstream walls. Each chamber would be supplied in three sections: two being 2.5m deep and one being 1.0 m deep, at a cost of £23,000.00 per chamber. Skilled personnel would attend to the assembly of the chambers on site and this plus the probable transport costs would be in the range of £5000.00; the overall costs for chamber fabrication would therefore be in the region of £50,000.00.

The second firm, Gendall Rainford Products, merely quoted a price well in excess of £20,000.00 per chamber due to the stress factors acting from both within the chamber and on its external walls, and suggested that alternative materials would be both more suitable and more economic.

These costings are for two chambers only and therefore include the fabrication of the necessary moulds, etc. The prices would decrease with increasing numbers of chambers and the viability of this system will depend upon the extent of the proposed project. The attributes of a plastic/GRP system such as its inherent lightness, durability and non-pollutive aspects may justify its extra cost in certain locations.

7.10 **Components Common to all Systems**

Those components of both the construction procedure and of the completed structure that are common to all the proposed systems irrespective of their composite materials or configuration include: site investigation, bank protection and bed preparation, the gate and trashrack, the turbine, generator and associated ducting and the necessary electrical switching facilities for grid connection.

7.10.1 Site Investigation

The site investigation cost includes percussion boreholes, undisturbed samples, standard penetration tests and relevant laboratory tests.

7.10.2 Bank Protection and Bed Preparation

The cost of the gabion wall at each bank (see Fig. 7.10) includes fabrication, supply and placing. These costs were supplied by Mr. R. Hutchings, a South West Water Authority Engineer. The downstream rockfill has been included to prevent scour from the cyclic surges of the emptying chambers and during overtopping of the structure in flood conditions. It is assumed that the initial bed preparation can be achieved using either bankside dragline or backactors with extended booms.

7.10.3 Site Set-up and Temporary Works

Some allowance must be made for the installation of site offices and access roads. This sum will be extremely site specific and the economics of developing a site could largely depend on its accessibility. It has been assumed here that no particular problem exists concerning accessibility, the main expense being the installation of those offices and facilities necessary to service a job of this size and the mobilizing of the necessary plant and equipment. It is assumed that the contractors carrying out the works will be specialist piling and riverworks contractors possessing the necessary materials for the construction of the required temporary works.

7.10.4 Additional Plant Costs

Although the plant costs are included in most of the civils prices shown in the appendices (ie those based on Wessex Database rates) due to the small quantities involved it is not felt that these plant prices are particularly realistic. Additional costing has therefore been included to cover the continuous use of necessary plant over periods varying from one to eight weeks.

7.10.5 Gate System

A possible design for the butterfly gate is shown in Fig. 7.26. It is proposed that the gate be constructed from steel plate supported by a steel framework. The layout shown is mainly for costing purposes and does not represent a working drawing. The gate rotates on a 70 mm diameter, steel bar via three water-lubricated B.T.R. Silverline bearings.

7.10.6 Trashrack

The proposed trashrack extends from the base of the intermediate wall to the line of the upstream, temporary cofferdam, a plan distance of 600 mm (see Fig. 7.27). The bars of the rack must be capable of carrying the full loading from the differential head if the screen becomes completely blocked. The basic costs of the gate and trashrack have been increased by 100% to allow for manufacturer's profit, site alignment and installation.

7.10.7 Turbine, Generator and Ducting

Costing experience of individual turbines is, at the moment, restricted to those required by the various prototype pneumatic devices (ie Benburgh, Borrowash and Islay). However, negotiations between Queens University, Belfast and turbine manufacturers should eventually result in production costs for a range of turbine sizes suited to various pressure differential 'envelopes' and, therefore, various rated outputs. Discussion with Dr. Trevor Whittaker of Queens University indicates that projected production costs of the turbine, generator and associated ducting would be in the region of £200 to £460 per kW dependent upon the expected output in relation to the various production envelopes, ie considering a production turbine designed for the 30 to 60 kW regime, cost per kW would increase as expected system output tended to the 30 kW end of the envelope. This would indicate that some tailoring of a particular system's potential output may be required to ensure that it remains in the upper portion of one particular regime rather than the lower portion of the next regime. However, for the purpose of this report a cost of £350.00 per kW is taken as an average representation.

7.10.8 Grid Connection

Discussion with Mr. F. Dixon, a planning engineer with the South West Electricity Board has resulted in the following breakdown of possible connection costs.

(Assuming parallel operation with the Electricity Board whereby on-site power requirements are satisfied and excess power is exported.)

Protection, changeover switching and metering:	£700.00
Transformer, 50 kVA three phase, plus pole and earthing:	£3200.00
200 m cabling @ £25.00/m:	<u>£5000.00</u>
TOTAL	£8900.00

These figures assume that on-site power requirements justify three phase supply (ie a large farm with milking and processing plant, Water Authority pumping station etc.) and that there is no existing connection to the grid. It is, therefore, a worst case scenario, indeed, the 200 m of cabling is the maximum distance over which a low voltage supply can be transmitted before losses become significant. The following figures represent the other end of the scale where an existing grid supply is established and the user is situated within 50 m of the PWE:

Protection, changeover switching and metering:	£700.00
50 m of LV cabling @ £25.00/m:	<u>£1250.00</u>
TOTAL	<u>£1950.00</u>

This illustrates the site specific nature of grid connection costing. For the purpose of this study it is therefore assumed that such costs will be in the region of £6000.00. (It is assumed that an asynchronous induction generator will be incorporated into the system thereby negating the need for the additional cost of rectification and inversion that would otherwise be necessary to integrate the supply with the grid.)

7.10.9 Professional Fees, etc

An amount equal to 20% percent of the total civils cost has been included to cover professional fees and insurance. The professional fees would include investigation into flow regimes, planning and Water Authority restrictions etc as well as detailed design and on-site quality control. A further 5% of the total civils cost has been added to cover an acceptable profit margin for the contractor carrying out the works.

The appropriate costing procedures for these common components can be found in Appendix IV.

7.11 Alternative System Configuration

It is now intended to carry out a somewhat briefer study of the likely capital cost of the Twin, Rectangular Chamber System incorporating the horizontal-axis radial gate (see Figs. 2.1 and 2.6). The initial parametric testing of this configuration via the mathematical model has shown that the greater width of the gate entrance and exits have made possible a higher average output than those of the twin chamber, butterfly gated system. However, weighed against this must be the energy

requirements of the gate drive and the problems associated with the construction and operation of a system incorporating gates of this size.

No outline design calculations have been included in this study, estimations of member size, pile drive depth etc being based on similar situations already investigated for the butterfly-gated system. The following design features have been incorporated in order to provide a basic model on which to establish the costing:

- 1) The chambers have been designed to be greater in width than in length (Fig. 7.28) in order to minimize the span of the gate arms and thereby reduce torque whilst still retaining an effective cross-sectional area.
- 2) It is assumed that the channel banks provide, along those lengths of the chambers that extend into them, a percentage of the overall support required to resist overturning and sliding forces. The remaining support is supplied via the isolated steel piles and the sheet pile cut-off wall.
- 3) The 5 m long radial gates are supported at three points along their length via hollow, rectangular section steel arms themselves connected to the 100 mm diameter steel drive shaft. The drive shaft is supported by the central steel piles with suitable bearings fitted at each of the interfaces (see Figs. 7.28 and 7.29).
- 4) The gate drive is supplied via three, double-acting pneumatic rams positioned along each of the drive shafts. The compressor is sited above the central partition and both it and the turbine/generator are supported by the rectangular section steel pile. Calculations have shown that a free air delivery of 73 m³/h would be required from a compressor capable of providing pressures up to 10 bar. Discussion with IMI Fluidair has resulted in the selection of suitable machines and cost estimates for both the compressor, double-acting pistons, receiver and air lines. The power requirement of the necessary compressor would be in the region of 11 kW.
- 5) It is assumed that construction will take place within a sheet-piled cofferdam alternatively enclosing areas on either side of the channel whilst still allowing flow via the remaining area. Costs for the driving and extraction of the cofferdam have been included and a 30% allowance has been added for the usage of the specialist contractor's temporary piles.
- 6) Although pre-cast concrete units have been costed for the chambers, the steel frame could accommodate a similar range of materials as those costed for the butterfly gated system. Estimates of the quantities required

for the construction of the system and the probable costing of these quantities can be found in Appendix IV. Again, the Civil Engineering Standard Method of Measurement has been used to provide the guidelines for quantity estimation although the results are presented in a less formal format. Prices have been provided in some instances by private suppliers or in the case of more general items, via the Wessex Database.

7.12 Summary of Overall Costs

Detailed costing procedures in accordance with the Civil Engineering Standard Method of Measurement can be found in Appendices IV. These have been inspected and considered satisfactory for the purpose of this document by a qualified Quantity Surveyor with much experience in both marine civil engineering projects and riverworks.

The overall costs of the varying systems are summarised on the following pages.

Twin Circular Chamber Configuration (Butterfly Gate)

(Turbine/generator costs based on average output of 72 kW @ £350.00 per kW).

	£	p
<u>Sheet Piled System</u>		
- granular soils.		
Civils:	53 029.06	
M and E:	33 288.04	

TOTAL:	86 317.10	
- clay soils.		
Civils:	48 188.06	
M and E:	33 288.04	

TOTAL:	81 476.10	
<u>Precast Concrete System</u>		
Civils:	55 502.68	
M and E:	33 288.04	

TOTAL:	88 790.72	
<u>In-Situ Concrete System</u>		
- open water construction.		
Civils:	51 566.42	
M and E:	33 288.04	

TOTAL:	84 854.46	
- construction within a cofferdam.		
Civils:	58 994.86	
M and E:	33 288.04	

TOTAL:	92 282.90	
<u>Steel Chamber System</u>		
Civils:	64 291.79	
M and E:	33 288.04	

TOTAL:	97 579.83	
<u>Plastic/GRP System</u>		
Civils:	108 498.63	
M and E:	33 288.04	

TOTAL:	141 786.67	

Twin Rectangular Chamber Configuration (Horizontal-axis, radial gate)

(Turbine/generator costs based on average output of 90 kW @ £350.00 per kW).

	£	p
Civils:	63 660.44	
M and E:	39 588.00	

<u>TOTAL:</u>	<u>103 248.44</u>	

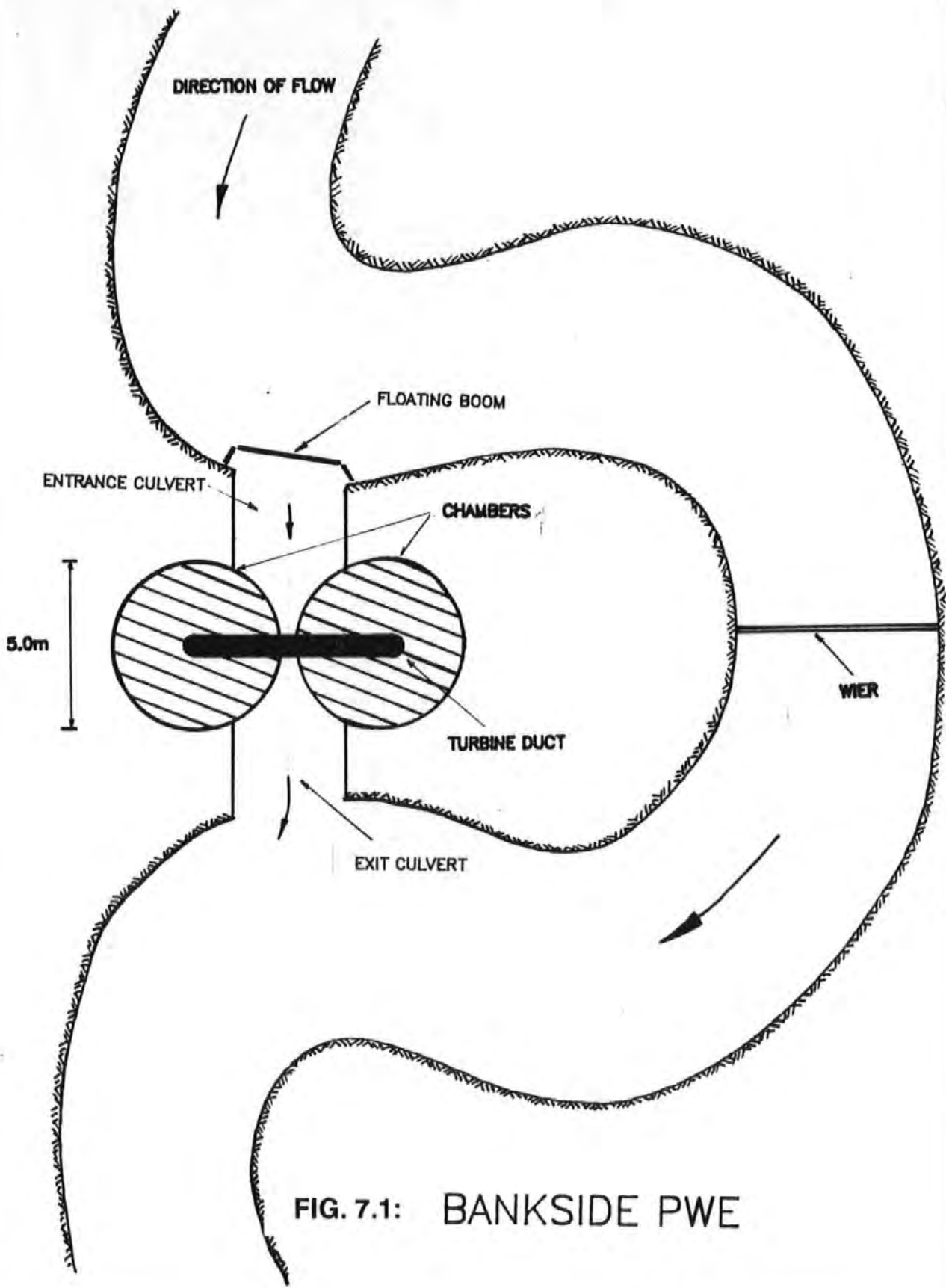


FIG. 7.1: BANKSIDE PWE

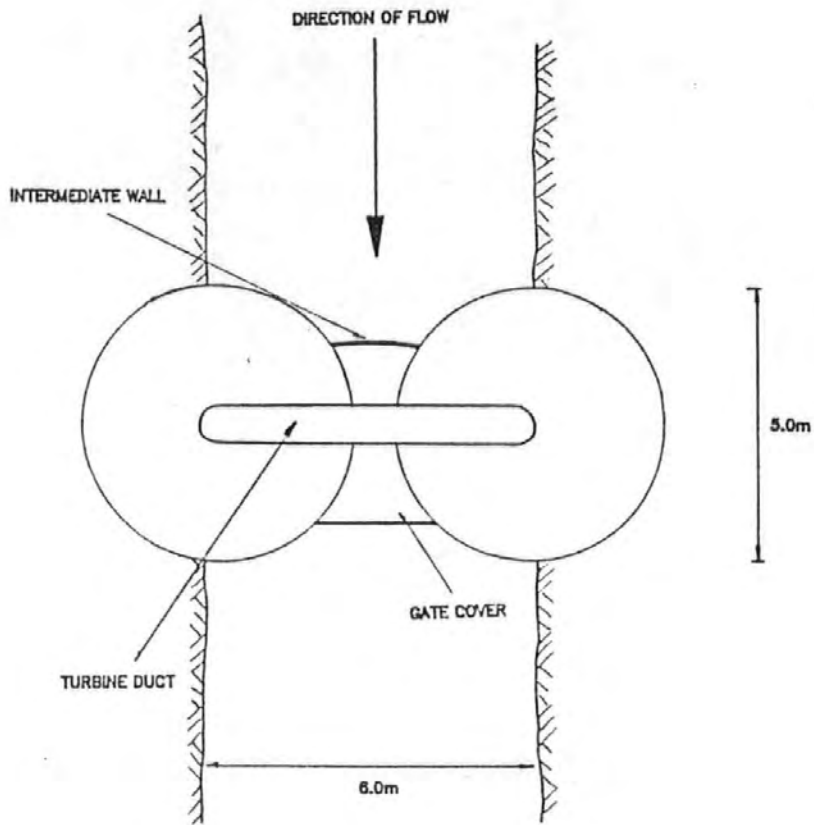


FIG. 7.2: P.W.E. BARRAGE WITH BANK SUPPORT

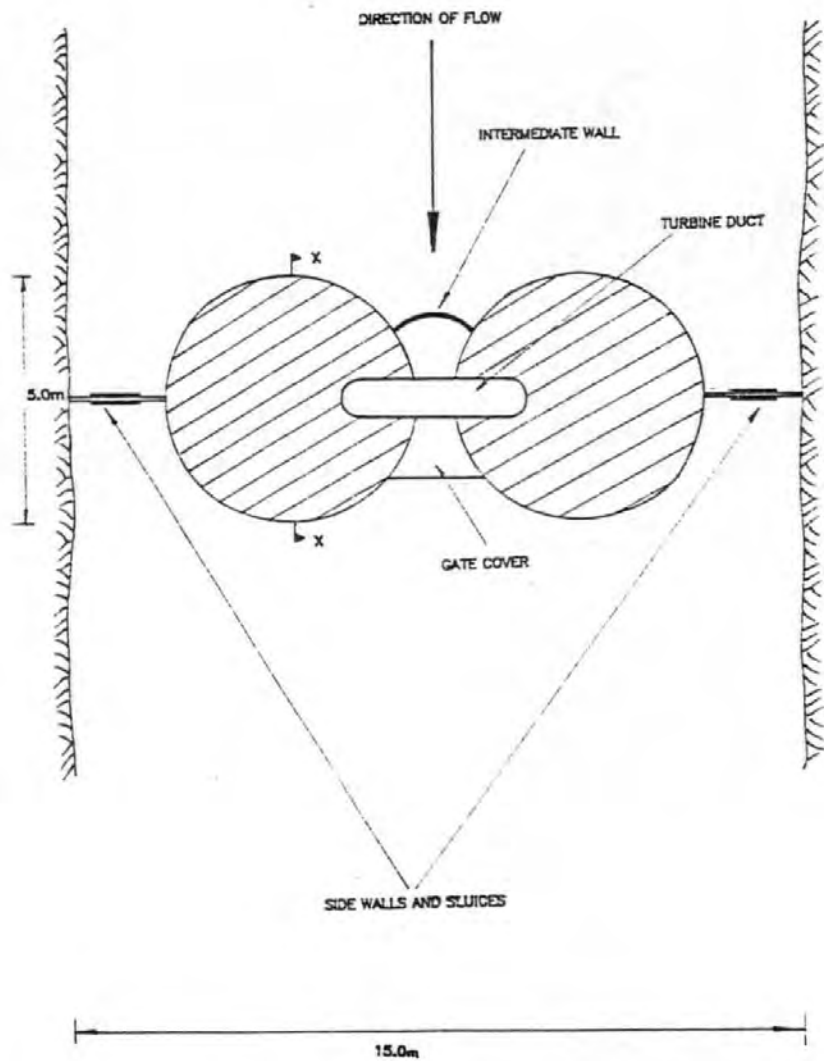


FIG. 7.3: FREE STANDING P.W.E. BARRAGE.

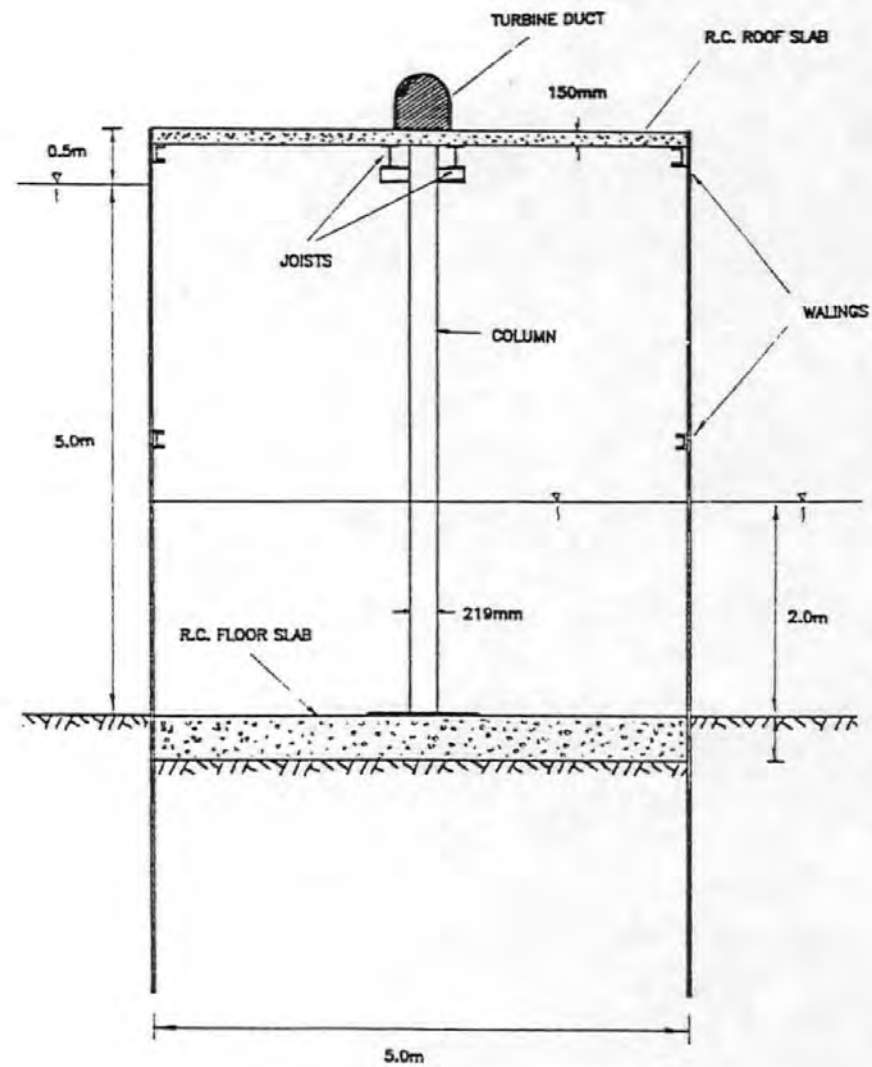


FIG. 7.4: SHEET-PILED SYSTEM
VERTICAL SECTION

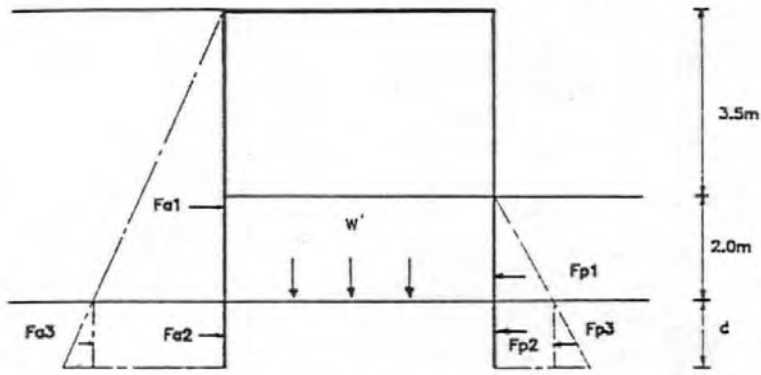


FIG. 7.5: SLIDING FORCES

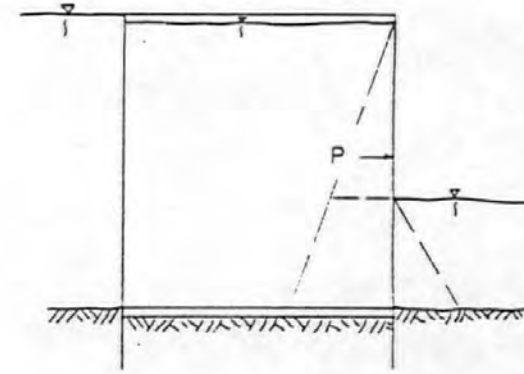


FIG. 7.7: WORST CASE-INTERLOCK TENSION

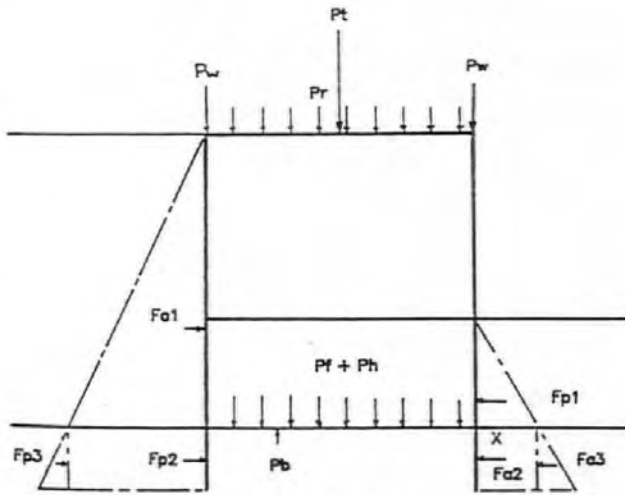


FIG. 7.6: OVERTURNING FORCES

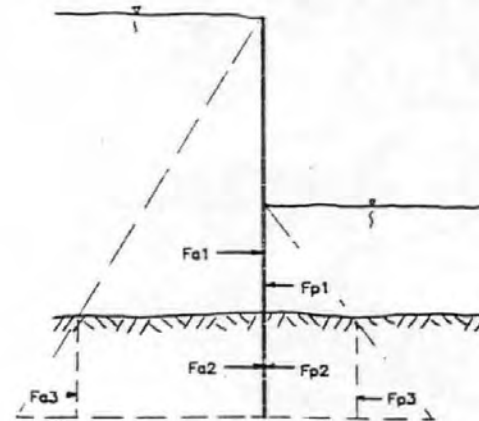


FIG. 7.8: ACTIVE AND PASSIVE PRESSURES-SIDE WALLS

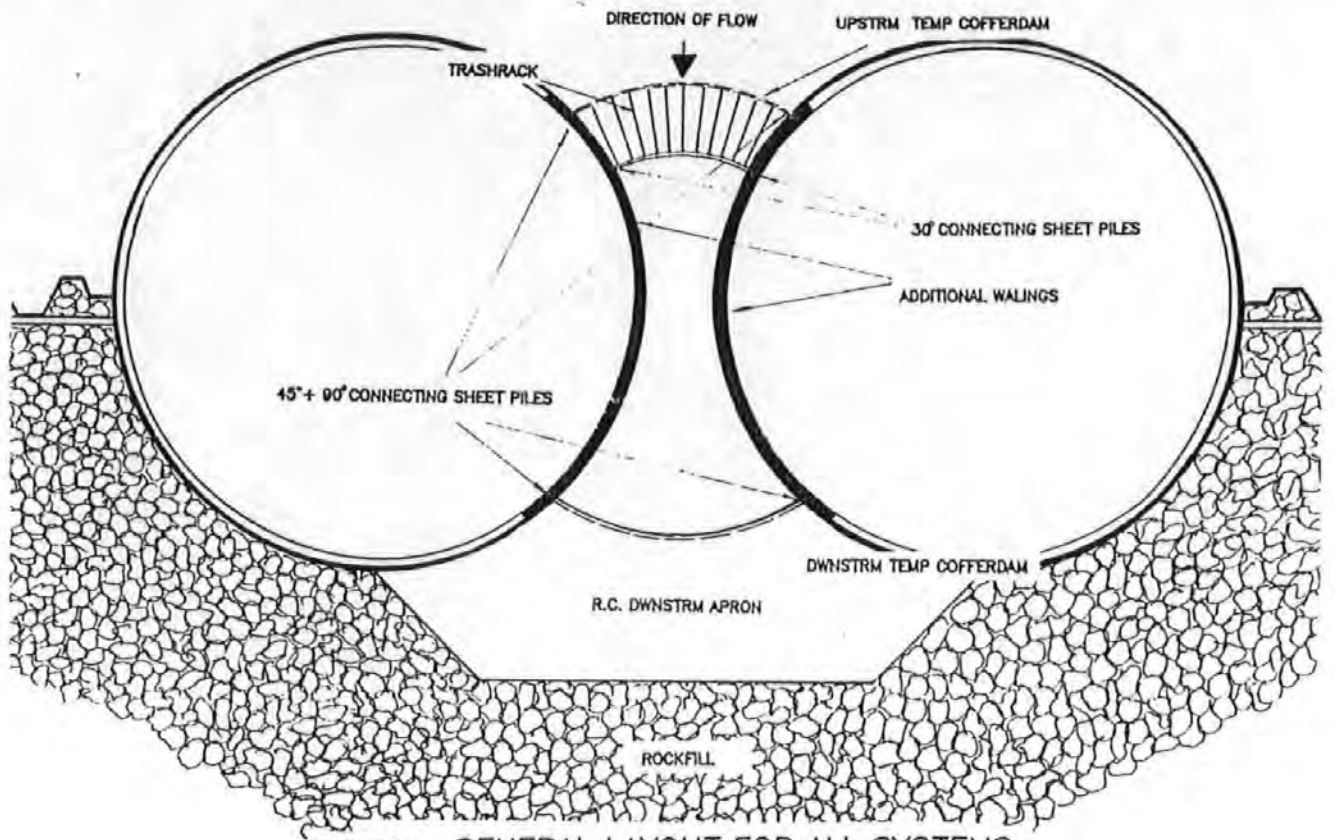


FIG. 7.9: GENERAL LAYOUT FOR ALL SYSTEMS

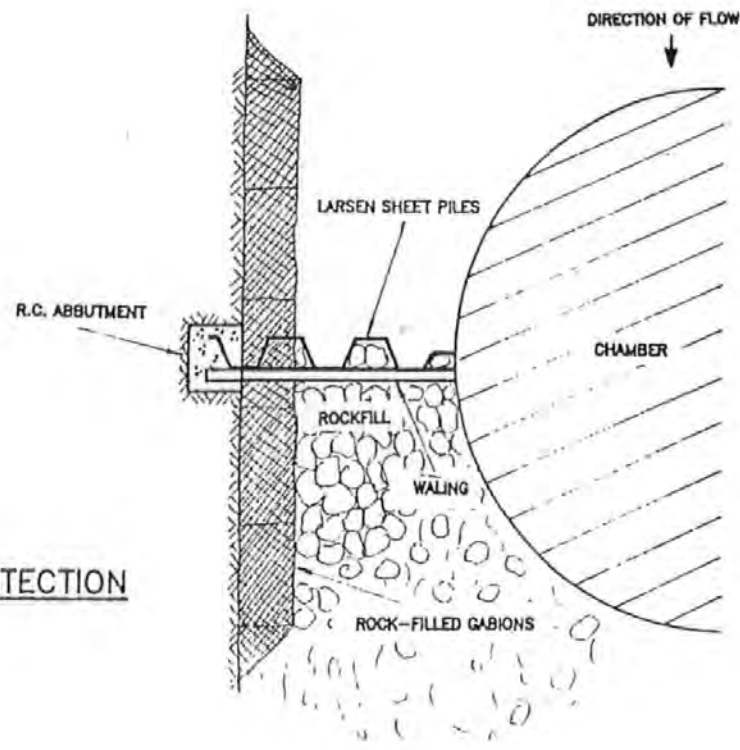


FIG. 7.10: BANK PROTECTION

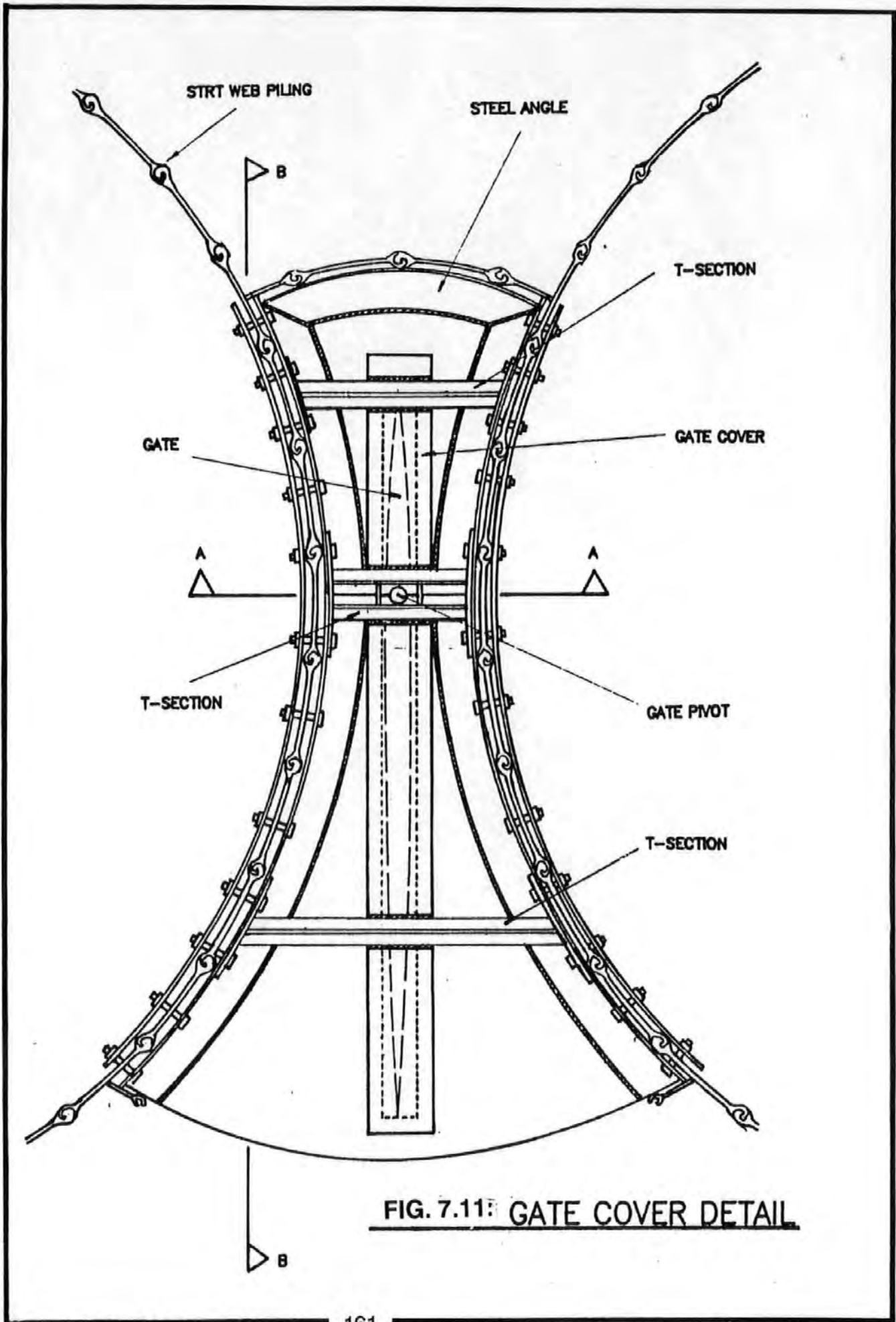


FIG. 7.11: GATE COVER DETAIL

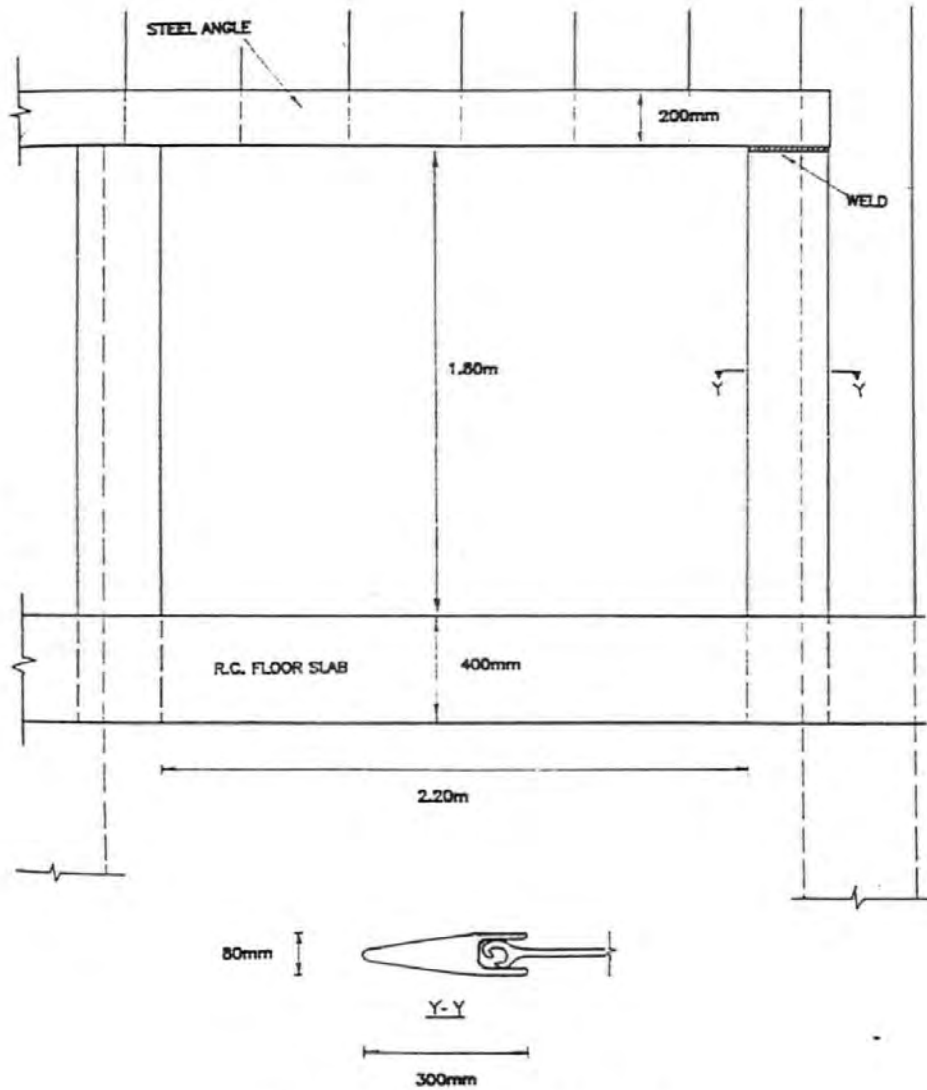


FIG. 7.12: GATE COVER DETAIL

VERTICAL SECTION ON B-B. (See FIG. 7.11)

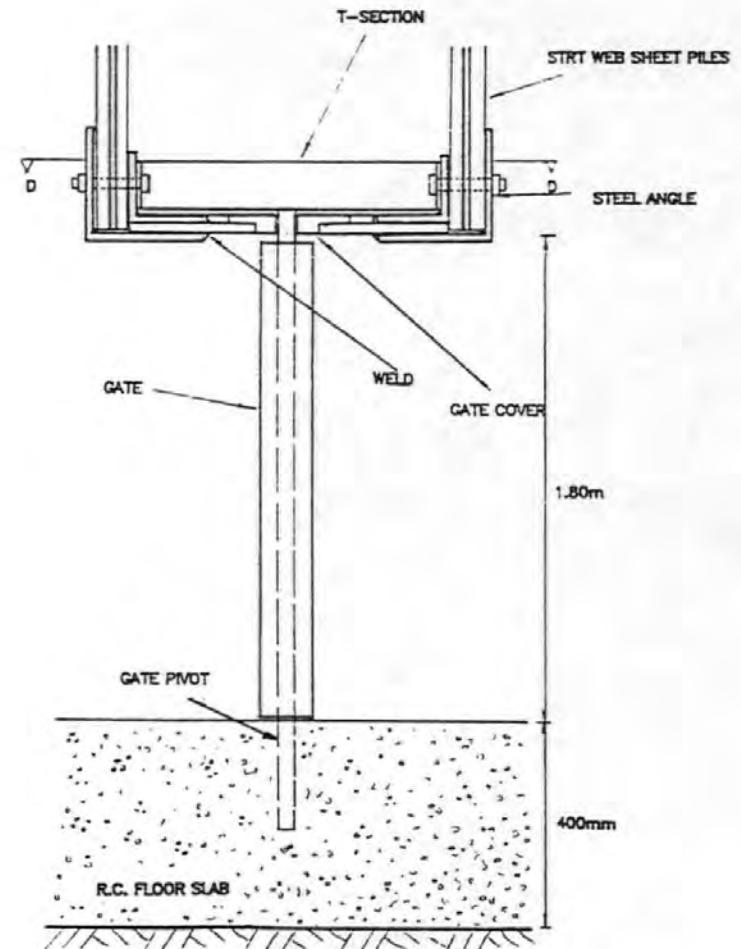


FIG. 7.13: GATE COVER DETAIL

VERTICAL SECTION ON A-A. (See FIG. 7.11:)

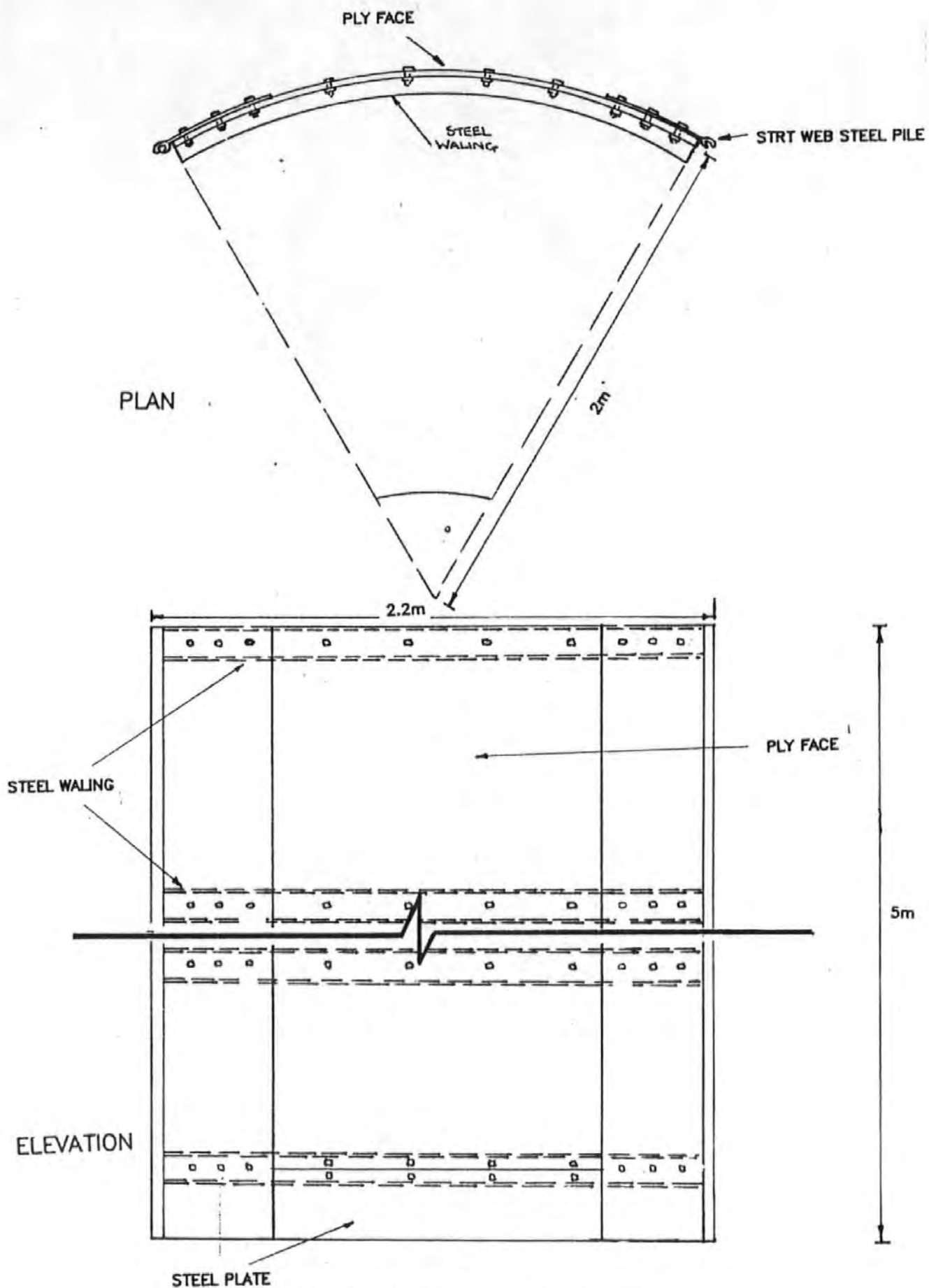


FIG. 7.14: TEMPORARY COFFERDAMS

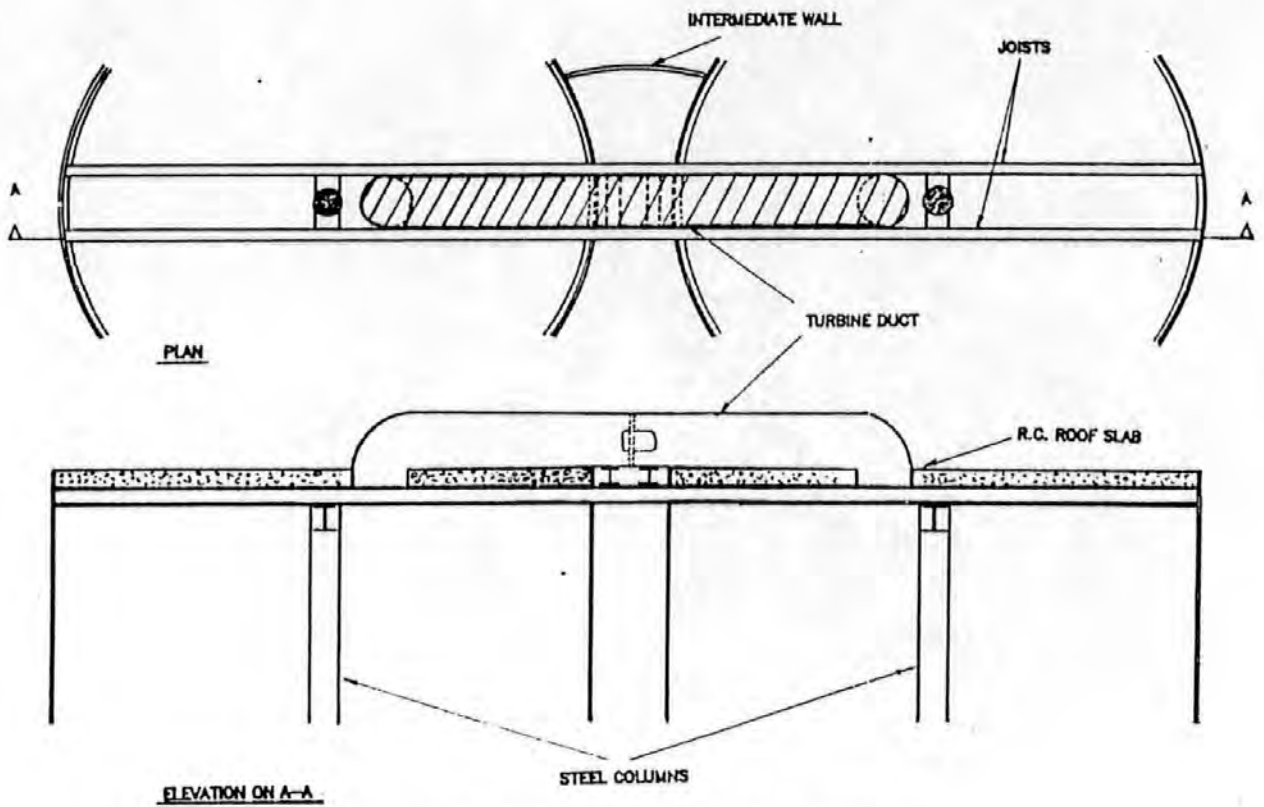
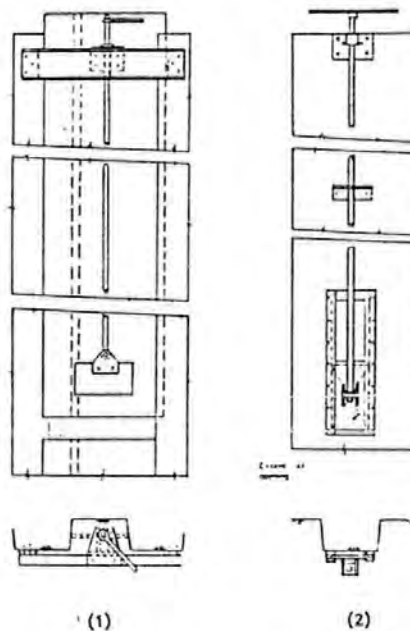


FIG. 7.15: TURBINE SUPPORT FRAME DETAIL



1) Gates formed by cutting a pair of piles and fitting them with screw gear so that the upper part of the piles can be raised to form an opening 750mm wide and of any desired depth.

2) Gates with an opening about 200mm wide by 400mm deep across the interlock of a pair of piles, with screw operating gear worked from the top of the cofferdam.

FIG. 7.16: TYPES OF SLUICE GATE

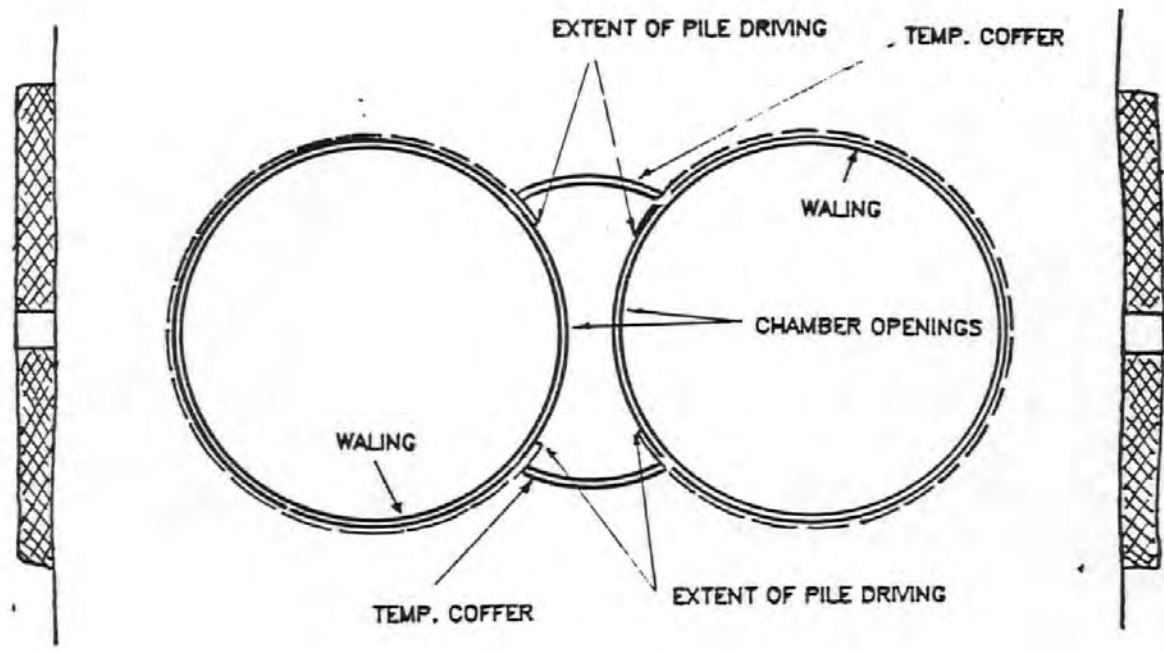


FIG. 7.17: STRUCTURE ACTING AS COFFERDAM

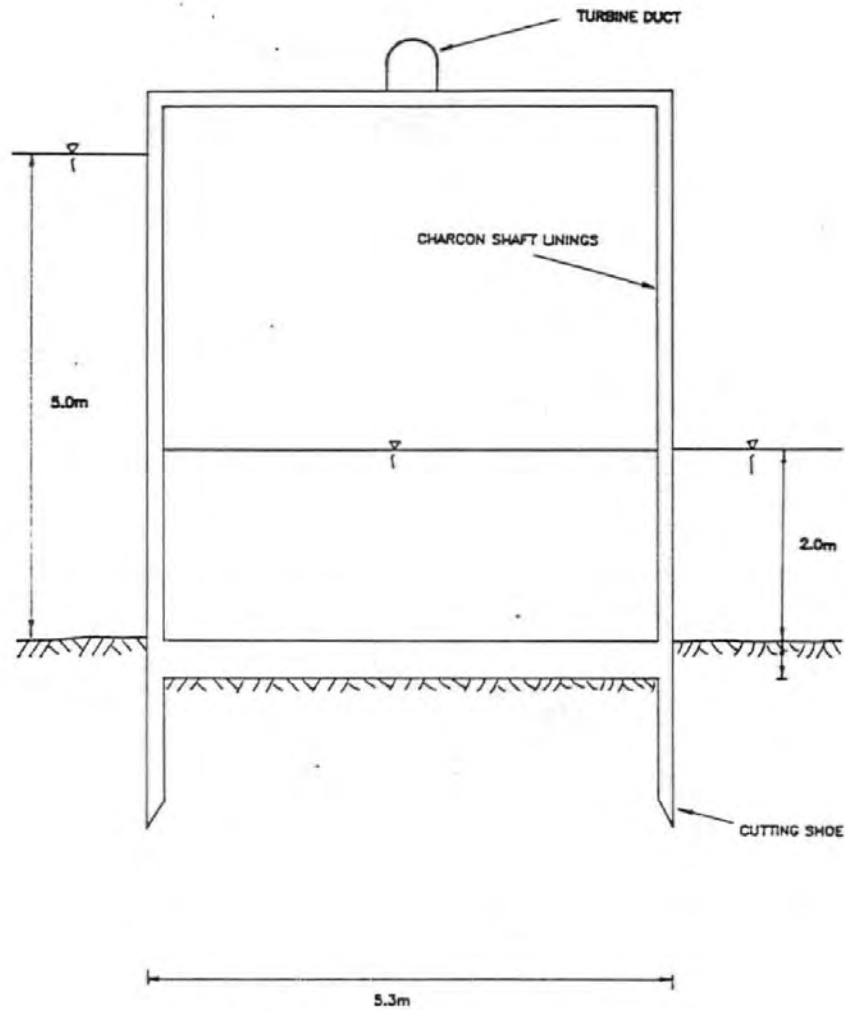


FIG. 7.18: PRECAST CONCRETE SYSTEM
VERTICAL SECTION ON X-X

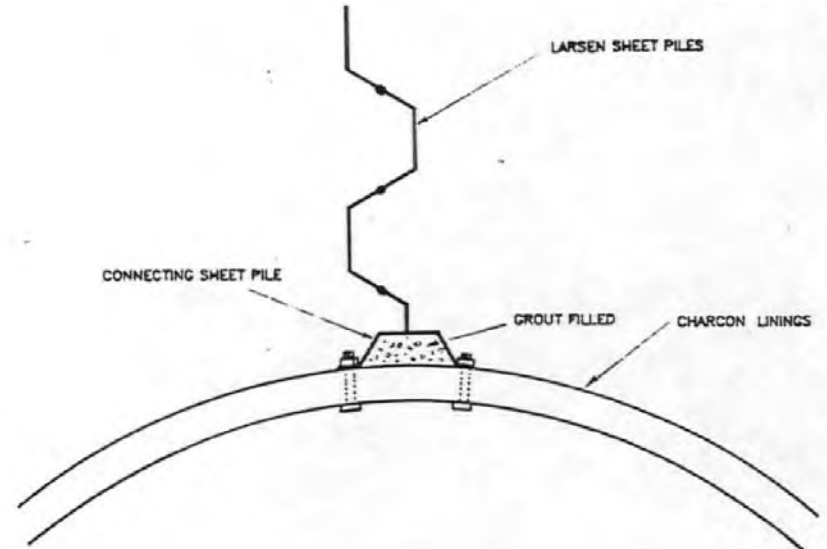


FIG. 7.19: DETAIL OF SIDE WALL AND CHAMBER INTERFACE

PROJECT THE PERFORMANCE AND ECONOMICS OF A P.W.E.		made	DEPARTMENT OF CIVIL ENGINEERING	
SECTION CHAPTER 7	date 15/2/88	JOB NO.	SHEET NO.	rev.

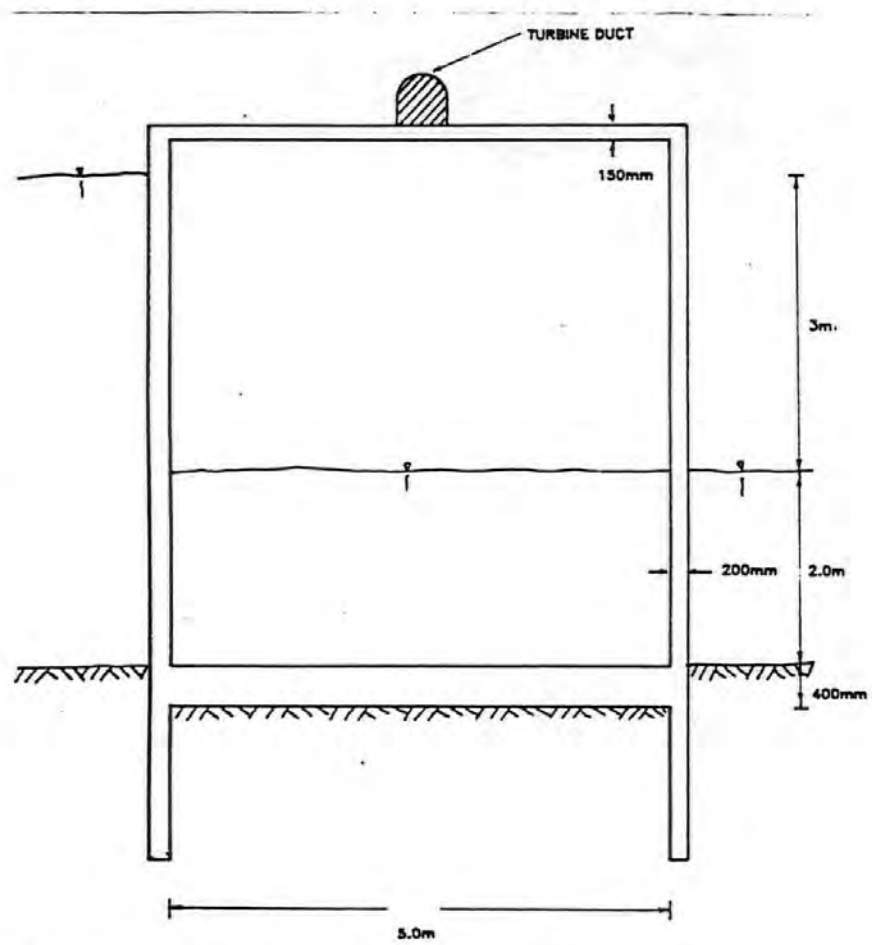


FIG. 7.20: IN-SITU CONCRETE SYSTEM USING COFFERDAM -
ELEVATION ON X-X (SEE FIG.)

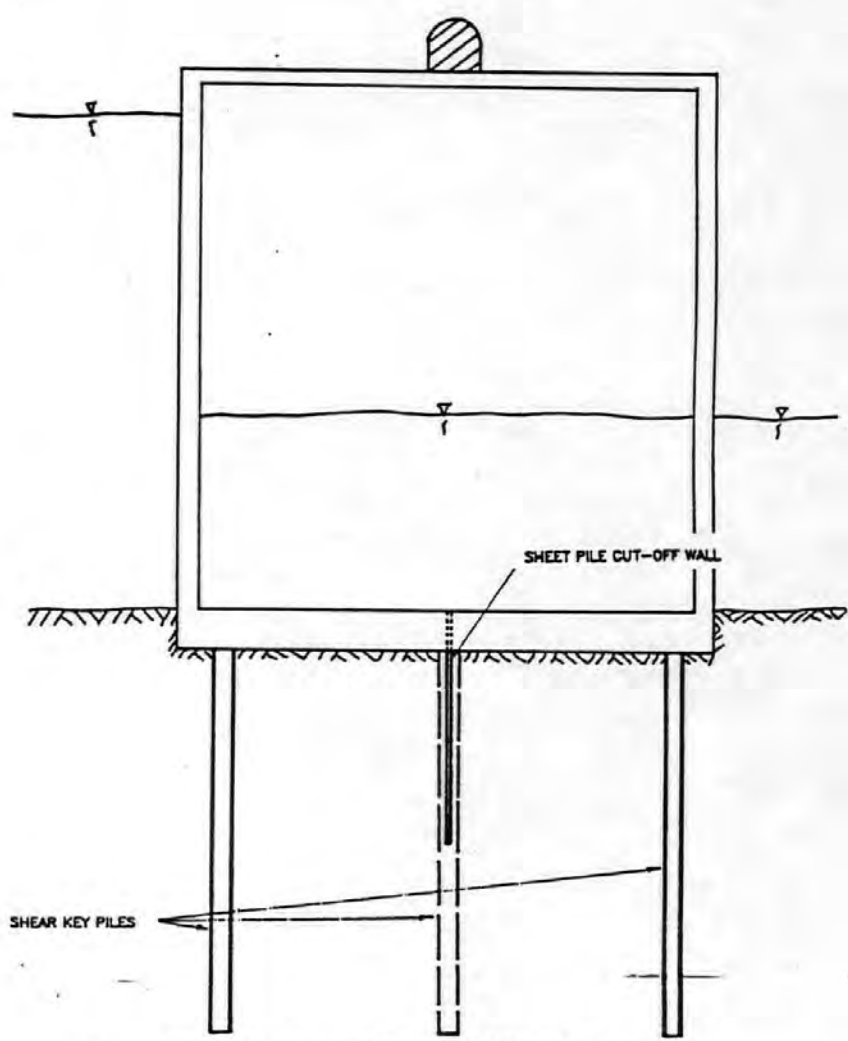
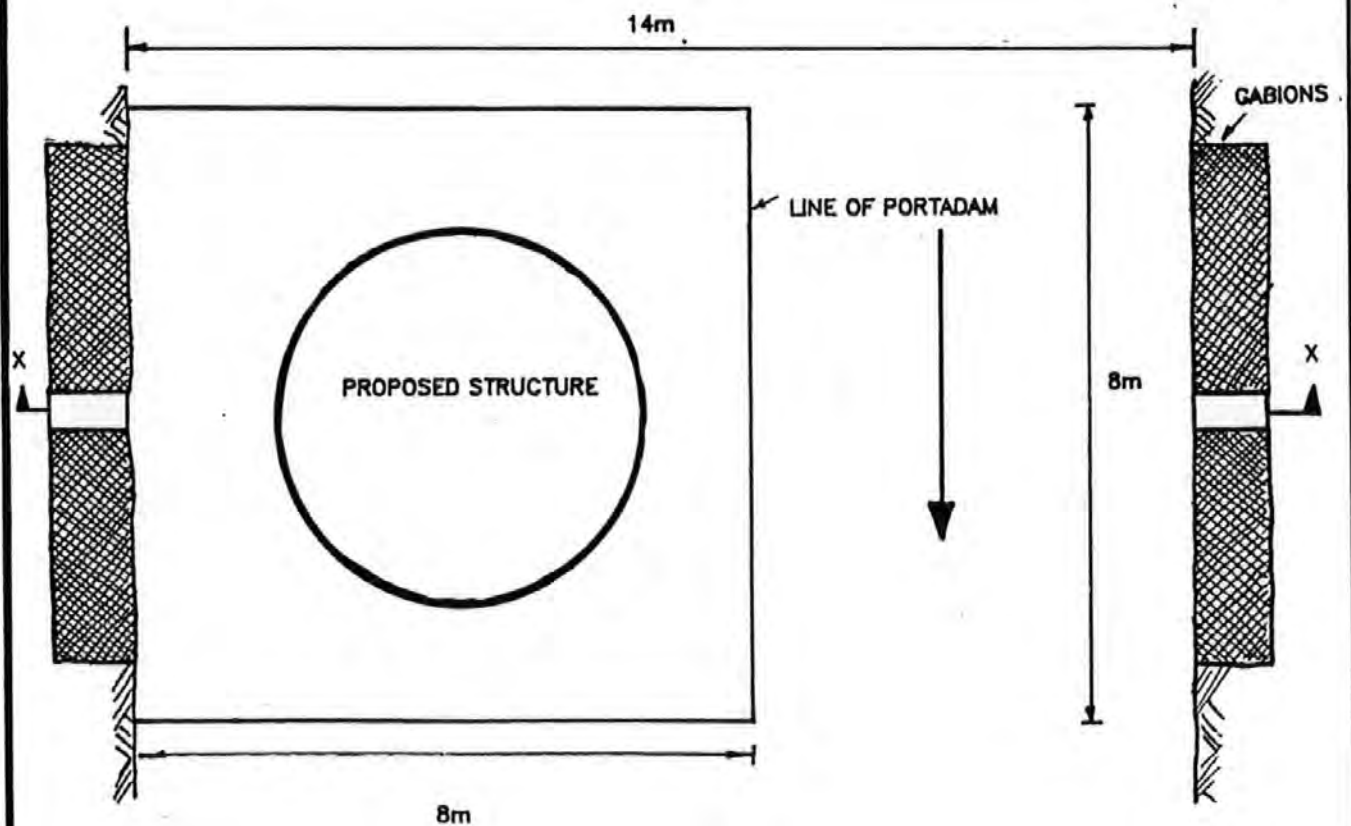
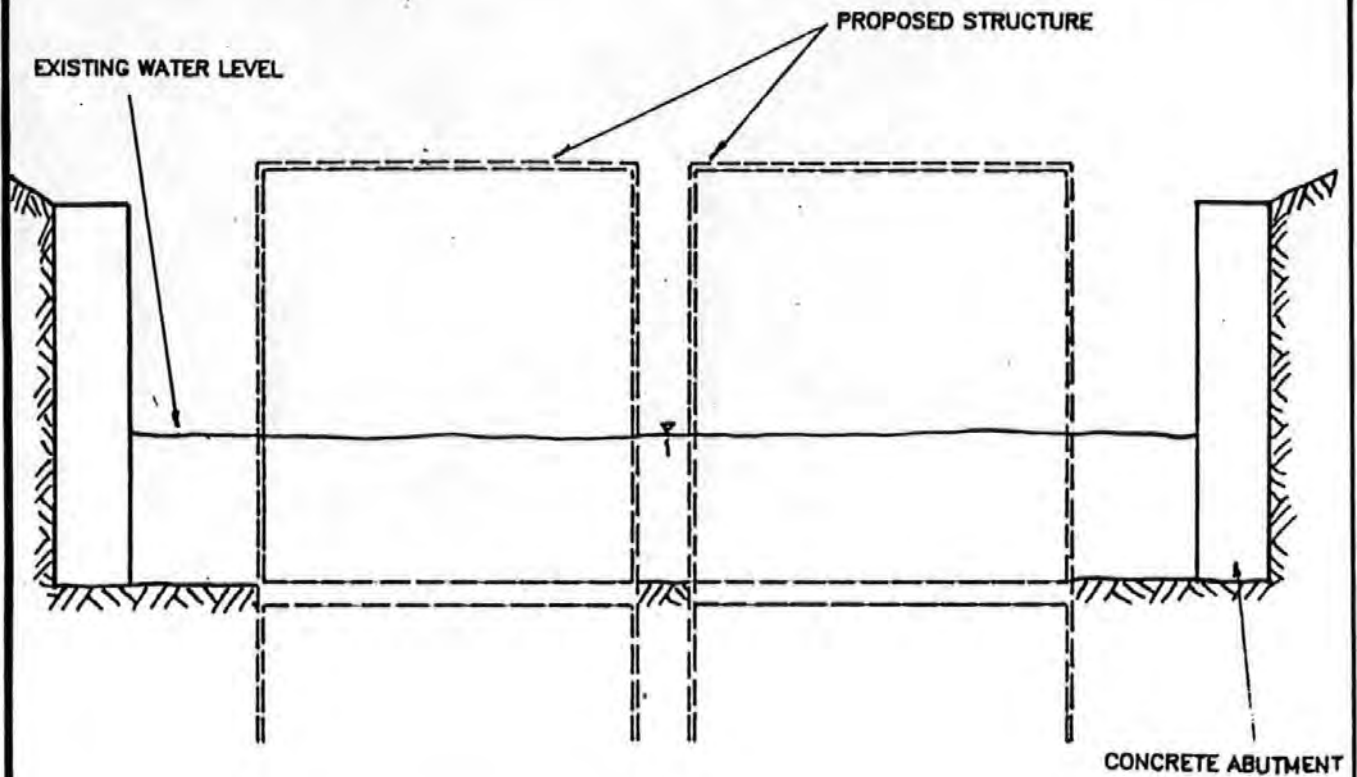


FIG. 7.21: IN-SITU CONCRETE SYSTEM
-OPEN WATER CONSTRUCTION

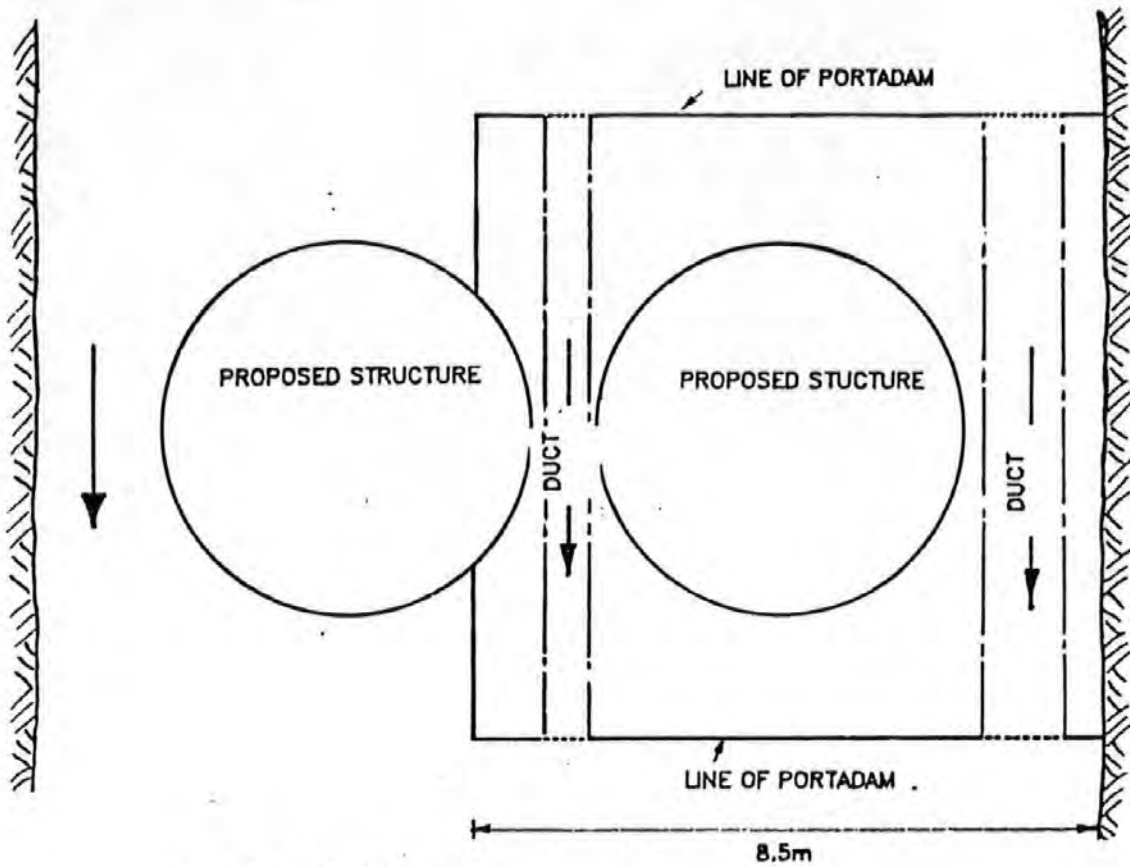
ELEVATION ON X-X



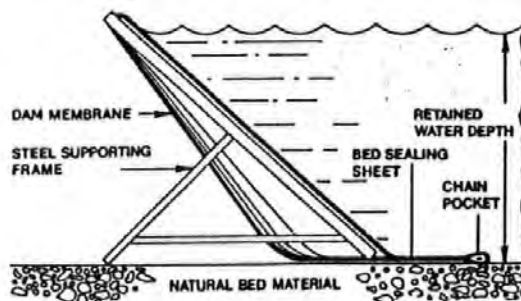
PLAN OF STAGE 1

FIG. 7.22: SUGGESTED LAYOUT OF PORTADAM

FIG. 7.22 (CONT):



PLAN OF STAGE 2



: CROSS-SECTION OF PORTADAM

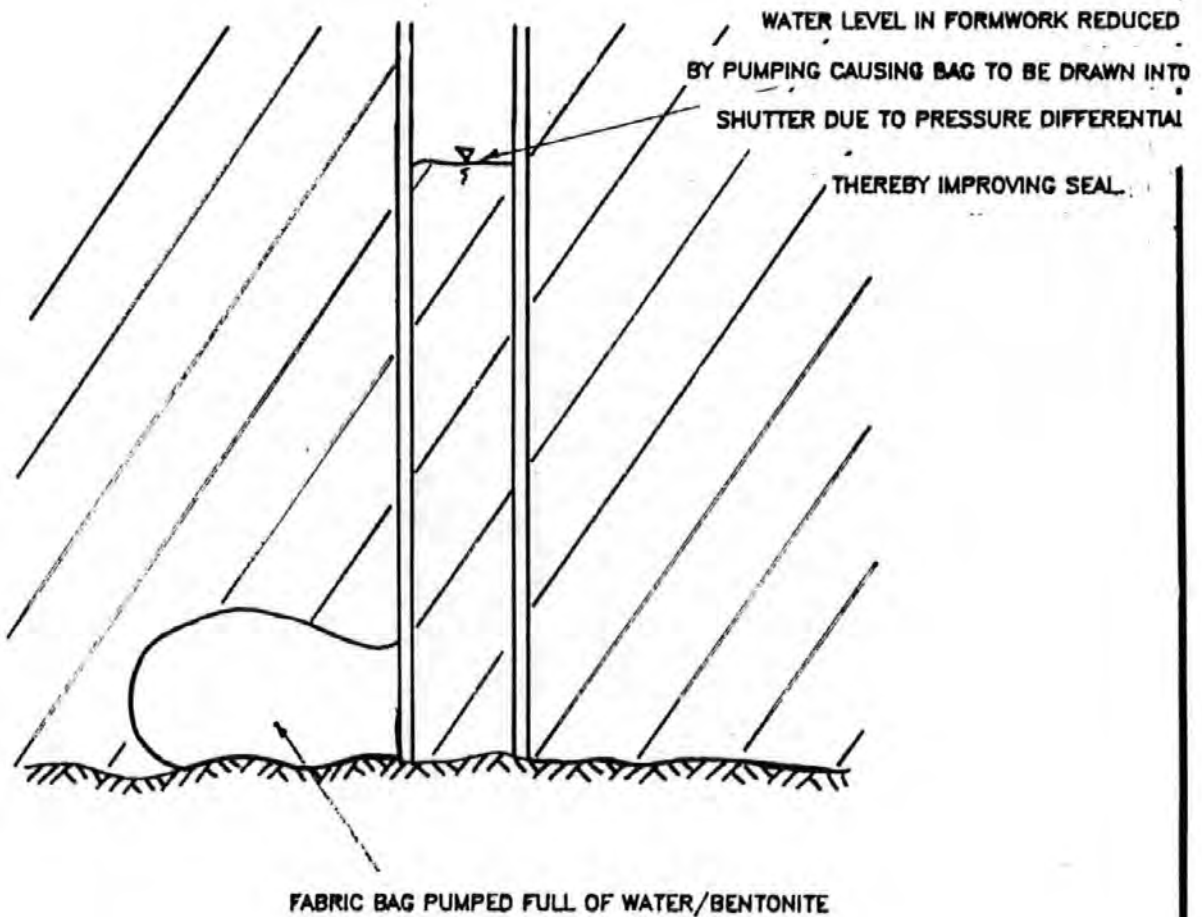
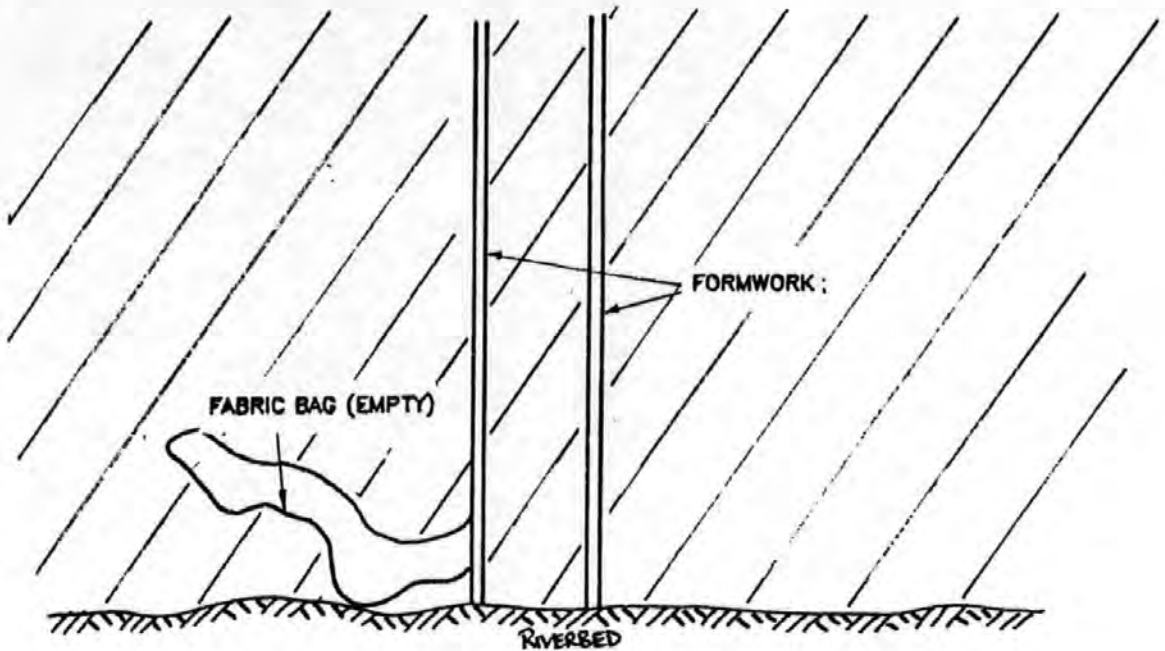


FIG. 7.23: SUGGESTED METHOD OF GROUT LEAK PROTECTION.

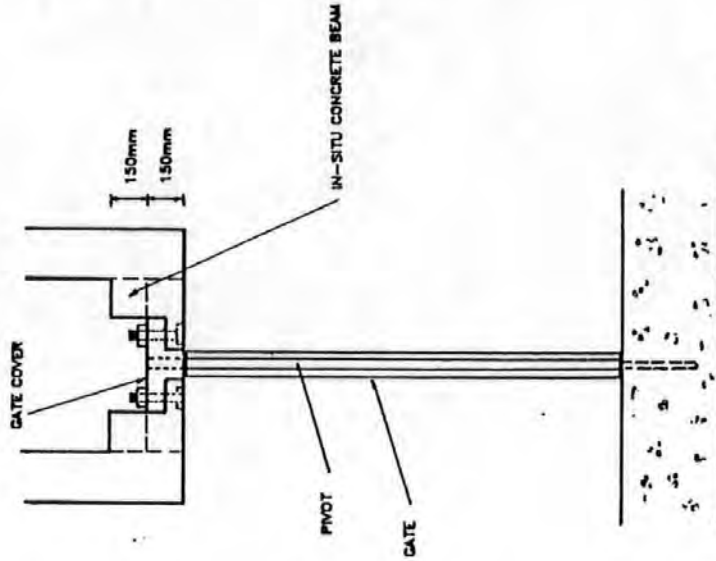


FIG. 7.25: IN-SITU CONCRETE GATE COVER
ELEVATION ON A-A (SEE FIG.)

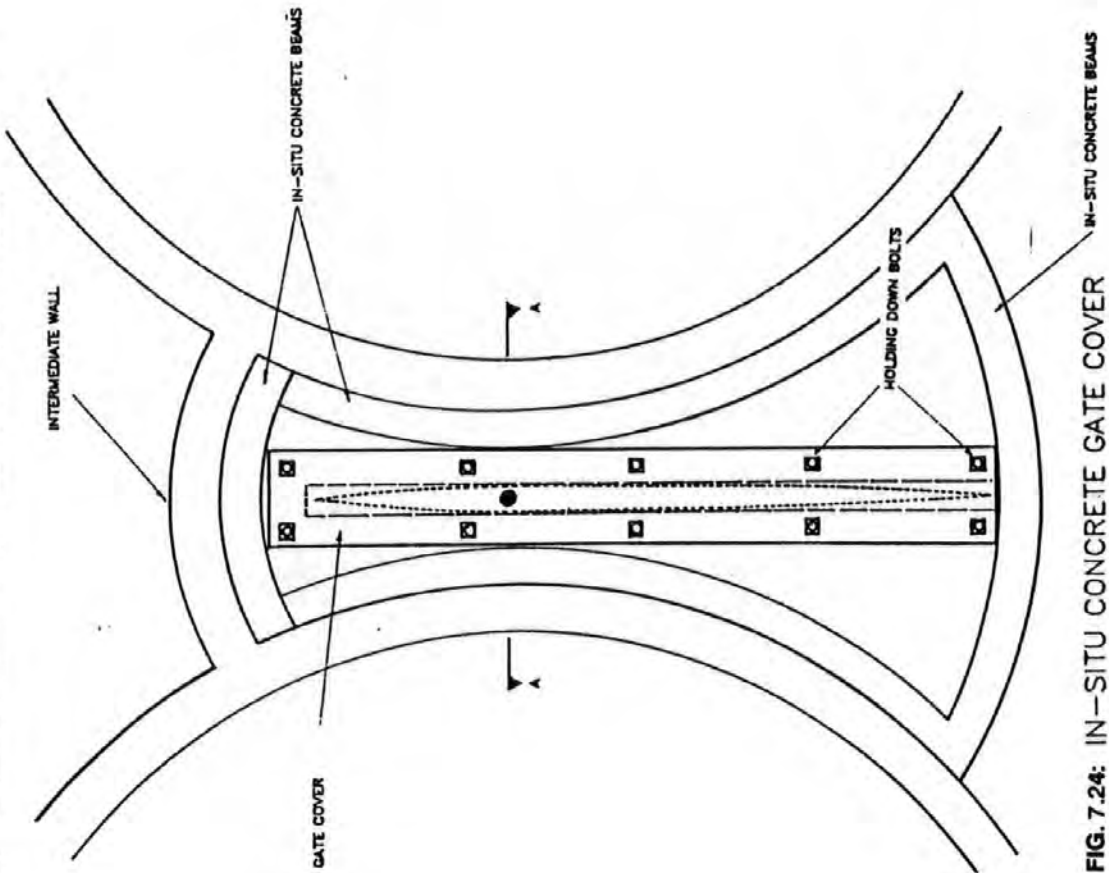
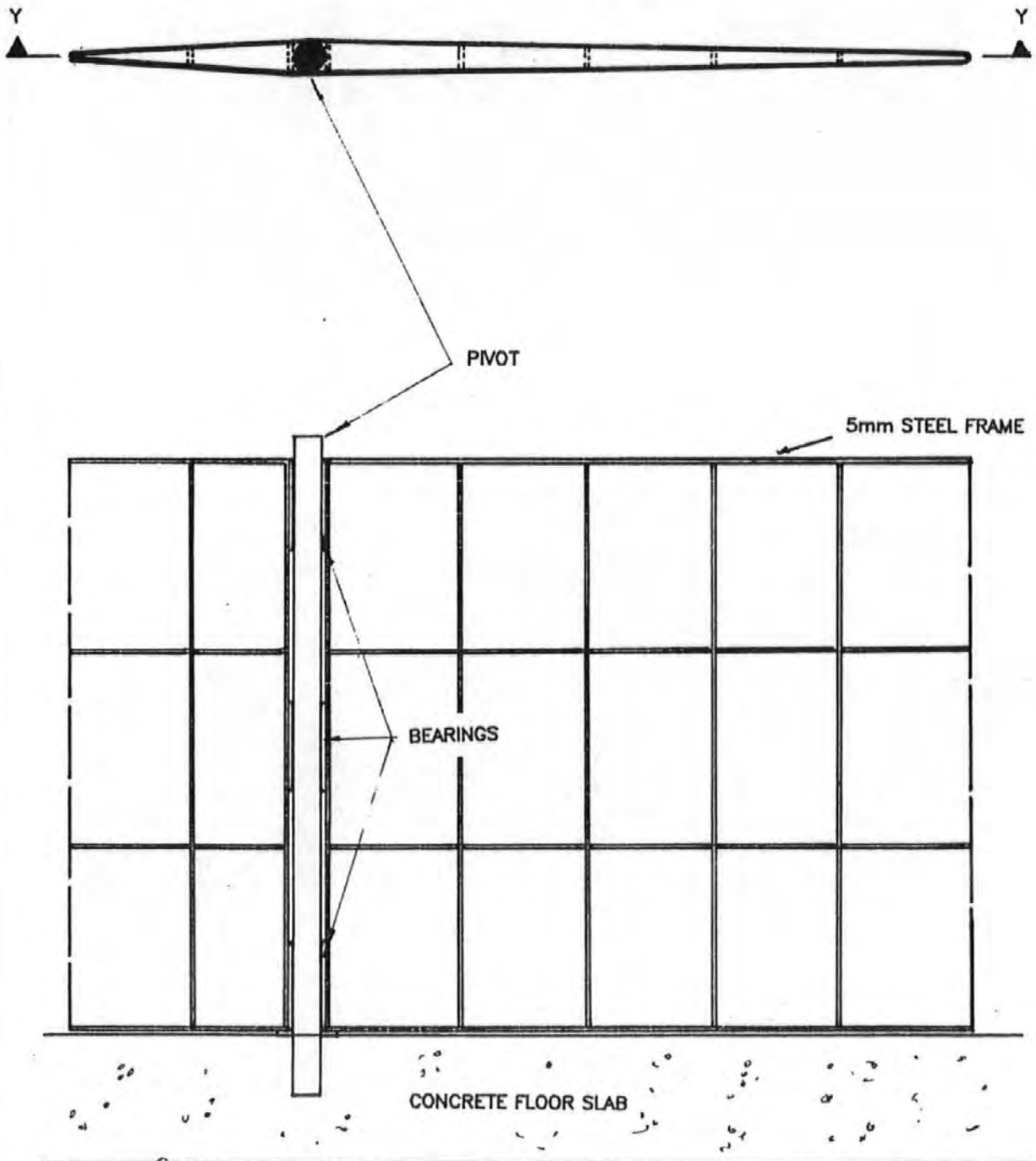


FIG. 7.24: IN-SITU CONCRETE GATE COVER

PLAN



ELEVATION ON Y-Y SHOWING FRAMEWORK

FIG. 7.26: POSSIBLE GATE DESIGN

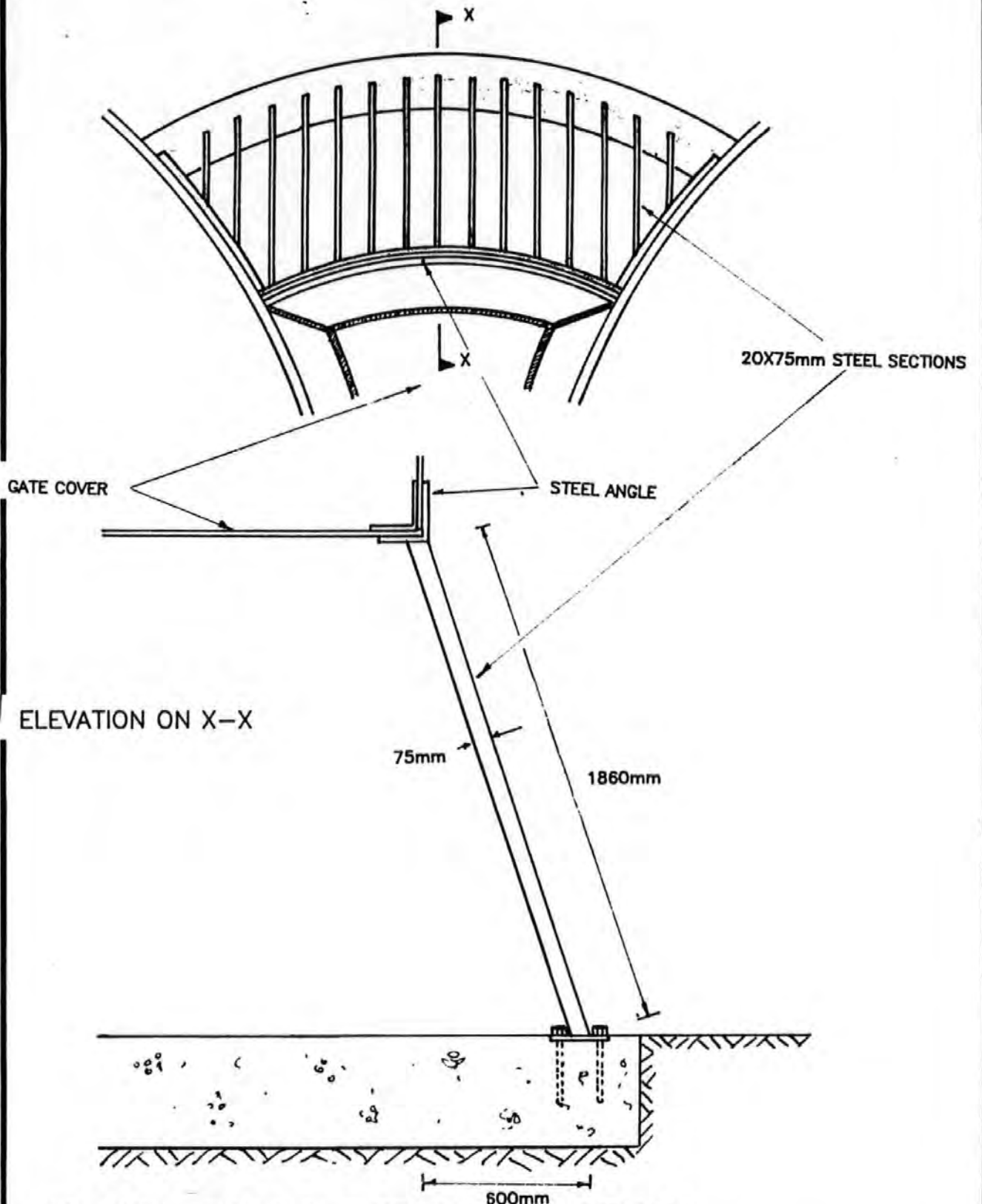


FIG. 7.27: POSSIBLE TRASHRACK DESIGN

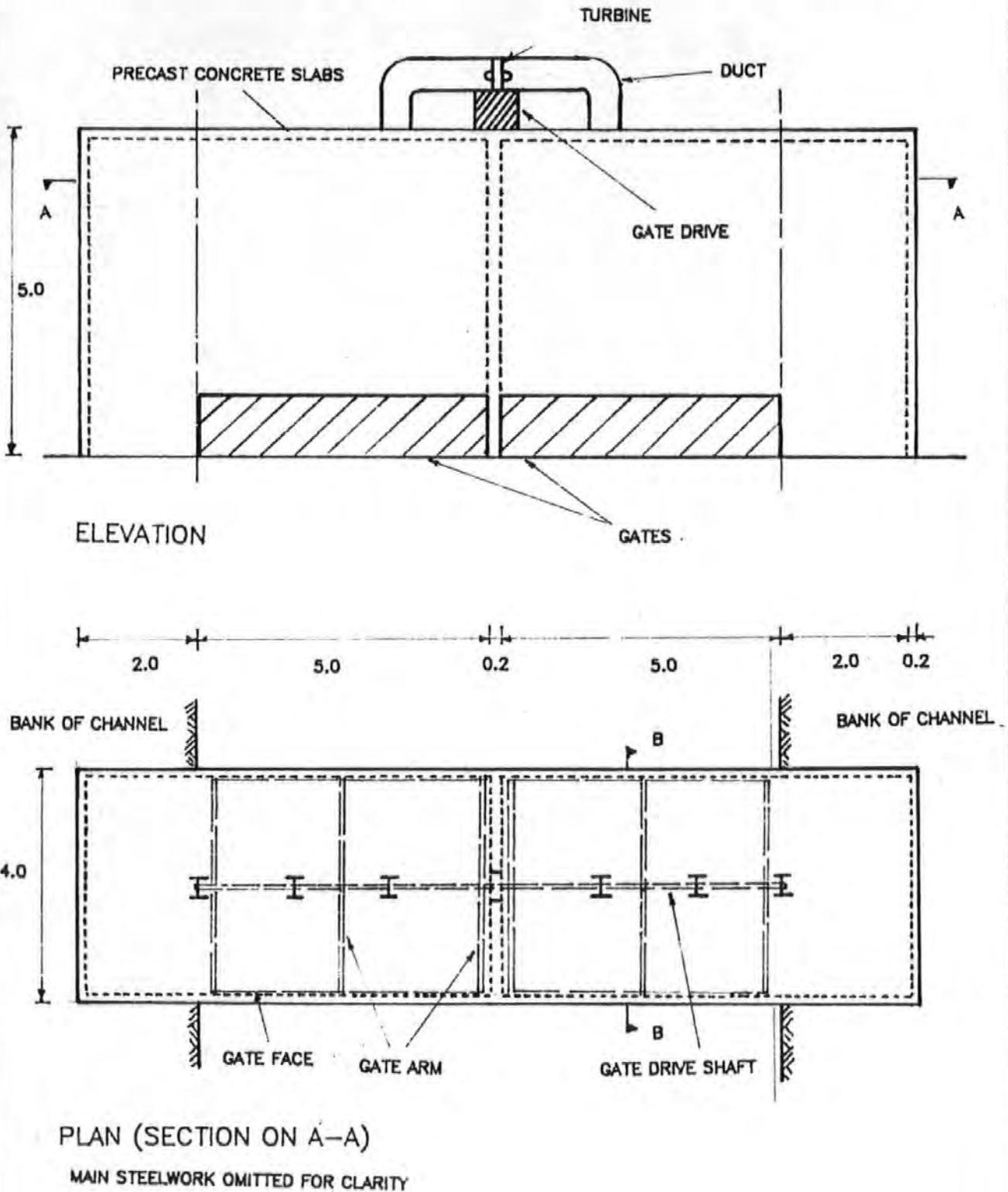
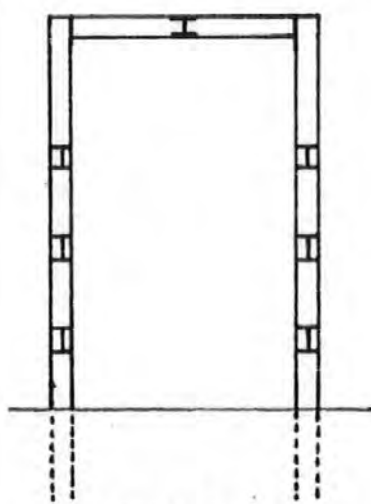
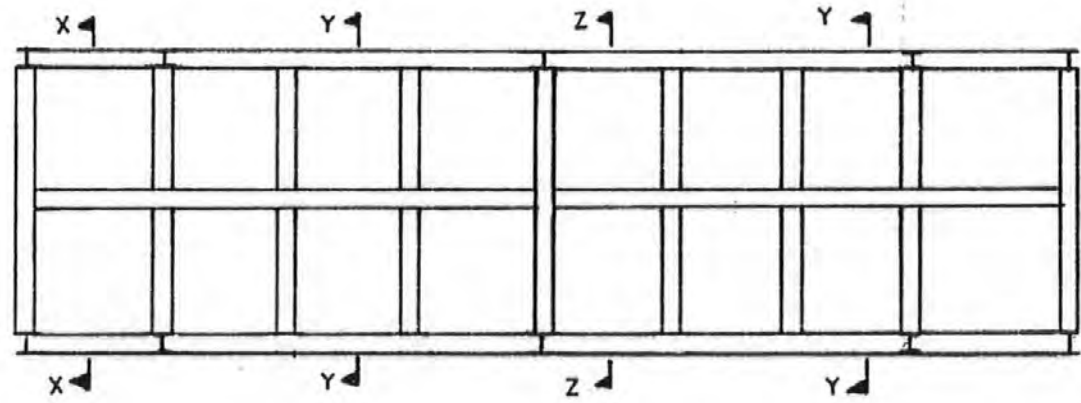
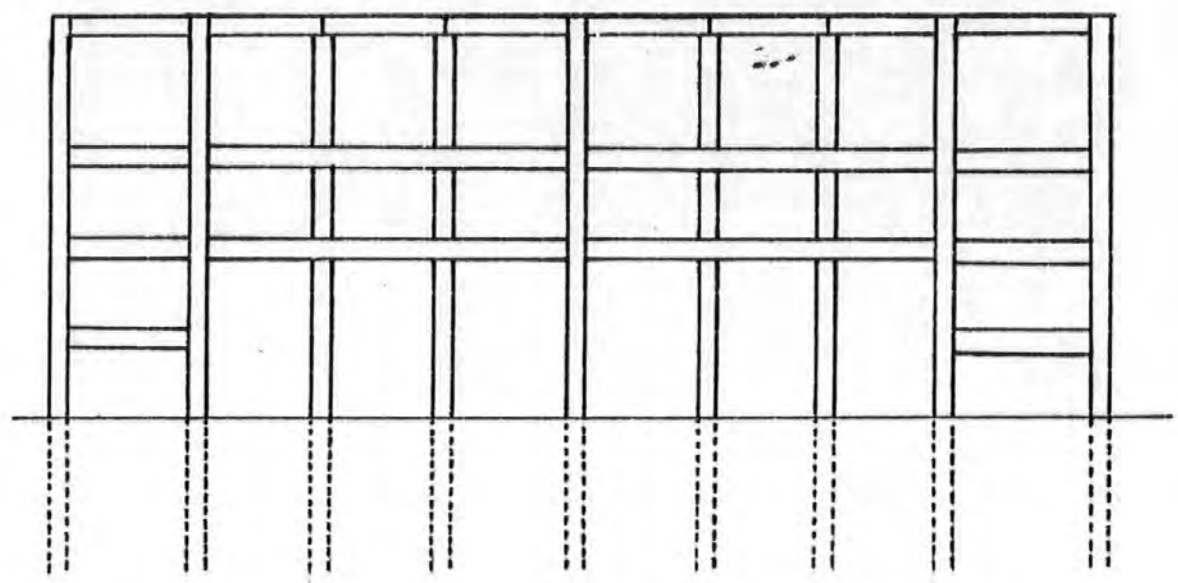
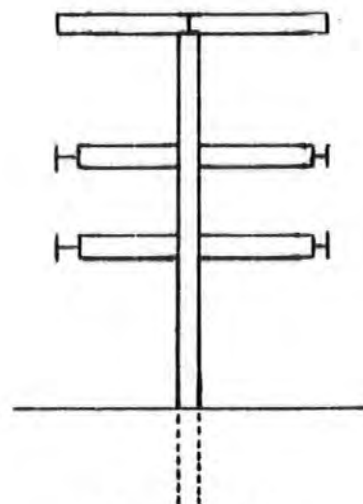


FIG. 7.28: HORIZONTAL-AXIS RADIAL GATE SYSTEM
 (OUTLINE DRAWINGS FOR APPROXIMATE COSTINGS)

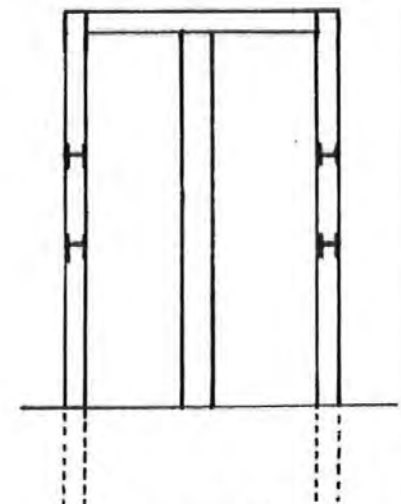
FIG. 7.28 (CONT): STEEL SUPPORTING FRAME



SECTION X-X



SECTION Y-Y



SECTION Z-Z

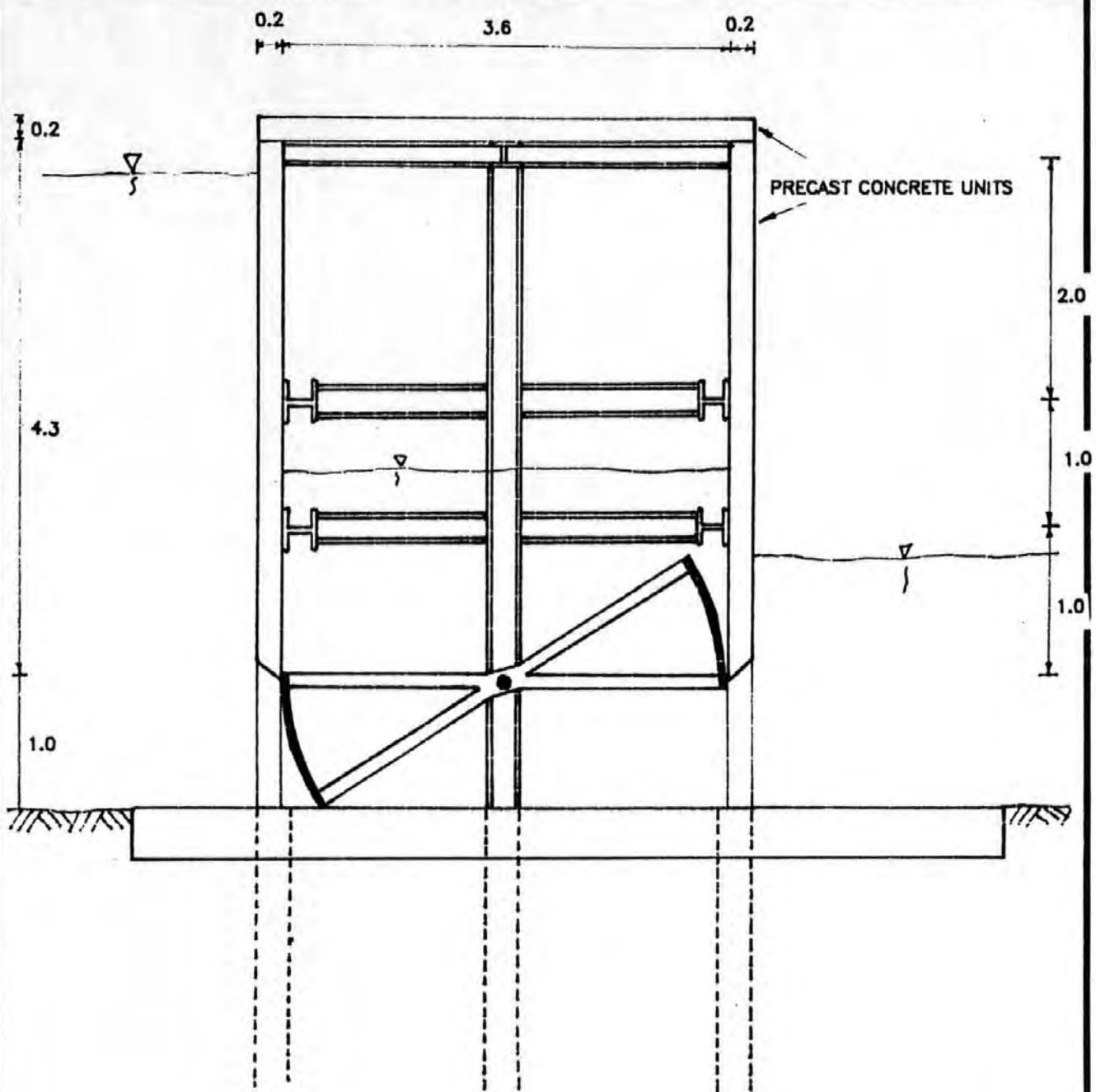
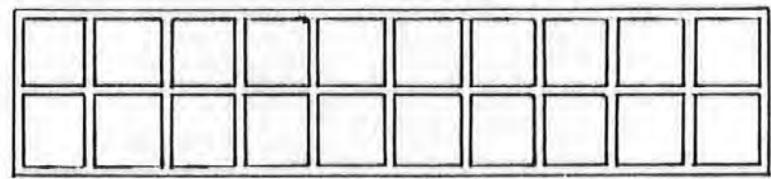


FIG. 7.28: (CONT.):ELEVATION ON B-B

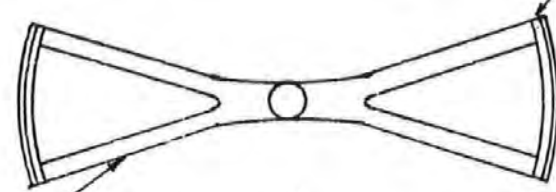
5



POSSIBLE FRAMEWORK FOR GATEFACE

60X60 SQUARE HOLLOW SECTION

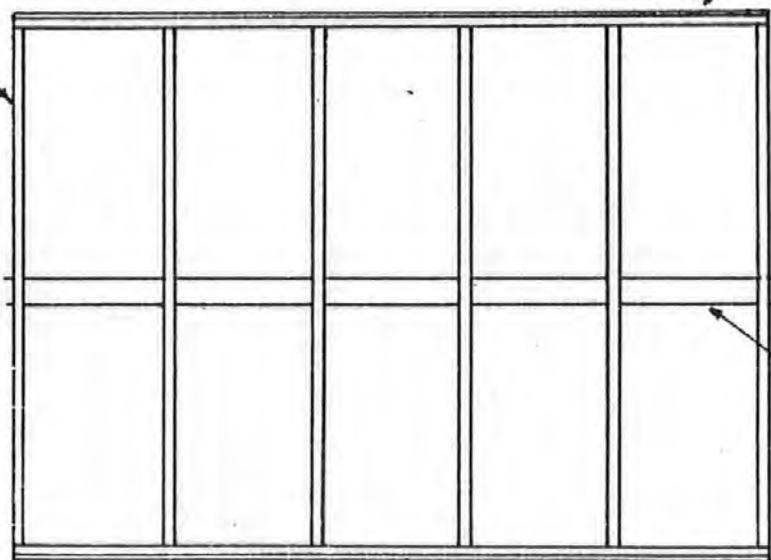
3.6



SIDE ELEVATION OF GATE AND PIVOT

20mm STEEL PLATE

60X120mm RECT. SECTION



DRIVE SHAFT

PLAN OF COMPLETE GATE SYSTEM

FIG. 7.29: SUGGESTED GATE DETAILS FOR COST ANALYSIS

8.0 : ECONOMIC ASSESSMENT OF THE PWE

8.1 Introduction

The capital costs of the two PWE configurations considered in the previous Chapter provide a basis for estimating the cost of the energy produced. However, before embarking upon a detailed economic assessment the annual costs likely to be incurred during the working life of a PWE must be investigated so that they can be included in the analysis.

Maintenance costs immediately come to mind when considering annual running costs of any hydropower system. In the case of small-scale hydropower installations a sum equivalent to 1% of the capital cost of the system is generally regarded³⁶ as sufficient to cover these costs. It is assumed therefore that such a percentage can be included in the following assessment of the PWE. Other factors to be taken into account include possible downtime per annum, Water Abstraction Charges imposed by local Water Authorities and Local Authority Rating. It is intended to investigate these factors more fully in the following sections.

8.2 Annual Charges

8.2.1 Downtime

Although annual downtime does not constitute a cost as such, it will significantly affect PWE output and therefore the potential annual income from the system. The effect of possible seasonal variation of river/channel flow upon annual PWE output has not been taken into account up to this point in the research programme. Such a consideration is difficult to include when one is dealing with a non site-specific study with a corresponding lack of flowrate data. It would seem reasonable to assume that the required flowrates defined by the parametric studies of Chapter 6 (ie approx. 10 m³/s) suggest that the PWE would need to be situated across a substantial watercourse both to supply its own needs and to provide any necessary compensatory flow. Such a situation may not be affected to any great extent by rapid fluctuation in flowrate. It is proposed therefore to introduce an annual downtime of 8%. This is the equivalent of a load factor of 92% as calculated for a conventional hydropower scheme and represents approximately 30 days per annum. A proportion of this can be assumed to be necessary for general maintenance whereas the remainder represents power production losses during the summer months when the flowrate available to the PWE may not be sufficient to maintain an optimum output. In real terms, assuming that maintenance requires an average annual shutdown period of seven

days then the remaining 23 days of lost production represents the operation of the PWE at 75% of its optimum output for a period of three months per annum.

Unless stated otherwise, the sensitivity analyses of Section 8.4 and the possible scenarios of Section 8.5.2 assume 8% downtime.

8.2.2 Water Abstraction Charges

When considering hydropower sites within the U.K. the charges levied by local Water Authorities for the abstraction of water from sources within their respective areas must be included in any economic analysis. These charges are generally based on such criteria as the source type, the quality of the abstracted water, the time of year during which abstraction is to take place and the purpose of the abstraction. A series of factors which vary with these criteria can then be applied to a standing charge per cumec of water abstracted. The factors governing the abstraction of water for power generation are comparatively low, as the passage of water through a turbine has no detrimental effect on water quality and there are no losses. Indeed, it could be argued that a device such as the PWE aerates the flow and therefore improves water quality. However, these charges are still very significant and in some areas, notably South and South-East England, they are sufficiently high to render the PWE non-economic before even considering the capital cost. Table 8.1 shows the annual charges for various regions. These charges have been calculated both for a required flow rate of 9.7 m³/sec for the twin circular chamber system (Case 1) and 10.5 m³/sec for the rectangular chamber system (Case 2). 8% downtime is taken into account in each case. The additional cost per kilowatt-hour is shown.

Water Authority	Case 1		Case 2	
	Annual Cost	p/kWh	Annual Cost	p/kWh
Severn/Trent	1860.23	0.29	2013.66	0.32
South West	15.00	-	15.00	-
Yorkshire	13789.00	2.38	14927.25	2.34
Welsh	21247.76	3.66	23000.15	3.61
Southern	41088.38	7.10	44477.11	7.00
North West	8160.39	1.41	8834.50	1.39
Thames	77392.50	13.34	83775.38	13.16

Table 8.1

The Energy Conservation Act of 1981 encouraged Water Authorities not to levy charges in individual cases where such charges inhibited the use of water as a

source of energy. Of the Water Authorities shown in Table 8.1 only three seem to take this into account. Upon enquiry the South West Water Authority stated early in 1988 that quantities of around 10 cumecs should be charged as if the water was to be used for cooling purposes. This charge would be in the region of £11250.00 per annum. However, a more recent conversation with the Authority has revealed that they would charge the minimum £15.00 licence fee irrespective of water quantity. The SWWA does stress, however, that the Authority would most likely set a prescribed flow condition to prevent abstraction in low flows. It is specifically stated in the Authority's literature that power generation should be viewed mainly as a winter activity to avoid abstraction during low summer flows. Although this would not greatly affect the individual generating power for his own domestic needs it would seriously upset the economics of a commercial generator.

The Welsh and North West Water Authorities have a definite policy regarding water abstraction for power generation. Upon receiving an application for a licence the relevant Authority will advise the prospective generator on those charges due under their scheme of Abstraction Charges. The applicant is then invited to indicate whether these charges will render his system uneconomic. If this is the case he can present a financial analysis of the scheme and the Authority will then offer an abated charge. However, the power to offer rebates is at the Authorities' discretion and no details of the criteria on which the economic status of a scheme is judged are offered^{37,38}.

At this time of writing the effects of the privatisation of the water supply industry upon abstraction charges are not known. However, the scenarios of Section 8.5.2 allow for a number of possible policy changes concerning hydropower generation.

8.2.3 Local Authority Rating

This is another area where annual costs can greatly differ depending upon system location and local policy. The Public Electricity Supply Industry in the U.K. has its rateable value determined by a statutory formula as laid down in Schedule 7 of the General Rate Act of 1967. Unfortunately this same formula does not, at this moment, apply to the private producer. Cecil Parkinson (then Secretary of State for Energy) stated in March, 1988 that: *'The Government has agreed in principle that Private Generators exporting electricity to the Electricity Supply Distribution Network should be rated on a comparable basis to the rest of the Electricity Supply Industry.'*³⁹ However, although Section 34A of the General Rates Act provides for the extension, by order, to other generators of electricity of the formula contained in Schedule 7, that formula is not currently in a form which can be applied to independent electricity suppliers.

Until this formula is presented in a suitable form the only precedent on which to base an assessment of the likely effect of local rates is that set by the case of the Slade Windmill, constructed at Ilfracombe, Devon. This was rated by conventional means, ie. its rateable value was determined from a percentage of the capital cost of construction and land value. Although the 1983 Energy Act allows the private generator to appeal against Local Authority rating, upon appeal the windmill was deemed fully rateable and its energy production was therefore rendered uneconomic.

It would therefore seem reasonable to assume for the purpose of this study, that a 'worst case' situation for the PWE would be to be assessed in the same manner. Assuming the proposed system was situated in the South West, this would entail setting its rateable value at six percent of the capital cost of its construction discounted to 1973 prices. The six percent is a national figure and the necessary discounting can be achieved by dividing the capital cost by 3.5. This factor is set by the Regional Building Surveyor and is based upon the trends in land and property values in the South West of England over the past 15 years⁴⁰. Taking an average commercial rate of £2.375p in the pound for the same area the resulting annual rate is as follows:

Case 1:

$$\begin{aligned} \text{Annual Rate} &= \frac{88550.00 \times 0.06}{3.5} \times 2.375 \\ &= \underline{\underline{\pounds 3605.25}} \end{aligned}$$

or, in terms of pence per kWh:

$$\frac{3605.25}{580262.4} = \underline{\underline{0.62\text{p/kWh}}}$$

Case 2:

$$\begin{aligned} \text{Annual Rate} &= \frac{103248.44 \times 0.06}{3.5} \times 2.375 \\ &= \underline{\underline{\pounds 4203.69}} \end{aligned}$$

or, in terms of pence per kWh:

$$\frac{4203.69}{636676.8} = \underline{\underline{0.66\text{p/kWh}}}$$

A 'best case' situation would be for the PWE to be charged a comparable rate to that charged the CEGB, ie approximately 0.18p/kWh at 1988 prices. Both situations are investigated in the following sections.

8.3 Economic Assessment

8.3.1 Methodology

Having established the annual costs that should be included within any economic analysis of the PWE it is now possible to calculate the cost per kilowatt-hour (kWh) of the energy thus produced.

This is achieved via the following process:

The Net Present Value (PV_1) of the Capital Cost (P_c) and the Annual Operating Costs (P_o) is calculated using:

$$PV_1 = P_c + \frac{P_o}{(1+i)^1} + \frac{P_o}{(1+i)^2} + \dots + \frac{P_o}{(1+i)^n} \quad (8.1)$$

where: i = real discount rate

n = working life of the system

The Net Present Value (PV_2) of the energy output is represented by similarly discounting the Annual Energy Output (E):

$$PV_2 = \frac{E}{(1+i)^1} + \frac{E}{(1+i)^2} + \dots + \frac{E}{(1+i)^n} \quad (8.2)$$

The Unit Cost of Energy Generation (U p/kWh) can now be calculated thus:

$$U = \frac{PV_1}{PV_2} \times 100 \quad (8.3)$$

No allowance is made for inflation in the following analyses and no interest is added during the construction period. The following real discount rates are applied:

- 1) $i = 0.05$: This represents the historical public sector discount rate.
- 2) $i = 0.08$: The present public sector discount rate and typical discount rate for a large, asset-rich utility company.
- 3) $i = 0.10$: Typical discount rate for a small utility company or a private investor.

8.3.2 Case 1: Circular Chamber, butterfly gated system

An average cost of £88550.18 has been taken as representative of the likely capital cost of this system. The Plastic/GRP chamber costing has not been included in this calculation. An optimum average output of 72 kW has been shown (via parametric testing) to be achievable. These two figures, therefore, provide the basis for the following costs per kilowatt hour of the probable electrical output of the system. Two scenarios are presented in order to illustrate the effects of Water Abstraction Charges and Local Authority Rating upon the Unit Cost of Generation. The Public Utility Rate of Scenario 2 is based upon the rate per kilowatt-hour paid by the CEGB (0.18p/kWh). A Payback Period of 25 years is assumed in each case.

Scenario 1:

Annual Operating Costs:

Maintenance: £900.00

Water Abstraction Charges (Severn/Trent): £1860.00

Local Authority Rates: £3605.00

Discount Rate	Unit Cost (p/kWh)	
	(A)	(B)
0.05	2.01	2.18
0.08	2.32	2.53
0.10	2.56	2.78

Column (A): Assuming 0% downtime

Column (B): Assuming 8% downtime

Table 8.2

The effects of increasing the capital cost of the system upon the unit cost of the electricity output is illustrated in Fig. 8.1. The annual costs of Scenario 1 have been included in this illustration.

Scenario 2:

Annual Operating Costs:

Maintenance: £900.00

Public Utility Rate: £1076.00

Discount Rate	Unit Cost (p/kWh)	
	(A)	(B)
0.05	1.30	1.42
0.08	1.62	1.76
0.10	1.86	2.02

Column (A): Assuming 0% downtime

Column (B): Assuming 8% downtime

Table 8.3

8.3.3 Case 2: Rectangular Chamber, horizontal-axis radial gated system.

In this case, the sole cost estimate of £103248.44 is taken to be representative of the likely capital cost of the system. An optimum average output of 90 kW has been achieved via parametric testing. However it has been established in Section 7.11 that the compressor providing the gate drive will require 11 kW leaving an optimum output of 79 kW. Again, the cost per kilowatt hour is based on these figures and two similar scenarios to those of Section 8.3.2 are presented.

Scenario 1:

Annual Operating Costs:

Maintenance: £1050.00

Water Abstraction Charges (Severn/Trent): £2014.00

Local Authority Rates: £4203.00

Discount Rate	Unit Cost (p/kWh)	
	(A)	(B)
0.05	2.11	2.29
0.08	2.45	2.66
0.10	2.69	2.93

Column (A): Assuming 0% downtime

Column (B): Assuming 8% downtime

Table 8.4

Scenario 2:

Annual Operating Costs:

Maintenance: £1050.00

Public Utility Rate: £1195.00

Discount Rate	Unit Cost (p/kWh)	
	(A)	(B)
0.05	1.38	1.50
0.08	1.72	1.87
0.10	1.97	2.14

Column (A): Assuming 0% downtime

Column (B): Assuming 8% downtime

Table 8.5

8.4 Sensitivity Analysis

In order to investigate the economic sensitivity of the system to variations of annual and capital costs a number of analyses have been carried out. These analyses involve the calculation of the Internal Rate of Return (IRR) over various payback periods for a series of differing situations. All calculations are based upon the twin chamber, butterfly-gated PWE (Case 1) of Section 8.3.2.

The effects of a 40% variation in downtime are shown in Fig. 8.2. In this case Water Abstraction charges have been fixed at the South West Water Authority's licence fee of £15.00. All other annual costs are as Scenario 1 of Section 8.3.2.

The value of the energy produced in each of these analyses has been estimated from Scale A of the South West Electricity Board's purchasing tariff for 1988. The details of this estimate can be found in the following section. In the graph of Fig. 8.3 the energy value itself is varied whilst the annual and capital costs remain identical to those of Scenario 1 (Section 8.3.2).

The curves of Fig. 8.4 illustrate the variation of the capital cost of the system whereas those of Fig. 8.5 show the effects of increasing the annual maintenance cost from 0 to 5% of the capital cost. All other costs are identical to those of the previous analysis.

8.5 Cost Projections

8.5.1 Introduction

When dealing with both Water Abstraction Rates and Local Authority Rates it becomes difficult to establish a definitive cost per kilowatt-hour due to the large variations in annual charges dependent upon the system's location. A comprehensive treatment of each of the Local Authority Rating areas coupled with the relevant Water Authority's Abstraction Charges would be excessively time consuming. This becomes even more apparent when one considers the advent of the Standardized Business rate or the likely introduction of a Public Utility rate. A revision of the Water Abstraction charging system following the privatization of the Water Supply Industry is also a distinct possibility.

The situation at the time of writing is such that a more general approach is necessary. An attempt to overcome the possible changes in policy has been made by presenting a series of scenarios which should be regarded as illustrations of the economics of the system rather than a definitive analysis. The various elements of each scenario are summarised in Section 8.5.3.

8.5.2 Possible Scenarios

Figs. 8.6 and 8.7 show cost projections over the working life of the system for five differing scenarios all involving the Twin Circular Chamber butterfly gated system. In each scenario 8% downtime is taken into account.

Scenarios one to three assume that the energy produced is to be sold to the CEGB. A rate of 2.82p/kWh has been calculated by averaging the various rates for differing seasons and times of day under Scale A of the South West Electricity Board's Purchase Tariff⁴¹ for April, '88. Assuming that the private generator is also receiving a supply from the Board via the same connection to the Board's system

then the various monthly charges will reduce this rate to 2.80p/kWh. The 8% downtime is assumed to occur mainly during the summer months i.e. during periods of low flow and so the resulting loss in revenue is calculated at the lower purchase rates for this period and subtracted from the overall annual value of the energy produced. The Purchase Tariff is directly related to the Bulk Supply Tariff and it is assumed that, in real terms, the BST remains constant over the 25 year period (this being one of the scenarios put forward by Carr⁴⁶ in his economic analysis of the Severn Barrage).

The first of these three scenarios assumes that the PWE is situated in a location rendering it liable to both significant Water Abstraction Rates and full Local Authority Rating. The Severn/Trent Water Authority's rate of £1860.23 per annum has been taken as representative of the maximum annual charge that the system's economics could tolerate (those annual charges of the Yorkshire, Southern and Thames Water Authorities being sufficient in themselves to render the PWE non-economic). The Local Authority Rate calculated in the previous section is assumed representative for the purpose of these illustrations.

The second scenario again involves case 1 but assumes that it is situated within an area where a minimum Water Abstraction Charge only is required (i.e. the South West or possibly Wales or the North West). The Local Authority Rate is as scenario one.

Scenario No. 3 assumes that the Local Authority Rating has been replaced by a system whereby the private generator is rated on a comparable basis to the rest of the Electricity Supply Industry. Water abstraction charges are set at a minimum on the assumption that this will be the case following privatisation of the water supply industry.

The two final scenarios illustrate an alternative and far more profitable method of selling the electricity. Scenario four assumes that the PWE is so positioned as to be able to offer a supply to a private, industrial concern either as an alternative or as a supplement to the CEGB's supply. The energy is offered at the competitive rate of 5p/kWh. It is also assumed that the relevant Water Authority/Company has adopted a reasonable attitude to the private hydro-generator and is therefore charging the minimum Abstraction Rate. A Public Utility Rate of 0.18p/kWh is also in force.

This is also the case in scenario five; however, here we look at the situation where a private industrial consumer or perhaps a Water Authority / Company has installed a PWE specifically to reduce its dependence on the CEGB supply. The energy value is set at 6p/kWh, which, it is suggested, represents a slightly

conservative estimate of the average cost of electricity to a small, industrial concern at the present time.

In order to assess the acceptability of the economics of the system to either the public or private sectors the Internal Rate of Return (IRR) is calculated for each scenario over various payback periods.

8.5.3 Summary of Scenarios One to Five

Scenario 1, (Fig. 8.6):

- (1) Twin, circular chamber, butterfly gated system.
- (2) Liable to full water abstraction charges (WA).
- (3) Liable to full Local Authority rating.
- (4) Energy value based on an average of the SWEB's purchase tariff.

Scenario 2, (Fig. 8.6):

- (1) Twin, circular chamber, butterfly gated system.
- (2) Liable to minimum water abstraction charges (WA).
- (3) Liable to full Local Authority rating.
- (4) Energy value based on an average of the SWEB's purchase tariff.

Scenario 3, (Fig. 8.6):

- (1) Twin, circular chamber, butterfly gated system.
- (2) Liable to minimum water abstraction charges (WA).
- (3) Liable to Public Utility rating (assumed equivalent to 0.18 p/kWh).
- (4) Energy value based on an average of the SWEB's purchase tariff.

Scenario 4, (Fig. 8.7):

- (1) Twin, circular chamber, butterfly gated system.
- (2) Liable to minimum water abstraction charges (WA).
- (3) Liable to Public Utility rating (assumed equivalent to 0.18 p/kWh).
- (4) Energy value is set at 5p/kWh, i.e. it is assumed that the energy is supplied to a private, industrial consumer at a competitive rate.

Scenario 5. (Fig. 8.7):

- (1) Twin, circular chamber, butterfly gated system.**
- (2) Liable to minimum water abstraction charges (WA).**
- (3) Liable to Public Utility rating (assumed equivalent to 18 p/kWh).**
- (4) Energy value is set at 6p/kWh, i.e. at a rate comparable with the present cost of electricity to a private, industrial consumer requiring an average supply in the region of 70 kW.**

FIG. 8.1: UNIT COST/CAPITAL COST

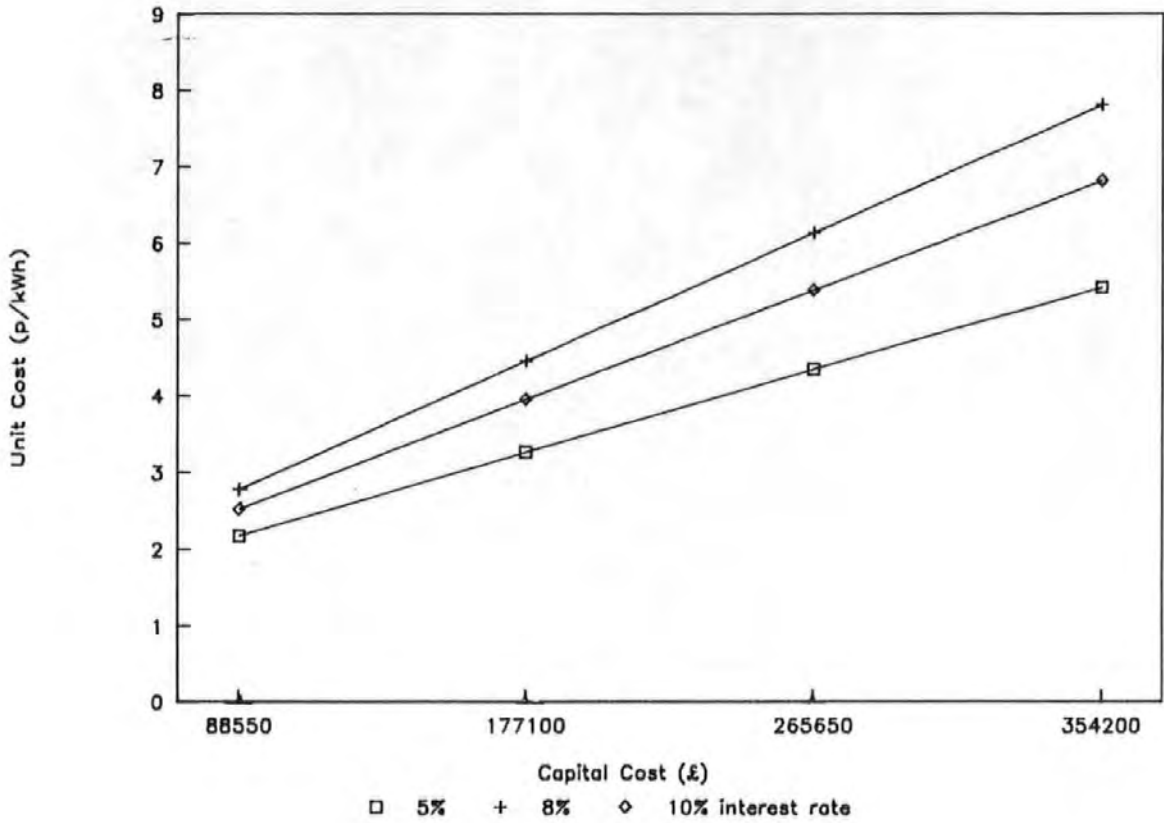


FIG. 8.2: VARIABLE DOWNTIME

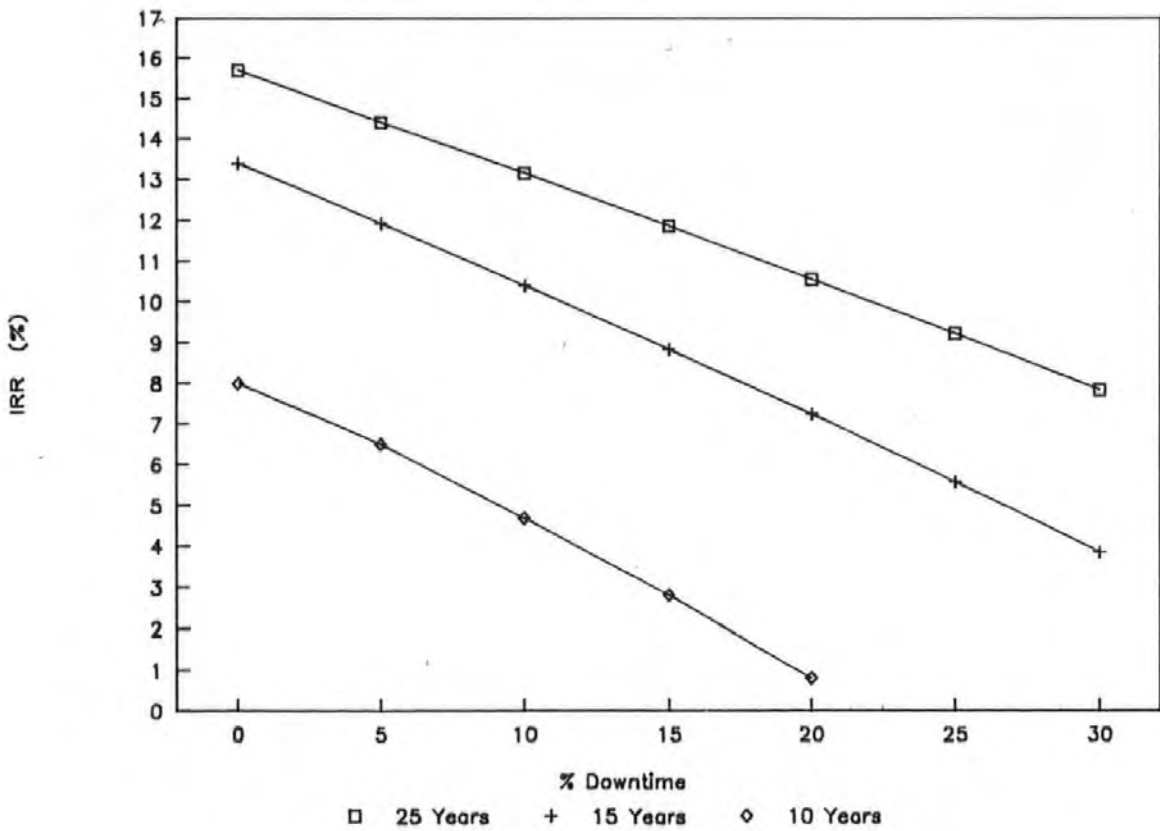


FIG. 8.3: VARIABLE ENERGY VALUE

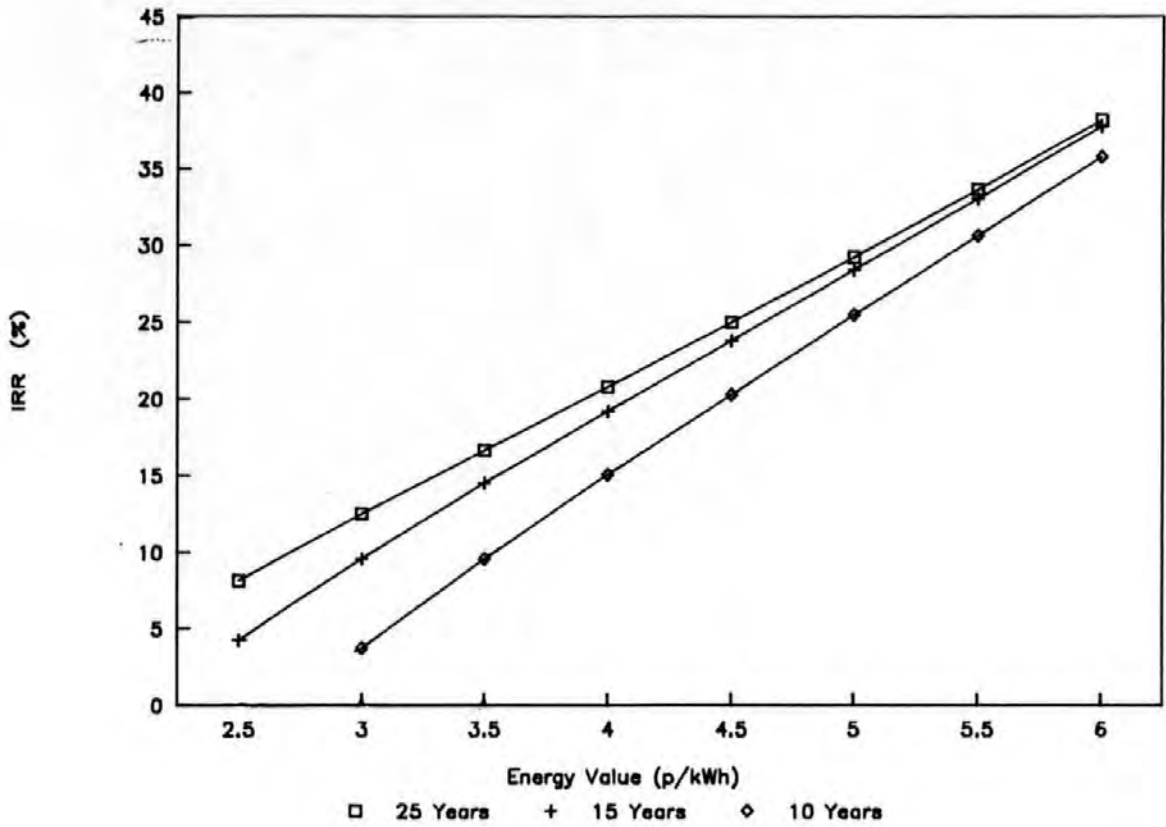


FIG. 8.4: VARIABLE CAPITAL COST

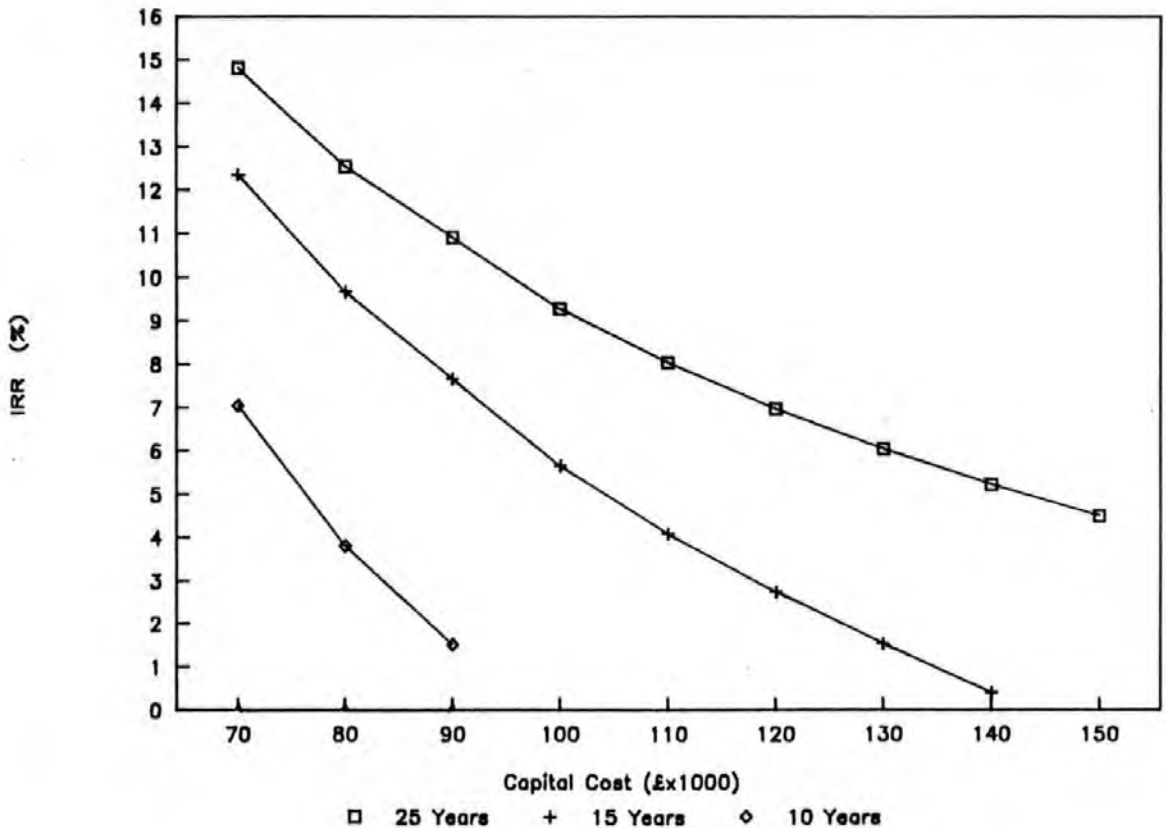


FIG. 8.5: VARIABLE MAINTENANCE COSTS

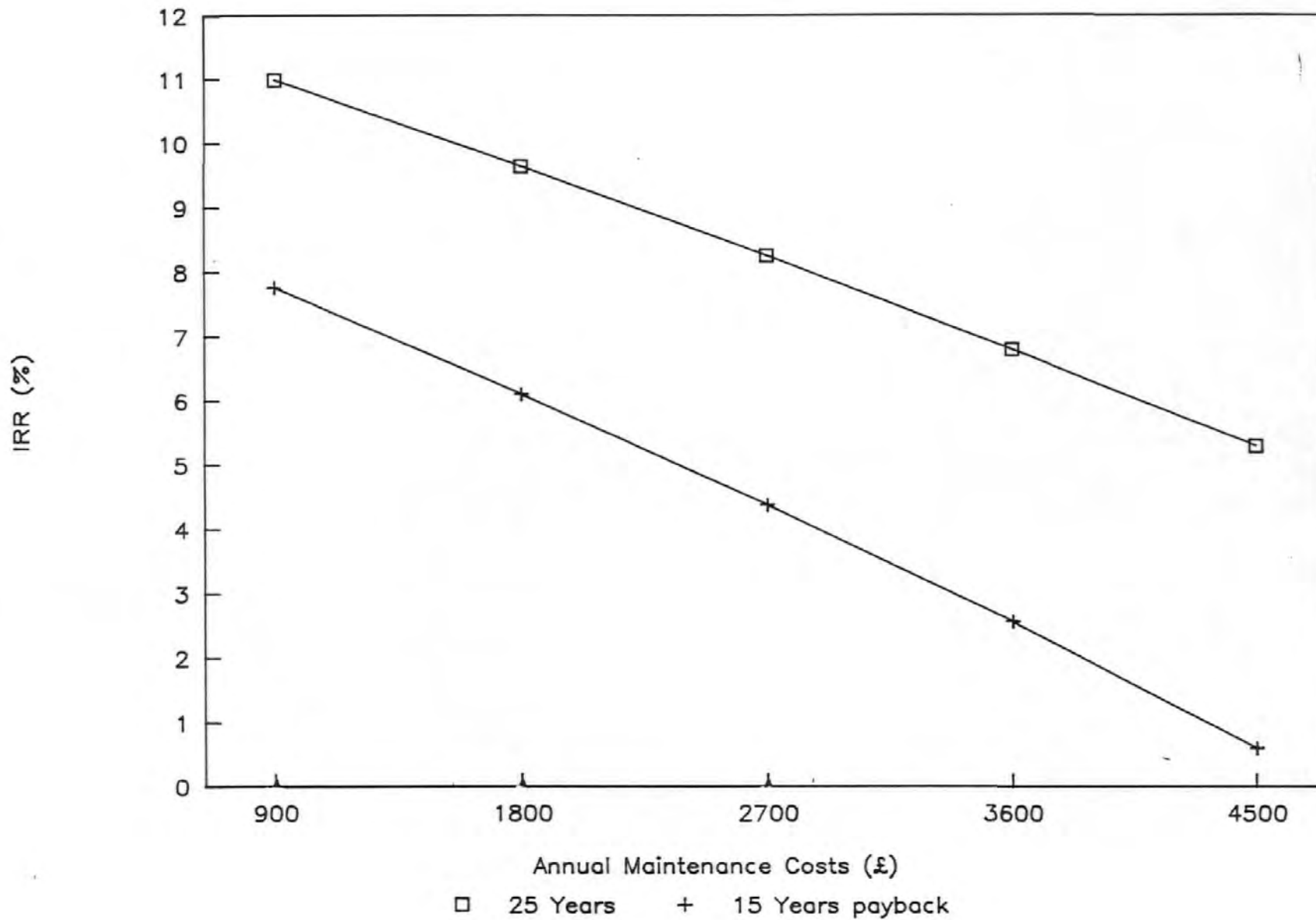


FIG. 8.6: COST PROJECTIONS

Scenarios 1 to 3

193

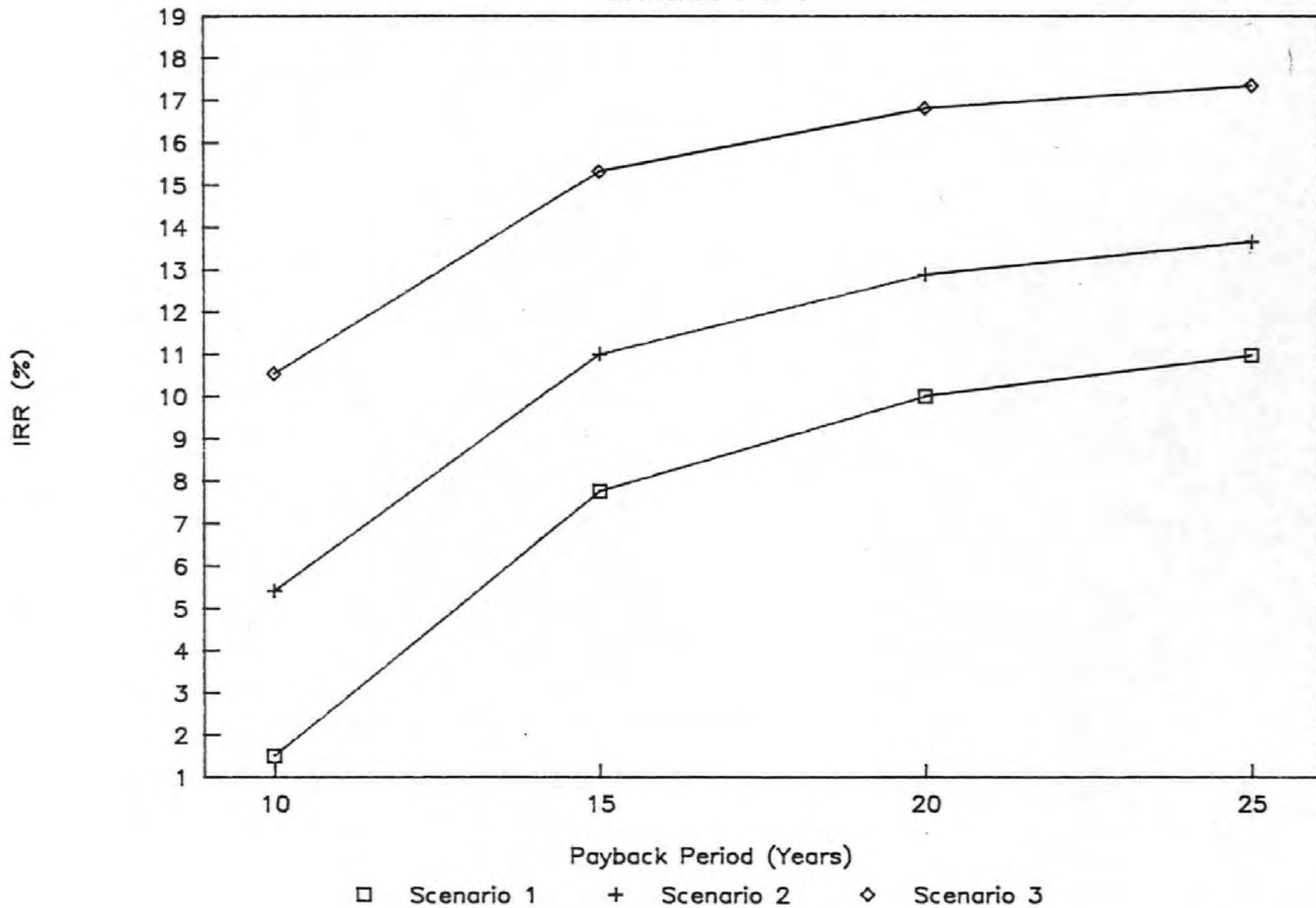
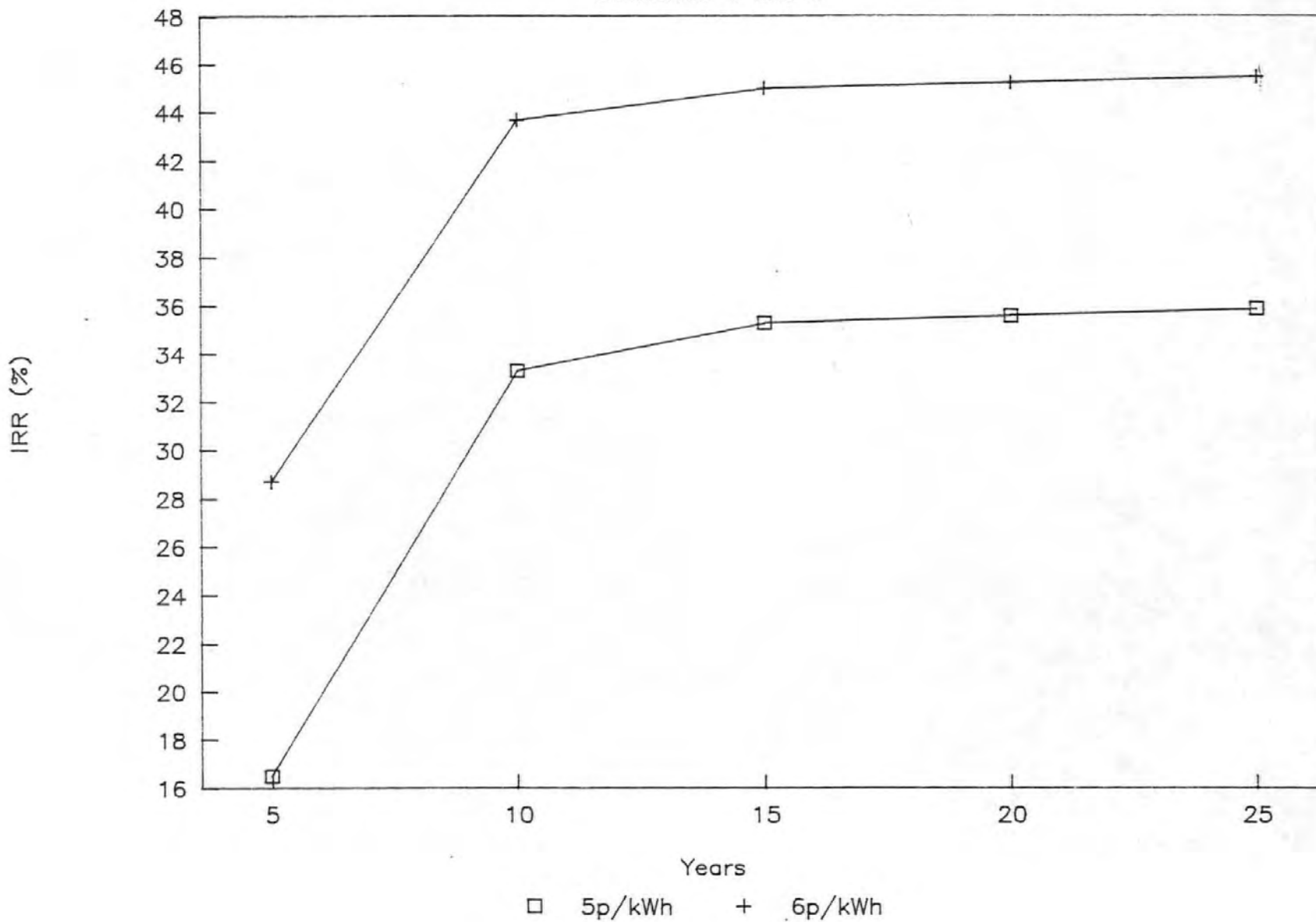


FIG. 8.7: COST PROJECTIONS

Scenarios 4 and 5



9.0 : SYSTEM OPTIMIZATION VIA GENETIC ALGORITHM

9.1 Introduction

The complex interaction of a selection of the PWE's many design variables was illustrated by the hydraulic model and parametric tests described in Chapters 3 and 6. Even though only a few parameters were considered, their optimization to achieve maximum average power output proved both difficult and time consuming. This chapter explores the potential of an alternative method of optimization which makes use of the genetic algorithm. The power of this 'Evolutionary Design' technique is demonstrated by applying it to the design of a twin, circular chamber PWE with similar dimensions to those considered in Section 6.3.

The severe physical restraints that apply to the upper and lower bounds of some of the design parameters of this type of PWE have already been discussed in Section 6.3.3. Two of the parameters affected are gate size and gate speed. Both the physical model tests and the parametric tests indicated that the gate should be as large as is practically possible and should move as quickly as possible. It can be assumed therefore that optimization of these particular parameters has already been achieved within their respective physical restraints (see test series 10 to 12 and 23 and 24 of Sections 6.3 and 6.4).

9.1.1 ZHCG, PADIFD and ST

Physical restraints also apply to the gate trigger level (ZHCG), design pressure differential (PADIFD) and turbine scale factor (ST) parameters. The upper and lower bounds of ZHCG are defined by the magnitude of the respective water column strokes under any given set of conditions. The upper bound of PADIFD is dependent upon the pressure regime of the PWE cycle whereas the scale of the turbine is restricted by the physical practicality of its installation and by cost. Unlike gate size and speed, there is no reason to suppose that the optimum values of these three parameters lie at their upper or lower bounds.

The interdependent nature of these three parameters was illustrated by the parametric tests. These tests also indicated how difficult it was to achieve an optimum combination of their respective values by traditional means.

9.1.2 Chamber Shape

All of the system configurations so far considered have assumed that the plan cross-sectional area of the chamber or chambers remains constant with elevation. Conceptually a gradual narrowing of the chambers with height could result in an

increase in average power output by improving water column velocities and increasing the mass air flow rate through the turbine. However such a narrowing could involve a lessening of the overall chamber capacity and this could have a detrimental effect upon the average mass flow rate of air over a complete PWE cycle. Maximum average power output must be dependent upon passing the largest mass of air through the turbine in the shortest possible period. There should exist therefore a chamber shape which will allow a compromise between air capacity, mass flow rate of the water columns and air flow rate through the turbine which results in an optimum average power output over the complete PWE cycle.

With a twin chamber system the chamber shape must provide an optimum solution in the situation where water columns are simultaneously rising and falling. Consequently, this situation involves all the air pressure, flowrate and compressibility characteristics of linked chambers. It is difficult, if not impossible, to visualise the resultant effect of chamber shape variation on all these interdependent parameters.

It would seem that in order to comprehend the extent of the problem a heuristic approach is necessary. This could take the form of the initial introduction of a number of chamber shapes to the PWETWO programme and subsequent analysis and discussion of the resulting effects. Such a process would define possible directions in which to proceed but a more efficient method of shape selection must be introduced in order that an optimum can be realized within an acceptable period of time.

In the following sections the very large numbers of parameter combinations and shape possibilities that exist are considered to represent the extent of the respective search spaces in which an optimum solution lies. A method is introduced that enables the negotiation of these search spaces in a far more efficient manner than the parametric test processes of Chapter 6.

9.2 The Search Space

9.2.1 Parameter Combination

In order to facilitate the realization of an optimum combination of ZHCG, PADIFD and ST values it is necessary to reduce the extent of the search space in which an optimum combination may lie. For present purposes this can be achieved by adopting a PWE configuration with identical physical characteristics to that investigated in Test Series 9. The following bounds seem appropriate when the results presented in Chapter 6 are taken into consideration:

Parameter	Lower Bound	Upper Bound	Increment
ZHCG	3.00 m	4.60 m	0.10 m
PADIFD	10,000.00 N/mm ²	26,000.00 N/m ²	250 N/m ²
ST	0.40	2.00	0.05

By introducing the increments shown above to each range of parameter values a search space consisting of 32,768 parameter combinations is created.

9.2.2 The Variation of Chamber Shape

The definition of the extent of the search space when considering an optimal chamber shape is more complex. The parametric testing of a variety of uniform conical shapes would prove relatively simple. However it is highly unlikely that an optimal shape would fall within this limited category. How then should the chamber shape be varied in order to provide the heuristic approach suggested in Section 9.1.2 whilst presenting a realistic opportunity of arriving at a near-optimal form? It must become necessary to adopt a methodology that allows the magnitude of the plan cross sectional area of the chambers to be freely varied at a number of chamber elevations. Such a methodology is fully developed and illustrated in Section 9.4. It is sufficient to indicate here that the introduction of even a limited area variation in the manner outlined above will result in the creation of a search space consisting of several million possible combinations of cross-sectional plan areas.

9.2.3 Negotiating the Search Space

The respective magnitudes of the search spaces outlined in the previous sections each present a daunting multi-dimensional optimization problem possibly involving numerous local optima. To attempt to isolate the optimum solutions using a similar format to that of the parametric tests described in Chapter 6 would represent a formidable task. A possible search process would involve a supplementary computer program that could randomly select parameter/area combinations and assess their performance via PWETWO. The probability of locating a global optimum solution in this manner without excessive testing would be very low. To determine with any certainty whether a particular high performance combination was in fact a global optimum and not one of many local optima would require its comparison to results obtained from many regions of the

search space. The compilation of such a comparative database would prove impractical.

An ideal methodology would involve random selection and subsequent testing in such a manner that those regions of the search space which contain high performance solutions are thoroughly investigated whilst those areas of primarily poor performance solutions receive a less rigorous appraisal.

A number of Evolutionary Design techniques exist in which a combination of random selection, testing, performance rating and subsequent reproduction of high performance solutions allows the development of an optimal path through a multi-dimensional search space. These 'Genetic Algorithms' use the principles of Cumulative Darwinian Evolution to develop successive generations of increasingly high performance solutions. This development progresses in such a manner as to avoid local optima via the introduction of relevant Genetic Operators.

It is suggested that the application of such techniques would provide suitable solutions to the optimization problems outlined in the previous sections. As most readers may be unfamiliar with Evolutionary Design techniques it is first intended to briefly explore their history and background before illustrating their basic methodology by presenting in detail their application to the three parameter combination of Section 9.1.1. It is envisaged that a better understanding of both the evolutionary process and its particular suitability to the optimization problems of the PWE can be promoted in this way.

For those readers already familiar with these Algorithms the optimum parameter combination and optimal chamber shape generated in this manner are presented and discussed in the final two sections of the Chapter.

9.3 History and Background of the Genetic Algorithm

The basic concept of evolutionary design consists of the development of successive generations of cumulative random variations of those parameters which significantly affect the overall design and performance of a system.

This process was pioneered by Professor J. Rechenburg⁴⁷ of the Department of Bionic and Evolution Technology of the Technical University of West Berlin. He has been applying such Cumulative Evolutionary techniques to engineering problems since 1964. His original problem consisted of the evolution of the configuration of a steel plate hinged in five places and placed in a wind tunnel as shown in Fig. 9.1. Each hinge could be set at any one of fifty-one positions. This created a search space consisting of some 345,025,251 possible plate configurations. He used a cumulative evolutionary technique whereby the

optimum configurations of the steel plate (ie those presenting the minimum drag) from an initially randomly selected combination of hinge positions were retained. These high performance plate configurations were then combined in a random manner in order to create the next generation of hinge positions. This process was repeated until the obvious best solution of a flat plate was reached within 300 generations. It is this survival of the best characteristics of each generation of possible combinations and the rejection of those characteristics that do not reach a desired 'fitness' criteria that is the trademark of all successful evolutionary techniques.

Although this original experiment was only of academic significance, similar processes were used by Rechenburg in 1973⁵⁴ to develop a right angled pipe bend with minimum flow resistance; by Schweffelin in 1970 to develop a two-phase supersonic flow nozzle⁴⁸, (the nozzle shape being optimized in order to achieve maximum thrust); and by Hoeffler in 1973⁴⁹ to develop a lattice frame with given loading to a minimum weight criteria. Other structural applications of the Evolution Strategy include those of Lawo and Thieraugh.⁵⁰ The technique has been adopted by several West German companies, namely Shearing for electro-chemical processes; Mercedes Benz and Audi for motor car components and Siemens for fan blades, strip-lighting and electrical switches. The West German Army is also reputed to have used such processes in the development of the Leopard Tank.⁵¹

It is however, in the field of Artificial Intelligence that Cumulative Evolutionary methods are currently showing the greatest potential. Studies at Michigan University have resulted in the development of rule-generating techniques based on Genetic Algorithms for the control of robotic, production-line machinery. These machines, at present, work to continuous sets of rules and tend to malfunction if the tasks they are presented with differ by even a slight degree to those they have been programmed to perform. Evolutionary Techniques allow the breeding of new rules based upon the originals to handle new situations as they occur. If the machine in question encounters a situation that is not recognized by its controlling programme then that programme will commence to develop, implement and assess new rules, rejecting those with a low performance and breeding from those that prove most successful. The high performance rules can also be stored for future reference thereby allowing a degree of 'machine learning' which facilitates the machine's ability to cope with future non-standard situations.

It would appear that it is within this field that the majority of current research involving Evolution Strategy is taking place. However, engineering applications other than those associated with the machine shop have been investigated, two notable examples being the optimization of gas supply and gas pipeline operation

implemented by D. E. Goldberg⁵⁵ and W. Pinebrook's thesis concerning the minimization of drag on a body of revolution⁵⁶.

A current leader in the field of Evolutionary Techniques or 'Genetic Algorithms' as they have now become known, is Professor J. Holland of Michigan University. He has presented a formal framework⁵² representing the Evolutionary Process and it is the methods suggested by Holland that have been adopted in the following optimization exercises.

9.4 Overall Methodology

The inherent strength of an Evolution Strategy when applied to system optimization relies almost entirely upon the concept of cumulative, as opposed to random selection, ie the performance of each combination of parameters is assessed in order to measure its 'fitness' in a particular environment before that combination is allowed to contribute to the production of the next generation of combinations. This concept of Cumulative Evolution is fully explored by Dr. R. Dawkins in the book, 'The Blind Watchmaker'⁵³ wherein the various analogies between the optimization of artificial systems and Cumulative, Darwinian Evolution theory are thoroughly discussed. It is this more general approach combined with Holland's formal framework which can provide an overall understanding of the main processes. It is intended here to provide an outline of the main predominant factors of the natural systems and the methods of simulation that can be utilized to harness their evolutionary powers.

9.4.1 The Natural System

When one considers natural systems of evolution and Darwinian theory it is apparent that the fitness of a particular offspring of any given species is determined by its ability to survive in that environment to which it is subjected. Hence, high fitness individuals are those that carry a more favourable genetic heritage allowing them to cope to a greater degree with those stresses and dangers of that environment. This genetic suitability both increases their survival rate and enhances their reproduction rate thereby ensuring that those genes responsible for their success are further exposed to other gene combinations with either positive or negative results. Constant coupling and reproduction allows a large number of offspring, each with a slightly different genetic structure to be exposed to the environment thereby allowing development (and to a constantly lessening extent, regression) to proceed in a parallel manner from various points within the overall population.

Within a natural adaptive system the controlling factors of the evolutionary process are the characteristics determined by the genes constituting an organism's

chromosomes. Each gene has several forms or alternatives known as alleles which cause variations in the characteristics of a gene by producing enzymes that control chemical reaction rates within a cell. Thus the genes and the enzymes they produce are the major determinants of the cell's form. However, the successful conclusion of a sequence of reactions depends totally upon the presence of all the necessary enzymes, if one is missing then the reaction will not take place. Therefore the affect of one allele is strongly dependent upon those other alleles present. Because of this it is impossible to determine what constitutes a 'good' or 'bad' allele, as one particular allele may provide an excellent result when combined with a particular set of alleles but may prove to be disastrous when combined with others. It becomes necessary therefore to be able to recognize the fitness of co-adapted sets of alleles, ie alleles of different genes which when combined cause an improvement in the performance of the overall organism or that part of the organism to which they directly relate.

It is this chromosome/gene/allele relationship that we wish to simulate in order to harness the natural selection procedure of the evolutionary process. If a reliable computer simulation can be achieved then the process could be significantly accelerated thereby providing a powerful optimization tool with a wide ranging application within the engineering field.

9.4.2 Artificial Systems

Returning to the initial optimization problem outlined in Sections 9.1.1 and 9.2.1; ie the optimization of Turbine Scale (ST), Gate Trigger Levels (ZHCG) and Design Pressure Differentials (PADIFD). The following suitable intervals across practical ranges for each of the parameters have already been established:

Range	Interval	No. of Alternatives
ST 0.4 - 2.0	0.050	32
ZHCG 3.0 - 4.6	0.100	16
PADIFD 10,000-26,000	250	64

In order to represent these parameters in a form directly analogous to the chromosome/gene/allele relationship described in the previous section it is necessary to adopt a binary notation. For instance, an ST value of 1.2 can be represented by the lower bound of 0.4 plus the binary notation (10000), the binary base being equal to 0.05. Similarly in order to achieve a ZHCG value of 4.2 m the increment of 1.2 m needed to be added to the lower bound of 3.0 m can be represented by (1100) where the binary base is equal to 0.1. A PADIFD value of 15,000 N/m² would be expressed by the lower bound of 10,000 N/m² plus the binary representation of 5,000 N/m² namely (010100); the binary base being

equal to 250 N/m². The combination of the variable parts of the three parameters can therefore be represented as follows:

ST	ZHCG	PADIFD
10000	1100	010100

Removing the bounds between each parameter results in the binary string:

100001100010100

This binary string can now be considered to represent a chromosome within which each binary digit or 'bit' can be regarded as a gene whereas the respective value of that gene represents an allele.

Having achieved a mathematical simulation of the natural structure it is now possible to subject this string format to various processes which are analogous to the cumulative selection procedures of the natural systems. This is achieved by applying the following Genetic Operators:

- i) Fitness Proportionate Reproduction.
- ii) Crossover.
- iii) Random Mutation.

9.4.3 The Fitness Proportionate Reproduction Operator

Having discretized the binary coding the first step of the Evolutionary Process is to randomly select a population of chromosomes/parameter combinations in order to create the starting generation. The bit values of this initial generation can be set via a random number generator. Let us therefore assume a starting population of ten chromosomes; a typical randomly selected starting population would therefore be:

Generation 1:

(1)	0	1	0	1	1	0	1	0	0	0	0	1	0	1	0
(2)	0	0	1	0	0	1	1	0	1	1	1	1	1	1	0
(3)	1	0	1	0	0	0	0	0	0	1	0	0	0	1	0
(4)	0	1	1	0	0	1	0	0	0	0	0	0	0	1	1
(5)	0	0	0	1	0	0	1	0	1	0	1	0	1	1	0
(6)	0	0	0	1	1	0	0	0	0	0	0	0	1	0	1
(7)	0	0	1	1	0	1	0	0	0	0	0	1	0	0	1
(8)	0	0	1	1	1	0	1	0	1	0	0	1	1	0	0
(9)	0	0	1	0	0	0	1	0	1	0	1	0	0	1	0
(10)	1	1	1	1	0	1	0	1	1	1	1	0	1	0	1

This population of ten chromosomes represents the following parameter combinations:

	ST	ZHCG (m)	PADIFD (N/m²)
(1)	0.95	3.50	12,500
(2)	0.60	4.40	25,500
(3)	1.40	3.10	18,500
(4)	1.00	3.90	10,750
(5)	0.50	3.60	15,500
(6)	0.55	3.10	11,250
(7)	0.75	3.60	13,000
(8)	0.70	3.90	12,250
(9)	0.60	3.60	14,500
(10)	1.90	4.20	23,250

The programme, PWETWO, can now be used as a tool by the Genetic Algorithm to process each of these chromosomes/parameter combinations and to determine the average power output of the PWE that can be achieved utilizing each combination.

It should be noted at this point that throughout the following Genetic exercises the isentropic version of PWETWO has been used; the average power output achieved after three complete cycles of the PWE being considered representative. This greatly reduces computation time and allows the use of the IBM PC/AT for the smaller population sizes. If the non-isentropic version had been used then up to twenty complete cycles of the PWE would have been necessary to achieve a representative average power output for each of the populations. The

computational time required to process even a small number of populations would have proved far too excessive for the IBM PC/AT.

Utilization of the first generation of chromosomes results in the following average power outputs (POWAV):

- (1) 49.357 kW
- (2) 40.815 kW
- (3) 54.761 kW
- (4) 38.709 kW
- (5) 42.157 kW
- (6) 22.680 kW
- (7) 44.795 kW
- (8) 36.978 kW
- (9) 44.613 kW
- (10) 15.877 kW

It is now necessary to instigate some form of selection procedure which will initially determine the fitness of each of the chromosomes using the above average power outputs. Then, by establishing an appropriate fitness criteria, it must be possible to determine to what extent each should be reproduced in order to contribute to the next generation whilst still retaining a constant overall population size.

This has been achieved by first normalizing the power output results. The curve thus produced can then be categorized, ie those chromosomes producing an average power output with a deviation from the mean of between $-0.75 \times SD$ and $+0.75 \times SD$ will be reproduced once whereas those producing a deviation above the mean of more than $0.75 \times SD$ will be reproduced twice (SD = Standard Deviation of the average power outputs of the chromosomes within each generation). The remainder ($< -0.75 \times SD$) are rejected. In this way a population of reproduced chromosomes remains at a near constant size although with smaller sized populations there can be a slight loss or gain of chromosomes which must be adjusted by a suitable 'topping-up' with high fitness individuals or a more severe cutting back of the lesser fit. To summarise, the initial chromosomes with their respective average power outputs and the resultant fitness reproduction counts are as follows:

Generation 1:

	ST	ZHCG (m)	PADIFD (N/m²)	POWAV (kW)	FRC
(1)	0.95	3.50	12,500	49.357	2
(2)	0.60	4.40	25,500	40.815	1
(3)	1.40	3.10	18,500	54.760	2
(4)	1.00	3.90	10,750	38.709	1
(5)	0.50	3.60	15,500	42.157	1
(6)	0.55	3.10	11,250	22.680	0
(7)	0.75	3.60	13,000	44.795	1
(8)	0.70	3.90	12,250	36.978	1
(9)	0.60	3.60	14,500	44.613	1
(10)	1.90	4.20	23,250	15.877	0

The average power output of this initial generation is 39.074kW with a Standard Deviation of 11.734.

The binary representations of each of the chromosomes can now either be reproduced or rejected depending upon their fitness reproductive count (FRC).

The upper and lower bounds of the variations from the mean can be varied by trial and error to suit any particular optimization problem; In addition the reproduction count need not necessarily peak at two although the problems of retaining a balanced population size increase with maximum fitness reproduction count.

This normalization procedure ensures that there exists a constantly self-adjusting criteria for each successive generation of chromosomes as they gradually improve. To use Rechenburg's terminology each generation creates its own 'evolution window' which ensures overall improvement. There are however pitfalls inherent in this narrowing of the sample size which can lead to premature focussing upon a local optima which will be discussed in the following sections.

9.4.4 The Crossover Operator

The Genetic representation of the duplicated chromosomes is as follows:

(1)	0	1	0	1	1	0	1	0	0	0	0	1	0	1	0
(2)	0	1	0	1	1	0	1	0	0	0	0	1	0	1	0
(3)	0	0	1	0	0	1	1	0	1	1	1	1	1	1	0
(4)	1	0	1	0	0	0	0	0	0	1	0	0	0	1	0
(5)	1	0	1	0	0	0	0	0	0	1	0	0	0	1	0
(6)	0	1	1	0	0	1	0	0	0	0	0	0	0	1	1
(7)	0	0	0	1	0	0	1	0	1	0	1	0	1	1	0
(8)	0	0	1	1	1	0	1	0	1	0	0	1	1	0	0
(9)	0	0	1	1	0	1	0	0	0	0	0	1	0	0	1
(10)	0	0	1	0	0	0	1	0	1	0	1	0	0	1	0

It is now necessary to allow a random interchange of genetic information between these chromosomes in order to create the next generation of possible parameter combinations. This can be achieved by first randomly 'pairing off' the above chromosomes and then randomly selecting 'Crossover' sites for each pair. For example:

No. 8 will exchange genetic information with No. 3 at site 8

No. 1	"	"													No. 6 at site 9
No. 5	"	"													No. 10 at site 1
No. 2	"	"													No. 7 at site 7
No. 4	"	"													No. 9 at site 13

In order to illustrate the manner in which the Crossover operator performs consider two chromosomes A1 and B1 comprising of genes a1 an and b1 bn respectively, i.e.

$$A1 = a1 \ a2 \ a3 \ a4 \ a5 \ a6 \ a7 \ a8 \ a9 \ a10 \ \dots \ a_n$$

$$B1 = b1 \ b2 \ b3 \ b4 \ b5 \ b6 \ b7 \ b8 \ b9 \ b10 \ \dots \ b_n$$

Assuming that site No. 4 has been randomly selected as that site at which crossover will take place between the two chromosomes, all the information contained in the genes to the right of a3 will be exchanged with that contained in the genes to the right of b3 thereby creating two new chromosomes A2 and B2, i.e.:

$$A2 = a1 \ a2 \ a3 \ b4 \ b5 \ b6 \ b7 \ b8 \ b9 \ b10 \ \dots \ b_n$$

$$B2 = b1 \ b2 \ b3 \ a4 \ a5 \ a6 \ a7 \ a8 \ a9 \ a10 \ \dots \ a_n$$

Applying this operator to the randomly paired chromosomes of the illustrative population at the randomly selected sites shown above, results in the following new generation:

Generation 2:

(1)	0	0	1	1	0	1	0	1	1	1	1	1	1	0
(2)	0	0	1	0	0	1	1	0	1	0	0	1	1	0
(3)	0	0	1	1	0	1	0	0	0	1	0	0	0	1
(4)	1	0	1	0	0	0	0	0	0	1	0	0	0	1
(5)	1	0	1	0	0	0	0	0	0	1	0	0	0	1
(6)	0	0	1	0	0	0	1	0	1	0	1	0	0	1
(7)	0	1	0	1	1	0	0	0	0	0	0	0	0	1
(8)	0	1	1	0	0	1	1	0	0	0	0	1	0	1
(9)	0	1	0	1	1	0	1	0	0	0	0	1	1	1
(10)	0	0	0	1	0	0	1	0	1	0	1	0	0	1

Subjecting the parameter combinations represented by these chromosomes to processing via PWETWO and Fitness Proportionate Reproduction results in the following average power outputs and reproduction counts:

	ST	ZHCG (m)	PADIFD (N/m ²)	POWAV (kW)	FRC
(1)	0.75	3.60	25,500	55.754	2
(2)	0.60	4.40	13,000	25.409	0
(3)	0.70	3.90	18,500	60.723	2
(4)	1.40	3.10	12,250	58.511	2
(5)	1.40	3.10	18,500	54.760	1
(6)	0.60	3.60	14,500	44.613	1
(7)	0.95	3.10	10,750	36.802	0
(8)	1.00	4.30	12,500	36.561	0
(9)	0.95	3.50	13,500	54.323	1
(10)	0.50	3.60	14,500	37.585	1

The average power output for this generation is 46.504 kW with a Standard Deviation of 11.936 (cf 39.074 kW and 11.734 of the first generation). It is useful at this stage to consider the analogy put forward by D. E. Goldberg⁵⁵ in partial explanation of how the Crossover Operator provides much of the Genetic Algorithm's power. He suggests that one should view each of the chromosome

strings as complete ideas or prescriptions of how to perform a task whereas the substrings transferred during crossover can be considered to contain notions of what is important or relevant to that task. The population of each generation therefore becomes a body of knowledge containing a multitude of notions. Performance Related Reproduction followed by Random Crossover combines various high performance notions to form new ideas which themselves will undergo performance testing. This analogy is represented in a more formal manner by the concept of schemata as described in Section 9.4.6.

9.4.5 The Random Mutation Operator

The function of the Random Mutation Operator is that of a rearguard action to ensure that any potentially useful information discarded via the Reproduction and Crossover Operators has a probability of being recovered and reintroduced into any current generation of chromosomes. This is achieved by randomly selecting a site/sites within the population after the introduction of the Crossover Operator and changing the value (ie allele) of the gene at that site from a 0 to a 1 or vice versa. It is this reintroduction of a lost allele to the current population that may allow the adaptive plan to escape a false peak as once an allele has been lost from a population there is no way that the Crossover Operator alone can replace it.

9.4.6 Schemata

Before continuing the optimization exercise it is worth pausing to consider the results of Fitness Proportionate Reproduction and subsequent Crossover in order that the concept of co-adapted alleles (see Section 9.4.1) and their artificial system's counterpart, Schemata, can be fully appreciated. A thorough understanding of the Genetic Algorithm's search technique can only be achieved via this appreciation.

In order to familiarize oneself with the basic concept of schemata it is first worthwhile to consider how an optimal route through a multi-dimensional search space can best be negotiated. Taking the optimization problem currently being considered, there will naturally exist within the search space regions of poor performance parameter combinations/chromosomes and regions of high performance combinations. Due to the extensive nature of the search space it is essential that most effort be expended searching the more promising regions. This is achieved via the processing of schemata (hyperplanes) which cut through and partition the search space in such a way that the search effort proceeds in a near-optimal manner. It is intended to adopt a slightly more formal approach to describe the manner in which the Genetic Algorithm utilizes and processes schemata. It is left to the reader however, to familiarize him/herself with the

detailed analyses of Genetic Algorithm behaviour to be found in the relevant works of Holland,⁵² De Jong,⁵⁷ and Bethke.⁵⁸

What are schemata? Bethke defines a SCHEMA (hyperplane) as a subset of the binary strings (chromosomes) of length, L , consisting of all the binary strings which match a specified pattern, h .

This definition can be satisfactorily illustrated by noting string similarities present in Generation 2 of our example. If chromosome 2.1 and chromosome 2.3 are compared the following similarity becomes evident:

$$h_1 = 0011****0*1****10$$

The asterisk represents a 'don't care' ie the value (allele) of the gene at the position denoted by * does not affect the overall fitness of the schema. As the mean average power output of the two chromosomes that are represented by this schema is equal to 58.239 kW then it would be reasonable to assume that this schema is of a relatively high fitness. It may help to visualize this schema as a hyperplane cutting through the search space and containing such chromosomes as:

```
001111101111110
001101000100010
001100101100010
etc.
```

Following chromosomes 2.1 and 2.3 through the Fitness Proportionate Reproduction process reveals that they both qualify for a reproduction count of 2. This ensures that the high fitness schema, h_1 , will be reproduced four times. Fitness Proportionate Reproduction therefore is directly responsible for the exponential growth of good schemata and thereby offers them a high allocation of trials. On a more formal footing let the reproduction count of a chromosome be simply represented by u/\hat{u} where u is equal to the average power output achieved by a chromosome and \hat{u} is the mean average power output of that population of chromosomes. It follows that for any schema, h , there exists $m(h,g)$ such schemata present in the population of a current generation, g . If, therefore, $u(h)$ represents the mean average power output of those chromosomes within the population containing the schema, (h) , it would be expected that there would exist $m(h,g) \times u(h)/\hat{u}(g)$ schemata, h , present within the population after reproduction.

Two other properties of schemata identified by Bethke are schema order, $o(h)$, and defining length, $d(h)$. The order of a schema is a measure of the specificity of the schema and is defined as the number of significant values present within that

schemata the number of gene positions with a value of 0 or 1. The defining length of a schema is the difference between the first gene position carrying a significant value and the last gene position carrying a significant value. It can therefore vary between 1 and (L-1). The schema h_1 is of the order 8 and of a defining length equal to 14. Consider however

the following schema:

$$h_2 = \text{*****010}$$

This would be of an order of 3 and a defining length of 2. We can consider h_1 and h_2 to represent long and short schemata respectively.

Having established the basic concept of schemata it is now possible to perceive that the initial, randomly selected population of generation 1 represents a vast database of information contained within schema of greatly differing length and order. As each gene within a chromosome can either possess a value of 0, 1 or 'don't care' the number of schemata present within that binary string must be equal to 3^L . Therefore the number of schemata present in a population consisting of N strings is equal to $N \times 3^L$ which, in the case of our illustrative population, is equal to 143,489,070. This represents a far greater search space than that represented by the 32,768 parameter combinations of Section 9.2.1. It is the processing procedure of the Genetic Algorithm with the exponential growth of good schemata and near optimal allocation of trials that causes a rapid convergence on a global optimum whilst ensuring that a significant number of options representing the complete spectrum of the search space have been tested.

How then does the Crossover Operator perform without badly disrupting the allocation of trials to good schemata? The defining length, $d(h)$, is the significant factor where the Crossover operator is concerned. As crossover depends upon the random selection of sites, short length schemata tend to remain unaffected. Consider the short length schemata, h_2 , there are 12 out of a possible 15 crossover sites that will ensure the survival of the schema whereas schema h_1 can only survive if crossed with a chromosome containing an identical schema. Therefore a conservative estimate of crossover survival probability is equal to

$$1 - (d(h)/(L-1)).$$

The Crossover Operator therefore badly disrupts the allocation of trials to long-definition schemata. It can, however, generate new instances of schema already present in the population as well as creating new schemata thereby supplying a structured, though randomized information exchange between chromosomes.

The probability of the Random Mutation Operator altering the value of a significant bit of a schema is dependant upon the order, $o(h)$, of the schema. This operator is more likely to disrupt the allocation of trials to high order schemata than to those of a low order. As the probability of mutation, p_m , is fixed within the algorithm the probability of a schema surviving intact is $(1-p_m)^{o(h)}$ or where $p_m \ll 1$ this probability can be approximated by $(1-(o(h) \times p_m))$. Taking the three Genetic Operators into account it is now possible to calculate the number of schemata, h , that can be expected to survive into the subsequent generation. This is simply the product of the expected number from reproduction alone and the survival probabilities of crossover and mutation.

$$\text{ie. } \frac{m(h,g+1) = m(h,g) \times u(h,g) \times (1-d(h)) \times (1-(o(h) \times p_m))}{\hat{u}(g) \times (L-1)}$$

To summarize, it is now evident that short schemata are allocated trials at a near-optimal rate whereas longer schemata are sampled correspondingly less frequently. Holland, recognizing the importance of these low-defining length schemata referred to them as 'Building Blocks' thereby indicating how the multiple testing and recombination of short length, high-performance schemata rapidly leads to the formation of equally high-performance chromosomes.

Holland has estimated that approximately N^3 schemata are tested in parallel during each generation of the adaptive plan. Therefore 1000 schemata are processed at each step of our illustrative 10 chromosome population. This simultaneous handling of schemata without any attempt to store, manipulate or recognize past schemata is termed 'implicit parallelism' by Holland; the processing of the schemata of a current generation implicitly involving the information processed in all preceding generations.

9.5 The Optimization of the ZHCG, PADIFD and ST Parameter Combination

The Evolutionary process described in the previous sections was implemented on the IBM PC/AT by a program developed in Fortran 77. This program, PWEVO, implements the Genetic Algorithm and utilizes PWETWO (renamed PWEVOL) as a subroutine. An outline of the program with its various subroutines is illustrated in the flow diagram of Fig. 9.2.

Initially the Random Mutation Operator of Section 9.4.5 was omitted as its significance was not fully appreciated. It soon became apparent however that without this Operator the algorithm would rapidly converge on a sub-optimum parameter combination. This was due to the small population of only 10

chromosomes being introduced to the algorithm. Unfortunately, it was necessary to keep the population as small as this in order to reduce computing time. Such small populations restrict the size of the genetic information database of the initially randomly selected population. Furthermore it amplifies the tendency of the Fitness Proportionate Reproduction Operator to reject useful genetic information. Consequently, within a very few generations the number of competing schemata within the population dramatically falls. The usefulness of the Crossover Operator then becomes seriously limited as the information being exchanged is very similar. Without the Random Mutation Operator no new genetic information is available and the algorithm becomes trapped with a sub-optimum solution.

This is illustrated by the 'No RM' curve of Fig. 9.3. After only 10 generations a sub-optimum average power output of 62.43 kW is achieved from the following parameter combination:

$$\text{ZHCG} = 3.10 \text{ m} \quad \text{PADIFD} = 18,500.00 \text{ N/m}^2 \quad \text{ST} = 0.75.$$

It was apparent that this was not the true optimum solution as slightly higher average power outputs had been achieved by individual chromosomes in previous generations. Unfortunately these high performance chromosomes had been destroyed during crossover.

A choice of Random Mutation probabilities ranging from zero to 0.1 were therefore offered to the program operator via PWEV0. As the population consisted of 150 genes a probability choice of 0.01 resulted in the value of one randomly selected gene being changed per generation. The result of such a selection can be seen from the relevant curves of Figs. 9.3 and 9.4. The disruption of the Standard Deviation of successive populations due to the possible introduction of a new competing schemata at each generation becomes more apparent as the algorithm approaches convergence. This disruption allows the algorithm to proceed to the seventeenth generation before converging upon an a near-optimum average power output of 63.30 kW with the following parameter combination:

$$\text{ZHCG} = 3.1 \quad \text{PADIFD} = 15,750.00 \text{ N/m}^2 \quad \text{ST} = 1.0.$$

This average power output was further improved upon by introducing a Random Mutation probability of 0.1. This meant that 15 randomly selected genes of each generation were subjected to a change of value. Radical disruption of the chromosome populations is evident from the high Standard Deviations of the first fourteen generations. However, the algorithm has identified the high performance area containing the optimum by this time and the 'evolution window' has sufficiently narrowed to ensure a thorough testing of those parameter

combinations lying within this region of the search space. The algorithm continued for a further fifteen generations negotiating this optimum region whilst constantly introducing fresh genetic material via the Random Mutation Operator. It finally converged upon an optimum average power output of 63.37 kW. The relevant

parameter combination was:

$$\text{ZHCG} = 3.60\text{m} \quad \text{PADIFD} = 18250.00\text{N/m}^2 \quad \text{ST} = 0.85.$$

As further increases in Mutation probability and population size failed to improve upon this parameter combination and its resulting average power output it is considered reasonable to assume that it represents the optimum solution.

9.6 The Evolutionary Design of the Chamber Shape

9.6.1 Methodology

The introduction of variable plan areas at selected chamber elevations was initially discussed in Section 9.2.2. In order to minimize the effect of such variations on the stability of the mathematical model in its present form, a twin, square chamber configuration was adopted in the following tests. This can be considered to represent the least complex twin chamber configuration of PWETWO as it does not include the modelling of the chamber vortices. Further simplification was achieved by adopting the isentropic option and allowing the two sluice-type gates of each chamber to be controlled by a single upper gate trigger level, ZHCG.

By allowing the chamber roof elevation (ZT) to be equal to 5.6 m and introducing nodes at 200 mm centres between it and the downstream water surface elevation (EDC=2m) eighteen positions were established where the plan cross-sectional area of the chambers could be varied. Again to avoid model instability an upper and lower bound of 28 m² and 12 m² respectively was applied to these plan cross-sectional areas. The resolution of any such variation was set at 0.25 m². Suitable gradients are calculated between the areas at successive nodes to ensure the chamber width and length expand or contract in a uniform manner. This scenario is adequately illustrated by the chamber profile of Fig. 9.5.1. The controlling Genetic Algorithm also ensured that the plan cross-sectional areas of each chamber varied in an identical manner.

The remaining PWETWO parameters were set as follows:

<u>Upstream Channel:</u>		<u>Upstream Gates:</u>	
CMUC	= 1.0	CUCG	= 0.6
BUC	= 10.0 m	BUG	= 4.4 m
EUC	= 5.0 m	TUG	= 2.0 s
		ZHCUG	= 4.1 m
<u>Chambers:</u>			
B (below 2.0 m elevation)		= 4.472 m	
L (below 2.0 m elevation)		= 4.472 m	
PADIFD	= 17000.00 N/m ²		
ST		= 1.00	
<u>Downstream Channel:</u>		<u>Downstream Gates:</u>	
CMUC	= 1.0'	CUCG	= 0.6
BUC	= 10.0 m	BUG	= 4.4 m
EUC	= 2.0 m	TUG	= 2.0 s
		ZHCUG	= 4.1 m

Table 9.1

The 0.25 m² resolution of the area variation creates 64 possible plan cross-sectional areas between the upper and lower bounds of each of the eighteen nodes. This results in a search space consisting of 3.245×10^{32} possible area combinations each representing a different chamber shape. Each plan cross-sectional area was represented by a six-bit binary form and population size was set at 10 area combinations/chromosomes. A Random Mutation probability of 1% was introduced (ie ten gene values were mutated in each generation). Two complete cycles of PWETWO were run for each chromosome.

The resulting evolution of the chamber shape can be seen in Figs. 9.5.1 to 9.5.6. Fig. 9.5.1 represents the worst case average power output of the randomly selected starting population. The subsequent shapes are those resulting in the average power output most similar to the mean average power output of that particular generation. The final chamber shape of Fig. 9.5.6 provided the highest average power output of the exercise. Improvement between successive generations at this point had become minimal, the maximum average power output alternately rising and falling about a 89.0 kW average. It was therefore

decided to terminate the programme and to accept that the 89.8 kW output represented a maximum and that an optimal chamber shape had been achieved.

The actual shape in which the chamber air volume above the maximum chamber water level is presented has no significance with regards to the present mathematical model. It is merely treated as a compressible volume of air. It is therefore possible to idealize the chamber shape containing this volume without unduly affecting the average power output. By selecting suitable cross-sectional areas for those nodes above the maximum chamber water surface elevation the air volume contained in the complex shape of Fig. 9.5.6 can be closely approximated. The resulting chamber shape with an average power output of 89.6 kW is shown in Fig. 9.6.

9.6.2 Discussion

In order to provide a comparison, identical parameters to those of Table 9.1 were introduced to a further chamber shape via PWETWO. To distinguish between the two systems in the following discussion the optimum variable plan area configuration of the previous section will be termed the VCA system (Variable Chamber Area) whereas the newly introduced configuration will be termed the UCA system (Uniform Chamber Area).

The chamber plan cross-sectional area of the UCA remained at a constant 20 m² irrespective of elevation. This particular area represents the mean of the range of variation of the plan areas of the VCA system. It is interesting to note that the total air volume between the starting elevations of the two water columns of the UCA system and their respective chamber roofs is very similar to that of the VCA system (see Table 9.2).

The most significant region of the pressure differential curves of Fig. 9.7 is region A. It is within this region that the increased energy output of the VCA system results in the improvement in average power output evident from Table 9.2. In order to understand how this increased output is achieved it is necessary to consider the air volume available to both the VCA and the UCA.

The Working Air Volume of each system is that volume between the minimum chamber water level and the maximum chamber water level. Using this volume the following comparison can be made:

	UCA	VCA
Working Air Volume:	34.14 m ³	37.12 m ³
*Turbine Air Volume:	68.27 m ³	74.24 m ³
Average Air Flow Rate:	7.41 m ³ /s	7.65 m ³ /s

*Turbine Air Volume = Volume of air passing through the turbine during a complete cycle.

From this comparison it is reasonable to assume that the improved average power output is primarily due to an increased average air flow rate through the turbine. However, one should also take into consideration the manner in which the air flow/pressure differential regimes of each system utilise the Design Pressure Differential relationship of Section 5.3. Upon relating the curves of Fig. 9.7 to the efficiency curve of Fig. 5.3 it becomes apparent that the turbine of the VCA is operating at an efficiency greater than 70% for approximately 80% of its cycle whereas the UCA turbine can only maintain such efficiencies for a period equal to 65% of its cycle time. The resulting increase in instantaneous power outputs produces a 12.6% increase in the energy harnessed per cycle (see Table 9.2). However, the significance of this increase is reduced by a longer cycle time caused by an 8.8% increase in swept volume (swept volume = Working Air Volume). The overall result is a 6.9% increase in average power output.

	VCA System	UCA System
Total air capacity of chambers	61.355 m ³	59.397 m ³
Average power dissipated over cycle	302.0 kW	300.8 kW
Energy harnessed during cycle	870.4 kW	772.8 kW
Average power output	89.64 kW	83.86 kW
Volume of water discharged	99.6 m ³	94.1 m ³
Swept volume of Chambers	74.2 m ³	68.2 m ³
Leakage	25.0%	27.5%
Hydraulic flow rate	10.26 m ³ /s	10.22 m ³ /s
Overall efficiency	29.7%	27.9%
Cycle time	9.71s	9.21s

Table 9.2

The hydraulic flow rates through the two systems are very similar. This indicates that, in the case of the VCA, a greater volume of water must enter and leave the chambers during those periods in which the upstream and downstream gates are simultaneously open (see Section 6.2.4) in order that the greater swept volume

can be accommodated. Straight through leakage is therefore reduced as shown by a fall in leakage percentage and an increase in overall system efficiency.

The shape of the VCA and the resulting flow regime may also, to some extent, be optimizing the relationship between the capacity of the chambers subjected to the incompressible water flow and the capacity of the chambers subjected to the compressible air flow. The air volume above a UCA chamber in which the water level is at its maximum elevation is 5% larger than the air volume above a VCA chamber in the same situation. As the water level falls in the chambers of both the VCA and the UCA systems so the air pressure above it decreases with a corresponding fall in air densities. The larger the air volume present the greater the relative expansion. This resulting expansion of the air is therefore greater in the case of the UCA system. This means that the falling water column of the UCA system must pass through a greater distance than that of the VCA in order to generate a similar negative air pressure within its second chamber. This would suggest that a higher percentage of the potential energy of the initial differential head between the chamber water levels and the downstream water levels is wasted in providing the necessary work to cause the increase in volume.

A useful analogy can be applied by regarding the airspace above the falling water columns as a spring and the volume of the space as a measure of the springs stiffness ie the greater the volume the less stiff the spring. The less stiff the spring the greater its extension under a given load; the greater the extension of the spring the lower the elevation of the load and the less its potential energy.

To summarize, the Evolutionary Design process has optimized the chamber shape of the PWE in a manner in which the resulting air flow/pressure differential regime better utilizes the Design Pressure Differential relationship of Section 5.3. This ensures a better overall performance over a complete PWE cycle. An improved relationship between the incompressible water flow and compressible air flow within the chambers may be a contributory factor to this better overall performance.

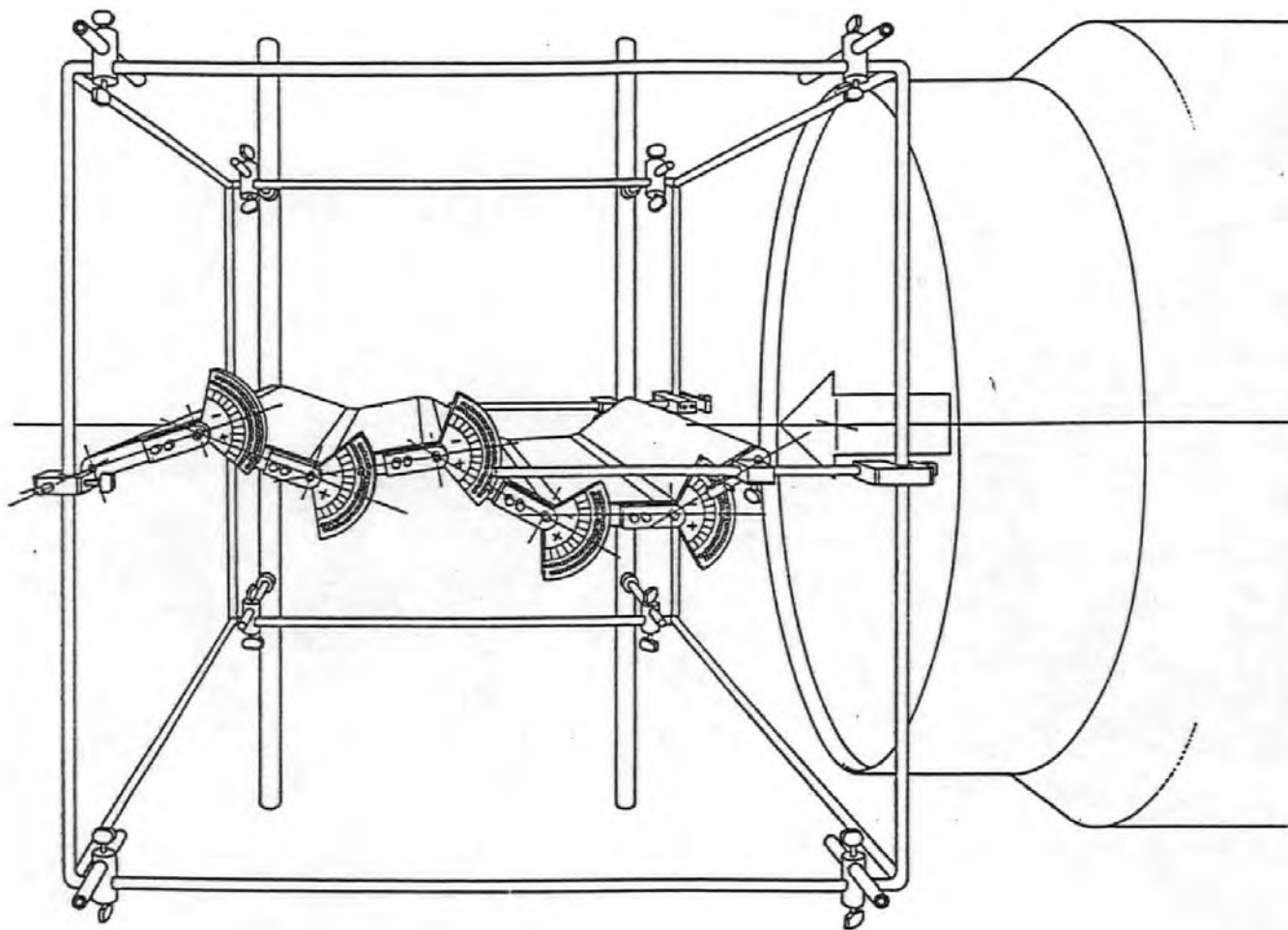


FIG. 9.1: The articulated plate: The experimental device was created to imitate Darwinian evolution in a wind tunnel.

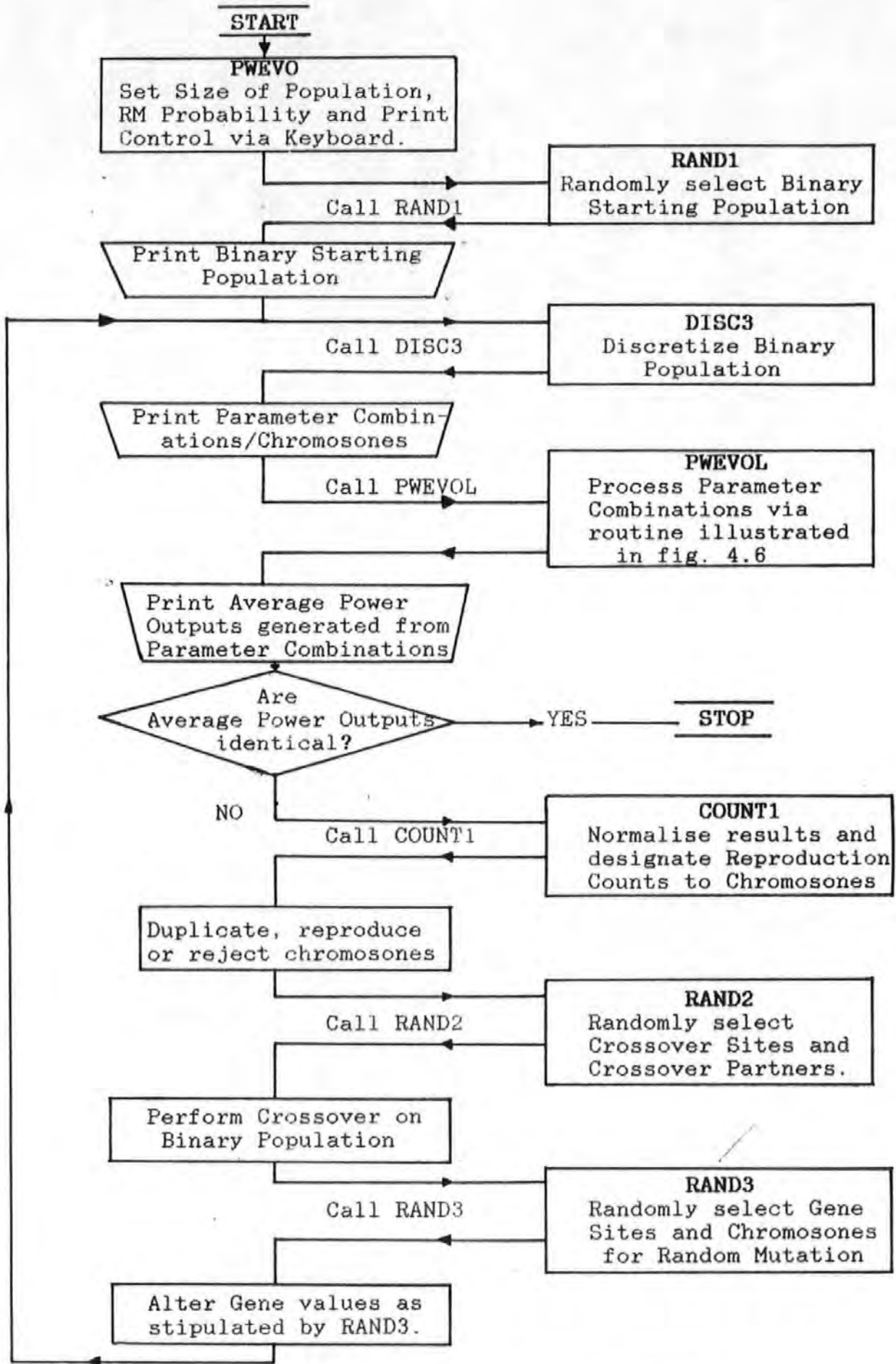


FIG. 9.2: FLOW DIAGRAM FOR PWEVO

FIG. 9.3: MEAN AVERAGE POWER OUTPUT
OPTIMIZATION OF ZHCG, PADIFD AND ST

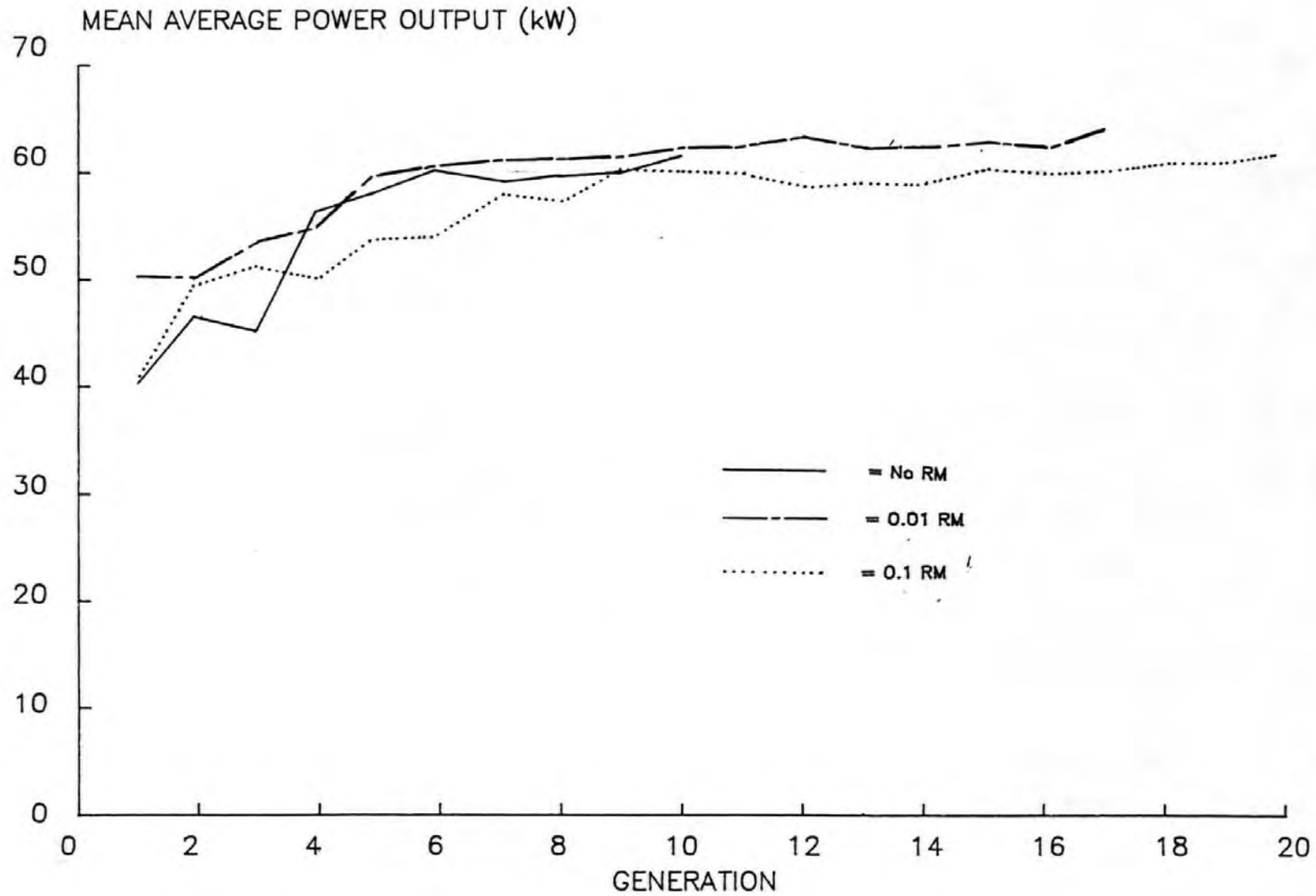
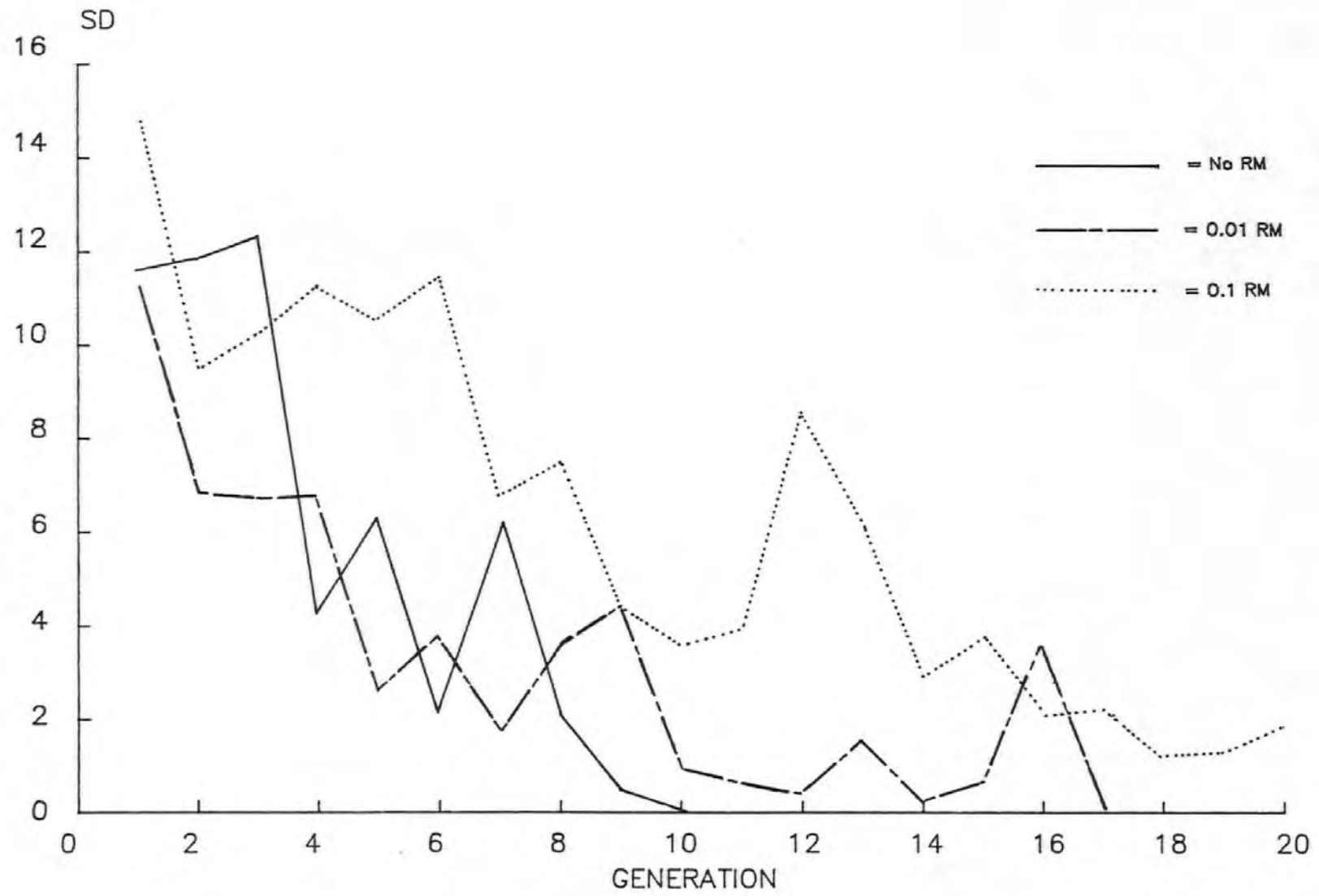
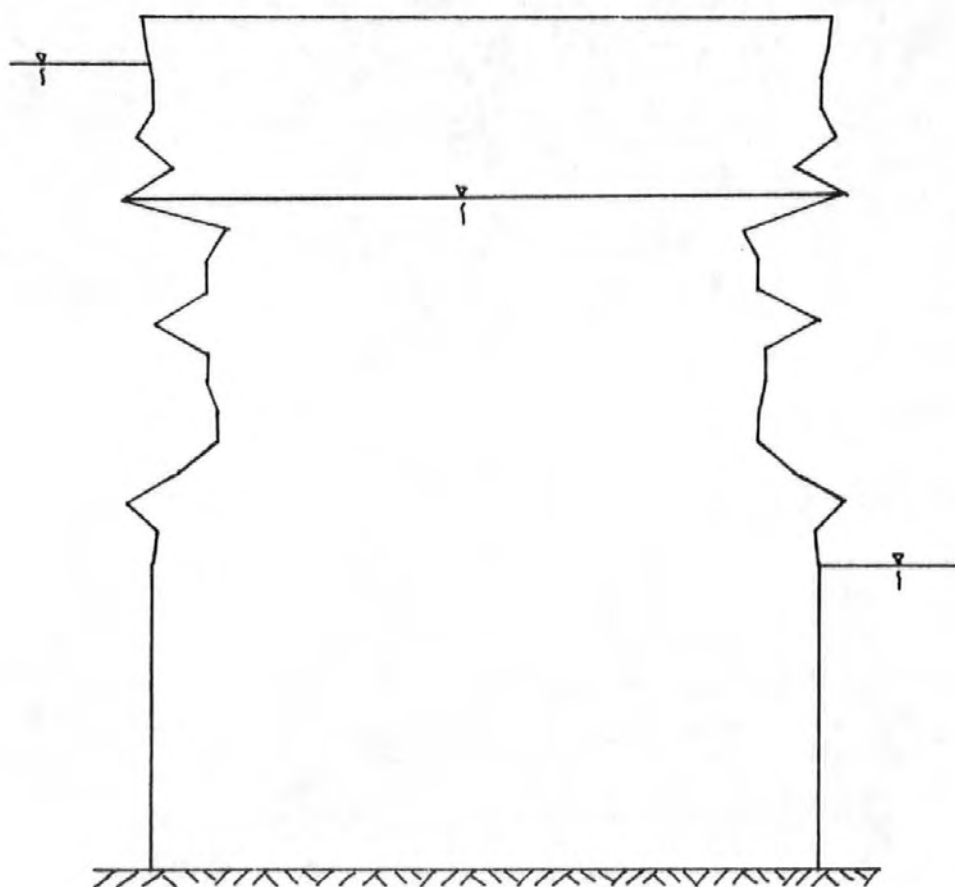


FIG.9.4: STANDARD DEVIATION
OPTIMIZATION OF ZHCG, PADIFD, AND ST



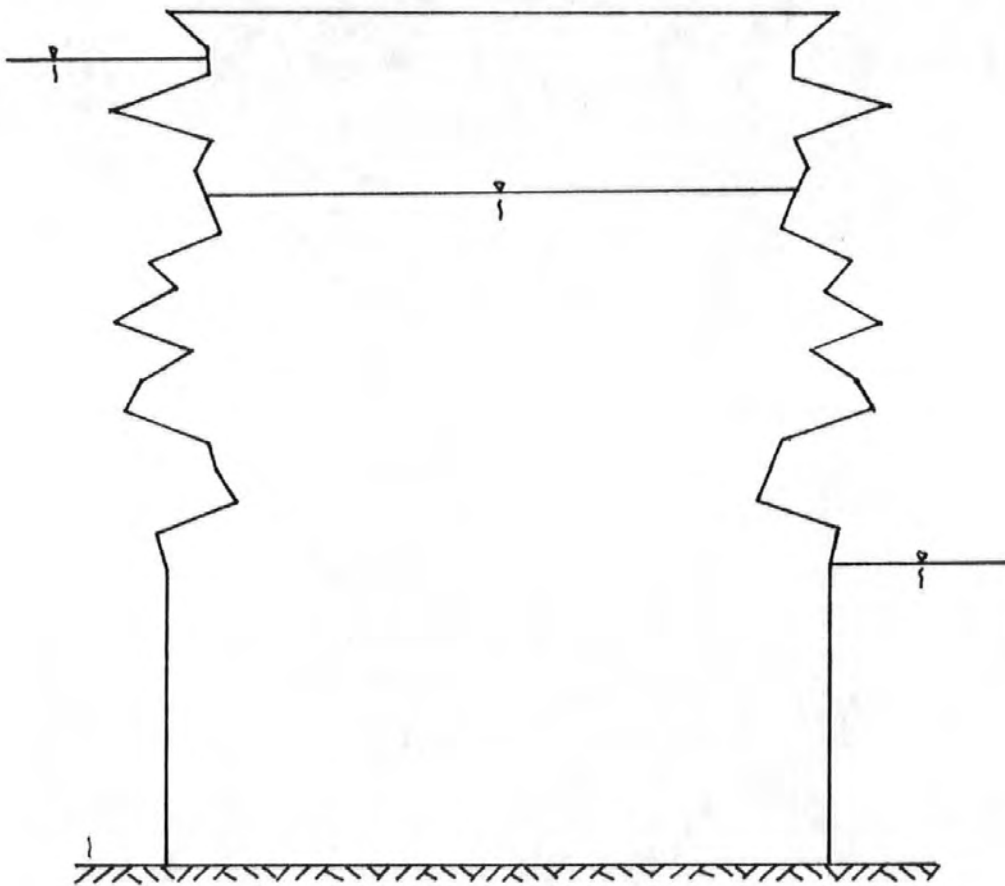
GENERATION 1



AVERAGE POWER OUTPUT = 79.70 kW

FIG. 9.5.1

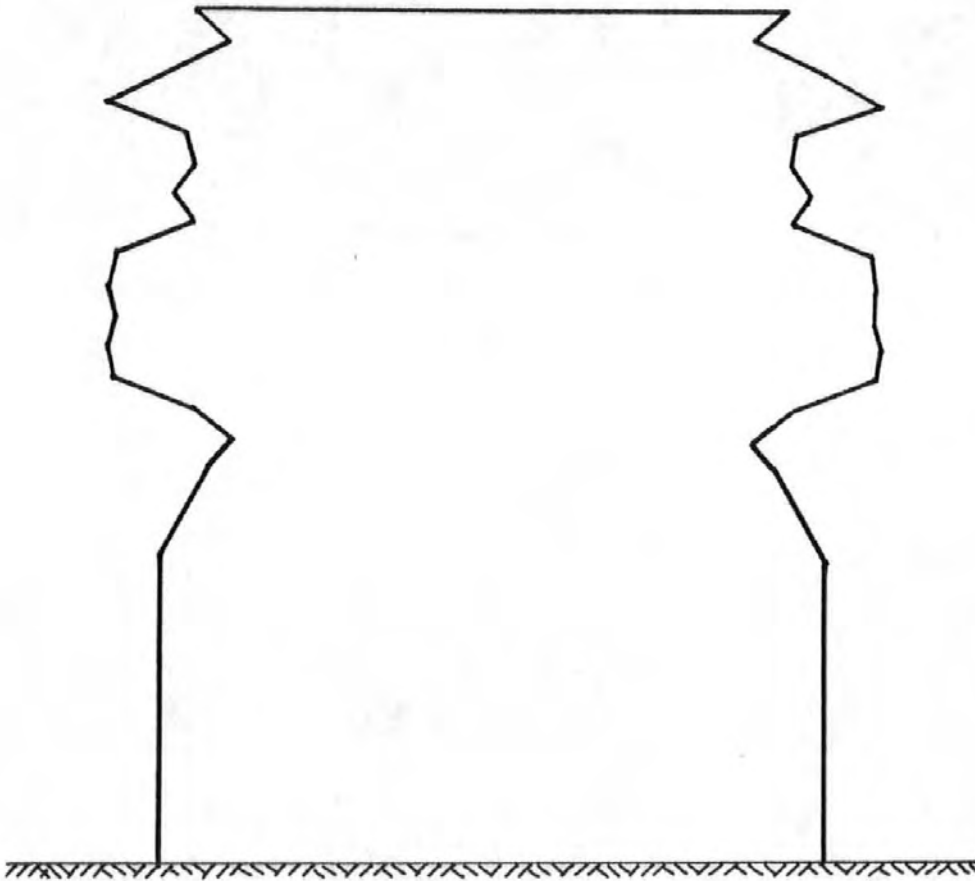
GENERATION 5



AVERAGE POWER OUTPUT = 85.70 kW

FIG. 9.5.2:

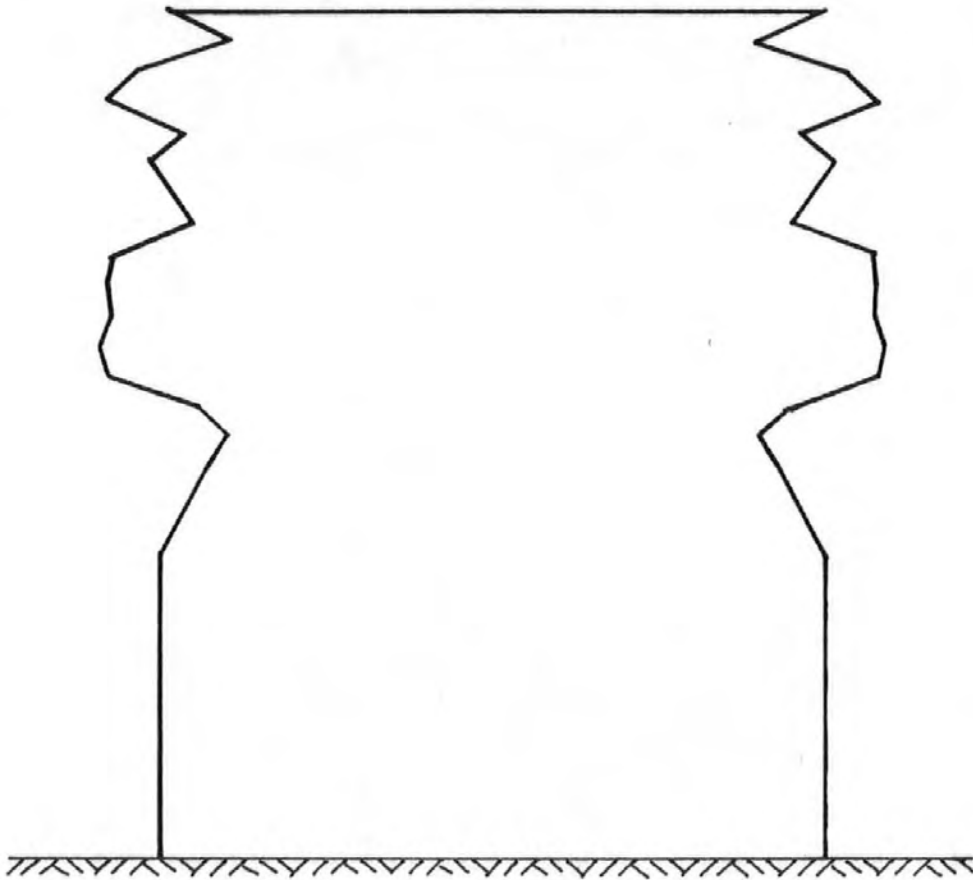
GENERATION 10



AVERAGE POWER OUTPUT = 88.71 kW

FIG. 9.5.3

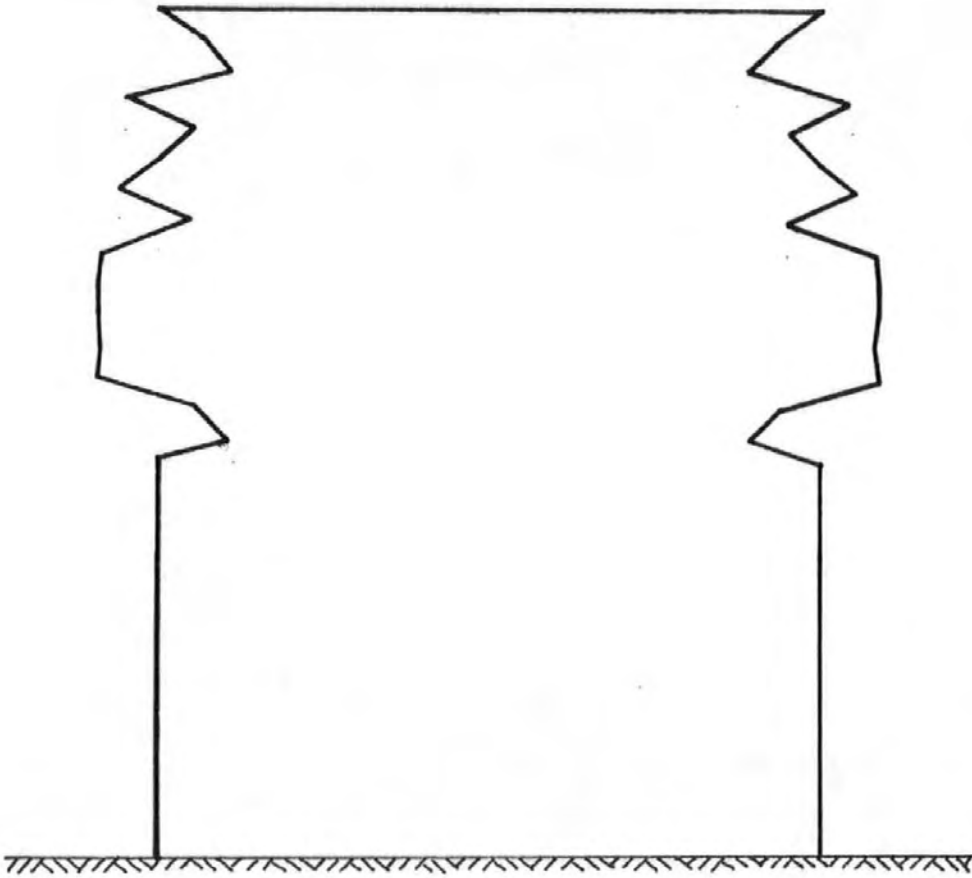
GENERATION 20



AVERAGE POWER OUTPUT = 89.09 kW

FIG. 9.5.4

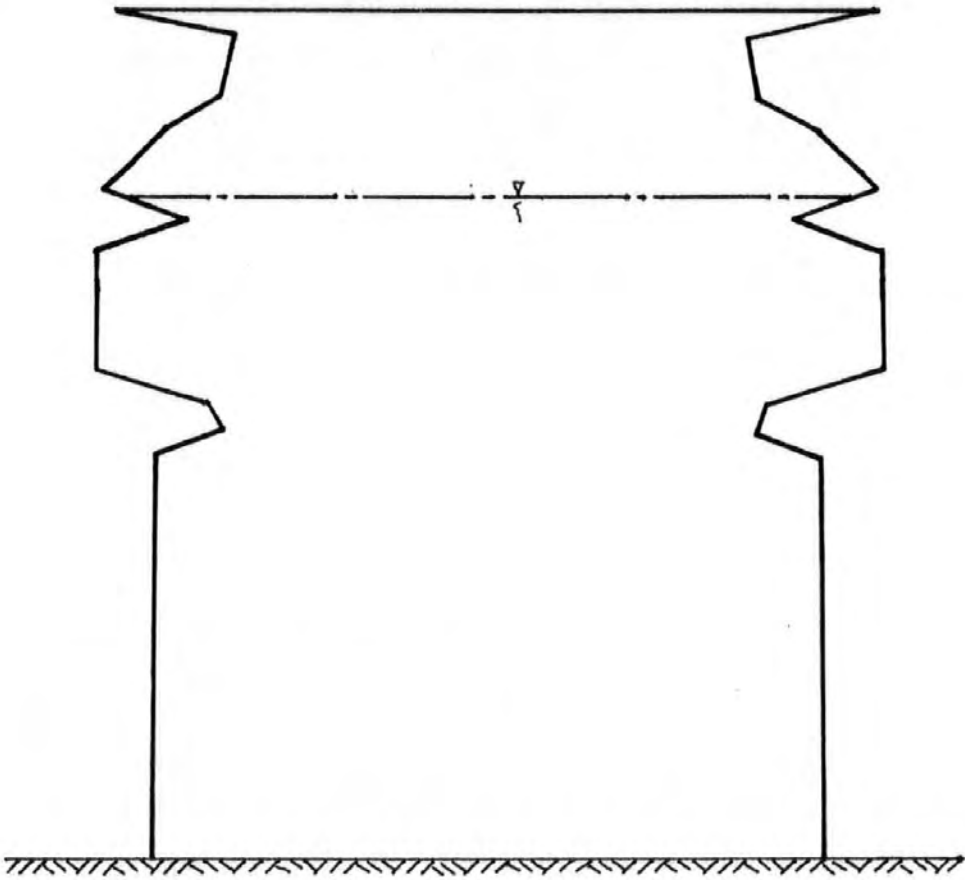
GENERATION 50



AVERAGE POWER OUTPUT = 89.69 kW

FIG. 9.5.5

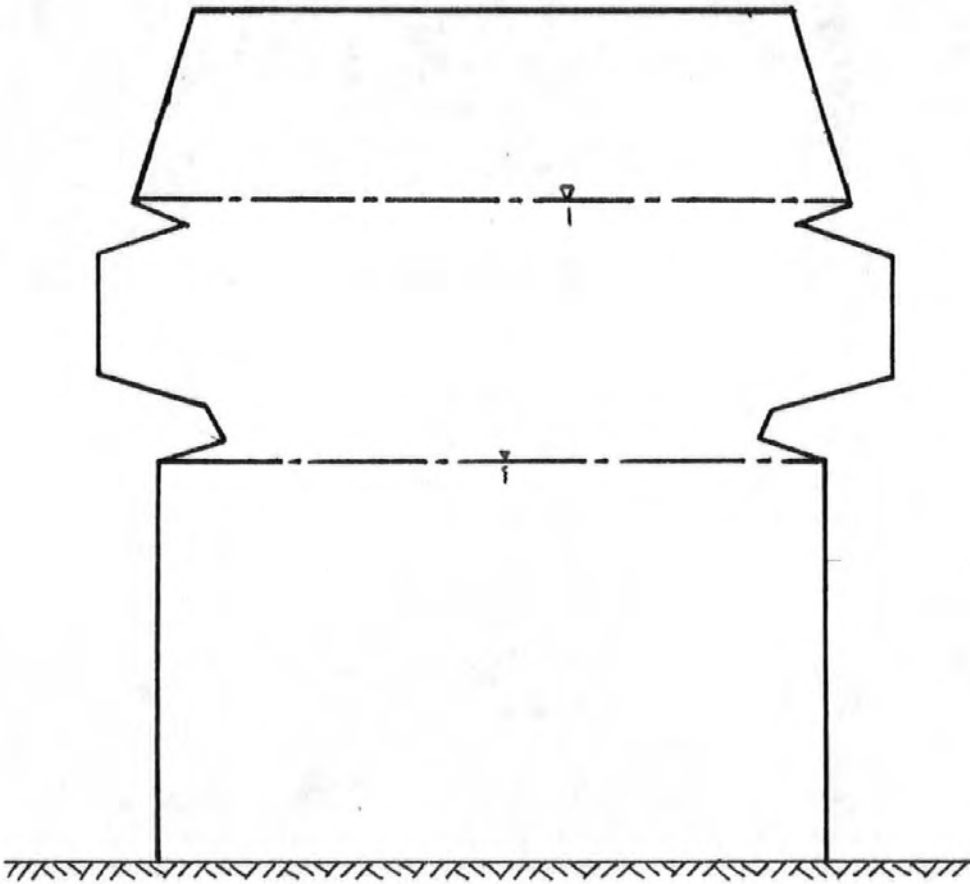
GENERATION 110



AVERAGE POWER OUTPUT = 89.88 kW

FIG. 9.5.6

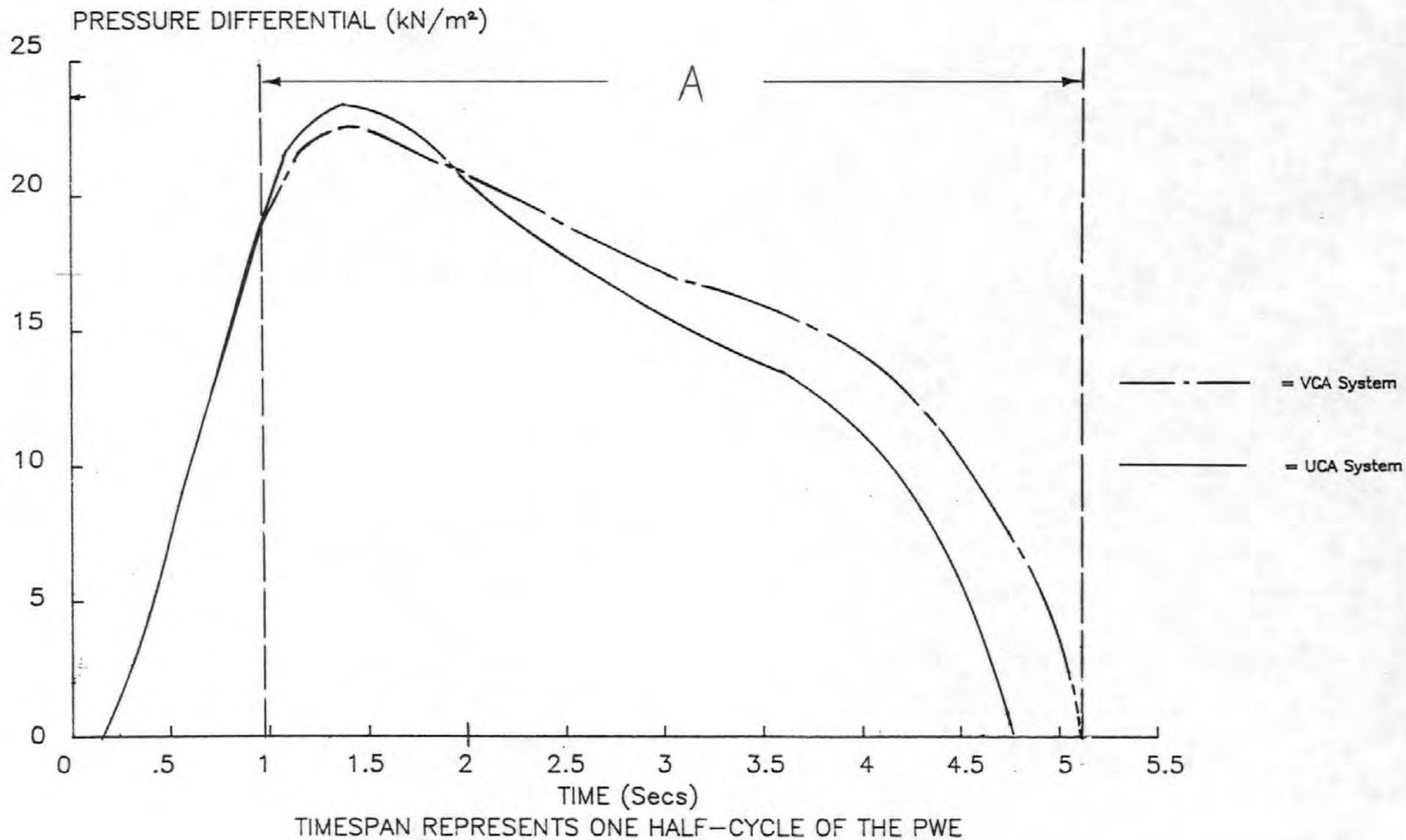
IDEALIZED AIRSPACE



AVERAGE POWER OUTPUT = 89.64 kW

FIG. 9.6

FIG. 9.7: PRESSURE DIFFERENTIALS
UNIFORM PLAN CSA VERSUS VARIABLE PLAN CSA



10.0 : CONCLUSIONS

10.1 Introduction

To conclude the study a summary of the contents of each chapter is presented and those aspects of the study considered to be of most significance are discussed. Firm conclusions will be drawn wherever possible and areas requiring future study are recognized and briefly explored. The thesis is finally brought to a close by an overall appraisal of the pneumatic hydropower systems in which their relationship to other hydropower devices is discussed and their development potential investigated.

10.2 Initial Concepts

The requirement and possible potential for a commercially viable method of harnessing energy from low-head hydraulic sources was established in Chapter 1. The state of the art of the development of both conventional and non-conventional methods of achieving such an energy capture was thoroughly investigated.

The Design Criteria of Chapter 2 provided the framework around which the design of a pneumatic hydropower device could be established. Adherence to this criteria led to the immediate dismissal of a number of concepts which were inherently weak. This allowed a greater effort to be expended upon those systems outlined in the chapter, in particular the twin-chamber, butterfly gated system shown in Fig. 2.3. This system conformed to the criteria to the greatest extent and was to become the predominant system throughout the remainder of the research project.

Subsequent parametric testing, costing and economic assessment has shown the butterfly gated system to be the most promising system in commercial terms. This would suggest that the selection procedure instigated by the design criteria represents a valid basic methodology for the successful outline design of a PWE system.

It was the complicity with the design criteria and the possibility of achieving a flow-assisted gate action that led to the extensive, small-scale laboratory testing of the butterfly gated system. The logical progression of the development of the flow-actuated gate depended to a large extent upon the observation of the flow characteristics of the system. This observation led to a greater understanding of the operation of the models and resulted in their development from the simple truncated representation of Section 3.2 to the fully adjustable models of Section 3.3.2.

The tests can be considered to have proved the basic feasibility of a flow-assisted gate and the resulting information from the complete series has been sufficient to support a successful patent application. The tests have also shown that the chambers need not be entirely circular in plan and that the gate height need not be uniform along its entire length.

Further laboratory testing of a model at a scale of around 1:5 would be desirable. The design detail of the flow-actuated gate could be finalised at this stage and monitoring and refinement of the "stepped" gate design of Section 3.6 could also take place. The effects of friction, surface tension and viscosity would be negligible at this larger scale.

Pneumatically operated gate latches as described in Section 3.3.5 would be introduced on this larger model. Their operation would be controlled by chamber water levels and the effects upon gate speed, chatter and leakage as well as the effects upon overall performance would be monitored. Variation in chamber shape based upon the optimisation process of Section 9.6 could also be considered at this stage.

It is suggested in Section 10.7.4 that the PWE may be best suited to an estuarial, tidal situation. In this case further modelling of the non-circular barrage chambers of Section 3.4 would be desirable. For the reasons outlined in Section 10.8.4 the following model studies would be of interest:

- (i) The effects of reversed flow through the gate system.
- (ii) The operation of the oscillating water columns when the downstream water level is below the level of the gate cover.
- (iii) Possible automatic gate realignment to allow flow actuation irrespective of flow direction.

10.3 The Mathematical Models and Parametric Testing

The results from the initial "open chamber" mathematical model were checked against the physical model results from the AUR Water Engine project (see Section 4.2.2). Considering that the physical model results could not be considered to be error free the agreement between the physical and computed results proved to be satisfactory. This satisfactory correlation was further confirmed towards the end of the mathematical model development when PWETWO results were checked against the behaviour of the Series 3 models (see Sections 3.5 and 4.8). The agreement between the two sets of data was considered to be sufficient to validate the mathematical model. Further validation

was provided by agreement between PWETWO's instantaneous power output and that of both TURB4 (see Section 5.4) and CEGB test data. This correlation particularly validates the concept of the Design Pressure Differential of Section 5.3.

PWETWO has proved to be an invaluable tool providing the capability to assess probable system behaviour and output over a wide range of operating conditions. It has excellent potential as a design tool especially when manipulated by the Evolutionary Processes of Chapter 9. PWETWO will continue to be of use in any future PWE development project.

The flexibility and robustness of the mathematical model was thoroughly demonstrated during the parametric tests of Chapter 6. This testing provided a wealth of information from which the following conclusions may be drawn:

- (i) Maximum air pressure differentials across the turbine fall far short of the head available to the system. This is due in part to the compressibility of the air within the chambers and to the inevitable head losses associated with the gate system. However, as air is constantly passing through the turbine, differential air pressures similar to the available pressure head will not be achieved unless the scale of the turbine is suitably reduced. The parametric tests clearly show that such a reduction will result in a severe drop in average power output.
- (ii) Maximum instantaneous power achieved during any PWE cycle far exceeds the average power output. Therefore the turbine will not have a high load factor.
- (iii) Gate size and the velocity of the gate motion should be maximised within the physical limits discussed in the text. Minimum chamber water levels suggest that the height of the gate can be safely increased to the full depth of the downstream flow without any air escaping from the emptying chamber.
- (iv) The volume of the air space above maximum chamber water level should be as small as possible. Care must be taken however to ensure that water does not reach the turbine. A minimal air space is easier to achieve in the circular chamber butterfly-gated system due to the nature of the flow within the chambers. The super-elevation of the chamber vortices would allow the water to reach the roof of the chamber at the periphery whilst a turbine duct placed at the centre of the roof would remain dry.
- (v) In the case of the twin circular chambered butterfly gated system the air pressures within the chambers will tend to be sub-atmospheric.

- (vi) A significant change in air temperature can be expected within the chambers during each cycle of the PWE and a net heat loss will occur from the system.

10.4 Outline Design and Costing

The use of a "top down" method of estimating the likely costs of a PWE system was initially suggested by ETSU. However, it was felt that the size and simplicity of the system was such that a reasonable outline design could be prepared upon which more realistic cost estimates would be based. Standard Civil Engineering practice has been applied to the preparation of these cost estimates. Such an approach offered the following advantages:

- (i) In order to produce an outline design of the system the logistics and practicalities of fabricating and installing a PWE in a waterway had to be studied to a greater extent. Such study involved focussing upon a large number of problem areas and the application of a variety of engineering solutions. This proved to be a very beneficial exercise which involved a degree of innovation and resulted in a much firmer concept of the siting of the system and the fabrication and construction of its component parts.
- (ii) The dimension sheets of Appendix IV can be considered to represent a useful database which can be manipulated in a number of ways. For example reliable cost estimates for different sized units could be obtained via suitable scaling of the existing dimensions.

The addition of further information to the database could eventually allow the development of a cost model specifically suited to run-of-river pneumatic devices. Once such a model had been established its involvement in a "top down" approach to the costing of any number of configurations could provide reliable cost estimates.

- (iii) The rates for the items listed in the Bills of Quantities of Appendix IV have been obtained either from the Wessex Database or from private suppliers. However, as the Bills of Quantities are now established, any organisation can now apply their own in-house rates to them and rapidly obtain a current estimate of the likely system costs for a variety of materials.

It is considered that the project as a whole benefits greatly from the design and costing exercises of Chapter 7. It is felt that a "top down" approach would have been less beneficial and would have resulted in a less realistic cost estimate.

10.5 Economic Assessment

The Economic Assessment of Chapter 8 was initially prepared before the privatisation of the water supply industry. At that time the current policies of the individual Water Authorities relevant to private hydro-power generation varied considerably. This restricted the development of any low-head potential to those areas of the UK under the control of Authorities who were taking heed of the 1981 Energy Conservation Act and adjusting their Water Abstraction charges accordingly.

It is still not clear as to what extent water privatisation will affect the economics of private hydro-power generation. The indications are however that the financial burden currently imposed will be significantly reduced. The private generator should also benefit from a long overdue introduction of the Public Utility Rate to replace the previous unfair imposition of Local Authority Rates. Upon privatisation of the electricity supply industry it will become necessary to ensure that all private generators are rated on a comparable basis. Other possible benefits resulting from the privatisation of the electricity supply industry and related to the renewable energy technologies are discussed in Section 10.7.2.

Hopefully, those scenarios of Chapter 8 which include either Water Abstraction Charges or Local Authority Rates will soon be considered of academic interest only. However, the wide range of scenarios presented in the Chapter represent a number of possible outcomes following the privatisation of both the water and the electricity supply industries.

The unit costs of the electricity produced by both a circular chamber PWE (case 1) and a rectangular chamber PWE (case 2) are presented in Section 8.3. The costs have been calculated for both a "worst case" scenario where Water Abstraction and Local Authority Rating charges are included and a "best case" scenario where Water Abstraction Charges are regulated and a Public Utility Rate equal to 0.18 p/kWh is introduced.

The unit costs vary as follows:

Discount Rate	Generation Cost (p/kWh)	
	Case 1	Case 2
0.05	1.30-2.01	1.38-2.29
0.08	1.62-2.32	1.72-2.66
0.10	1.86-2.78	1.97-2.93

These costs compare most favourably with the following recently published⁵⁵ unit costs of conventional electricity production:

Discount Rate	Generation Cost (p/kWh)	
	New PWR Plant	New Coal-Fired Plant
0.05	2.24	2.50
0.08	3.09	2.97
0.10	3.80	3.35

It is evident from the 10% discount rate curve of Fig. 8.1 that the capital cost of the PWE system could be increased by at least 50% before the unit cost of electricity generation was equal to that of a new PWR plant.

The sensitivity analyses of Section 8.4 would be of interest to a potential investor. Minimum Rates of Return between 8 and 10% would be required in order to attract investment from the private sector. Using this IRR 'envelope' the following upper and lower bounds can be obtained from the curves of Figs. 8.2 to 8.5:

	Payback Period (years)		
	10	15	25
Downtime (%)	0	11.3-18.0	22.5-30.0
Maintenance Costs (% of capital)	0	0-0.8	1.8-3.2
Energy Value (p/kWh)	3.4-3.5	2.8-3.0	2.5-2.7
Capital Cost (£x10 ³)	62.0-66.5	78.7-89.0	96.0-111.4

It can be concluded from the above figures and from the scenario 1 curve of Fig. 8.6 that the Case 1 circular chamber, butterfly-gated PWE could provide an Internal Rate of Return (IRR) on the capital invested of approximately 8% over a payback period of 15 years.

A considerably improved situation becomes apparent as the annual costs incurred by the PWE are reduced in the scenarios of Section 8.5.2. The relevant curves of Fig. 8.6 show that under the conditions of scenario 2 an IRR of 10% can be achieved assuming a payback period of approximately 14 years. Examination of the scenario 3 curve reveals that the introduction of the Public Utility Rate further increases the IRR to a more realistic 15% when a payback period of 15 years is considered.

It is the curves of Fig. 8.7 that provide the most promising economic assessment. Payback periods of 5 years can be achieved from the relevant scenarios providing

Internal Rates of Return of between 15 and 25%. It is suggested that such figures represent the true requirements of the private sector. Scenarios 4 and 5 therefore establish the economic viability of the PWE when operated under appropriate physical and economic conditions.

10.6 System Optimisation

10.6.1 The Evolutionary Technique

The Economic Assessment of Chapter 8 was based upon the optimum average power outputs achieved during the parametric studies of Chapter 6. It was apparent from these studies that there was a need for the development of a less time-consuming method of optimising PWE performance. The Evolutionary Design processes of Chapter 9 seemed best suited to this optimisation problem for the following reasons:

- (i) The Evolutionary Design technique involves a combination of random selection, testing, performance rating and subsequent reproduction of high performance parameter combinations. Thus the technique offers a method of developing an optimal path through the multi-dimensional search spaces of both the parameter combination of Section 9.1.1 and the chamber shape problem of Section 9.1.2.
- (ii) The nature of the optimisation problems of the aforementioned sections would suggest that there exists a large number of local optima upon which a more conventional optimisation process may converge. In the case of the evolutionary design technique this possibility of premature convergence can be eliminated by introducing the Random Mutation Operator to the Genetic Algorithm.

10.6.2 The Application of the Technique

The evolutionary process was implemented on the IBM PC/AT by a program developed in Fortran 77. The Genetic Algorithm uses PWETWO as a tool to provide average power outputs for the parameter combinations/chamber shapes that it generates. Unfortunately, as it was necessary to run three complete cycles of PWETWO to obtain a reasonable degree of stability, the process required an extensive amount of computer time. It was therefore only possible to consider the isentropic version of PWETWO and, in the case of the chamber shape optimisation, to introduce a small population size only.

The optimisation of ZHCG, PADIFD and ST illustrated the significance of the Random Mutation Operator. With no Random Mutation the Algorithm rapidly

converged upon an optimum average power output of 62.43 kW. However, by increasing the probability of Random Mutation to 0.1 an output of 63.37 kW was achieved. Increases in population size failed to improve upon this output and so it is reasonable to assume that this represents the global optimum average power output for a PWE of the stated dimensions operating isentropically.

The chamber shape problem of Section 9.6, with its 3.25×10^{32} possible area combinations, presented an even greater task to the processing powers of the IBM PC/AT. Time restrictions were such that only one complete run with a 10 chromosome population and a Random Mutation probability of 0.01 was possible. However, it was possible to repeat this exercise using an identical population size and RM probability but varying the starting point on a number of occasions using a Vax 8200 mini-computer. The resulting chamber shape is shown in Fig. 9.5.6. This shape provided an average power output of 89.87 kW. A degree of uniformity was introduced to the air space above the maximum chamber water level. This idealised chamber shape provided average power output of 89.64 kW and can be seen in Fig. 9.6.

Fabrication and installation costs were not taken into account during the chamber optimisation process. Any deviation from a uniform cross-sectional plan area will introduce cost penalties which may negate the usefulness of the increased average power output. However, the differing cross-sectional areas need not necessarily be represented in the uniform manner shown in Fig. 9.6. When considering a square or rectangular chamber the necessary increase or decrease in chamber plan area with elevation could be achieved by varying one side of the chamber only. Similarly, with a circular chamber, that part of the chamber adjacent either to the gate cover or to the side walls could be suitably distended to accommodate a required increase in plan area. Local reductions in plan area could be achieved by introducing bolt-on steel or glass-fibre inserts to the distorted chambers (Fig. 10.1).

A simple low-cost method of achieving variable cross-sectional plan areas would involve the introduction of the aforementioned inserts where plan areas need to be reduced and of simple pipe "galleries" at those elevations where an increase in plan area is required. None of these proposed deformations need necessarily destroy the chamber vortices.

10.6.3 Further Work

The next logical step in the design process would be to combine the optimisation of the parameters of Section 9.1.1 with the chamber shape problem of Section 9.1.2. A study involving this combination however should include the non-isentropic circular chamber, butterfly-gated option of PWETWO. This would

provide an optimum average power output on which to base a further economic assessment.

PWETWO would require some alteration to ensure sufficient stability in the operation of the vortex model of the circular chamber option and to achieve some reduction in the computation required for each PWE cycle. An improvement in the overall performance of the Genetic Algorithm may be achieved by allowing the RM probability to constantly vary in relation to the Standard Deviation of the average power outputs of each generation. Such an improvement may result in a reduction in the number of generations required to achieve convergence.

To summarise, the Evolutionary processes of Chapter 9 provide the methodology required to achieve an optimum PWE design. The optimisation exercises show that a significant improvement in PWE performance can be achieved. Further work would result in an optimum design of the PWE chambers, the air turbine and the gate operation characteristics. If this design can be fabricated and installed with a minimum cost penalty then a substantial improvement in the economics of the PWE could be obtained.

10.7 Further Development Of The Pneumatic Water Engine

10.7.1 PWE or Conventional Water Turbine?

It is intended in this final section to discuss the potential for further development of the PWE. In the first instance it is necessary to consider how the economics of the PWE compare to the economics of currently available, conventional water turbines. Such a comparison is made extremely difficult by the site specific nature of any system costing or economic assessment.

The installation of a conventional water turbine can be greatly facilitated by the presence of existing flow control works. Such control works may for instance consist of the millpool/millrace of an earlier hydro-power scheme. These existing facilities can significantly reduce the requirement for both temporary and permanent civil works. A number of turbine manufacturers produce mechanical and electrical packages that are particularly suitable for installation in such situations. It is claimed that overall capital costs of supplying and installing these packages can be as low as £1000.00/kW.

It is doubtful whether the presence of existing flow control facilities would facilitate the installation of a PWE to the same extent. However, an existing weir may influence the choice of site for a PWE and any existing facilities that provided complete or even partial river diversion would allow a substantial saving in construction cost.

It seems reasonable to assume that in the case of the installation of conventional water turbines the presence of existing flow control facilities would reduce the extent of both the temporary and permanent works whereas in a similar situation the installation of a PWE may only benefit from a reduction in the amount of temporary works required. It is suggested therefore that the competitiveness of the PWE economics would be severely weakened in this situation.

When one considers installation at a "green field" site however the PWE must be considered to present the most economically attractive option. Discussion with suppliers has indicated that the minimum cost of the mechanical and electrical components of a water turbine system suitable for operation under a 3 m head would be in the region of £750.00/kW. Assuming that these component costs constitute 25% of the total cost of the installation of a conventional system at a "green field" site then the overall capital cost would be in the region of £3000.00/kW. This cannot compete with the £1230.00/kW cost of a PWE installation at a similar site.

Referring back to Section 1.1, the Severn-Trent survey took into consideration only those low-head sites that provided existing civil engineering works that might facilitate the installation of a hydro-power system. A potential of some 132 GWh/annum was estimated to be available from sites where the available head was 3 m or less. Returning to the previous argument and taking the Severn-Trent survey into account the following conclusion may be drawn. In the short term the potential of such low-head sites is most likely to be realised by the installation of technically proven conventional hydro-power systems as any economic advantage offered by the installation of a PWE would probably be marginal. A PWE would only be considered where choice of site was restricted to the "green field" variety.

However, it must be remembered that PWE technology is in its infancy. There is every reason to assume that improved performance will lead to greater economic competitiveness. For example, the introduction of the gate "latching" system of Section 3.3.5 would result in an improvement in the gate operation by increasing the gate velocities. This would reduce leakage through the system and therefore increase overall system efficiency. Introduction of the stepped gate of Section 3.6 would further increase system output. Further significant increases in system output resulting from the optimization studies in Chapter 9 have already been discussed. Conventional water turbines however have a long history and it is debatable as to whether further significant improvement in their design is feasible.

In the long term, for the PWE to develop as a run-of-river hydro-power device, collaboration between those contracting organisations that manufacture and

install conventional water turbines and those organisations involved in the research and development of pneumatic hydro-power systems is essential. The scenarios of Section 8 show that in the right circumstances the PWE can be economically attractive. It is now necessary for the appropriate industries to contribute knowledge, experience and, along with the public sector, further financial assistance for its final development.

10.7.2 The 1989 Electricity Act

The Electricity Bill 1989 is a piece of enabling legislation concerning the Licences covering the generators, the new public supply companies and the transmission company of a privatised electricity supply industry within the UK⁵⁶.

The Act seeks to encourage diversity of supply by obliging the public supply companies to contract for a required minimum of non-fossil fuelled generation. This obligation is expected to represent approximately 20% of the UK electricity requirement and should remain in force at least until the year 2000.

Although originally intended as a measure to protect the UK nuclear industry until it can compete with fossil-fuelled generators the obligation was expected to cover both nuclear and renewable sources of energy. However, to prevent this requirement being monopolised by the nuclear industry, a smaller, additional obligation exclusive to renewables is to be introduced. From 1992 the public electricity suppliers will be required to contract for a minimum 600 MW of equivalent, renewable capacity over the years to 2000.

To prevent the electricity suppliers suffering undue economic disadvantage from this obligation a charge can be levied on the fossil-fuelled electricity that they supply. In effect this removes the need for independent renewable generators to compete with either nuclear or fossil-fuelled generators. Their only competition therefore will be between each other. Such a situation is likely to result in an increase in the value of the energy produced from renewable sources. This would have a significant beneficial effect upon the rates of return on any capital invested with a possible reduction in payback period as illustrated in Fig. 8.3.

All is not good news however. In order to qualify for inclusion under the 600 MW obligation each independent renewable generator will, in the first instance, have to have a minimum rated output of several Megawatts. This capacity will be reduced over the period up to 2000 but it seems likely that the smaller renewable generator providing less than, say, 500 kW will benefit directly within the near future.

It would appear that the 600 MW tranche is designed, in the main, for larger scale renewable generation such as the Windfarm project, the burning of dry combustible waste/biogas or the smaller tidal power schemes. The PWE would only qualify for inclusion if sited in a barrage configuration with an overall capacity equal to or greater than the required minimum. This provides a strong argument for moving the PWE out of the run-of-river situation and into the tidal regime as proposed in Section 10.11.

10.7.3 The PWE in the Developing World

If the PWE is to be of benefit to small communities in the developing world as suggested in Section 1.1 it will be necessary to attract significant funding from the relevant overseas aid organisations to provide financial assistance for its manufacture and installation. In a number of cases the amount of funding available depends upon to what extent the system is to be manufactured within the UK. Unfortunately, the site-specific nature of the PWE design does not easily lend itself to the fabrication of modular units. It is more likely that the PWE would be constructed in-situ using local materials. The manufacture of the mechanical and electrical components offers some scope for UK involvement although it is understood that since the withdrawal of Howdens from the renewable energy field it may be necessary to approach either Norwegian or Japanese turbine manufacturers for the provision of the Wells Turbine.

The PWE concept provides a low-technology, low-maintenance device capable of generating useful quantities of electricity. It is therefore ideally suited to small communities within the developing world. It is suggested however that its utilization in such a situation is more suited to a do-it-yourself approach involving a degree of barefoot engineering. As a community project the construction of the PWE could be achieved using local materials and manpower. It is possible that a simple Wells Turbine could also be fabricated locally, although turbine efficiencies may well suffer.

It is possible that the PWE system could only be considered as an export commodity when the scale of the works involved is as discussed in the following section.

10.8.4 The Operation of a PWE In a Tidal Situation

The present study has been restricted to run-of-river systems. To conclude, it is considered worthwhile to discuss the possible potential of the inclusion of a number of PWE units within a tidal barrage. Such a barrage may possess either PWE units only or a combination of PWE units and conventional water turbine sets.

It has been shown that essentially the PWE is a low efficiency device that requires a substantial flowrate. Although this may reduce the number of suitable run-of-river sites, it may prove to be less of a disadvantage in a tidal situation. In addition, the ability of the PWE to be operated successfully in shallow water may well be considered to be advantageous when the following factors are taken into account:

- (i) Conventional large diameter water turbines need to be situated in a sufficient depth of water to ensure that the correct degree of submergence is achieved. For this reason their installation within a tidal barrage is restricted to that portion that spans any existing deep water channel. This would generally result in the re-routing of shipping lanes to and from a lock facility situated at another point in the barrage. This operation involves considerable civil engineering works at substantial cost. Installation of PWE units would allow shipping lanes to remain within any existing deep water channel whilst ensuring that a far greater percentage of the barrage length would be utilised for energy production.
- (ii) A PWE tidal barrage could be successfully operated in those estuaries that possess the required tidal range but do not possess the necessary depth to accommodate conventional water turbines. For the same reasons, a PWE barrage could enclose large shallow bays or inlets that would otherwise be considered unsuitable.
- (iii) The installation of a tidal barrage combining both conventional turbine sets and PWE units would allow electricity generation to take place along much of the barrage length. Both deep water sections and shallow sections could be fully utilised. If PWE units were not installed however, "blind" caissons would most likely take their place in order to achieve closure. PWE units are particularly suited to caisson construction and it is reasonable to assume that construction and installation costs of PWE chamber caissons would be similar to those of the otherwise required "blind" caissons. It is suggested therefore that any economic assessment of the additional power output from the PWE units would only need to take into account the capital cost of the fabrication and installation of the mechanical and electrical components and gate system. This would reduce the installed cost per kW by approximately 25%. A further reduction may be achieved by the introduction of continuous construction techniques for the installation of the PWE caissons.
- (iv) It is possible that the volumetric flow rate through the PWE units of a tidal barrage combining both systems may allow a reduction in the sluicing

facilities that would otherwise be required if the barrage utilised conventional turbines only. It may be necessary to phase the operation of the different units during a half-tide cycle in order that an optimum average power output can be achieved whilst a sufficient volume of water is passed through the barrage. The ability to position the butterfly gate of a circular chamber PWE in the central position in order to create a sluicing facility could provide an added operational advantage.

- (v) Much interest has been shown in recent years in the installation of tidal barrages for the sole reason of allowing the development of the upstream basin. The increased minimum water level upstream of a barrage can be utilised for the development of marinas and other leisure facilities. Such facilities can greatly improve opportunities for tourism and thus significantly increase local revenue and employment prospects.

Amenity barrages in the main would not provide the necessary head differential nor the required depth to allow the utilisation of conventional water turbines. However, the economics of installing PWE units to realise the potential of the lesser head differentials could prove attractive. This may be especially so if cellular caisson barrage construction is planned. Such an installation could provide a reasonable rate of return on the capital investment in addition to the increased local revenue from the leisure facilities.

- (vi) An increase in sea level due to Global Warming and the resulting thermal expansion of the oceans would appear to be a distinct possibility within the foreseeable future. A massive investment would be required to upgrade or install the necessary coastal and estuarial protection works to accommodate any such rise. This introduces another possible role for the tidal barrage. A suitably positioned barrage could prevent extensive estuarial flooding by providing control of the upstream basin water level. This would remove the need for extensive investment in estuarial flood protection works. The cost savings thus achieved must be taken into account when assessing the economics of a barrage.

For reasons already stated, in many cases the installation of conventional water turbines in a barrage may not be practicable or economic. The installation of a PWE barrage however could provide an annual income that would allow the payback of the capital cost of the scheme. No such repayment would be possible from the conventional estuarial flood protection works that would otherwise be required.

The installation of a tidal energy/flood protection barrage falls to some extent within the category of sustainable development and can be considered to benefit the environment in two ways. Whilst the flood protection aspect would accommodate any rise in sea level caused by Global Warming, the electricity production aspect would allow some reduction in the fossil fuel burning that contributes to the CO₂ problem.

The installation of a PWE barrage in shallow offshore waters (see Fig. 10.2) could provide substantial protection to low lying coastal regions whilst allowing significant cost savings in coastal protection works and the opportunity to generate revenue.

Although there are a number of regions around the UK coastline that may benefit from such a barrage it is when the concept is applied to the developing world that the true potential of an offshore PWE barrage becomes apparent. Taking Bangladesh as an example, vast low lying areas of this country are under constant threat of flooding both from the extensive river systems and from the possibility of surge tides in the Bay of Bengal. Any rise in sea level would significantly add to the existing problems.

To provide adequate flood protection along the much indented coastline and estuaries of such a country would possibly involve a greater investment than that required for the establishment of a number of shallow water, offshore barrages incorporating PWE units. The electricity output from such barrages could allow substantial development without contributing to global air pollution. It may also represent a valuable export commodity.

The possible savings in fossil fuel consumption is a significant factor. The developed nations have recognised that financial and technological support must be made available to the developing countries so that their energy requirements can be met with minimal environmental damage. If the developing world follows a similar development path to our own (which relied upon the massive consumption of fossil fuels) then they will seriously undermine any attempt by the developed world to reduce CO₂ emissions. Funding may therefore be available from international sources to finance tidal power schemes especially if such schemes provide significant protection against flooding.

Although the above factors are conjectural at this point in time, they are founded upon a firm basis provided by the preceding study. A substantial research programme involving further physical model testing would be required to establish the true potential of a tidal PWE barrage.

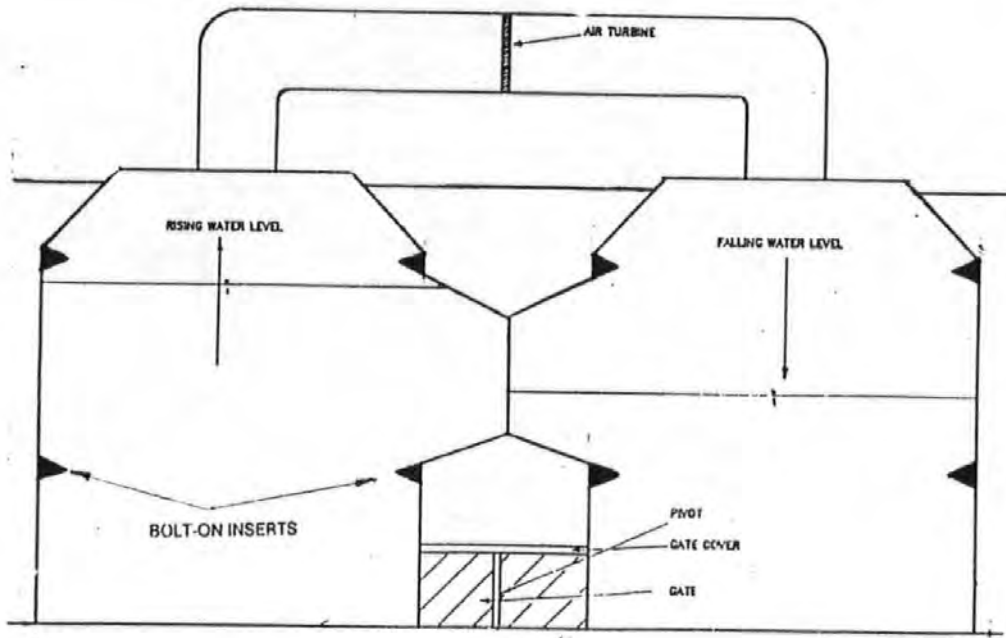
It is not intended to expand upon the requirements of such a study other than to suggest that the following areas will require investigation:

- (i) The overall operating characteristics of a tidal PWE barrage may differ to those of a tidal barrage incorporating conventional turbine sets. A study will therefore be required to establish the system's optimum mode of operation.
- (ii) If the PWE system is to generate during the ebb tide only then the butterfly gates must be held at the central, sluicing position when the tide is flooding. When the basin water level reaches its maximum it will be necessary to hold the gates at a "closed" position until the tide has ebbed enough to provide the required head differential between the basin and the sea. Similar gate operation will be required if the barrage is to generate during the flood tide only.

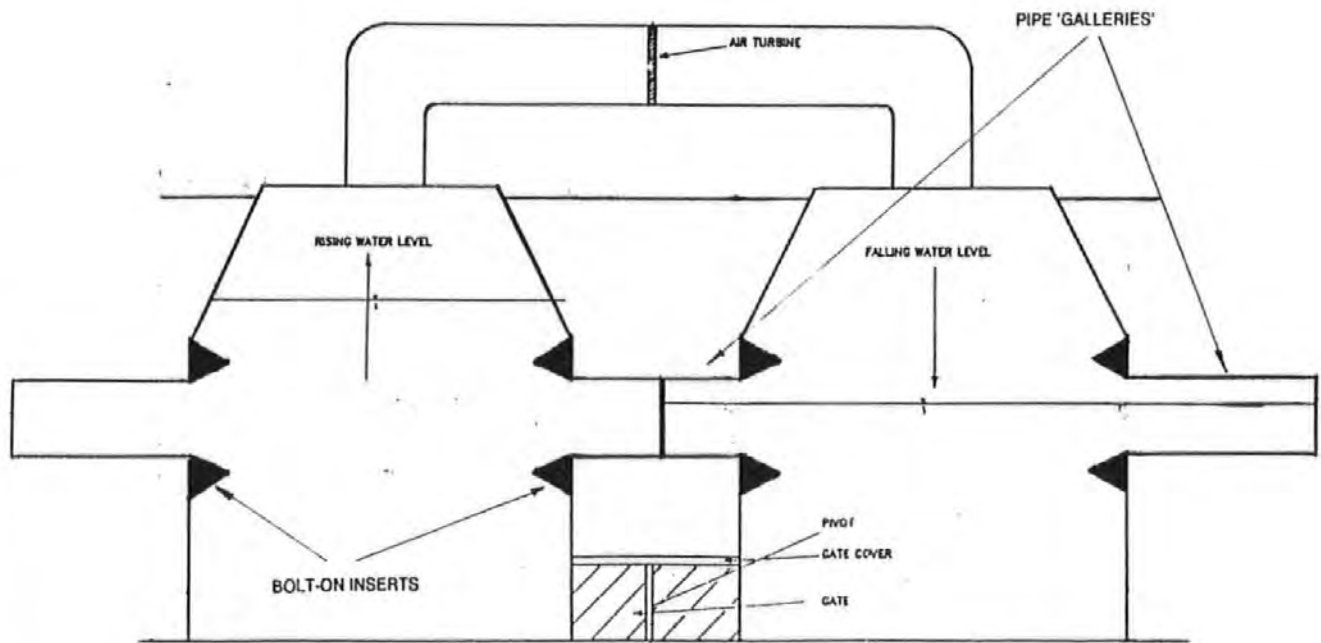
It may be found that the optimum mode of operation involves generation during both the flood and ebb tides. If this is the case then it is possible that suitable automation could enable the pivot point of the gates to be altered and the chamber openings to be realigned to allow flow actuation when the tide is flowing either into or out of the basin. Physical model testing will be required to establish the feasibility of each of these modes of operation.

- (iii) In shallower regions of the barrage the gating system may require protection from wave action on the seaward side. This could be provided by independent, deflecting wave walls.
- (iv) An automatic venting system to allow air to either enter the chambers or to escape from them will be required to ensure that an appropriate air volume is maintained during periods of generation.

The transition from run-of-river scheme to tidal scheme will greatly increase the scale of the civil works and of the mechanical and electrical requirement. Such an increase may provoke greater interest from the construction industry and from the turbine manufacturing industry. As has been previously stated, the full potential of the PWE will not be realised without such support from the private sector.



SECTION OF DISTENDED CIRCULAR CHAMBER SYSTEM



SECTION OF CIRCULAR CHAMBER SYSTEM INCORPORATING PIPE 'GALLERIES'

FIG. 10.1: CHAMBER SHAPE

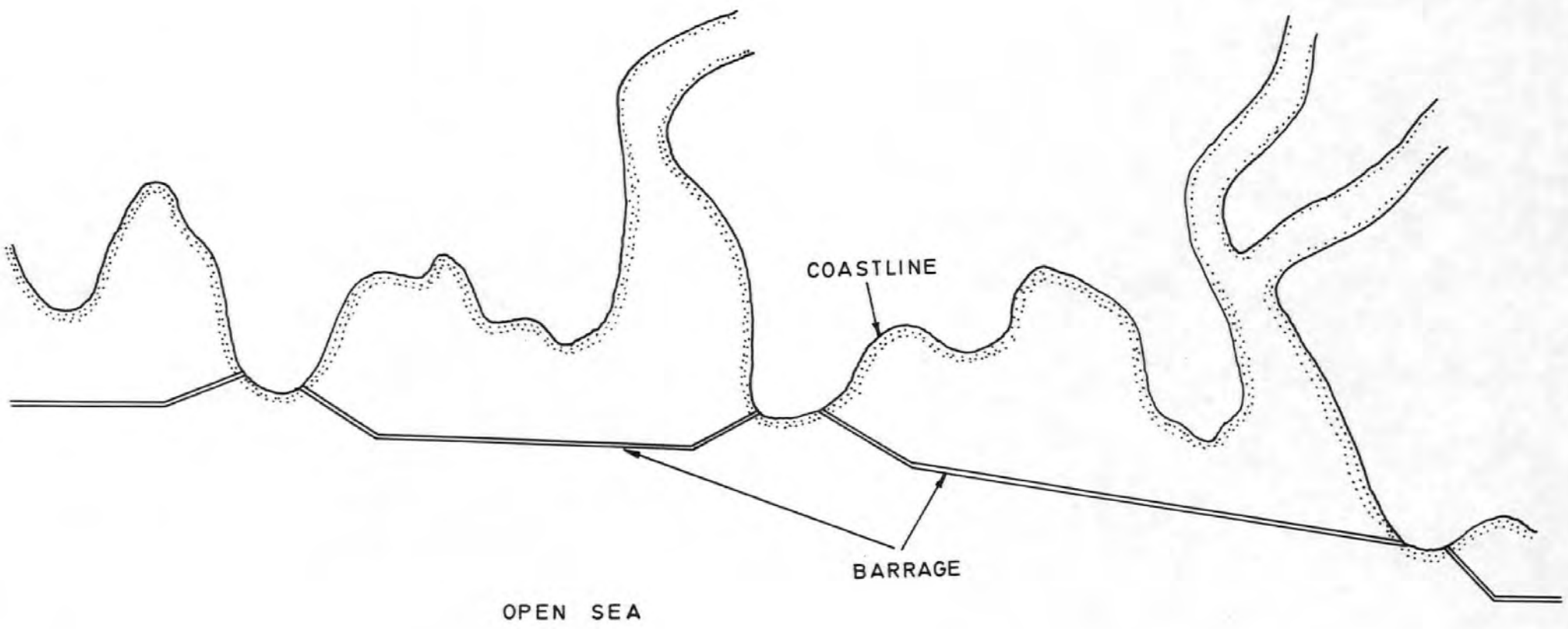


FIG. 10·2 SHALLOW WATER, OFFSHORE ENERGY BARRAGE

REFERENCES

- (1) Bullock, G.N. **Developments in the Utilization of Hydraulic Energy.** Ch.1, Energy - Present and Future Options, Volume 1. Edited by D. Merrick and R. Marshall, John Wiley and Sons Ltd., 1981.
- (2) **Latest Tidal Power Device to be Revealed at Nova Scotia.** International Water Power and Dam Construction, June 1982, pp.39-41.
- (3) Hydro Energy Associates Ltd. **Feasibility Studies of Pneumatic Hydro-Electric Systems.** Report for the Department of Energy, 1987.
- (4) Salford Civil Engineering Ltd. **Small Scale Hydro-electric Generation Potential in the UK.** ETSU Report, Department of Energy, Vol. 1, 1989.
- (5) Syson, L. **The Watermills of Britain.** David and Charles, London 1980.
- (6) The Severn Barrage Committee. **Tidal Power From the Severn Estuary.** Energy Paper No. 46 for the Department of Energy, HM Stationary Office.
- (7) Wilson, E.M. **The Annapolis Royal Power Station.** Proceedings: Symposium of Tidal Power, ICE 1986.
- (8) **Water Power From Wiessenburg.** Ossberger-Turbenfabrik, Wiessenburg, West Germany.
- (9) Gorlov, A.M. **Hydropneumatic Approach to Tidal Energy.** Paper presented at "New Approaches to Tidal Power" Conference, Bedford Institute of Oceanography, Dartmouth, Nova Scotia, 1982.
- (10) Whittaker, T.J.T., McIlhagger, D.S., Barr, A.G., Thompson, A. **Electrical Considerations With Wave Powered Navigation Aids.** Department of Civil Engineering, The Queen's University, Belfast.
- (11) Drew, S. **Wave Energy - The Small Scale Application of an Oscillating Water Column Device.** Paper - "Rural Power Sources" Conference, Newcastle Polytechnic, March 1983.
- (12) Mier, R. **The Development of the Oscillating Water Column Device.** Proceedings - "Wave Energy" Conference, Heathrow Hotel, London, 1978.
- (13) Raghunathan, S. **Theory and Performance of a Wells Turbine.** Paper WE/80/13R, The Queen's University, Belfast, 1980.




- (14) **Whale - Wave Activated Turbine Generator.** Munster Simms Engineering Ltd., Belfast, Northern Ireland.
- (15) Whittaker, T.J.T., White, P.R.S. **Wave Power.** Paper, Energy Engineering Group, ICE, 1987.
- (16) Peatfield, A.M., et al. **Wave Energy - A British Way Forward With the Circular Sea Clam.** Proceedings - "Energy Options - The Role of Alternatives in the World Energy Scene", Conference Publication 276, Institute of Electrical Engineers, 1987.
- (17) Bellamy, N.W. **Pneumatic Conversion for Low-Head Hydropower.** Proceedings - "The Role of Alternatives in the World Energy Scene", Conference Publication 276, Institute of Electrical Engineers, 1987.
- (18) Peatfield, A.M., et al. **Energy From Low-Head Water Sources.** Proceedings - "Alternative Energy Systems, Electrical Integration and Utilization", Coventry Polytechnic, Pergamon Press, 1984.
- (19) Bullock, G.N., Parmee, I.C. **The Performance and Economics of a Pneumatic Water Turbine.** ETSU Report No. SSH 4043, Department of Energy, 1989.
- (20) Private Communication: Salford Civil Engineering.
- (21) Johnson, L.W., Dean Riess. **Numerical Analysis.** Second Edition, Addison-Wesley Publishing Company, Massachusetts, 1982.
- (22) Grant, R.J., Johnson, C.G. **Performance Tests on a Single Stage Wells Turbine.** Confidential Report for the CEGB, 1979.
- (23) Hoskin, R.E., Count, B.M., Nichols, N.K., Nicol, D.A.C. **Phase Control for the Oscillating Water Column.** Proceedings - "Hydrodynamics of Ocean Wave - Energy Utilization", IUTAM Symposium, Lisbon, 1985.
- (24) White, P.R.S. **Developments in Norwegian Wave Energy.** Conference Proceedings - "Wave Energy Devices", Whitefriars Museum, Coventry, UK ISES, 30/11/89.
- (25) Whittaker, T.J.T. Private Communication, The Queen's University, Belfast, 1987.
- (26) Grant, R.J., Johnson, C.G., Sturge, D.P. **Performance of a Wells Turbine in a Wave Energy System.** I.E.E. Conference Publication No. 192, Jan. 1981.

- (27) Raghunathan, S., Tan, C.P. **Performance Prediction of the Wells Self-Rectifying Air Turbine.**
- (28) Private Communication, S. Raghunathan, Department of Aeronautical Engineering, The Queen's University, Belfast.
- (29) Jacobs, E.N., Sherman, A. **Airfoil Section Characteristics as Affected by Variations of the Reynolds Number.** Report No. 586, National Advisory Committee for Aeronautics, 1937.
- (30) The Institution of Civil Engineers. **The Civil Engineering Standard Method of Measurement.** 2nd Edition, Thomas Telford, London, 1985.
- (31) **Wessex Database for Civil Engineering.** 1st Edition, Wessex Electronic Publishing Ltd., Dorset, 1986.
- (32) Private Communications:
- British Steel Corporation Ltd., West Midlands
 - Plastic Installations Ltd., Glamorgan
 - Gendall Rainford Products, Cornwall
 - Mr. R. Peabody, Liegh Flexible Structures Ltd., Walsall
 - Mr. Whitham, Charcon Tunnel Linings Ltd., Notts.
 - Mr. Marshall, Spun Concrete, Burton-on-Trent
 - Mr. N. Thomas, C.V. Buchan, Middlewich
 - Mr. S. Brown, Barnshaw Section Benders Ltd., West Midlands
 - Mr. B. Hutchings, S.W.W.A., Exeter
 - Teignbridge Engineering, Newton Abbott
- (33) Property Services Agency. **Price Adjusted Formulae for Construction Contracts.** October 1987.
- (34) Lacroix, Y, Melvin, I., Luscher, E. and U. **Design, Construction and Performance of Cellular Cofferdams.** Proceedings - "Lateral Stresses in the Ground and Design of Earth Retaining Structures", Cornell University, New York, 1970, ASCE New York.
- (35) British Steel Corporation. **Piling Handbook.** 4th Edition, BSC, 1984.
- (36) University of Salford, Civil Engineering Department. **The Development of Small Scale Hydro-Electric Power Plants; Volume 1 - Technical Guide/Volume 2 - Demonstration Projects.** Report for the Department of Energy.

- (37) **Notes for the Developers of Small Scale Hydropower in the Welsh Water Area.** Welsh Water Authority, 1987.
- (38) Private Communication, North West Water.
- (39) **Comparable Rating for Independent Electricity Supplies.** Energy Management - Journal of the Department of Energy, Issue 1, April 1988, pp.4.
- (40) Private Communication. Mr. Sitter, District Valuer and Valuation Officer, Barnstaple, North Devon.
- (41) South West Electricity Board Supply Tariff, Leaflet MSTA/88, April 1988.
- (42) Carr, J.G. **The Economics and Possible Financing of the Two Severn Barrages.** Proceedings - "Symposium on Tidal Power", Institute of Civil Engineers, 1986.
- (43) Private Communication, Professor Ingo Rechenburg, Technische Universitat Berlin, Ackerstrasse 71-76 1000 Berlin 65, Germany.
- (44) Schweffel, H.P., Klockgether, J. **Two Phase Nozzle and Hollow Core Jet Experiments.** Proceedings of the 11th Symposium on Engineering Aspects of MagnetoHydrodynamics, Pasadena, California Institute of Technology, 1970.
- (45) Hoeller, A., Leysner, U., Wiedemann, J. **Optimization of the Layout of Trusses Combining Strategies Based on Mitchell's Theorem and on the Biological Principles of Evolution.** AGARD Conference Proceedings 123, A1-A8, 2nd Symposium on Structural Optimization, Milan, Italy, 2-4th April 1973.
- (46) Lawo, M., Thierauf, G. **Optimal Design for Dynamic, Stochastic Loading, A Solution by Random Search.** In: Eschenauer, H., Olhoff, N. **Optimization Methods in Structural Design.** (Euromech-Colloquium 164, University of Siegen 1982), Bibl. Inst., Mannheim 1983.
- (47) BBC Television. "Horizon" production. **The Blind Watchmaker**, 1987.
- (48) Holland, J.H. **Adaptation in Natural and Artificial Systems.** The University of Michigan Press, 1975.
- (49) Dawkins, R. **The Blind Watchmaker.** Longman Scientific and Technical, 1986.




- (50) Rechenberg, I. **The Evolution Strategy - A Mathematical Model of Darwinian Evolution.** In: Frehland, E. **Synergetics - From Microscopic to Macroscopic Order.** Springer Series In Synergetics, Vol. 22, Springer, Berlin-Hiedelberg 1984.
- (51) Goldberg, D.E. **Computer Aided Gas Pipelline Operation Using Genetic Algorithms and Rule Learning.** PhD Dissertation, University of Michigan, 1983.
- (52) Pinebrook, W.E. **Drag Minimization on a Body of Revolution.** PhD Dissertation, University of Houston, Texas, 1982.
- (53) De Jong, K.A. **Analysis of the Behaviour of a Class of Genetic Adaptive Systems.** PhD Dissertation, University of Michigan, 1981.
- (54) Bethke, A.D. **Genetic Algorithms as Function Optimizers.** PhD Dissertation, University of Michigan, 1981.
- (55) CEGB. **Evidence to the Hinkley C Enqulry.** 1989.
- (56) Andrews, S.A. **The Role of Independent Power Producers in the UK Energy Supply.** Proceedings-'Energy Policy and the Environment', UK ISES, London. 1989.

APPENDIX I

Configuration & Final Position (Dotted)	Size of Aerofoil	Position of Aerofoil	Size of Fin	Position of Fin	Force* Reqd (1 to 10)	Close/ Not Close	COMMENTS
	None	None	None	None	7	Close	<u>SYMMETRICAL GATE</u> Gate remains firmly closed. Appreciable force required to move gate through distance 'A'. From this point gate will travel to opposite closed position with no force applied.
	None	None	None	None	4	Close	<u>LONG TAILED GATE (250mm)</u> Gate remains in closed position. However, when gate is moved through distance 'A' using external force, it will then travel to opposite closed position with no external force applied.
	None	None	None	None	None	Close	<u>LONG-TAILED GATE (270mm)</u> Gate remains closed until water level in chamber is approximately equal to upstream head. Gate then swings across to opposite closed position and process is repeated.

*The 'Force Required' column in this and subsequent tables, refers to a notational force (i.e. manual operation) required to pass the gate through any area that it otherwise would not pass. The scale 1-10 is meant to be interpreted in a comparative sense only.

TABLE 1. MODEL 1:0, TRUNCATED TEST MODEL, 65° ARC

Configuration & Final Position (Dotted)	Size of Aerofoil	Position of Aerofoil	Size of Fin	Position of Fin	Force* Reqd (1 to 10)	Close/ Not Close	COMMENTS HUC = 300mm HDC = 150mm
2:1 Flow 	None	None	None	None	6	Not Close	<u>205mm GATE</u> The gate will not close completely and remains in position shown. Appreciable external force has to be exerted to pass gate through central area 'Y' to corresponding position on other side.
2:2 	-	-	-	-	4	Not Close	<u>230mm GATE</u> As above. However, significant reduction in magnitude of external force required to pass gate through central area, 'Y'.
2:3 	-	-	-	-	4	Not Close	<u>250mm GATE</u> As 2:1. Slightly less force required to pass gate through central area, 'Y'.

HUC = Head in upstream channel
HDC = Head in downstream channel

TABLE 2:0 MODEL NO. 2 COMPLETE CHAMBERS, NO COVERS, 65° ARC (SEE FIG. 1)

Configuration & Final Position (Dotted)	Size of Aerofoil	Position of Aerofoil	Size of Fin	Position of Fin	Force* Reqd (1 to 10)	Close/ Not Close	COMMENTS
2:4 Flow ↓ 	None	None	30mm x 5mm	Adjacent to gate opening	7	Close	<u>205mm GATE</u> Gate now closes but remains in closed position for a very short period before swinging to position shown. Greater force required to pass gate through central area than for 2:1.
2:5 	-	-	30mm x 5mm	Adjacent to gate opening	4	Not Close	<u>230mm Gate</u> As Gate 2:2.
2:6 	-	-	30mm x 5mm	Adjacent to gate opening	6	Not Close	<u>250mm Gate</u> As Gate 2:3. Slightly greater force needed to pass gate through central area.

TABLE 2:1 MODEL NO. 2

Configuration & Final Position (Dotted)	Size of Aerofoil	Position of Aerofoil	Size of Fin	Position of Fin	Force* Reqd (1 to 10)	Close/ Not Close	COMMENTS HUC = 300mm HDC = 150mm
2:7 Flow ↓ 	None	None	30mm x 5mm	At tail of gate	3	Not Close	<u>230mm GATE</u> Gate will not close. However when held at close position and then released. It moves rapidly to central position shown & remains there. No great force required to move gate back over to close position.
2:8 	None	None	30mm x 5mm	At tail of gate	3	Close	<u>250mm GATE</u> Gate remains closed until chamber head is approximately level to upstream head and then swings across to position shown. Light force only required to close gate on opposite side.
2:9 	40mm x 10mm	At leading edge of gate	30mm x 5mm	At tail of gate	3	Close	<u>250mm GATE</u> Gate remains closed until chamber head is approximately equal to half that of the head differential then swings across to position shown.
2:91 	40mm x 5mm	At leading edge of gate	30mm x 5mm	At tail of gate	2	Close	<u>250mm GATE</u> Gate remains closed until chamber head approximately equals upstream head and then swings to position shown. Will occasionally complete arc to opposite close position but action is erratic.

TABLE 2:2 MODEL NO. 2




Configuration & Final Position (Dotted)	Size of Aerofoil	Position of Aerofoil	Size of Fin	Position of Fin	Force* Reqd (1 to 10)	Close/ Not Close	COMMENTS HUC = 280mm HDC = 130mm
3:1 Flow 	None	None	None	None	8	Close	<u>SYMMETRIC GATE</u> Rise Time = 7 Secs Fall Time = 6.5 Secs Gate remains very firmly closed. Substantial external force required to move gate through area 'Y'. Gate then crosses over with no external force.
3:2 	-	-	-	-	5	Not Close	<u>140mm GATE</u> RT = 6 Secs FT = 6 Secs When released from 'closed' position gate will swing across to position 1 and then return to position 2 and stabilize there.
3:3 	-	-	-	-	5	Close [1 sec]	<u>155mm GATE</u> RT = 8 Secs FT = 7.5 Secs When released from 'closed' position gate swings across to opposite closed position, remain there for approximately 1 sec and then returns to position shown.

TABLE 3.0 MODEL 3:3.

ENCLOSED SYSTEM 45° ARC





Configuration & Final Position (Dotted)	Size of Aerofoil	Position of Aerofoil	Size of Fin	Position of Fin	Force* Reqd (1 to 10)	Close/ Not Close	COMMENTS HUC = 280mm HDC = 130mm
3:4 Flow 	None	None	10mm x 5mm	At tail of gate	4	Not Close	<u>140mm GATE</u> When released from 'closed' position gate swings to position shown and remains there. Positive movement.
3:5 	None	None	10mm x 5mm	At tail of gate	4	Not Close	<u>155mm GATE</u> When released from 'closed' position, gate swings to position 1 (very positive movement) and then returns to position 2 and oscillates about this position.
3:6 	None	None	20mm x 5mm	At tail of gate	4	Not Close	<u>140mm GATE</u> As 3:4
3:7 	None	None	20mm x 5mm	At tail of gate	1	Close [1+2]	<u>155mm GATE</u> When released from 'closed' position gate will swing to opposite closed position, remain there for 1-2 secs and then return to position 2 and oscillate between 1 and 2 (Positive movement)

TABLE 3:1 MODEL 3:3, PIVOT NO.

Configuration & Final Position (Dotted)	Size of Aerofoil	Position of Aerofoil	Size of Fin	Position of Fin	Force [†] Reqd (1 to 10)	Close/ Not Close	COMMENTS
							HUC = 280mm HDC = 130mm
3:8 Flow [†] 	None	None	30mm x 6mm	At tail of gate	7	Not Close	<u>140mm GATE</u> When released from 'closed' position gate will swing to position 1 and then return to position 2 and stabilize there.
3:9 	None	None	30mm x 6mm	At tail of gate	4	Not Close	<u>155mm Gate</u> Gate oscillates between two 'closed' positions without any external force being applied. Gate begins swing when chamber water level is at half the head differential.
3:91 	10mm x 5mm	At leading edge of gate	30mm x 6mm	At tail of gate	-	Not Close	<u>155mm Gate</u> Gate oscillates between two 'close' positions - action more positive than 3:9 and chamber now fills to $\frac{1}{2}$ of the head differential. Slight 'hover' at 'closed' position.
3:92 	30mm x 5mm	At leading edge of gate	30mm x 6mm	At tail of gate	-	Not Close	<u>155mm Gate</u> Very positive movement - 'hover' disappeared. Gate starts 1-2 secs after 'chamber full' condition.

TABLE 3:2 MODEL 3:3 PIVOT NO 1.

Configuration & Final Position (Dotted)	Size of Aerofoil	Position of Aerofoil	Size of Fin	Position of Fin	Force [†] Reqd (1 to 10)	Close/ Not Close	COMMENTS
							HUC = 180mm HDC = 130mm
3:93 Flow [†] 	None	None	None	At tail of gate	3	Not Close	<u>140mm GATE</u> When released from 'closed' position gate swings to position 1 and then returns to 2. Rise Time = 5.75 SECS Fall Time = 8.00 SECS
3:94 	None	None	20mm x 5mm	At tail of gate	2	Close (less than one sec)	When released from 'closed' position gate swings to opposite 'closed' position then immediately returns to position shown.
3:95 	None	None	40mm x 5mm	At tail of gate	2	Close (less than one sec)	As 3:94
3:96 	30mm x 5mm	At leading edge of gate	40mm x 5mm	At tail of gate	1	Close (less than one sec)	When released from closed position gate swings to opposite closed position then immediately swings to position 1 and oscillates between 1 and 2. The same pattern occurs for 10 & 20mm aerofoils only slightly less positive movements.

TABLE 3:3 MODEL NO. 3:3 PIVOT NO. 2 140MM GATE

Configuration & Final Position (Dotted)	Size of Aerofoil	Position of Aerofoil	Size of Fin	Position of Fin	Force [†] Reqd (1 to 10)	Close/ Not Close	COMMENTS
							HUC = 180mm HDC = 130mm
3:97 Flow [†] 	None	None	None	None	3	Not Close	RT = 6 SECS FT = 6.5 SECS When released from 'closed' position gate swings to 1 and then returns to 2.
3:98 	None	None	40mm x 5mm	At tail of gate	2	Close (less than one sec)	When released from 'closed' position gate swings to opposite 'closed' position and immediately swings back to position 1 and oscillates between 1 and 2.

TABLE 3.4 MODEL NO 3:3 PIVOT NO. 3 140mm GATE

NOMENCLATURE

GL	=	Gate Length
HUC	=	Head - Upstream Channel
HDC	=	Head - Downstream Channel
$Y_{max,min}$	=	Maximum and Minimum Chamber Water Levels
T10	=	Time Taken for 10 Complete Cycles
Gu,Gd	=	As Fig. 3.3
WEN	=	Width of Entrance
WEX	=	Width of Exit

RISE AND FALL / GATE DATA

45° MODEL

COVERS AND CONNECTOR

GL(mm)		120	130	130/F4	130/F8	140	155
HUC(mm)		300	310	310	310	310	300
HDC(mm)		150	150	150	150	150	150
Y_{max} (mm)		200	205	270	240	225	215
Y_{min} (mm)		115	115	120	120	125	130
T10(secs)		75	108	137	104	100	82
Gu(mm)		30	30	30 ⁿ	30	40	40
Gd(mm)		90	100	100	100	100	115
WEN(mm)		24	24	24	24	28	28
WEX(mm)		45	48	41	45	45	57

COMMENTS: On all gates bar the flanged, 130mm models, rapid, pronounced oscillation of the gate at the closed position was evident. Those models incorporating the flange showed a much reduced tendency to oscillate, the oscillations only commencing when the head of the emptying chamber had become within 20mm of its lowest point. The oscillations that then occurred were of a much lesser magnitude and force than those of the other gates.

The 155mm gate showed a less positive action than those of a lesser length.

TABLE 4.0

COVERS ONLY

GL(mm)	120	130	130/F4	130/F8	140	155
HUC(mm)	310	310	310	310	310	310
HDC(mm)	150	150	150	150	150	150
Ymax(mm)	200	190	220	225	230	230
Ymin(mm)	115	120	115	115	115	115
T10(secs)	70	63	80	80	65	84
Gu(mm)	30	30	30	30	40	40
Gd(mm)	90	100	100	100	100	115
WEN(mm)	24	24	24	24	28	28
WEX(mm)	47	43	41	48	46	57

COMMENTS: As for previous Table.

TABLE 4.1

NO COVERS

GL(mm)	120	130	130/F4	130/F8	140	155
HUC(mm)	300	300	300	310	300	310
HDC(mm)	150	150	150	150	150	150
Ymax(mm)	195	200	220	210	220	250
Ymin(mm)	105	100	115	115	115	115
T10(secs)	63	78	93	64	65	86
Gu(mm)	30	30	30	30	40	40
Gd(mm)	90	100	100	100	100	115
WEN(mm)	24	24	24	24	28	28
WEX(mm)	52	52	44	49	48	53

COMMENTS: Oscillation of flanged gates hardly noticeable, even more reduced than those of the flanged gates of the previous configurations. The oscillation of the other gates, however, remain as pronounced as before.

TABLE 4.2

55° MODEL

COVERS AND CONNECTOR

GL(mm)	170	170/F8	190	190/F8
HUC(mm)	310	310	290	290
HDC(mm)	150	150	150	150
Ymax(mm)	260	230	260	260
Ymin(mm)	120	130	120	120
T10(secs)	116	---	115	145
Gu(mm)	50	50	50	50
Gd(mm)	120	120	140	140
WEN(mm)	40	40	40	40
WEX(mm)	67	72	63	64

COMMENTS: 170mm: Pronounced oscillation throughout cycle.

170mm/8mm Flange: Gate would not completely close, tended to hover 2 to 3mm off the fully closed position. This introduced substantial leakage.

190mm: Pronounced oscillation throughout cycle. Erratic action, difficult to time 10 consecutive cycles.

190mm/8mm Flange: Pronounced oscillation throughout cycle. However, action was far more positive than the straight 190mm gate.

TABLE 5.0

COVERS AND CONNECTORS

GL(mm)	120	130	130/F4	140	155
HUC(mm)	310	300	290	310	320
HDC(mm)	150	150	150	150	150
Ymax(mm)	245	220	200	280	270
Ymin(mm)	125	120	120	120	110
T10(secs)	146	132	122	196	192
Gu(mm)	30	30	30	40	40
Gd(mm)	90	100	100	100	115
WEN(mm)	30	30	30	35	35
WEX(mm)	55	60	62	61	65

COMMENTS: Gates 130mm, 140mm and 155mm showed pronounced oscillation throughout the cycle. Both the 120mm and the flanged 130mm gates showed no apparent oscillation whatsoever. In addition, the 120mm gate's action was noticeably more positive than the larger gates and that of the 120mm gate when incorporated in the 45 model. In contrast the action of the flanged 130mm gate was weak possibly due to the flange interfering with the chamber sides before the gate had reached the fully closed position.

TABLE 5.1

COVER ONLY

GL(mm)		170	170/F8	190	190/F8
HUC(mm)		310	---	310	300
HDC(mm)		150	---	150	150
Ymax(mm)		300	---	300	250
Ymin(mm)		120	---	120	120
T10(secs)		150	---	---	72
Gu(mm)		50	50	50	50
Gd(mm)		120	120	140	140
WEN(mm)		40	40	40	40
WEX(mm)		63	---	66	63

COMMENTS: 170mm: Pronounced oscillation throughout cycle. Gate action very erratic, tendency to hover at various positions.

170/F8: Will not operate satisfactorily; impossible to find cowl correct cowl position; gate either remains closed or hovers 3-4mm off the closed position.

190mm: Gate action very erratic; proved impossible to achieve sufficient number of similar, consecutive cycles.

190/F8: Slight oscillation evident, commencing when head of the emptying chamber was within 20mm of its lowest point.

TABLE 5.2

NO COVERS

GL(mm)		120	130	130/F4	140	155
HUC(mm)		310	300	290	300	320
HDC(mm)		150	150	150	150	150
Ymax(mm)		245	220	200	270	290
Ymin(mm)		120	120	130	120	125
T10(secs)		130	89	93	113	149
Gu(mm)		30	30	30	40	40
Gd(mm)		90	100	100	100	115
WEN(mm)		30	30	30	35	35
WEX(mm)		55	60	62	65	65

COMMENTS: As Table 4.2

TABLE 5.3

NO COVERS

GL(mm)		170	170/F8	190	190/F8
HUC(mm)		300	300	300	300
HDC(mm)		150	150	150	150
Ymax(mm)		245	255	260	270
Ymin(mm)		115	115	115	115
T10(secs)		70	---	---	80
Gu(mm)		50	50	50	50
Gd(mm)		120	120	140	140
WEN(mm)		40	40	40	40
WEX(mm)		66	---	---	58

COMMENTS: 170mm: Pronounced oscillation throughout cycle.

170/F8: As 'cover only' table.

190mm: Erratic gate action prevented sufficient number of consecutive, similar cycles to be recorded.

190/F8: Very slight oscillation for 1-2secs before gate begins swing.

TABLE 5.4

APPENDIX II

NOTATION

Main Symbols

A	Area (m^2)
B	Breadth of chamber or feature indicated by subscript (m) e.g. B_{UG} = breadth of upstream gate
CC	Coefficient of contraction
CF	Coefficient of friction
CH	Thermal conductance ($W/^\circ K$)
CM	Coefficient of added mass
CV	Specific heat of air at constant volume (J/kgK)
CP	Specific heat of air at constant pressure (J/kgK)
D	Depth of flow in channel (m)
DIAM	Diameter of a circular chamber (m)
DT	Increment of time
E	Specific energy of flow in channel (m)
EFFT	Efficiency of air turbine
EN	Energy (kWs)
EPSILA	Absolute error criterion
EPSILR	Relative error criterion
g	Acceleration due to gravity (m/s^2)
H	Variable dimension of gate opening (m) e.g. height of a sluice gate.

HMAX Maximum value of H (m)

K A loss coefficient

L Length of chamber measured in the direction of flow (m)

MOMEN Variable proportional to the momentum of a circular vortex (m^4/s)

NDT Integer used in the calculation of DT

NDTMAX Maximum value of NDT

NDTMIN Minimum value of NDT

P Gauge pressure (N/m^2)

PDIF Pressure differential across air turbine (N/m^2)

PDIFD Design prssure differntial across air turbine (N/m^2)

POW Power (kw)

Q Discharge (m^3/s)

QH Heat Transfer rate (W)

QM Mass flow rate (kg/s)

RGC Gas constant (J/kg K)

S Entropy (J/K)

SS Specific entropy (J/kg K)

ST Scale of air turbine

T Time (s)

TEMPK Absolute temperature (K)

TMAX Maximum value of T (s)

V	Velocity (m/s)
VJ	Velocity at the vena contracta of the jet of flow passing through a gate (m/s)
VOL	Volume (m ³)
VT	Tangential velocity adjacent to the wall of a chamber (m/s)
Y	Mean elevation of the water surface in a chamber (m). Used as a generalised co-ordinate measured positive upwards from the defined datum.
Z	Elevation above datum (m). Used for the bed of a channel, a chamber or the centre of a gate opening. Subscripts indicate which use is intended.
ZHC	Elevation of higher control water level for a gate (m).
ZLC	Elevation of lower control water level for a gate (m).
ρ	Density (kg/m ³).

Subscripts

A	Air
C	Channel or vena contracta
CY	Cycle
D	Downstream or first time derivative
DD	Second time derivative
G	Gate
I	Inside
N	New value after timestep

O Outside

P Chamber

T Turbine

U Upstream

W Water

APPENDIX III

ENERGY TEST 1: VARIABLE SCALE
FACTOR AND GATE TRIGGER LEVELS

SINGLE AND TWIN CHAMBERS

E.T. 1.0

INITIAL VALUES:

Upstream Channel:

BUC = 10.000 m ZUC = 0.000
EUC = 5.000 m CMUC = 1.000

Downstream Channel:

BDC = 10.000 m ZDC = 0.000
EDC = 2.000 m CMDC = 1.000

Upstream Gate:

BUG = 4.472 m HUGMAX = 1.000 m
TUG = 1.000 s HUG1 = 0.005 m
ZHCUG = 4.999 m HUG2(TWIN CHMBR) = 1.000 m
ZLCUG = 2.001 m CCUG = 0.600

Downstream Gate:

BDG = 4.472 m HDGMAX = 1.000 m
TDG = 1.000 s HDG1 = 1.000 m
ZHCDG = 4.999 m HDG2(TWIN CHMBR) = 0.005 m
ZLCDG = 2.001 m CCDG = 0.600

Chamber:

B = 4.472 m L = 4.472 m
A = 19.999 m² ZT = 6.000 m

ST = SINGLE CHMBR: 0.5>5.0
TWIN CHMBR: VARIABLE

E.T. 1.1

All values as E.T. 1.00 excepting the following:

ZHCUG = 4.950 m ZHCDG = 4.950 m
ZLCUG = 2.050 m ZLCDG = 2.050 m
ST = TWIN CHMBR: 1.5>6.0

E.T. 1.2

All values as E.T. 1.00 excepting the following:

ZHCUG = 4.900 m ZHCDG = 4.900 m
ZLCUG = 2.100 m ZLCDG = 2.100 m
ST = TWIN CHMBR: 1.5>6.0

E.T. 1.3

All values as E.T. 1.00 excepting the following:

ZHCUG = 4.850 m ZHCDG = 4.850 m
ZLCUG = 2.150 m ZLCDG = 2.150 m
ST = TWIN CHMBR: 1.0>6.0

E.T. 1.4

All values as E.T. 1.00 excepting the following:

ZHCUG = 4.800 m ZHCDG = 4.800 m
ZLCUG = 2.200 m ZLCDG = 2.200 m
ST = TWIN CHMBR: 1.0>3.5

A3.2

E.T. 1.5

All values as E.T. 1.00 excepting the following:

ZHCUG = 4.700 m ZHCDG = 4.700 m
 ZLCUG = 2.300 m ZLCDG = 2.300 m
 ST = TWIN CHMBR: 1.0>3.5

E.T. 1.6

All values as E.T. 1.00 excepting the following:

ZHCUG = 4.600 m ZHCDG = 4.600 m
 ZLCUG = 2.400 m ZLCDG = 2.400 m
 ST = TWIN CHMBR: 1.0>5.0

E.T. 1.7

All values as E.T. 1.00 excepting the following:

ZHCUG = 4.500 m ZHCDG = 4.500 m
 ZLCUG = 2.500 m ZLCDG = 2.500 m
 ST = TWIN CHMBR: 1.0>3.5

NOMENCLATURE

ST = Scale of turbine.
 YMAX = Maximum chamber water level during cycle.
 YMIN = Minimum
 CT = Duration of cycle.
 PAMAX = Maximum chamber air pressure during cycle.
 PAMIN = Minimum
 IPMAX = Maximum instantaneous power
 EFF = Overall efficiency.
 AP = Average power output during cycle.

E.T. T1.0

ST	Y MAX. (M)	Y MIN (M)	CT (SEC)	PA MAX (N/M ²)	PA MIN (N/M ²)	IP MAX. (KW)	EFF. (%)	AP (KW)
2.00	5.003	1.998	15.6	8523	-7424	238.7	31.3	77.30
2.50	5.016	1.990	13.7	7588	-5834	217.9	27.1	77.00
3.00	5.030	1.981	12.9	6977	-4588	198.5	23.9	73.10
3.50	5.042	1.973	12.4	6481	-3704	181.2	21.4	68.40
4.00	5.052	1.966	12.0	6077	-3019	166.3	19.4	63.90
4.50	5.060	1.960	11.8	5808	-2568	153.4	17.7	59.70
5.00	5.067	1.995	11.6	5472	-2257	142.1	16.3	55.90
5.50	5.073	1.951	11.4	5252	-2015	132.4	15.0	52.40
6.00	5.078	1.947	11.3	5105	-1830	124.0	14.0	49.40

A3.3

E. T. T1.1

ST	Y MAX. (M)	Y MIN (M)	CT (SEC)	PA MAX (N/M ²)	PA MIN (N/M ²)	IP MAX (KW)	EFF. (%)	AP (KW)
1.50	4.995	2.040	16.1	11257	-7731	270.1	36.9	86.3
2.00	4.972	2.029	13.8	9534	-6143	245.5	31.4	86.6
2.50	4.990	2.018	12.8	8431	-4852	221.4	27.3	82.4
3.00	5.005	2.008	12.1	7662	-3939	200.0	24.2	76.9
3.50	5.018	1.999	11.7	7050	-3263	181.8	21.6	71.4
4.00	5.027	1.992	11.4	6560	-2811	166.3	19.5	66.4
4.50	5.035	1.986	11.3	6156	-2465	153.1	17.8	61.8
5.00	5.042	1.982	11.1	5877	-2181	141.9	16.4	57.7
5.50	5.047	1.977	11.0	5564	-1968	132.0	15.1	54.0
6.00	5.052	1.974	10.9	5413	-1778	123.5	14.1	50.8

E. T. T1.3

ST	Y MAX. (M)	Y MIN (M)	CT (SEC)	PA MAX (N/M ²)	PA MIN (N/M ²)	IP MAX (KW)	EFF. (%)	AP (KW)
1.00	4.856	2.129	17.0	14900	-9716	292.1	44.7	94.0
1.50	4.885	2.111	13.6	12158	-7230	274.7	37.3	99.3
2.00	4.911	2.094	12.2	10234	-5595	245.9	31.9	95.4
2.50	4.931	2.080	11.5	9003	-4479	219.8	27.8	88.8
3.00	4.947	2.069	11.0	8173	-3718	197.9	24.5	81.9
3.50	4.959	2.060	10.7	7376	-3155	179.3	21.9	75.5
4.00	4.969	2.053	10.5	6929	-2730	163.9	19.8	69.7
4.50	4.975	2.047	10.4	6401	-2415	150.6	18.0	64.7
5.00	4.982	2.042	10.3	6039	-2147	139.4	16.6	60.3
5.50	4.987	2.039	10.2	5789	-1930	129.7	15.3	56.4
6.00	4.992	2.035	10.1	5551	-1752	121.5	14.2	52.9

E. T. T1.2

ST	Y MAX. (M)	Y MIN (M)	CT (SEC)	PA MAX (N/M ²)	PA MIN (N/M ²)	IP MAX (KW)	EFF. (%)	AP (KW)
1.50	4.919	2.076	14.6	11780	-7380	273.8	37.1	94.1
2.00	4.942	2.061	12.9	10059	-5722	246.9	31.7	91.7
2.50	4.962	2.048	12.0	8867	-4556	221.3	27.6	86.0
3.00	4.977	2.037	11.5	7971	-3765	199.3	24.4	79.7
3.50	4.989	2.028	11.2	7301	-3189	180.8	21.8	73.7
4.00	4.999	2.021	11.0	6728	-2754	165.4	19.7	68.2
4.50	5.006	2.016	10.8	6342	-2427	152.1	17.9	63.4
5.00	5.012	2.011	10.7	5993	-2162	140.7	16.5	59.1
5.50	5.019	2.007	10.6	5759	-1942	131.0	15.2	55.3
6.00	5.022	2.004	10.5	5508	-1762	122.5	14.2	52.0

E. T. T1.4

ST	Y MAX. (M)	Y MIN (M)	CT (SEC)	PA MAX (N/M ²)	PA MIN (N/M ²)	IP MAX (KW)	EFF. (%)	AP (KW)
1.00	4.815	2.169	15.6	15166	-9690	293.6	44.7	99.4
1.50	4.85	2.147	12.8	12272	-7123	273.1	37.6	103.4
2.00	4.879	2.127	11.6	10297	-5533	243.9	32.1	98.4
2.50	4.899	2.113	11.0	9052	-4430	217.7	27.9	91.0
3.00	4.915	2.101	10.6	8033	-3697	195.7	24.6	83.7

E. T. S1.0

ST	Y MAX. (M)	Y MIN (M)	CT (SEC)	PA MAX (N/M ²)	PA MIN (N/M ²)	IP MAX (KW)	EFF. (%)	AP (KW)
0.50	4.999	2.001	155	22789	-23646	139.8	56.6	8.40
1.00	4.999	2.001	77.8	18378	-18327	168.9	56.6	15.00
1.50	4.999	2.001	51.4	15268	-14957	174.8	52.2	20.20
2.00	4.999	2.001	37.5	13007	-12640	169.2	47.4	24.60
2.50	5.000	2.001	28.7	11306	-11301	159.8	42.8	28.90
3.00	5.005	2.001	23.9	9986	-9877	149.6	39.0	31.80
3.50	5.015	2.001	20.9	8935	-8899	139.7	35.9	33.40
4.00	5.026	2.001	18.8	8079	-8078	130.6	33.1	34.30
4.50	5.037	2.001	17.1	7371	-7390	122.9	30.7	34.80
5.00	5.046	2.001	15.8	6776	-6807	115.8	28.6	35.20

E. T. S1.2

ST	Y MAX. (M)	Y MIN (M)	CT (SEC)	PA MAX (N/M ²)	PA MIN (N/M ²)	IP MAX (KW)	EFF. (%)	AP (KW)
0.50	4.902	2.099	63.3	22351	-23581	139.0	61.5	19.20
1.00	4.907	2.097	33.5	18108	-18544	171.9	58.1	33.00
1.50	4.913	2.095	23.9	15.121	-15229	173.9	52.7	41.60
2.00	4.921	2.091	19.3	12945	-12910	167.6	47.7	46.50
2.50	4.933	2.088	16.6	11303	-11205	159.7	43.3	48.80
3.00	4.945	2.084	15.0	10026	-9899	150.8	39.5	49.40
3.50	4.958	2.079	13.9	9007	-8866	142.0	36.2	48.90
4.00	4.970	2.074	13.2	8176	-8028	133.7	33.4	47.80
4.50	4.981	2.069	12.7	7485	-7335	126.1	31.0	46.30
5.00	4.990	2.064	12.2	6902	-6752	119.1	28.9	44.60

E. T. S1.1

ST	Y MAX. (M)	Y MIN (M)	CT (SEC)	PA MAX (N/M ²)	PA MIN (N/M ²)	IP MAX (KW)	EFF. (%)	AP (KW)
0.50	4.951	2.050	77.2	22566	-23660	140.0	61.3	16.30
1.00	4.952	2.049	40.3	18237	-18556	172.2	58.0	28.30
1.50	4.955	2.048	28.2	15193	-15240	174.2	52.5	36.10
2.00	4.959	2.047	22.3	12983	-12927	168.6	47.3	41.00
2.50	4.966	2.046	18.8	11320	-11231	160.2	42.9	43.90
3.00	4.977	2.044	16.7	10030	-9932	150.9	39.1	45.10
3.50	4.988	2.043	15.3	9001	-8902	141.8	35.9	45.20
4.00	5.000	2.040	14.3	8164	-8064	133.3	33.1	44.60
4.50	5.011	2.037	13.6	7472	-7370	125.6	30.7	43.60
5.00	5.020	2.034	13.1	6890	-6784	118.7	28.6	42.30

E. T. S1.3

ST	Y MAX. (M)	Y MIN (M)	CT (SEC)	PA MAX (N/M ²)	PA MIN (N/M ²)	IP MAX (KW)	EFF. (%)	AP (KW)
0.50	4.854	2.148	55.1	22145	-23391	136.8	61.4	21.20
1.00	4.862	2.145	29.5	17974	-18425	169.7	58.1	36.40
1.50	4.872	2.140	21.3	15031	-15142	172	53.0	45.40
2.00	4.884	2.134	17.4	12882	-12840	166	48.0	50.20
2.50	4.898	2.128	15.2	11259	-11145	158.5	43.6	52.10
3.00	4.912	2.121	13.9	9994	-9845	149.8	39.8	52.30
3.50	4.926	2.115	13.0	8983	-8818	141.2	36.5	51.40
4.00	4.938	2.108	12.4	8158	-7984	133.1	33.7	49.90
4.50	4.948	2.101	11.9	7470	-7293	125.6	31.3	48.10
5.00	4.958	2.095	11.6	6889	-6713	118.6	29.1	46.30

E.T. S1.4

ST	Y MAX. (M)	Y MIN (M)	CT (SEC)	PA MAX (N/M ²)	PA MIN (N/M ²)	IP MAX (KW)	EFF. (%)	AP (KW)
0.50	4.806	2.197	49.2	21942	-23132	133.8	61.1	22.90
1.00	4.818	2.191	26.6	17836	-18262	166.7	58.1	39.00
1.50	4.831	2.184	19.4	14931	-15026	169.3	53.1	48.40
2.00	4.846	2.175	16.1	12807	-12750	164.0	48.3	53.10
2.50	4.862	2.167	14.2	11202	-11072	156.8	43.9	54.70
3.00	4.878	2.158	13.0	9950	-9782	148.5	40.1	54.60
3.50	4.892	2.15	12.3	8946	-8762	140.1	36.8	53.30
4.00	4.905	2.141	11.8	8127	-7934	132.1	33.9	51.50
4.50	4.915	2.134	11.4	7443	-7428	124.6	31.5	49.60
5.00	4.925	2.127	11.1	6864	-6672	117.8	29.3	47.50

E.T. S1.6

ST	Y MAX. (M)	Y MIN (M)	CT (SEC)	PA MAX (N/M ²)	PA MIN (N/M ²)	IP MAX (KW)	EFF. (%)	AP (KW)
0.50	4.617	2.390	34.2	21140	-21794	118.7	59.6	27.50
1.00	4.642	2.373	19.2	17245	-17424	151.8	57.7	46.30
1.50	4.666	2.355	14.6	14482	-14444	157.3	53.4	56.40
2.00	4.690	2.337	12.4	12456	-12313	155.2	48.7	60.50
2.50	4.712	2.322	11.3	10917	-10718	149.0	44.4	61.30
3.00	4.731	2.307	10.6	9711	-9484	141.5	40.6	60.10
3.50	4.747	2.295	10.1	8739	-8503	133.6	37.3	53.60
4.00	4.760	2.285	9.8	7942	-7704	126.2	34.4	55.70
4.50	4.771	2.276	9.6	7273	-7042	119.0	31.9	53.10
5.00	4.780	2.268	9.4	6707	-6483	112.5	29.7	50.60

E.T. S1.5

ST	Y MAX. (M)	Y MIN (M)	CT (SEC)	PA MAX (N/M ²)	PA MIN (N/M ²)	IP MAX (KW)	EFF. (%)	AP (KW)
0.50	4.711	2.294	40.5	21540	-22501	126.6	60.5	25.50
1.00	4.729	2.283	22.4	17544	-17865	159.6	58.0	43.10
1.50	4.749	2.269	16.7	14713	-14751	163.2	53.4	53.00
2.00	4.769	2.256	14.0	12640	-12543	159.8	48.6	57.40
2.50	4.788	2.244	12.6	11067	-10904	153.1	44.2	58.60
3.00	4.806	2.231	11.7	9839	-9641	145.2	40.4	57.80
3.50	4.822	2.222	11.1	8851	-8640	137.1	37.1	56.10
4.00	4.834	2.211	10.7	8043	-7823	129.4	34.2	54.00
4.50	4.846	2.204	10.4	7366	-7151	122.1	31.7	51.70
5.00	4.854	2.196	10.2	6794	-6581	115.4	29.5	49.40

E.T. S1.7

ST	Y MAX. (M)	Y MIN (M)	CT (SEC)	PA MAX (N/M ²)	PA MIN (N/M ²)	IP MAX (KW)	EFF. (%)	AP (KW)
0.50	4.522	2.485	29.1	20745	-21042	110.7	58.5	29.10
1.00	4.553	2.462	16.7	16943	-16951	143.7	57.2	48.80
1.50	4.583	2.439	12.9	14247	-14116	152.2	53.2	59.00
2.00	4.610	2.418	11.2	12266	-12065	150.5	48.7	62.90
2.50	4.634	2.399	10.2	10756	-10520	144.6	44.5	63.20
3.00	4.654	2.382	9.7	9571	-9319	137.4	40.7	61.70
3.50	4.671	2.370	9.3	8615	-8360	129.9	37.4	59.40
4.00	4.683	2.357	9.1	7831	-7576	122.6	34.5	56.80
4.50	4.695	2.350	8.8	7172	-6928	115.7	32.0	54.10
5.00	4.704	2.342	8.7	6613	-6380	109.3	29.8	51.50

E.T. T1.5

ST	Y MAX. (M)	Y MIN (M)	CT (SEC)	PA MAX (N/M ²)	PA MIN (N/M ²)	IP MAX (KW)	EFF. (%)	AP (KW)
1.00	4.739	2.247	13.7	15386	-9639	291.3	44.9	107.5
1.50	4.781	2.219	11.5	12301	-7031	267.4	37.9	109.4
2.00	4.811	2.198	10.6	10372	-5439	238.4	32.4	102.8
2.50	4.832	2.181	10.1	8991	-4393	212.6	28.2	94.5
3.00	4.847	2.170	9.78	7935	-3642	191.1	24.8	86.5
3.50	4.858	2.160	9.58	7188	-3113	173.0	22.2	79.3

E.T. T1.7

ST	Y MAX. (M)	Y MIN (M)	CT (SEC)	PA MAX (N/M ²)	PA MIN (N/M ²)	IP MAX (KW)	EFF. (%)	AP (KW)
1.00	4.586	2.406	11.0	15110	-9326	274.2	45.1	117.7
1.50	4.633	2.369	9.57	11704	-6915	252.2	38.3	117.0
2.00	4.664	2.343	8.98	9718	-5393	224.9	32.7	108.2
2.50	4.685	2.328	8.65	8453	-4351	200.6	28.4	98.5
3.00	4.700	2.316	8.45	7593	-3619	180.4	25.0	89.6

E.T. T1.6

ST	Y MAX. (M)	Y MIN (M)	CT (SEC)	PA MAX (N/M ²)	PA MIN (N/M ²)	IP MAX (KW)	EFF. (%)	AP (KW)
1.00	4.663	2.327	12.2	15306	-9495	283.6	45.1	113.1
1.50	4.708	2.294	10.5	11985	-6939	260.1	38.2	113.9
2.00	4.738	2.269	9.7	9949	-5408	231.8	32.6	106.1
2.50	4.761	2.253	9.3	8699	-4362	206.9	28.3	96.9
3.00	4.774	2.242	9.1	7685	-3631	185.7	25.0	88.4
3.50	4.787	2.233	8.9	7135	-3080	168.4	22.3	80.8
4.00	4.794	2.225	8.8	6542	-2690	153.6	20.1	74.3
4.50	4.804	2.219	8.7	6122	-2367	141.4	18.3	68.6
5.00	4.809	2.216	8.6	5813	-2092	130.8	16.8	63.7

A3.7

SERIES 10: VARIABLE SCALE FACTOR AND VARIABLE GU
Circular Twin Chambers

INITIAL VALUES:

Upstream Channel:

BUC	=	10.000 m	ZUC	=	0.000
EUC	=	5.000 m	CMUC	=	1.0

Downstream Channel:

BDC	=	10.000 m	ZDC	=	0.000
EDC	=	2.000 m	CMDC	=	1.00

Upstream Gate:

BUG	=	2.000 m	HUGMAX	=	0.852-0.983 m
TUG	=	3.000 s			
ZHCUG	=	4.000 m	HUG2(TWIN CHMBR)	=	0.852-0.983 m
			CCUG	=	0.6

Downstream Gate:

BDG	=	2.000 m	HDGMAX	=	1.533-1.769 m
TDG	=	3.000 s			
ZHCDG	=	4.000 m	HDG2(TWIN CHMBR)	=	1.533-1.769 m
			CCDG	=	0.7

Chamber:

A	=	19.998 m ²	ZT	=	5.5 m
		ST = 0.2 - 1.0			

SERIES 10: VARIABLE WIDTH OF ENTRANCE.

Gu = 1.040m

ST	CT (SEC)	Y MAX. (M)	Y MIN. (M)	PA MAX (N/M ²)	PA MIN (N/M ²)	dPA MAX (N/M ²)	L'KAGE %	IP MAX (KW)	EFF. (%)	AP (KW)
1.00	14.23	4.177	2.394	-3069	-20842	17773	26.96	120.7	25.3	50.9
0.80	14.61	4.167	2.432	-1380	-21083	19703	27.62	126.0	28.4	54.5
0.60	15.37	4.157	2.493	1700	-21121	19421	28.83	126.9	31.8	56.4
0.40	16.80	4.112	2.588	5920	-20679	26599	30.68	116.4	34.9	53.4
0.20	21.88	4.043	2.745	11509	-19686	31195	35.64	80.6	35.3	38.2

Gu = 1.080m

ST	CT (SEC)	Y MAX. (M)	Y MIN. (M)	PA MAX (N/M ²)	PA MIN (N/M ²)	dPA MAX (N/M ²)	L'KAGE %	IP MAX (KW)	EFF. (%)	AP (KW)
1.00	14.04	4.181	2.387	-3438	-21041	17603	27.67	126.1	25.5	52.7
0.80	14.43	4.170	2.426	-1169	-21261	20092	28.37	131.3	28.5	56.3
0.60	15.23	4.162	2.489	1950	-21267	23217	29.63	131.7	31.8	57.8
0.40	16.65	4.111	2.585	6183	-20763	26946	31.58	120.0	34.6	54.2
0.20	21.85	4.046	2.745	11745	-19804	31549	36.74	82.4	34.8	38.4

Gu = 1.110m

ST	CT (SEC)	Y MAX. (M)	Y MIN. (M)	PA MAX (N/M ²)	PA MIN (N/M ²)	dPA MAX (N/M ²)	L'KAGE %	IP MAX (KW)	EFF. (%)	AP (KW)
1.00	13.90	4.182	2.380	-3312	-21184	17872	28.20	130.1	25.6	54.1
0.80	14.31	4.173	2.421	-1013	-21386	22399	28.92	135.2	28.6	57.5
0.60	15.11	4.163	2.486	2135	-21369	23504	30.22	135.2	31.8	58.9
0.40	16.54	4.109	2.583	6377	-20820	27197	32.27	122.6	34.4	54.8

Gu = 1.120

ST	CT (SEC)	Y MAX. (M)	Y MIN. (M)	PA MAX (N/M ²)	PA MIN (N/M ²)	dPA MAX (N/M ²)	L'KAGE %	IP MAX (KW)	EFF. (%)	AP (KW)
1.00	13.86	4.183	2.379	-3268	-21229	17961	28.37	131.4	25.6	54.60
0.80	14.28	4.174	2.421	-960	-21426	20458	29.10	136.5	28.6	58.00
0.60	15.08	4.164	2.485	2195	-21402	23597	30.40	136.4	31.8	59.20
0.40	16.50	4.109	2.583	6442	-20838	27280	32.50	123.4	34.4	55.00

Gu = 1.160m

ST	CT (SEC)	Y MAX. (M)	Y MIN. (M)	PA MAX (N/M ²)	PA MIN (N/M ²)	dPA MAX (N/M ²)	L'KAGE %	IP MAX (KW)	EFF. (%)	AP (KW)
1.00	13.7	4.186	2.373	-3100	-21406	18306	29.05	136.7	25.8	56.3
0.80	14.12	4.176	2.415	-759	-21584	20825	29.82	141.6	28.7	59.6
0.60	14.96	4.168	2.482	2434	-21530	23964	31.19	140.9	31.8	60.5
0.40	16.38	4.108	2.581	6692	-20909	27601	33.8	126.8	34.1	55.8

Gu = 1.200m

ST	CT (SEC)	Y MAX. (M)	Y MIN. (M)	PA MAX (N/M ²)	PA MIN (N/M ²)	dPA MAX (N/M ²)	L'KAGE %	IP MAX (KW)	EFF. (%)	AP (KW)
1.00	13.54	4.188	2.364	-2939	-21579	18640	29.71	141.8	25.9	58.10
0.80	13.98	4.180	2.410	-558	-21733	21175	30.52	146.6	28.7	61.20
0.60	14.85	4.171	2.479	2669	-21651	24320	31.91	145.3	31.7	61.80
0.40	16.26	4.106	2.578	6937	-20973	27910	34.23	130.1	33.8	56.50

SERIES 11 : VARIABLE SCALE FACTOR AND GATE HIEGHT
Circular Twin Chambers

INITIAL VALUES:

Upstream Channel:

BUC	= 10.000 m	ZUC	= 0.000
EUC	= 5.000 m	CMUC	= 1.0

Downstream Channel:

BDC	= 10.000 m	ZDC	= 0.000
EDC	= 2.000 m	CMDC	= 1.000

Upstream Gate:

BUG	= 2.0-2.2 m	HUGMAX	= 0.983 m
TUG	= 3.000 s	HUG1	= 0.005 m
ZHCUG	= 4.000 m	HUG2(TWIN CHMBR)	= 0.983 m
		CCUG	= 0.6

Downstream Gate:

BDG	= 2.0-2.2 m	HDGMAX	= 1.769 m
TDG	= 3.000	HDG1	= 1.769 m
ZHCDG	= 4.000 m	HDG2(TWIN CHMBR)	= 0.009 m
		CCDG	= 0.7

Chamber:

A	= 19.998 m ²	ZT	= 5.500 m
---	-------------------------	----	-----------

ST = 0.4 - 1.0

SERIES 11: VARIABLE GATE HIEGHT.

BG = 2.050m.

ST	CT (SEC)	Y MAX. (M)	Y MIN. (M)	PA MAX (N/M)	PA MIN (N/M)	dPA MAX (N/M)	L'KAGE %	IP MAX (KW)	EFF. (%)	AP (KW)
1.00	13.45	4.191	2.359	-2828	-21699	18671	30.10	145.5	26.0	59.4
0.80	13.90	4.182	2.405	-423	-21845	21422	30.94	150.2	28.8	62.4
0.60	14.78	4.173	2.475	2822	-21723	24545	32.26	148.3	31.7	62.6
0.40	16.17	4.103	2.575	7097	-20996	28093	34.77	132.3	33.6	57.0

BG = 2.100m.

ST	CT (SEC)	Y MAX. (M)	Y MIN. (M)	PA MAX (N/M)	PA MIN (N/M)	dPA MAX (N/M)	L'KAGE %	IP MAX (KW)	EFF. (%)	AP (KW)
1.00	13.37	4.193	2.353	-2718	-21814	19096	30.49	149.1	26.1	60.6
0.80	13.82	4.185	2.402	-289	-21947	21658	31.35	153.7	28.8	63.4
0.60	14.72	4.176	2.471	2970	-21790	24760	32.61	151.3	31.7	63.4
0.40	16.08	4.101	2.572	7251	-21017	28268	35.28	134.5	33.5	57.4

BG = 2.150m.

ST	CT (SEC)	Y MAX. (M)	Y MIN. (M)	PA MAX (N/M)	PA MIN (N/M)	dPA MAX (N/M)	L'KAGE %	IP MAX (KW)	EFF. (%)	AP (KW)
1.00	13.28	4.195	2.347	-2612	-21933	19321	30.86	152.7	26.2	61.7
0.80	13.76	4.188	2.397	-163	-22039	21876	32.24	157.0	28.9	64.5
0.60	14.66	4.177	2.466	3111	-21848	24959	32.97	154.2	31.7	64.2
0.40	15.98	4.098	2.570	7399	-21034	28433	35.81	136.7	33.3	57.9

BG = 2.200m.

ST	CT (SEC)	Y MAX. (M)	Y MIN. (M)	PA MAX (N/M)	PA MIN (N/M)	dPA MAX (N/M)	L'KAGE %	IP MAX (KW)	EFF. (%)	AP (KW)
1.00	13.20	4.198	2.341	-2511	-22046	19535	31.23	156.2	26.3	62.9
0.80	13.69	4.192	2.392	-38	-22128	22090	32.54	160.3	28.9	65.5
0.60	14.60	4.179	2.462	3248	-21903	25151	33.31	156.9	31.6	64.9
0.40	15.90	4.096	2.567	7544	-21049	28593	36.30	138.7	33.1	58.4

SERIES 12: VARIABLE SCALE FACTOR AND GATE TIMINGS
Circular Twin Chambers

INITIAL VALUES:

Upstream Channel:

BUC	= 10.000 m	ZUC	= 0.000
EUC	= 5.000 m	CMUC	= 1.0

Downstream Channel:

BDC	= 10.000 m	ZDC	= 0.000
EDC	= 2.000 m	CMDC	= 1.0

Upstream Gate:

BUG	= 2.200 m	HUGMAX	= 0.983
TUG	= 2.4-2.8 s	HUG1	= 0.005
ZHCUG	= 4.000	HUG2(TWIN CHMBR)	= 0.983
		CCUG	= 0.6

Downstream Gate:

BDG	= 2.200	HDGMAX	= 1.769
TDG	= 2.4-2.8 s	HDG1	= 1.769
ZHCDG	= 4.000	HDG2(TWIN CHMBR)	= 0.009
		CCDG	= 0.7

Chamber:

A	= 19.998	ZT	= 5.500
	ST = 0.4 - 1.0		

SERIES 12: VARIABLE GATE TIMES.
TG = 2.8 Secs

ST	CT (SEC)	Y MAX. (M)	Y MIN. (M)	PA MAX (N/M)	PA MIN (N/M)	dPA MAX (N/M)	L'KAGE %	IP MAX (KW)	EFF. (%)	AP (KW)
1.00	12.92	4.194	2.338	-2466	-22321	19855	29.13	162.4	27.5	65.1
0.80	13.39	4.187	2.391	15	-22392	22407	30.42	165.5	30.2	67.6
0.60	14.29	4.175	2.464	3319	-22163	25482	31.16	160.9	33	66.7
0.40	15.59	4.092	2.57	7611	-21280	28891	34.21	141	34.4	59.6

TG = 2.6 Secs

ST	CT (SEC)	Y MAX. (M)	Y MIN. (M)	PA MAX (N/M)	PA MIN (N/M)	dPA MAX (N/M)	L'KAGE %	IP MAX (KW)	EFF. (%)	AP (KW)
1.00	12.63	4.188	2.335	-2431	-22614	20183	26.93	168.7	28.7	67.4
0.80	13.09	4.181	2.39	70	-22666	22736	28.15	170.9	31.6	69.8
0.60	13.95	4.169	2.466	3385	-22440	25825	28.94	165.1	34.4	68.7
0.40	15.27	4.087	2.573	7669	-21530	29199	31.96	143.4	35.8	60.9

TG = 2.4 Secs

ST	CT (SEC)	Y MAX. (M)	Y MIN. (M)	PA MAX (N/M)	PA MIN (N/M)	dPA MAX (N/M)	L'KAGE %	IP MAX (KW)	EFF. (%)	AP (KW)
1.00	12.33	4.181	2.333	-2398	-22905	20507	25.11	175.3	30	69.8
0.80	12.78	4.175	2.389	111	-22951	23062	25.82	176.7	33	72
0.60	13.63	4.164	2.468	3441	-22728	26169	26.57	169.6	35.9	70.6
0.40	14.95	4.083	2.577	7712	-21803	29515	29.52	146	37.2	62.1

ENERGY TEST 21: VARIABLE SCALE
FACTOR AND GATE TRIGGER LEVELS

TWIN CIRCULAR CHAMBERS

$$\delta = 1.4 \quad \eta = 1.0$$

E. T. 21.0

INITIAL VALUES:

Upstream Channel:

BUC	= 10.0m	ZUC	= 0.0m
EUC	= 5.0m	CMUC	= 1.0

Downstream Channel:

BDC	= 10.0m	ZDC	= 0.0m
EDC	= 2.0m	CMDC	= 1.0

Upstream Gate:

BUG	= 2.0m	HUGMAX	= 0.82m
TUG	= 3.0s	ARCMAX	= 55.0
ZHC	= 3.5 to 4.5m	CCUG	= 0.6
GU	= 1.0m		

Downstream Gate:

BDG	= 2.0m	HDGMAX	= 1.48m
TDG	= 3.0s	CCDG	= 0.7
ZHC	= 3.5 to 4.5m		

Chamber

D	= 5.046m	L	= 4.472m
A	= 19.999m	ZT	= 5.500m
CF	= 0.1	EFFT	= 1.0

ST = 0.2 to 1.4

SERIES 21: VARIABLE TRIGGER LEVEL

ZHCUG=4.50m

ST	CT (SEC)	Y MAX. (M)	Y MIN (M)	PA MAX (M H ₂ O)	PA MIN (M H ₂ O)	dPA MAX (M H ₂ O)	L'KAGE %	IP MAX (KW)	EFF. (%)	AP (KW)
0.20	48.53	4.524	2.382	1.493	-2.284	3.469	25.28	117.00	52.4	36.8
0.40	38.29	4.544	2.328	0.862	-2.206	2.779	24.25	149.8	44.0	46.0
0.60	28.67	4.549	2.303	0.427	-2.088	2.283	23.83	151.3	36.6	44.3
0.80	27.04	4.548	2.295	0.135	-1.965	1.919	23.59	142.4	30.9	39.6

ZHCUG=4.25m

ST	CT (SEC)	Y MAX. (M)	Y MIN (M)	PA MAX (M H ₂ O)	PA MIN (M H ₂ O)	dPA MAX (M H ₂ O)	L'KAGE %	IP MAX (KW)	EFF. (%)	AP (KW)
0.20	33.98	4.297	2.580	1.386	-2.184	3.215	29.51	102.20	48.4	40.7
0.40	23.56	4.336	2.476	0.759	-2.223	2.667	27.15	139.8	43.0	54.7
0.60	20.55	4.357	2.413	0.292	-2.206	2.238	25.94	146.5	37.0	55.4
0.80	19.22	4.366	2.380	-0.037	-2.154	1.906	25.35	141.0	31.7	51.5
1.00	18.53	4.370	2.362	-0.270	-2.094	1.649	25.07	131.9	27.5	46.6
1.20	18.11	4.371	2.352	-0.437	-2.036	1.449	25.00	122.2	24.1	42.0
1.40	17.85	4.372	2.348	-0.562	-1.984	1.290	25.02	113.0	21.4	37.9

ZHCUG=4.00m

ST	CT (SEC)	Y MAX. (M)	Y MIN (M)	PA MAX (M H ₂ O)	PA MIN (M H ₂ O)	dPA MAX (M H ₂ O)	L'KAGE %	IP MAX (KW)	EFF. (%)	AP (KW)
0.20	22.76	4.068	2.787	1.285	-2.053	2.921	34.24	88.60	42.5	42.4
0.40	16.81	4.113	2.635	0.690	-2.174	2.511	30.49	129.7	40.7	60.1
0.60	15.25	4.160	2.538	0.219	-2.239	2.159	28.15	140.9	36.6	63.2
0.80	14.44	4.175	2.479	-0.129	-2.249	1.868	27.29	138.6	32.1	60.5
1.00	14.04	4.185	2.442	-0.383	-2.233	1.635	26.73	131.5	28.3	55.8
1.20	13.81	4.194	2.419	-0.572	-2.207	1.448	26.40	123.0	25.0	51.0
1.40	13.64	4.198	2.404	-0.716	-2.178	1.296	25.79	114.5	22.4	46.5

ZHCUG=3.75m

ST	CT (SEC)	Y MAX. (M)	Y MIN (M)	PA MAX (M H ₂ O)	PA MIN (M H ₂ O)	dPA MAX (M H ₂ O)	L'KAGE %	IP MAX (KW)	EFF. (%)	AP (KW)
0.40	11.46	3.882	2.811	0.658	-2.093	2.278	36.60	118.1	35.2	59.5
0.60	11.09	3.947	2.686	0.212	-2.205	2.009	32.20	133.0	36.6	63.2
0.80	10.86	3.978	2.604	-0.135	-2.251	1.771	30.30	133.6	31.3	65.1
1.00	10.70	3.992	2.550	-0.396	-2.263	1.570	29.31	128.3	28.1	61.5
1.20	10.60	4.001	2.515	-0.593	-2.258	1.403	28.82	120.8	25.2	57.0
1.40	10.52	4.005	2.491	-0.746	-2.246	1.265	28.56	113.0	22.8	52.6

APPENDIX IV

SHEET PILE SYSTEM

QUANTITIES

PILING WORKS - SHEET PILE SYSTEM

	SAND		Column 1	CLAY		Column 2
2/	15.71 8.10	254.4	Chmbr total area, strt web. SW1 sheet piles. 27.9cm ² /m, 55.32kg/m. (P813)	2/ 15.71 7.00	219.9	Dtto clmn 1.
2/	2.60 4.60	23.92	Ddt gate opening.	2/ 2.60 3.50	18.20	Dtto clmn 1.
2/	15.71 2.60	81.67	Chmbr drvn area, strt web. SW1 sht piles. (P812)	2/ 15.71 1.50	47.12	Dtto clmn 1.
2/	2.60 2.60	13.52	Ddt gate opening.	2/ 2.60 1.50	7.80	Dtto clmn 1.
2/	8.10	16.20	30° Cnctng sht piles, strt web. (P811)	2/ 7.00	14.00	Dtto clmn 1.
4/	8.10	32.40	45° Cnctng sht piles, strt web. (P811)	4/ 7.00	28.00	Dtto clmn 1.
2/	8.10	16.20	90° Cnctng sht piles, strt web. (P811)	2/ 7.00	14.00	Dtto clmn 1.
	1.44 3.70	5.33	Interm wall total area. SW1 strt web sht piles. 27.9cm ² /m, 55.32kg/m. (P813)	1.44 3.70	5.33	Dtto clmn 1.
	4.00 11.50	46.00	Side walls total area. 2N Larsen sht piles. 1101cm ² /m, 55.32kg/m. (P833)	4.00 8.50	34.00	Dtto clmn 1.
	4.00 6.00	24.00	Side walls drvn area. 2N Larsen sht piles. 1101cm ² /m 48.8kg/m. (P832)	4.00 3.00	12.00	Dtto clmn 1.

SHEET PILED SYSTEM (Cont.)

2/	19.63 0.10	3.93	IN-SITU CONCRETE Provsn blndg chmbr floors. 100mm thick (F163)	2/ 19.63 0.15	5.89	Provsn chmbr roof, 150mm thick (30n/mm ²) (F163)
2/	19.63 0.10	3.93	Do. placing. (F411)	2/ 0.79 0.15	0.24	Ddt circ turb void
2/	19.63 0.30	11.78	Provsn chmbr floors 300mm thick (30N/mm ²) (F163)	2/ 19.63 0.15	5.89	Do placing. (F531)
2/	19.63 0.30	11.78	Do. placing. (F521)	2/ 0.79 0.15	0.24	Ddt circ turb void
	11.00 0.10	1.10	Provsn blndg gate area floors and dwnstrm apron 100mm thick. (F163)	2/ 19.63	39.26	CONC. ANCILLS. Fmwrk to chmbr roof rgh fin. plane horiz. (G115)
	11.00 0.10	1.10	Do. placing. (F411)	0.30 6.70	2.01	Fmwrk to dwnstrm apron, rgh fin. (G145)
	11.00 0.30	3.30	Provsn gate area and dwnstrm apron 300mm thick, (30N/mm ²) (F163)	2.00	2.00	Fmwrk to turb void (G271)
	11.00 0.30	3.30	Do. placing. (F522)	2/ 15.71	31.42	Hydrotite wtrstp for r.c. floor and sheet pile intrfce. (G681)
2/	5.50 0.50 0.50	2.75	Provsn abutments (30N/mm ²) (F163)	2/ 19.63	39.26	Wood flt fin to chmbr roofs. (G811)
2/	5.50 0.50 0.50	2.75	Dtto. placing. (F554)	2/ 1.00	2.00	Grtnng under clmn supp pads. (G843)

ABSTRACT

METALWORK - SHEET PILE SYSTEM

2/	0.28	0.57	Fab.circ.hollow sect. 219.1mm diam 5.5m long. 51.6kg/m (M311)	2/	0.12	0.24	Fab.steel supp. pad for clmn. 15mm thick. (M121)
2/	0.27	0.55	Fab.joists 203x102 10.8m long. 25.33kg/m (M321)	2/	0.12	0.24	Erect.steel supp. pad. (M720)
			Fab.gate cover. 2 equal angles, 200x 200x16mm thick, 48.5 kg/m. 2 equal angles, 120x 120x15mm thick, 26.6 kg/m. 1 equal angle, 150x 150x15mm thick, 33.8 kg/m 1 equal angle, 200x 200x16mm thick, 45.8 kg/m. All curved on plan. (M422)	1.40	1.40		Erect.gate cover (M720)
	0.73	0.73		40.00	40.00		Black bolts.HSFG higher grade. (M753)
			Fab.gate cover: 4 channels, 102x51 x15mm thick, 10.42 kg/m 2 T sections, 146x 127x12.7mm thick, 22.0kg/m. 1 steel plate, 3.5m . 20.0mm thick. All strght on plan. (M421)	4/	15.71	62.83	MISC. METALWORK
	0.67	0.67		3/	1.25	3.75	Waling, 127x64, grade 43 steel channel, 14.90kg/m. Int.chmbr walls. (N260)
2/	0.28	0.57	Erect.circ.hollow sects.Turb.support frame. (M620)	8/	2.09	16.76	Dtto.Interm.wall (N260)
2/	0.27	0.55	Erect.joists.Turb. support frame. (M620)	8/	2.00	16.00	Dtto.Extra to chmbr wall,gate area. (N260)
							Dtto.Upstrm and dwnstrm coffer. (N260)
							Dtto.Side walls. (N260)

PILING WORKS - SHEET PILED SYSTEM

SAND	S/	CLAY
	Total area, strt web, sht piles, 27.9 cm ² /m, 55.32kg/m. (P813)	
254.42 5.33 259.75 23.92 <u>235.83</u>	Dct. 23.92	219.87 Dct. 5.33 225.10 18.20 <u>206.90</u>
	S/ Drvn area, strt web, SW1 sht piles, 27.9 cm ² /m, 55.32kg/m. (P812)	
81.67 13.52 <u>68.15</u>	Dct. 13.52	47.12 Dct. 7.80 <u>39.32</u>
	L/ Spcl cncctng sht piles, strt web. (P811)	
16.20 32.40 16.20 <u>64.80</u>		14.00 28.00 14.00 <u>56.00</u>
	S/ Total area, Larsen 2N, sht piles, 1101 cm ² /m, 48.8 kg/m. (P833)	
<u>46.00</u>		<u>34.00</u>
	S/ Drvn area, Larsen 2N sht piles, 1101cm ² /m 48.8kg/m. (P832)	
<u>24.00</u>		<u>12.00</u>

A4.3

ABSTRACT
IN-SITU CONCRETE - SHEET PILED SYSTEM

<p>C/ Provsn conc presc mix for ord struct conc (30N/mm²) 20mm agg. (F163)</p> <p>3.93 Ddt 11.78 0.12 1.10 3.30 5.50 <u>5.89</u> 31.50 <u>0.12</u> <u>31.38</u></p>	<p>C/ Placing of chmbr roof, 150mm thick. (F531)</p> <p>5.89 Ddt <u>0.12</u> 0.12 <u>5.77</u></p> <p align="center">CONC. ANCILLS</p> <p>S/ Fmwrk to chmbr roofs rgh fin. (G115)</p> <p align="center"><u>39.26</u></p>	<p>L/ Hydrotite wtrstp for conc floor/sheet pile intrfce. (G661)</p> <p align="center"><u>31.42</u></p> <p>Nr/ Grouting under clmn support pad. (G843)</p> <p align="center"><u>2.00</u></p>
<p>C/ Placing of bldng 100mm thick (F411)</p> <p>3.93 <u>1.10</u> <u>5.03</u></p>	<p>S/ Fmwrk to dwnstrm apron, rgh fin (G145)</p> <p align="center"><u>2.01</u></p>	
<p>C/ Placing of chmbr and gate area floors and dwnstrm apron. 300mm thick. (F522)</p> <p>11.78 <u>3.30</u> <u>14.08</u></p>	<p>Nr/ Fmwrk to turb void. smooth fin. (G271)</p> <p align="center"><u>2.00</u></p> <p>S/ Wood float fin to chmbr roofs. (G811)</p> <p align="center"><u>39.26</u></p>	
<p>C/ Placing of conc abbtmnts. (F554)</p> <p align="center"><u>5.50</u></p>		

METALWORK - SHEET PILED SYSTEM

<p>t/ Fabrication 219.1mm hollow steel sects. grade 43.5.5m long, 51.6kg/m.</p> <p align="center">(M311)</p> <p align="center"><u>0.57</u></p>	<p>t/ Fabrication steel supp. pad for clmn. (M121)</p> <p align="center"><u>0.24</u></p>	<p>m/ Walings. 127x64. grade 43 steel channel 14.90kg/m. (N260)</p> <p align="center">62.83 3.75 15.71 16.76 <u>16.00</u> <u>115.05</u></p>
<p>t/ 25.33kg/m steel joists, 10.8m long. (M321)</p> <p align="center"><u>0.55</u></p>	<p>t/ Erect. turbine supp. frame. (M620)</p> <p align="center">0.57 <u>0.55</u> <u>1.12</u></p>	
<p>t/ Fabrication gate cover; angle sects. all curved on plan. (M422)</p> <p align="center">0.73</p>	<p>t/ Erect. steel supp. pad and gate cover. (M720)</p> <p align="center">0.24 <u>1.40</u> <u>1.64</u></p>	
<p>t/ Fabrication gate cover; channel, T, and plate sects. All strght on plan. (M421)</p> <p align="center"><u>0.67</u></p>	<p>nr/ Black bolts. HSFG higher grade. (M753)</p> <p align="center"><u>40.0</u></p>	

BILL OF QUANTITIES - SHEET PILED SYSTEM ON SAND.

No.	Description	Unit	Quantity	Rate	Amount
	<u>Piling to Chambers and Walls</u>				
	Interlocking, grade 43A steel sheet piles, straight web, section modulus 27.9cm ³ /m.				
P811	Length of connecting piles.	m	64.80	28.00	1814.40
P812	Driven area.	m ²	68.15	22.00	1499.30
P813	Area of piles of length not exceeding 14m, treated with two coats protective paint.	m ²	235.83	58.00	13678.14
Q671	Cutting off of surplus length.	nr	80.00	6.00	480.00
P832	Interlocking, grade 43A steel sheet piles, Larsen type 2N; section modulus 1101cm ³ /m.				
P832	Driven area.	m ²	24.00	23.00	552.00
P833	Area of piles of length not exceeding 14m, treated with two coats protective paint.	m ²	46.00	64.00	2944.00
Q673	Cutting off of surplus lengths.	nr	10.00	8.00	80.00
					21047.84
INDICES ADJUSTMENTS:					1704.87
TOTAL:					<u>22752.72</u>

BILL OF QUANTITIES - SHEET PILED SYSTEM ON CLAY.

No.	Description	Unit	Quantity	Rate	Amount
	<u>Piling to Chambers and Walls</u>				
	Interlocking, grade 43A steel sheet piles, straight web, section modulus 27.9cm ³ /m.				
P811	Length of connecting piles.	m	56.00	28.00	1568.00
P812	Driven area.	m ²	39.32	22.00	865.04
P813	Area of piles of length not exceeding 14m, treated with two coats protective paint.	m ²	206.90	58.00	12000.20
Q671	Cutting off of surplus length.	nr	80.00	6.00	480.00
P832	Interlocking, grade 43A steel sheet piles, Larsen type 2N; section modulus 1101cm ³ /m.				
P832	Driven area.	m ²	12.00	23.00	276.00
P833	Area of piles of length not exceeding 14m, treated with two coats protective paint.	m ²	34.00	64.00	2176.00
Q673	Cutting off of surplus lengths.	nr	10.00	8.00	80.00
					17465.24
INDICES ADJUSTMENTS:					1414.68
TOTAL:					<u>18879.92</u>

A4.5

SHEET PILED SYSTEM (Cont.)

No.	Description	Unit	Quantity	Rate	Amount
<u>IN-SITU CONCRETE</u>					
Provision of Concrete					
F163	Ordinary prescribed mix, grade C30, cement to BS 12, 20mm aggregate to BS 882. (Readymix)	m ³	26.35	40.00	1054.00
Placing of Concrete					
F411	Mass blinding for gate area, chamber floors and downstream apron; 100mm thick.	m ³	5.03	8.94	44.97
F522	Chamber and gate area floors and downstream apron; 300mm thick.	m ³	13.98	7.46	104.29
F531	Circular chamber roofs 150mm thick.	m ³	5.77	9.83	56.72
F554	Concrete abutments, 0.25m cross-sectional area.	m ³	5.50	11.17	61.44
INDICES ADJUSTMENTS:					1321.42
					58.73
REINFORCEMENT:					1380.15
					1054.00
TOTAL:					<u>2434.15</u>

SHEET PILED SYSTEM (Cont.)

No.	Description	Unit	Quantity	Rate	Amount
<u>CONCRETE ANCILLARIES</u>					
G115	Formwork, rough finish for chamber roofs; horizontal width: 5.0m	m ²	39.26	40.00	1570.40
G145	Formwork to downstream apron, rough finish; underwater placing, vertical, left in.	m	2.01	48.00	80.40
G271	Formwork to turbine void, smooth finish, 150mm depth.	Nr	2.00	11.89	23.78
G661	Hydrotite waterstop 150mm wide.	m	31.42	1.25	39.28
G881	Finishing of top surfaces, chamber roofs; wood float.	m ²	39.26	0.43	16.88
G843	Grouting under column support pad.	Nr	2.00	7.23	14.46
INDICES ADJUSTMENTS:					1745.20
					148.38
TOTAL:					<u>1893.58</u>

SHEET PILE SYSTEM (Cont.)

No.	Description	Unit	Quantity	Rate	Amount
STRUCTURAL METALWORK					
Turbine Support Frame Dwrng. No. Steel Grade 43A					
Fabrication of members for frames; straight on plan.					
M121	Plates	t	0.24	500.00	120.00
M311	Columns	t	0.57	782.00	445.74
M321	Beams	t	0.55	828.00	455.40
Erection of turbine support frame.					
M620	Frame members	t	1.36	150.00	240.00
Gate Cover and Support Dwrng No. Steel Grade 43A					
Fabrication of other members; curved on plan:					
M422	Beams straight on plan:	t	0.73	980.00	715.40
M421	Beams and plate	t	0.67	825.00	552.75
Erection of other members.					
M720	Beams	t	1.64	150.00	246.00
M753	Black Bolts	nr	40.00	4.50	180.00
MISCELLANEOUS METALWORK					
Walings for Chambers and Walls. Dwrng. Nos. Steel Grade 43A					
N260	Walings	m	115.05	14.60	1679.73
INDICES ADJUSTMENTS:					4635.02
					310.47
TOTAL:					<u>4945.50</u>

A4.7

OVERALL COSTS OF CIVILS WORK FOR SHEET PILED SYSTEM

Construction on Sand:

	P
Site investigation:	1371.90
Earthworks:	2494.40
Sheet piling works:	22752.72
In-situ concrete:	2434.15
Formwork, etc:	1893.58
Structural metalwork:	4940.50
Plant:	3536.00
Site set-up, temporary works etc:	3000.00

	42423.25
20% overheads	
(professional fees, insurance etc):	8484.65
5% profit margin:	2121.16

TOTAL:	<u>53029.06</u>

Construction on Clay:

Site investigation:	1371.90
Sheet piling works:	18879.92
Main civils costs:	18298.63

	38550.45
20% overheads:	7710.09
5% profit margin:	1927.52

TOTAL:	<u>48188.06</u>

PRECAST CONCRETE SYSTEM

QUANTITIES - PRECAST CONCRETE SYSTEM

		<u>Precast conc.</u>					
2/	19.63 2.60	102.8	Exc strt shaft with- in lining, mat to be used as fill. (T145)	2/	3.70	7.40	30 cncctng sht piles strt web. (P811)
2/	14.00	28.00	Pref conc sgmntl shaft lining, 150mm thick, 600mm deep, 3.55t per ring. (T615)				Bank Protection and Bed levelling. As for System No.1
2/	450.0	900.0	Wtrprfng of jnts using Hydrotite rbb seal. (T674)				
<u>In-Situ Conc.</u>							
2/	0.20 0.20 5.50	0.44	As for system No.1 plus: Provsn of conc to cncctng sht pile, 30 N/mm ² , 10mm agg. (F161)				
2/	0.20 0.20 5.50	0.44	Flcng of conc to cncctng sht pile, 30 N/mm ² , 10mm agg. (F452)				
<u>Steel Sheet Piles</u>							
As for sheet piled system re intermed- iate wall and side walls, plus:							
2/	11.50	23.00	90 cncctng sht piles, Larsen type 3C, 2N, 73.20kg/m. (P811)				
4/	2.50	10.00	45 cncctng sht piles strt web. (P811)				

ABSTRACT - PRECAST CONCRETE SYSTEM

<u>PRECAST CONC.</u>	<u>IN-SITU CONC.</u>	<u>STEEL SHEET PILES</u>
C/ Excav strt shaft, mat to be used as fill. (T145) <u>102.80</u>	As for system No.1 plus: C/ Provsn conc to cncctng sht pile, 30N/mm ² , 10mm agg. (F161) <u>0.44</u>	As for system No.1 re intermediate walls and side walls plus: L/ Spcl cncctng sht piles. (P811) 23.00 10.00 7.40 <u>40.40</u>
NR/ Pref conc sgmntl shaft lining, 150mm thick, 600mm deep, 3.55t per ring. (T615) <u>28.00</u>	C/ Flcng conc to cncctng sht pile, 30N/mm ² , 10mm agg. (F452) <u>0.44</u>	
L/ Wtrprfng of jnts using Hydrotite rbb seal. (T674) <u>900.00</u>		

BILL OF QUANTITIES - PRECAST CONCRETE SYSTEM.

No.	Description	Unit	Quantity	Rate	Amount
<u>CHAMBER CONSTRUCTION</u>					
T145	Shaft excavation, diameter 5.0m, material to be used as filling, straight.	m ³	102.80	40.00	4112.00
T615	Preformed concrete segmental shaft lining 150mm thick, 800mm deep, 3.55t per ring.	nr	28.00	555.00	15540.00
T674	Waterproofing joints using Hydrotite expanding rubber seal.	m	900.00	1.40	1260.00
In-Situ Concrete and Ancillaries: Brought forward from system No.1:					4327.73
F161	Provision of ordinary prescribed mix, grade C30, cement to BS 12, 10mm aggregate to BS 882.	m ³	0.44	47.25	20.79
F452	Placing to connecting sheet pile.	m ³	0.44	19.66	8.65
Steel Sheet Piles. Brought forward from system No.1:					4199.83
P811	Length of connecting piles.	m	40.40	30.27	1222.83
<u>METALWORK</u> Brought forward from system No.1:					1808.01
TOTAL					<u>32499.84</u>

(Inclusive of indices adjustments.)

OVERALL COSTS OF CIVILS WORK FOR PRECAST CONCRETE SYSTEM.

	P
Site investigation:	1371.90
Earthworks:	2494.40
Main civils works:	32499.84
Plant:	3536.00
Sluices:	1500.00
Site set-up, temporary works, etc:	3000.00

	44402.14
20% overheads (professional fees, insurance etc):	8880.43
5% profit margin:	2220.11

	<u>55502.68</u>

IN-SITU REINFORCED CONCRETE SYSTEMS

QUANTITIES - IN-SITU REINFORCED CONCRETE CHAMBERS

A4.10	2/	16.34 0.20 5.75	37.58	<u>CASES 1 AND 2</u> Provsn.Reinf.conc. Chmbr.walls.200mm thick.(30N/mm ²) (F161)	5.26 0.30	1.58	Provsn.Reinf.conc. gate area flrs.300 mm thick.(30N/mm ²) (F163)
	2/	16.34 0.20 5.75	37.58	Do.Placing.(F542)	5.26 0.30	1.58	Do.Placing.(F521)
	2/	2.60 0.20 2.20	2.28	Ddt.Gate opening in each chmbr.	1.30 0.20 3.70	0.96	Provsn.reinf.conc. Central barrage.200 mm thick(30N/mm ²) (F161)
	2/	19.63 0.10	3.93	Blinding.Chmbr.flrs. Provsn.100mm thick (F163)	1.30 0.20 3.70	0.96	Do.Placing.(F542)
	2/	19.63 0.10	3.93	Do.Placing.(F411)	2.00 0.20 5.00	4.00	Provsn.Reinf.conc. Side walls.200mm thick.(30N/mm ²) (F161)
	2/	19.63 0.30	11.78	Provsn.Reinf.conc. Chmbr.flrs.300mm thick.(30N/mm ²) (F163)	2.00 0.20 5.00	4.00	Do.Placing.(F542)
	2/	19.63 0.30	11.78	Do.Placing.(F521)	1.00 0.50 5.00	5.00	Provsn.Reinf.conc. abutments.1000mmx 500mm(30N/mm ²) (F163)
		5.26 0.10	0.53	Provsn.Blinding Gate area flr.100mm thick(F163)	1.00 0.50 5.00	5.00	Do.Placing.(F552)
		5.26 0.10	0.53	Do.Placing(F411)			

IN-SITU R.C. CHAMBERS.(CONT.)

2/	22.90 0.15	6.87	Provsn.Reinf.conc. Chmbr.covers.150mm thick(30N/mm ²) (F163)	16.18 0.15 1.60	3.88	Do.Placing. (F541)
2/	22.06 0.15	6.87	Do.Placing.(F531)			<u>CONC. ANCILLARIES</u> <u>CASES 1 AND 2</u>
2/	0.79 0.15	0.24	Ddt.voids for tur- bine ducts.	2/ 15.70 5.75	180.6	Fwk.to chmbr.walls 1 rad(2.5m)/1 plane Ro.fin.(G155)
	4.00 0.15	0.60	Provsn.Reinf.conc. Gate cover.150mm thick.(30N/mm ²) (F161)	2/ 16.96 5.75	195.0	Fwk.to chmbr.walls 1 rad(2.7m)/1 plane Ro.fin.(G155)
	4.00 0.15	0.60	Do.Placing.(F531)	1.40 3.70	5.18	Fwk.to central bar- rage.1 rad.(1.4m)/ 1 plane.Ro.fin. (G155)
	18.40 0.15 0.15	0.42	Provsn.reinf.conc. Beams 150mmx150mm to side walls.inter wall and gate cover. (30N/mm ²) (F161)	1.20 3.70	4.44	Fwk.to central bar- rage.1 rad.(1.2m)/ 1 plane.ff.(G255)
	18.40 0.15 0.15	0.42	Do.Placing (F561)	2/ 2.00 5.00	20.00	Fwk.to side walls. 1 rad(1.4m)/1 plane Ro.fin.(G:55)
			CASE 1 ONLY	2/ 2.00 5.00	20.00	Fwk.to side walls. 1 rad(1.2m)/1 plane ff.(G255)
2/	16.34 0.20 1.60	10.45	Provsn.reinf.conc. chmbr.walls 200mm thick.(30N/mm ²) (F161)	2/ 5.00 5.00	5.00	Fwk.to abbtmts.Ccs 1000mmx500mm.Ro.fin (G182)
				4.00 4.00	4.00	Fwk.to gate cover Ro.fin.(G115)
				18.40 18.40	18.40	Fwk.to beams.Ccs. 150mmx150mm.ff. (G281)

ABSTRACT

IN-SITU R.C.CHAMBERS (CONT.)

2/	22.90	45.80	Fwk.to roof slabs. Hrzntrl.Ro.fin. (G115)	6/	4.00	24.00	Ttl drvn depth of unvsl clmns,203x 203mm,60kg/m.(P742)
	4.00	4.00	Fwk.to gate cover Hrzntrl.Ro.fin. (G115)				<u>METALWORK</u>
	2	2	Fwk.to circ.voids in chmbr.covers. 1000mm diam.(G271)	2/	3.00	6.00	Fab joists 152x127 3.0m long,37.2kg/m (M321)
	2	2	Fwk.to gate open- ings.1800mm hi. 3000mm wi.(G277)	2/	3.00	6.00	Erect joists,turb. support frame. (M620)
	100	100	Rubber waterstops at all const.joints req.wp.or airtight seals.(G652)				
2/	22.90	45.80	Wood float fin.to chmbr.covers.5400mm diam.(G811)				
	15.70	50.24	CASE 1 ONLY: Fwk.to chmbr.walls 1 rad.(2.5m)/1plane Ro.fin.(G155)				
	1.60	54.28	Fwk.to chmbr.walls 1 rad.(2.7m)/1plane Ro.fin.(G155)				
	1.60	54.28					
			<u>PILING WORKS</u>				
	15.00	30.00	Ttl area,strt web, SW1 sheet pile,cut- off wall.27.9cm ³ /m, 55.32kg/m. (P813)				
	4.00	9.00	Case 2 Only: Add to ttl area. (P813)				
	2.25	9.00					
	15.00	26.25	Drvn area,strt web, SW1 sheet pile cut- off wall.(P812)				
	1.75	26.25					
	6	6	Isltd unvsl clmns. 203X203mm,60kg/m, 9.5m long.(P742)				

IN-SITU REINFORCED CONCRETE CHAMBERS

C/ Provsn.of conc. presc.mix for ord. struct.conc(30N/mm ²) 10mm agg.(F161)	C/ Placing conc. Walls 200mm thick (F542)	CONCRETE ANCILL.
Cases 1 and 2:	37.58 Ddt. 0.96 2.28 4.00	S/ Fwk.1 rad(1.4,2.5, 2.7m)/1 plane.Ro.fin (G155)
37.58 Ddt. 0.96 2.28 4.00 0.60 0.42	42.54 2.28	180.60 195.00 5.18 20.00
43.56 2.28	<u>40.26</u>	<u>400.78</u>
	Case 1 Only:	Case 1 Only:
	40.26 10.45	400.78 104.52
Case 1 Only:	<u>50.71</u>	<u>505.30</u>
41.28 10.45	C/ Placing of blinding 100mm thick (F411)	S/ Fwk.1 rad./1 plane (1.2m)ff. (G255)
<u>51.73</u>	3.93 0.53	4.44 20.00
	<u>4.46</u>	<u>24.44</u>
C/ Provsn.of conc. presc.mix for ord struct. conc. (30N/mm ²)20mm agg. (F163)	C/ Placing conc. abutmnts.1000mmx 500mm(F552)	S/ Fwk.Ro.fin.Horiz. (G115)
3.93 11.78 0.53 1.58 5.00 6.87	<u>5.00</u>	45.80 4.00
<u>29.69</u>	C/ Placing conc.chmbr floors.300mm thick. (F522)	<u>49.80</u>
C/ Placing conc. slabs.150mm thick (F531)	11.78 1.58	L/ Fwk.to clmns.ro. fin..Ccs 1000x500mm (G182)
6.87 0.60	<u>13.36</u>	<u>5.00</u>
<u>7.47</u>		

IN-SITU R.C.CHAMBERS (CONT.)

L/ Fwk. to beams. Ccs 150x150mm. ff. (G281) <u>18.41</u>	S/ Drvn. area. strt web SW1 sheet piles. 27.9cm ³ /m. 55.32kg/m (P812) <u>28.25</u>
Nr/ Fwk. to voids not excdng 0.5m depth. (G271) <u>2</u>	Nr/ Ctting. off of surplus length. (Q671) <u>37.00</u>
Nr/ Fwk. to voids not excdng 2.0m. (G277) <u>2</u>	Nr/ Isltd. unvsl. clms. 203X203mm, 60kg/m. 9.5m long. (P742) <u>6</u>
L/ Rubber waterstops Flat dumbell. (G552) <u>100.00</u>	L/ Ttl. drvn. depth of unvsl. clms. 203x 203mm, 60kg/m. (P742) <u>24.00</u>
S/ Wood float fin. to roof slab. (G811) <u>45.80</u>	<u>METALWORK</u>
<u>PILING WORKS</u>	t/ Fab. joists, 152x127mm 37.2kg/m, 3.0m long. (M321) <u>0.22</u>
S/ Ttl. area, strt web, SW1 sheet piles. 27.9cm ³ /m. 55.32kg/m. (P813) <u>30.00</u>	t/ Erect joists, 152x127 mm, 37.2kg/m, 3.0m long. (M620) <u>0.22</u>
Case 2 only: 30.00 9.00 <u>39.00</u>	

BILL OF QUANTITIES

IN-SITU REINFORCED CONCRETE CHAMBERS (Case 2)

No.	Item Description	Unit	Quantity	Rate	Amount
	<u>IN-SITU CONCRETE</u>				
	Provision of concrete				
F161	Ordinary prescribed mix grade C30 cement to BS12 10mm aggregate to BS882	m ³	41.28	40.00	1651.20
F163	Grade C30 cement to BS12 20mm aggregate to BS882	m ³	29.69	40.00	1187.60
	Placing of concrete				
F411	Mass blinding thickness not exceeding 150mm	m ²	4.46	8.94	39.87
F531	Reinforced Suspended slabs thickness not exceeding 150mm	m ²	7.47	9.83	73.43
F542	Walls thickness not exceeding 200m	m ²	39.08	9.83	384.16
F552	Columns cross-sectional area 0.3-1.0m	m ²	5.00	19.66	98.30
F522	Floors	m ²	13.36	7.46	99.67
					3534.23
					103.19
					3637.42
					2838.80
					<u>6476.22</u>

A4.13

IN-SITU R.C.SYSTEM (Cont.)

No.	Item Description	Unit	Quantity	Rate	Amount
<u>CONCRETE ANCILLARIES</u>					
G115	Formwork rough finish horizontal width exceeding 1.22m.	m ²	49.80	40.00	1992.00
G155	Formwork rough finish vertical curved to one radius in one plane; radii 1.4, 2.5 and 2.7m, upstream faces of side walls and central barrage plus inner and outer chamber walls.	m ²	400.78	25.96	10404.25
For concrete components of constant cross-section:					
G182	Columns: 1000x500mm Rough finish.	m	5.00	30.94	154.70
G281	Beams: 150x150mm, ff.	m	18.40	8.00	147.20
For voids:					
G271	Formwork to small voids depth not exceeding 0.5m.	nr	2	13.10	26.20
G277	Formwork to large voids depth 1-2m.	nr	2	39.45	78.90
Joints:					
G652	Rubber flat dumbbell waterstop 150mm wide.	m	100.00	12.12	1212.00
Accessories:					
G811	Finishing of top surfaces wood float.	m	45.80	0.43	19.70
					14043.95
INDICES ADJUSTMENT:					1184.25
TOTAL:					<u>15228.20</u>

IN-SITU R.C. SYSTEM (Cont.)

No.	Item Description	Unit	Quantity	Rate	Amount
<u>PILING WORKS</u>					
Piling to cut-off wall interlocking, grade 43a steel sheet piles, straight web, section modulus 27.9cm ³ /m.					
P812	Driven area:	m ²	26.25	22.00	577.50
P813	Area of piles of length not exceeding 14m, treated with two coats of protective paint.	m ²	30.00	58.00	1740.00
Q671	Cutting off of surplus length.	nr	37	6.00	222.00
Isolated steel piles:					
P741	Number of piles 9.5m long, universal columns 203X203mm, 60kg/m.	nr	6	55.00	330.00
P742	Driven depth.	m	24.00	28.50	684.00
					3553.50
INDICES ADJUSTMENT:					355.35
					<u>3908.85</u>
No.	Item Description	Unit	Quantity	Rate	Amount
<u>METALWORK</u>					
Turbine support frame.					
Fabrication of members for frames: straight on plan. Steel grade 43A.					
M321	Beams.	t	0.23	861.13	198.06
Erection of members.					
M620	Beams.	t	0.23	171.74	39.50
					TOTAL:
					<u>237.56</u>

(Inclusive of indices adjustments.)

ADDITIONAL QUANTITIES FOR CASE 1. (Inclusive of indices adjustments)

No.	Item Description	Unit	Quantity	Rate	Amount
IN-SITU CONCRETE					
Provision of concrete					
F161	Ordinary prescribed mix grade C30 cement to BS12 10mm aggregate to BS882	m ³	10.45	40.00	418.00
Placing of concrete					
F542	Walls thickness not exceeding 200mm.	m ³	10.45	9.83	102.72
CONCRETE ANCILLARIES					
G155	Formwork rough finish vertical curved to one radius in one plane; radii 2.5 and 2.7, inner and outer chamber walls.	m ²	104.52	28.17	2944.04
PILING WORKS					
Piling to cut-off wall interlocking, grade 43A steel sheet piles, straight web, section modulus 27.9cm ³ /m.					
P813	Deduct area of piles of length not exceeding 14m, treated with two coats of protective paint.	m ²	-9.00	58.00	-522.00
					<u>2942.76</u>

OVERALL CIVILS COSTS FOR IN-SITU, REINFORCED CONCRETE SYSTEM.

Construction Without Cofferdam:

	P	
Site investigation:	1371	90
Earthworks:	2494	40
In-situ concrete:	6476	22
Formwork, etc:	15228	20
Piling works:	3908	85
Metalwork:	237	56
Plant:	3536	00
Sluices:	3000	00
Site set-up, temporary works, etc:	5000	00

	41253	13
20% overheads		
(Professional fees, insurance etc):	8250	63
5% profit margin	2062	66

	<u>51566</u>	<u>42</u>

Construction With Cofferdam:

Site investigation:	1371	90
Earthworks:	2494	40
In-situ concrete:	6476	22
Formwork, etc:	15228	20
Piling works:	3908	85
Metalwork:	237	56
Plant:	3536	00
Sluices:	3000	00
Fabric cofferdam:	5000	00
Site set-up, temporary works, etc:	3000	00

	44253	13
Additional costs:	2942	76

	47195	89
20% overheads		
(Professional fees, insurance etc)	9439	18
5% profit margin	2359	79

Total:	<u>58994</u>	<u>86</u>

STEEL CHAMBER SYSTEM

QUANTITIES STEEL CHAMBER SYSTEM

			<u>METALWORK</u>			
29.68	29.68		Fab of chamber walls: 8 no. rings, 2.0m deep; 15mm thick, each in three equal segments; grade 43 steel. Curved on plan. (M402)			
29.68	29.68		Erection of chmbr walls. (M720)			
			As for sheet piled system re gate cover and frame.			
			<u>MISCELLANEOUS METALWORK.</u>			
			As for sheet piled system.			
			<u>SHAFT EXCAVATION</u>			
			As for pre-cast concrete system.			
			<u>IN-SITU REINF. CONC.</u>			
			As for sheet piled system.			
			<u>PILING</u>			
			As for sheet piled system re intermed- iate wall and side walls.			
			As for pre-cast system re connecting sheet piles.			

BILL OF QUANTITIES - STEEL CHAMBER SYSTEM.

No.	Description	Unit	Quantity	Rate	Amount
	<u>STRUCTURAL METALWORK</u> Chamber walls				
M402	Fabrication of plate wall segments.	t	29.68	593.00	17600.24
M720	Erection of wall seg- ments.	t	29.68	150.00	4452.00
	Gate Cover and Frame.				
	Brought forward from sheet piled system.				1805.96
	Miscellaneous Metalwork.				
	Brought forward from sheet piled system.				1815.79
	Piling				
	Brought forward from sheet piled system and pre-cast concrete system.				5417.65
	In-situ Reinforced Concrete				
	Brought forward from sheet piled system.				4327.73
	Shaft Excavation				
	Brought forward from pre-cast concrete system				4112.00
	TOTAL:				<u>39531.13</u>

(Inclusive of indices adjustments)

OVERALL COSTS OF CIVILS WORKS FOR STEEL CHAMBER SYSTEM

Site investigation:	P 1371.90
Earthworks:	2494.40
Main civils works:	39531.13
Plant:	3536.00
Sluices:	1500.00
Site set-up, temporary works, etc:	3000.00

	51433.43
20% overheads (professional fees, insurance, etc.)	10286.69
5% profit margin:	2571.67

	64291.79

PLASTIC /GRP CHAMBER SYSTEM

BILL OF QUANTITIES - PLASTIC/G.R.P. CHAMBER SYSTEM

No.	Description	Unit	Quantity	Rate	Amount
	<u>CHAMBERS</u>				
	Composite fibreglass/polypropelene rings, 5.0m in diameter, 6.0m deep.	No.	2	23000.00	56000.00
	Site assembly, transport and placing.				6000.00
	<u>TURBINE SUPPORT FRAME</u>				
	Brought forward from section 1.0.				1345.26
	<u>PILING WORKS</u>				
	Brought forward from section 1.0.				5417.65
	<u>GATE COVER</u>				
	Brought forward from section 1.0.				1805.96
	<u>IN-SITU REINFORCED CONCRETE</u>				
	Brought forward from section 1.0.				4327.73
				TOTAL:	<u>74896.60</u>

OVERALL COSTS OF CIVILS WORK FOR PLASTIC/GRP SYSTEM

Site investigation:	1371.90
Earthworks:	2494.40
Main civils work:	74896.60
Plant:	3536.00
Sluices:	1500.00
Site set-up, temporary works etc.	3000.00

	86798.90
20% overheads (professional fees, insurance etc):	17359.78
5% profit margin:	4339.95

	<u>108498.63</u>

COMPONENTS COMMON TO ALL SYSTEMS

SITE INVESTIGATION QUANTITIES

4	4	Light cable percuss. boreholes. 8m deep. (B212)	6	6	Moisture content. (B711)
4	4	Ditto (B232).	6	6	Spec. gravity (B713)
8	8	Open tube samples (B421)	4	4	Ph values. (B723)
12	12	Standard pen. tests. (B513)	6	6	Undrained Triax. (B761)

BILL OF QUANTITIES - SITE INVESTIGATION.

No.	Description	Unit	Quantity	Rate	Amount
<u>Site Investigation</u>					
B212	Light percussive boreholes.	No.	4	50.00	200.00
B232	Depth of drive.	m.	32.00	11.50	368.00
B421	Two open tube samples per borehole.	No.	8	6.50	52.00
<u>Site Tests</u>					
B513	Three standard penetration tests per borehole	No.	12	6.50	78.00
<u>Lab. Tests</u>					
B711	Moisture content.	No.	6	0.80	4.80
B713	Specific gravity.	No.	6	1.80	10.80
B723	Ph values.	No.	4	2.00	8.00
B761	Triaxial compression: undrained.	No.	6	10.50	63.00
					784.60
Indices adjustment:					130.00
					914.60
Professional services @ 50% :					457.30
TOTAL:					1371.90

**QUANTITIES
GATE SYSTEM AND TRASHRACK.**

		METALWORK			
0.13	0.13	Fab of gate frame, grade 43 steel, 5mm thick and gate pivot; 70mm diam. (M361)	0.11	0.11	Fab of trashrack frame, grade 43 steel 1 equal angle, 150x 150mm thick, 33.8kg/m 1 steel plate, 200x 20mm, 2.1m long. All curved on plan. (M472)
0.25	0.25	Fab of gate sides, grade 43 steel, 3mm thick. (M402)	0.38	0.38	Erection and installation of gate. (M720)
0.31	0.31	Fab of trashrack screen, grade 43 steel, 14x75mmx 20mm bars, 1.9m long. All stright on plan. (M471)	0.42	0.42	Erection and installation of trashrack. (M720)

ABSTRACT

t/ Fab of gate frame and pivot, grade 43 steel. (M361) <u>0.13</u>	t/ Fab of trashrack frame, grade 43 steel 1 equal angle, 150x 150mm thick, 33.8 kg/m. 1 plate, 200x20mm, 2.1m long. All curved on plan. (M472) <u>0.11</u>	t/ Fab of trashrack screen, 14 no. 75x 20mm bars, grade 43 steel, all stright on plan. (M471) <u>0.31</u>
t/ Fab of gate sides, 3mm thick plate, grade 43 steel. (M402) <u>0.25</u>		t/ Erection and installation of gate and trashrack. (M720) <u>0.80</u>

**BILL OF QUANTITIES
GATE SYSTEM AND TRASHRACK**

No.	Description	Unit	Quantity	Rate	Amount
STRUCTURAL METALWORK					
	Gate system and trashrack, drwg nos. Grade 43 steel.				
	Fabrication of members				
M361	Bracings and pivot	t	0.13	500.00	65.00
M402	Plate	t	0.25	470.47	117.62
M471	Plate	t	0.31	825.00	255.75
M472	Beams	t	0.11	980.00	107.80
	Erection:				
M720	Gate and trashrack members.	t	0.80	300.00	240.00
	Miscellaneous:				
	Water-lubricated bearings.	nr	3	85.95	257.85
					<u>1044.02</u>

+100% = 2088.02

OVERALL COSTS OF COMPONENTS COMMON TO ALL SYSTEMS

M. and E.

Gate and Trashrack system:	2088.04
Wells Turbine, generator and ducting:	25200.00
Grid connection and housing:	<u>6000.00</u>
TOTAL:	<u>33288.04</u>

Civils

Bank protection and bed preparation:	<u>2494.40</u>
--------------------------------------	----------------

RECTANGULAR CHAMBER, HORIZONTAL-AXIS RADIAL GATED PWE

QUANTITIES

Site Investigation

As for butterfly gated system.

Excavation and Bank Protection

<u>CESMM code</u>	<u>Description</u>	<u>Quantity</u>
(E423)	Bed Preperation	30m ³
(E512)	Trimming	60m ²
(----)	Gabion Supply + Placement	25m ³
(E426)	Bank Excavation	384m ³

Precast Concrete Units

(H535)	ROOF: 4.0x2.0x0.2 units	7 No
	WALLS, Upstrm and Dwnstrm:	
(H521)	2.0x1.0x0.2 units	4 No
(H535)	7.0x1.0x0.2 units	8 No
(H546)	7.0x2.0x0.2 units	4 No
(H535)	WALLS, Interm. and end	8 No

Structural Metalwork

FRAME: Assuming 203x133 UBMs throughout:

(M321)	Fabrication	2.60 t
(M620)	Erection	2.60 t

GATE SYSTEM: Assuming 10mm plate for faces:

(----)		1.73 t
--------	--	--------

Assuming 60x60 square hollow sections
for support frame to gate face:

(M321)	Fabrication	0.70 t
(M620)	Erection	0.70 t

Assuming 120x60 rectangular hollow sections for gate arms:

(M321)	Fabrication	0.93 t
(M620)	Erection	0.93 t
(----)	100mm diam. drive shaft	0.65 t

Piling

Assuming 305x305x20.7 Universal Bearing Piles driven to a depth of five metres and one 450x250x10.0 hollow rectangular steel pile at intermediate wall.

(P751)	Isolated steel piles	7 No
(P752)	Driven depth	80.00m

Piling (cont)

<u>CESMM code</u>	<u>Description</u>	<u>Quantity</u>
-------------------	--------------------	-----------------

Assuming 2N Larsen sheet piles driven to a depth of 2m to form cut-off wall:

(P832)	Driven area	28.00m ²
(P833)	Total area	35.00m ²

In-situ Concrete

(F163)	Provision	52.50m ³
(F411)	Placing (blinding)	10.50m ³
(F523)	Placing (reinforced)	42.00m ³
(G145)	Formwork	22.00m ²

Cofferdam

Assuming main cost to be driving and extracting of piles as specialist contractor will reuse sheet piling from previous works:

(P832)	Driven area, 5m drive depth	150.00m ²
--------	-----------------------------	----------------------

(Percentage of total cost to be added for extraction and materials usage.)

Gate Drive System

(----)	RPK 65H Rotapak Fluidair Compressor	1 No
(----)	100mmx118.6mm double acting pistons	6 No
(----)	Reciever plus airlines etc.	1 No

COSTING

Site Investigation

	£	p
As butterfly gated system:		
TOTAL:		<u>1371.91</u>

Excavation and Bank Protection

<u>CESMM code</u>	<u>Quantity</u>	<u>Rate</u>	
(E423)	30m ²	1.35	40.50
(E512)	60m ²	1.09	65.40
(E426)	384m ³	2.05	787.20
Gabions:	25m ³	80.00	<u>2000.00</u>
			2893.10
		Indices adjustment:	<u>100.00</u>
		TOTAL:	<u>2993.10</u>

Precast Concrete Units

(H521)	4 No	75.00	300.00
(H535)	23 No	150.00	3450.00
(H546)	4 No	230.00	<u>920.00</u>
			4670.00
		Indices adjustment:	<u>630.50</u>
		TOTAL:	<u>5300.00</u>

Structural Metalwork

(M321)	3.88 t	828.00	3212.64
(M620)	3.88 t	150.00	582.00
Steel plate:	1.73 t	490.00	847.70
Drive shaft:	0.65 t	520.00	<u>338.00</u>
			5823.14
		Indices adjustment:	<u>313.00</u>
			6136.14

50% of total gate cost to cover assembly, installation, etc.		<u>1389.57</u>
TOTAL:		<u>7525.71</u>

Piling

(P751)	17 No -	55.00	935.00
(P752)	80m	88.00	7040.00
(P832)	28m ²	23.00	644.00
(P833)	35m ²	64.00	<u>2240.00</u>
			10859.00
	Indices Adjustment:		<u>1085.90</u>
			11944.90

Piling (cont)

<u>CESMM code</u>	<u>Quantity</u>	<u>Rate</u>	£	p
Cofferdam:				
(P832)	150m	23.00	3450.00	
	Indices Adjustment:		<u>345.00</u>	
			15739.00	
50% to cover extraction and materials usage:				<u>1897.50</u>
		TOTAL:	<u>17636.50</u>	

In-Situ Concrete

(F163)	52.5m ³	40.00	2100.00
(F411)	10.5m ³	8.94	93.00
(F523)	42.0m ³	3.24	136.08
(G145)	22.0m ²	48.78	<u>1073.16</u>
			3403.11
	Indices adjustment:		<u>232.03</u>
		TOTAL:	<u>3635.14</u>

Gate Drive

(----)	Compressor	4830.00
(----)	6 No Pistons	500.00
(----)	Reciever, airlines etc.	<u>600.00</u>
	TOTAL:	<u>5930.00</u>

OVERALL COST OF CIVILS WORK

Site investigation:	1371.90
Earthworks:	2993.10
Precast concrete:	5300.00
Structural Metalwork:	7525.71
Piling:	17636.50
In-situ concrete:	3635.14
Gate drive:	5930.00
Plant:	3536.00
Site set-up, temporary works etc.	<u>3000.00</u>
	50928.35
20% overheads	
(Professional fees, insurance etc):	10185.67
5% profit margin:	<u>2546.42</u>
TOTAL:	<u>63660.44</u>